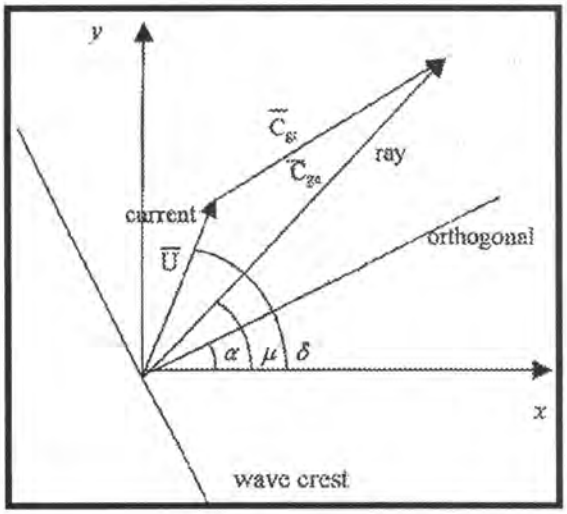

Figure 5-4. Wave and current vectors used in STWAVE. Subscript *a* denotes values in the *absolute* frame of reference, and subscript *r* denotes values in the *relative* frame of reference (with currents).

Model Domain and Bathymetry. Wave modeling consists of a regional coarse model grid (200 m x 200 m grid cells) as well as three fine grids (25 m x 25 m grid cells), which provide a detailed solution in areas of interest. The solution from the coarse wave model is mapped onto the offshore boundary of each of the fine grid, providing a detailed and spatially varying boundary condition for each of the fine grid runs.

Limits of the coarse grid (the largest rectangle in Figure 5-5) were chosen so the offshore boundary falls at the same latitude as WIS Station 156, which was chosen to supply the boundary conditions for wave runs. Lateral extents of the coarse grid are taken far from the fine grids to ensure the solution at the boundary of the fine grids is free of any edge effects. The inshore extent of the coarse grid is somewhat immaterial, provided it passes beyond the outer boundaries of the fine grids. The solution from the coarse wave grid was used only to formulate the boundary conditions for fine wave grids.

Three different fine grid domains were chosen so each area of interest could be examined with the required amount of detail. The two fine grids located along Dauphin Island and Morgan Peninsula were developed to achieve a detailed view of wave refraction and breaking in the nearshore region. Both these grids are comprised of 25 m x 25 m grid cells. The central fine grid encompasses the ebb shoal complex, Pelican Island, and Mobile pass, as well as a portion of the adjacent beaches. It also extends into Mobile Bay, so this same grid can be used for CMS-

M2D model runs as well. Because of the larger size of this grid, cell sizes were increased to 50 m x 50 m to keep model run times reasonable. A summary of the properties for each grid is given in Table 5-1.

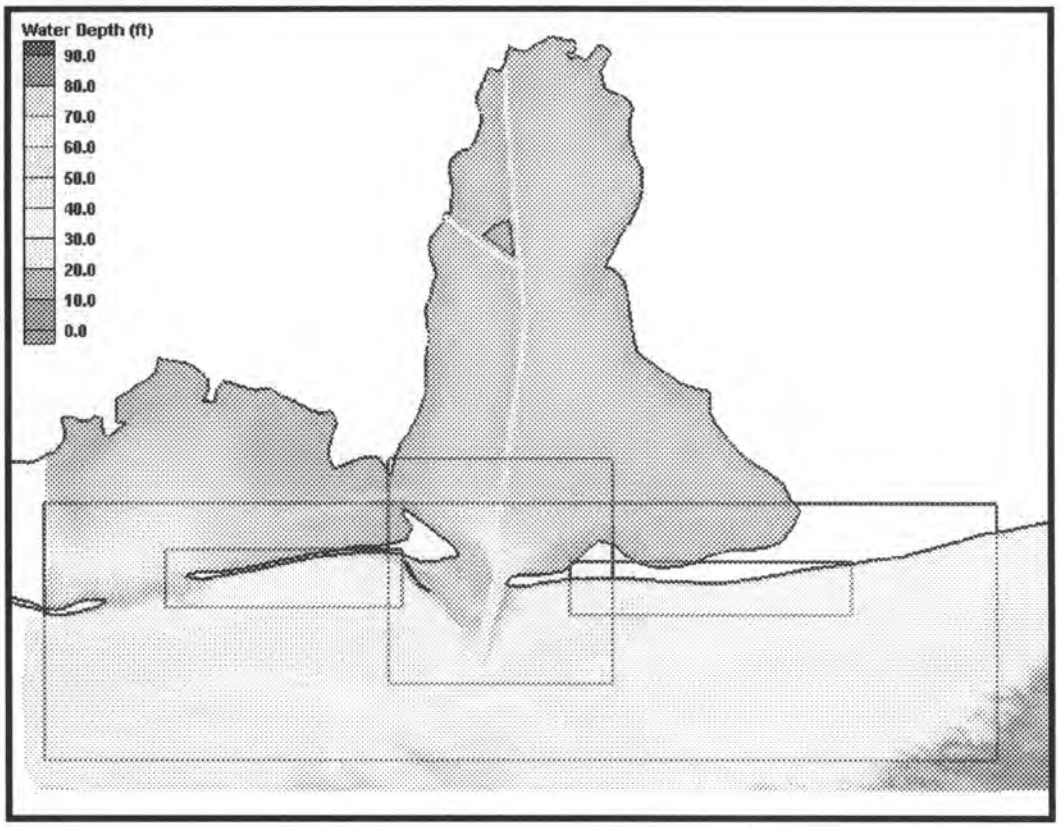

Figure 5-5. STWAVE bathymetry and model grid domains.

Table 5-1. Grid dimensions for offshore (coarse) and nearshore (fine) wave grids

	Cell Size	Grid Dimensions	Number of Water Cells	Typical Run Time (10 Wave Cases)
Coarse Grid	200 m x 200 m	430 rows x 115 columns	37,220	~11 min
West Fine Grid	25 m x 25 m	814 rows x 153 columns	88,888	~13 min
Center Fine Grid	50 m x 50 m	436 rows x 416 columns	167,970	~25 min
East Fine Grid	25 m x 25 m	1016 rows x 192 columns	138,182	~21 min

Bathymetry data were gathered from several sources and combined to provide a single data set which covered the study area. The offshore bathymetry is comprised of data collected in 1982/1988. All bathymetry along the ebb-tidal delta and within 3 miles of the Dauphin Island and Fort Morgan Peninsula shorelines was surveyed in 2002. Mississippi Sound and Mobile Bay bathymetry was taken from a 1960/1962 data set. Despite its age, this data set represents the most recent bathymetry covering Mobile Bay and Mississippi Sound. A detailed description of these data, including their original sources, datum adjustments applied, and other details can be found in Chapter 3.

Boundary Conditions. STWAVE input spectra were developed using a numerical routine that recreates a two dimensional spectrum for each individual wave condition in the WIS record, from 1980 to 1999. The program computes the frequency and directional spread of a wave energy spectrum based on significant wave parameters (i.e., wave height, peak period, and peak direction) and wind speed (Goda, 1985). The frequency spectrum $S(f)$ is computed using the relationship

$$S(f) = 0.257 H_{1/3}^2 T_{1/3} (T_{1/3} f)^{-5} \exp\left[-1.03 (T_{1/3} f)^{-4}\right] \tag{5.4}$$

known as the Bretschneider-Mitsuyasu spectrum, where $H_{1/3}$ is the significant wave height, f is the discrete frequency where $S(f)$ is evaluated, and $T_{1/3}$ is the significant period, estimated from the peak wave frequency (f_p) by

$$T_{1/3} = 1/(1.05 f_p). \tag{5.5}$$

To compute the two-dimensional energy spectrum, a directional spreading function $G(f,\theta)$ must be applied to the frequency spectrum such that

$$S(f,\theta) = S(f) G(f,\theta). \tag{5.6}$$

In this method, the directional spreading function is computed using the relationship

$$G(f,\theta) = G_o \cos^{2s}\left(\frac{\theta}{2}\right) \tag{5.7}$$

where s is a spreading parameter related to wind speed and frequency, θ is the azimuth angle relative to the principle direction of wave travel, and G_o is a constant dependent on θ and s. The spreading parameter s is evaluated using the expression

$$s = \begin{cases} s_{\max} \cdot (f/f_p)^5 : f \le f_p \\ s_{\max} \cdot (f/f_p)^{-2.5} : f \ge f_p \end{cases} \tag{5.8}$$

where $s_{\max} = 11.5(2\pi f_p U/g)^{-2.5}$. Wind speed U therefore to controls the directional spread of the spectrum by increasing the directional spread with increasing wind speed. Finally, the constant G_o is computed by evaluating the integral

$$G_o = \left[\int_{\theta_{\min}}^{\theta_{\max}} \cos^{2s}\left(\frac{\theta}{2}\right) d\theta \right]^{-1} \tag{5.9}$$

The result is a wave energy spectrum that is based on parameters from the WIS record, and that distributes spectral energy based on wave peak frequency and wind speed. An example of a two-dimensional spectrum generated by this method is presented in Figure 5-6.

After recreating a two-dimensional spectrum from the parameters given in the WIS record, each individual spectrum is sorted, or "binned", by peak direction and peak period. Wave spectra computed from wave parameters that occur within the limits of individual direction and period bins are added, and a mean spectrum for all waves in each bin is computed based on total number of wave events in the bin. In total, ten direction bins and one period bin were used to characterize wave data. These ten bins were selected based on percent occurrence and percent energy for conditions in each bin.

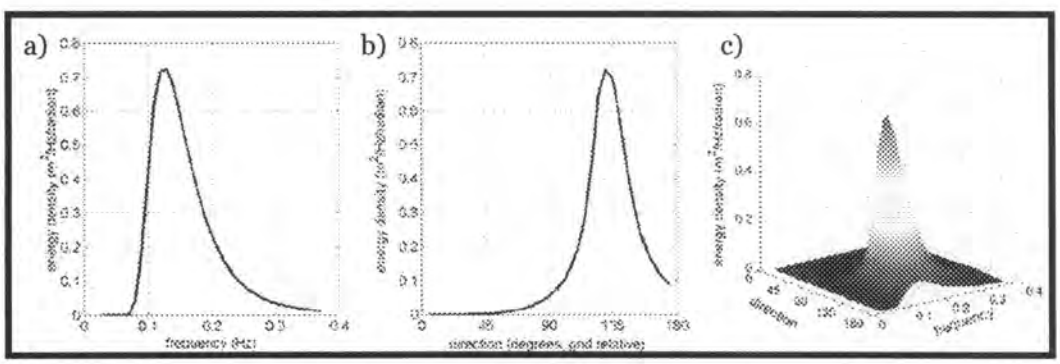

Figure 5-6. STWAVE input spectrum developed using WIS 20-year hindcast data with Goda (1985) method of computing frequency and direction spectrum. Plots show a) frequency distribution of energy at peak direction, b) directional distribution of energy at peak frequency, and c) surface plot of two-dimensional energy spectrum (H_{mo} = 0.9 m, θ_{mean} = 130 deg).

Selected conditions have a percent occurrence greater than 1%, and also contain more than 1% of the energy of the entire wave record. Conditions selected for the base model run are shown in Table 5-2, with the significant parameters of each input spectrum. The percent occurrence values do not add up to 100% as the WIS record reports waves which are traveling offshore. The waves accounted for in this work are only those which contribute energy to shorelines in the study area.

Table 5-2. Input wave spectra parameters used for 20-year average cases, WIS Station 156.

STWAVE Model Input Case	Percent Occurrence	H_{mo} Wave Height (ft)	Peak Wave Period, T_p (sec)	Peak Wave Direction, θ_p (deg true north)
1	10.81	3.2	5.9	105
2	4.75	3.2	5.9	130
3	10.72	2.9	5.9	145
4	12.49	4.1	6.7	160
5	9.27	4.9	7.7	170
6	4.53	4.2	6.7	185
7	3.30	3.4	6.7	200
8	2.17	2.9	5.3	215
9	1.76	3.1	5.9	230
10	5.18	3.2	5.3	260

Model Results. Results for the coarse grid were used to provide offshore boundary conditions for each of the 3 nested fine grids. However, a review of coarse wave results can provide an overview of the wave processes in the area and provide some guidance for what to look for in the nested grid results. Color contour and vector plots for Cases 5 and 10 are shown below in Figures 5-7 and 5-8 respectively. All wave modeling results are illustrated in Appendix H.

A larger energy event simulated in Case 5 (Figure 5-7) reveals significant wave breaking across the ebb shoal complex on both sides of the navigational channel at Mobile Pass. There is a significant sheltering effect provided by Pelican Island as well, where wave heights are reduced shoreward of the island. Some amount of shoaling can be seen across Dixie Bar while wave breaking again is seen across Petit Bois Pass to the west.

For the milder Case 10 results, there was a reduction of wave heights within Mobile Pass, but the strong gradient in wave heights denoting breaking is not seen here (Figure 5-8). There was a significant reduction in wave height between Pelican

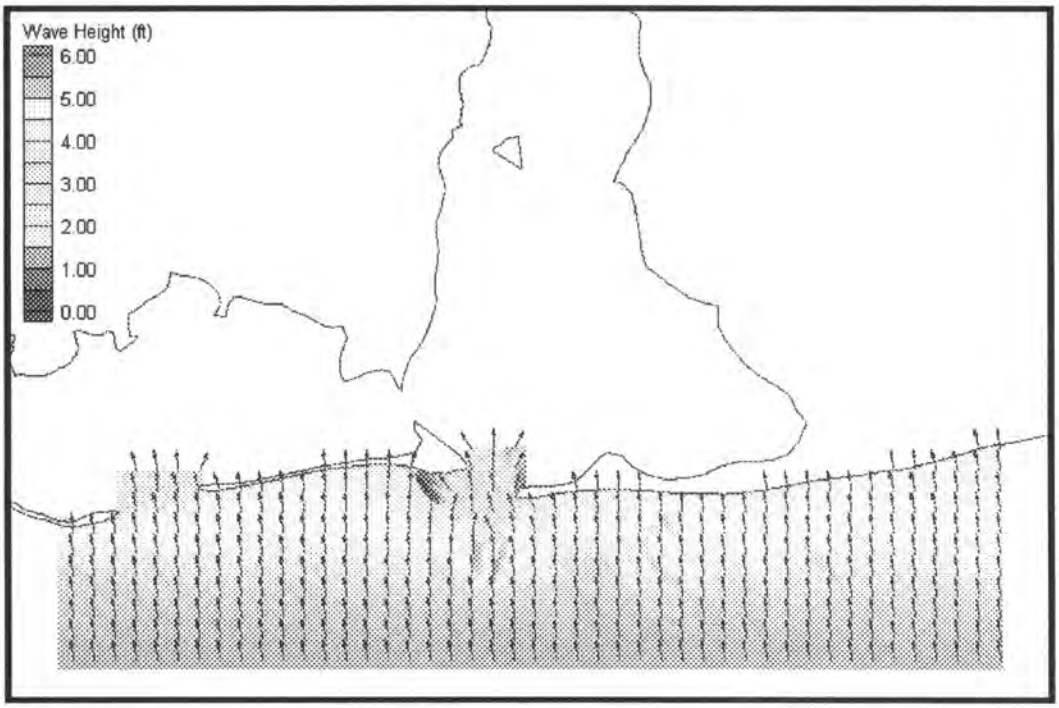

Figure 5-7. Coarse grid (200 m x 200 m) wave results for Case 5. Wave heights are shown by color while wave direction is indicated by the arrow direction.

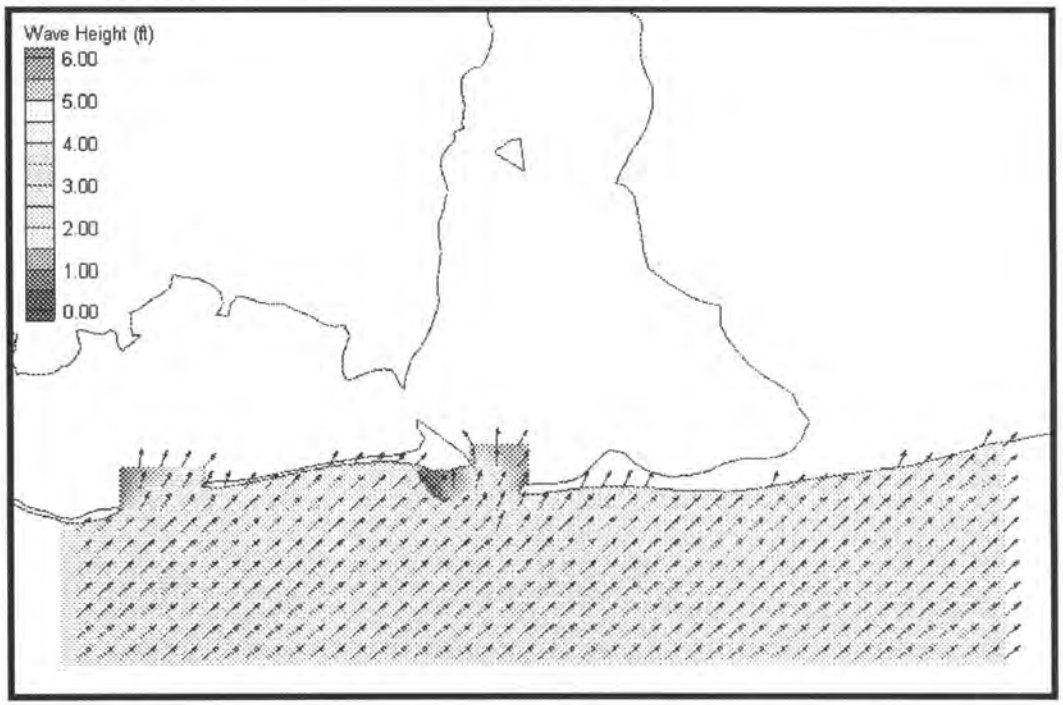

Figure 5-8. Coarse grid (200 m x 200 m) wave results for Case 10. Wave heights are shown by color while wave direction is indicated by the arrow direction.

Island and Dauphin Island. Wave propagation over the ebb-shoal complex and Dixie Bar appear to refract wave energy away from the western end of the Fort Morgan Peninsula, resulting in an area of somewhat reduced wave heights immediately east of Mobile Pass. There is little to no wave breaking at Petit Bois Pass for these smaller waves incident from the southwest.

In both cases it was observed that nearshore wave heights and directions along open coastal areas, such as central Dauphin Island and Fort Morgan Peninsula, were refracted normally as they approach the shoreline. In the absence of significant bathymetric features, these regions of the wave solution showed no drastic changes in wave height or direction.

Fine grid model results for Dauphin Island are shown for Cases 5 and 10 in Figures 5-9 and 5-10, respectively. The results for Case 5 show wave breaking at both ends of the grid. At the western end of the island, the shoal extending into Petit Bois Pass has a strong influence on wave heights and directions. At the east end of the model grid, the shoal extending between Pelican Island and Dauphin Island also causes these larger waves to break. Throughout the center portion of Dauphin Island, there is normal wave refraction, as expected. It is notable that along this section of the shoreline, waves from Case 5 are almost shore-normal adjacent to the shoreline. This fact serves to illustrate that shoreline orientation of the central portion of the island has adjusted to become perpendicular to the most significant direction of wave energy. As such, sediment transport predictions based on these results will be sensitive to wave angle for these high-energy contributions.

Wave results for Case 10 along Dauphin Island show little variation. Again the shoal at the west end of the island is causing wave refraction, but breaking observed in the higher energy waves from the southeast is absent (Figure 5-10). For the majority of the model domain, waves are seen to continue their refraction as they approach the shoreline, with breaking observed immediately adjacent to the beach.

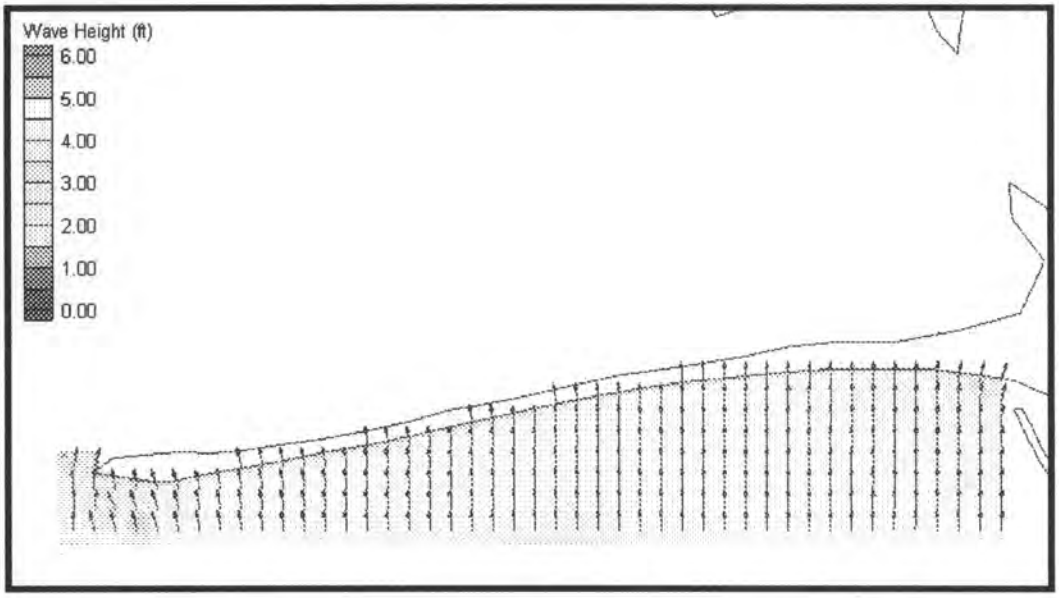

Figure 5-9. Fine grid (25 m x 25 m) wave results for Case 5, Dauphin Island. Wave heights are shown by color while wave direction is indicated by arrow direction.

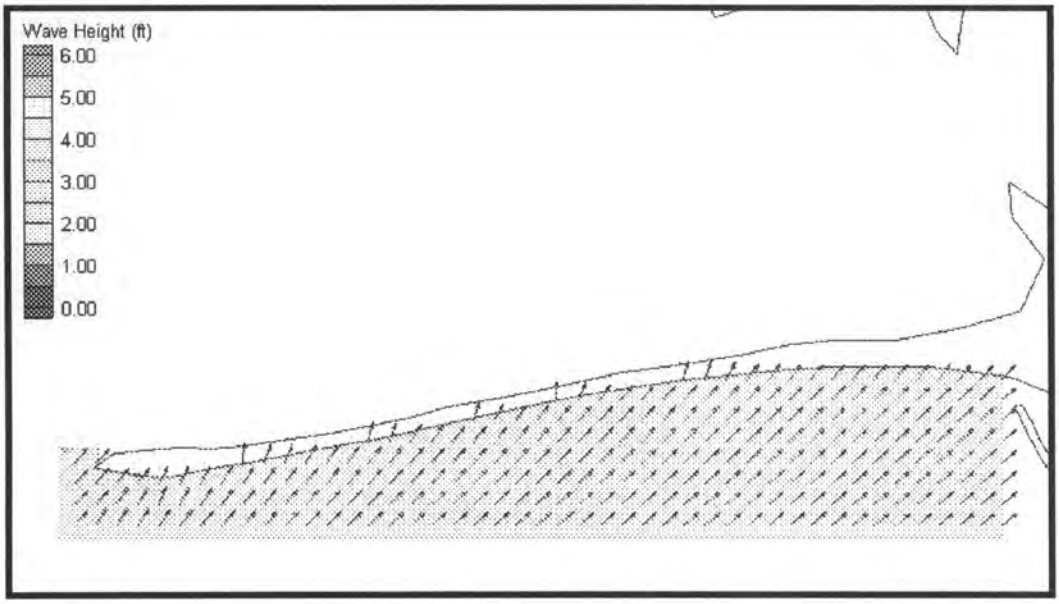

Figure 5-10. Fine grid (25 m x 25 m) wave results for Case 10, Dauphin Island. Wave heights are shown by color while wave direction is indicated by arrow direction.

Detailed wave results for Mobile Pass are shown in Figures 5-11 and 5-12. For Case 5 (Figure 5-11), the ebb-shoal complex dominates wave transformation seaward of the inlet. Wave steepening and breaking are observed along the outer edge of the ebb-tidal delta on either side of the navigation channel. The sheltering effect of Pelican

Island is apparent while there is strong refraction in the lee of the island, with waves traveling to the west. Inside the inlet, there is diffraction of wave energy as expected. The navigational channel within Mobile Bay promotes wave refraction to the east slightly, resulting in a decrease in wave height along the main channel.

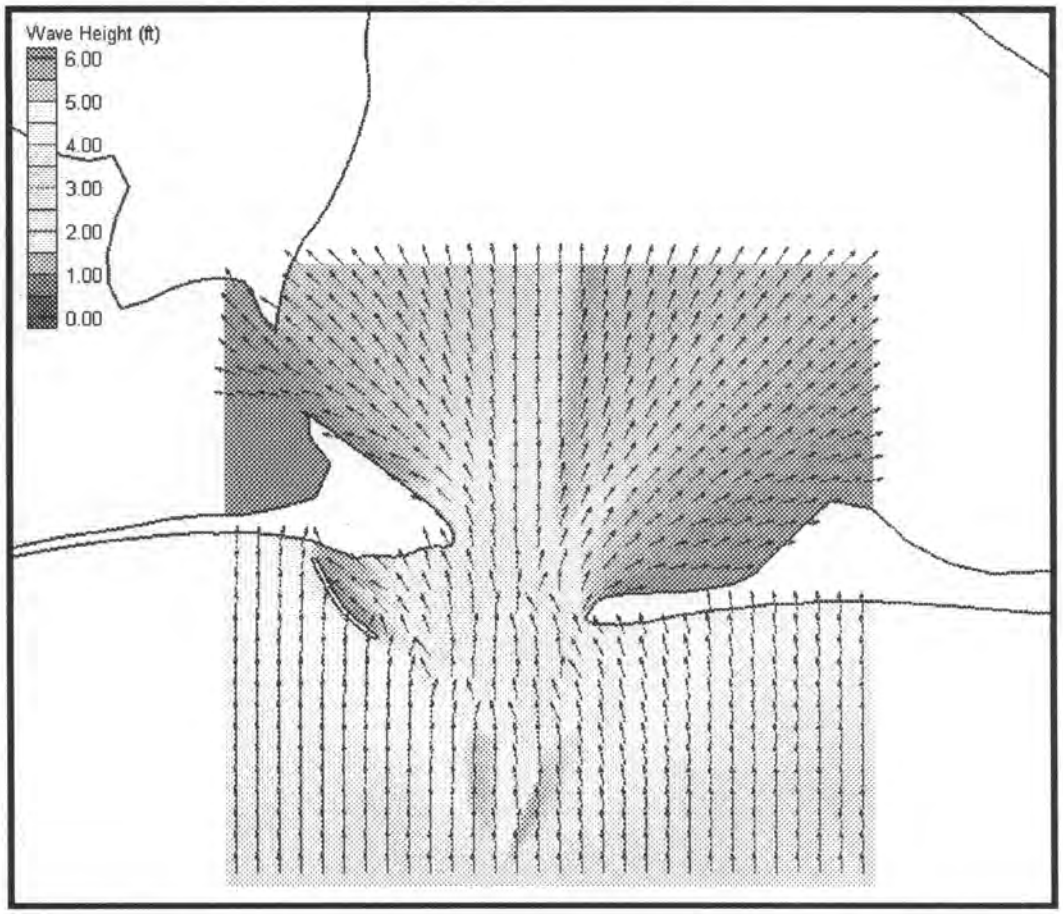

Figure 5-11. Fine grid (50 m x 50 m) wave results for Case 5, Mobile Pass. Wave heights are shown by color while wave direction is indicated by the arrow direction.

The smaller energy event modeled in Case 10 (Figure 5-12) shows some wave steepening over the ebb shoal but there is not the strong breaking that was illustrated in Case 5. Wave sheltering of Pelican Island is broader for these waves from the southwest, while refraction behind the island again orients the waves strongly to the west. The similarity of wave directions in the lee of Pelican Island for two different incident wave conditions serves to highlight the major influence the ebb-shoal complex has on wave transformation in the area, regardless of offshore conditions. Within the inlet itself, normal diffraction is observed. The influence of the

navigational channel is still evident, although the difference in wave height caused by wave refraction at the channel is smaller than in Case 5.

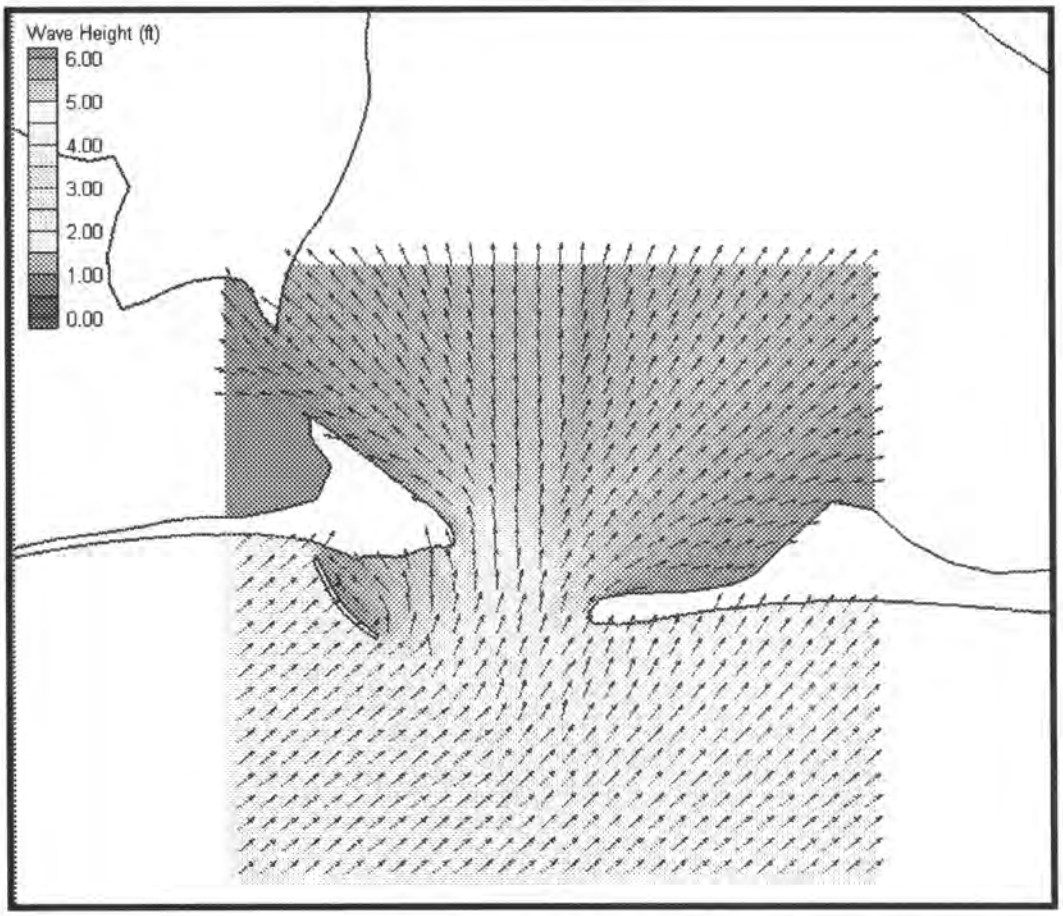

Figure 5-12. Fine grid (50 m x 50 m) wave results for Case 10, Mobile Pass. Wave heights are shown by color while wave direction is indicated by the arrow direction.

Figure 5-13 shows the results for Case 5 along Morgan Peninsula. Waves at the edge of the grid are almost shore normal, and there is little change in direction as the waves propagate towards the shoreline. The influence of Dixie Bar is seen in more detail here, with some wave steepening evident across the shoal. There is little wave refraction associated with the shoal in this case as the waves are essentially perpendicular to shoal orientation.

For waves from the southwest (Figure 5-14), Dixie Bar can be seen to have some influence on wave directions. There is a small gradient in wave height along the edge of the shoal, where waves traveling along the shoal are refracted to the east, whereas those waves which pass to the west of the shoal continue to the shoreline unaffected.

Aside from this slight focusing of wave energy, wave transformation along this stretch of open coast is typical of what is expected.

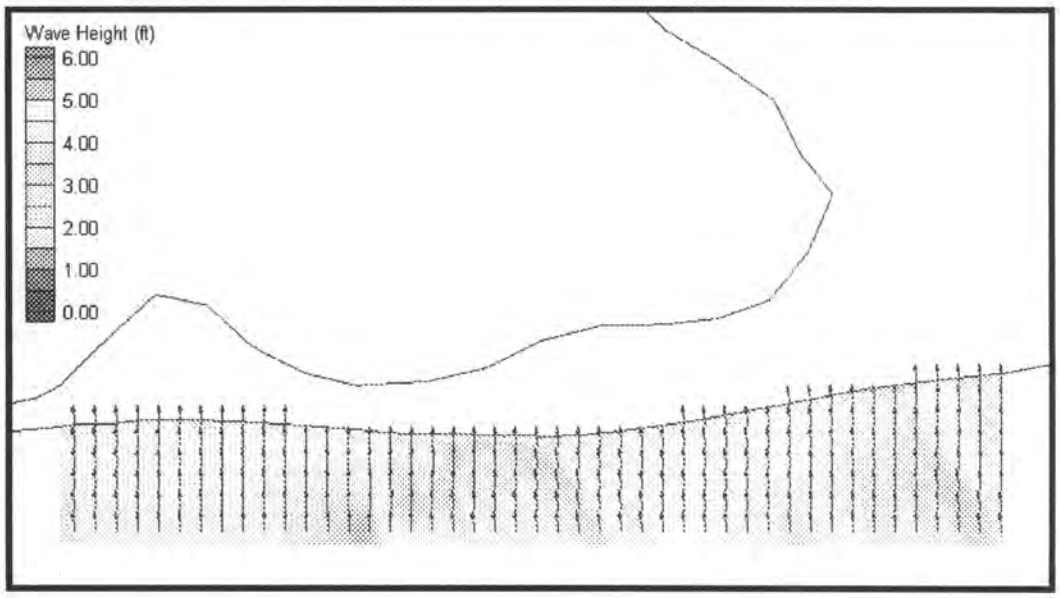

Figure 5-13. Fine grid (25 m x 25 m) wave results for Case 5, Morgan Peninsula. Wave heights are shown by color while wave direction is indicated by the arrow direction.

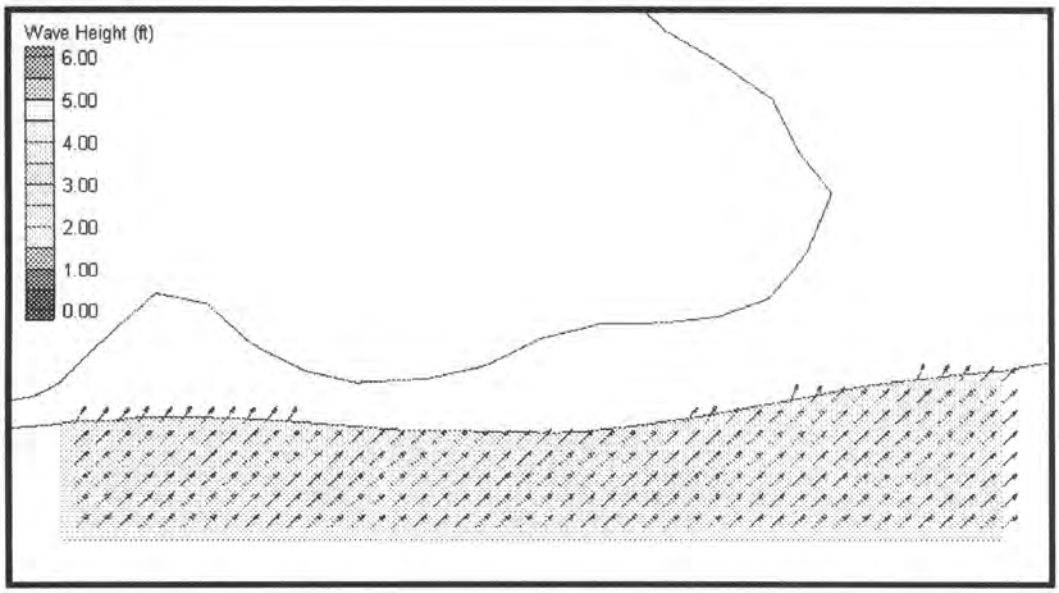

Figure 5-14. Fine grid (25 m x 25 m) wave results for Case 10, Morgan Peninsula. Wave heights are shown by color while wave direction is indicated by the arrow direction.

Longshore Sediment Transport Potential

Overview of Regional Sediment Transport Processes. Nearshore sediment transport is a complex process, which governs erosion and accretion of beaches. Sediment is moved alongshore and cross-shore (on and offshore) by physical coastal processes, such as wind, waves, tides, currents, and sea-level rise. The time scales of sediment transport and shoreline change vary from the initial formation of headlands and coasts on geologic time scales (thousands of years) to severe coastal erosion over a few days or hours during tropical storms and hurricanes.

In addition to physical coastal processes, sediment transport patterns are dependent upon the characteristics and sediment supply. Grain size is the most important characteristic of the sediment. The quantity of sediment moved is inversely proportional to its grain size. Sediment transport rates decrease with increasing grain size, because heavier sediment requires more time and energy to be mobilized and transported. Sediment density, durability, and shape also affect transport rates. In addition, the supply of sediment governs sediment transport rates, because transport rates are reduced where sediment is in short supply (e.g. along armored shorelines).

When waves break at an angle to the beach, alongshore-directed currents are generated, capable of lifting and moving sediment along the coast. For example, waves approaching the Gulf Shores shoreline from the east tend to move sand alongshore from east-to-west towards Mobile Pass. Because wave direction changes frequently, sand is moved back-and-forth along the beach. On an annual basis, however, there typically is a dominant wave direction that occurs most frequently on seasonal time scales.

Determination of Longshore Sediment Transport Potential. To estimate typical values of longshore sediment transport potential along Dauphin Island and Morgan Peninsula, wave modeling results were used to calculate the maximum quantity of sand transport possible based on a sediment-rich environment. Results from the spectral wave modeling formed the basis for quantifying changes in sediment transport rates along the beach because wave-induced transport is a function of wave breaker height, wave period, and wave direction. Longshore transport depends on long-term fluctuations in incident wave energy and the resulting longshore current. Therefore, annual transport rates were calculated from long-term wave statistics.

In general, the longshore sediment transport rate is proportional to longshore wave energy flux at the breaker line, which is dependent on wave height and direction.

Because the transport equation was calibrated in sediment-rich environments, it is typically considered an upper bound for sediment transport rates. However, it provides a useful technique for comparing erosion/accretion trends along a shoreline of interest and for comparing relative magnitudes along different sections of the shoreline.

Longshore Sediment Transport Calculations. The volumetric longshore sand-transport rate, Q_ℓ, past a point on a shoreline is computed using the relationship:

$$Q_\ell = \frac{I_\ell}{(s-1)\rho g a'} \qquad 5.10$$

where I_ℓ is the immersed-weight longshore sand-transport rate, s is the specific gravity of the sediment, a' is the void ratio of sediment, g is the acceleration of gravity, and ρ is the density of seawater.

This study estimates the value of I_ℓ as described by Kamphuis (1990). This approach includes a dependency on median grain diameter of beach sand (d_{50}) and the surf similarity parameter (Irabarren number), ξ_b, which is expressed as

$$\xi_b = \frac{m}{(H_b / L_0)^{0.5}} \qquad 5.11$$

where m is the bottom slope, H_b is the wave-breaker height, and L_0 is the incident deep-water wave length. The complete expression from Kamphuis (1990) is given by

$$I_\ell = K^* \rho g \left(\frac{g}{2\pi}\right)^{0.75} \xi_b T^{0.5} (m d_{50})^{-0.25} H_s^{2.5} \sin^{0.6}(2\theta_b) \qquad 5.12$$

where the coefficient $K^* = 0.0013$, T is the wave period, H_s is the significant wave height, and θ_b is the wave angle of approach to the shoreline at breaking.

Sediment transport computations were based on wave height, period, and direction at breaking for each grid cell along the modeled coastline. The wave model grids provided the basis for determining shoreline orientation. Computations of sediment transport rates for each of the 10 wave cases listed in Table 5-2 was performed and then weighted by the annual percentage occurrence.

Longshore Sediment Transport Modeling Results. Figure 5-15 illustrates calculated net and gross transport rates predicted for the Dauphin Island and Morgan Peninsula shorelines. Positive values indicate transport from west to east, whereas westerly directed transport is given a negative value. Gross easterly transport is shown as a blue dashed line, gross westerly transport is shown as a red dashed line, and the net transport is a solid black line.

Initial model results for Dauphin Island showed a portion of the island having net easterly directed transport. Although certain storm or even seasonal scale conditions may cause temporary reversals in transport direction, the current analysis shows the composite effect of 20 years. With the morphological data indicating unequivocally that the net direction of transport along Dauphin Island is to the west, a closer look at model results was merited.

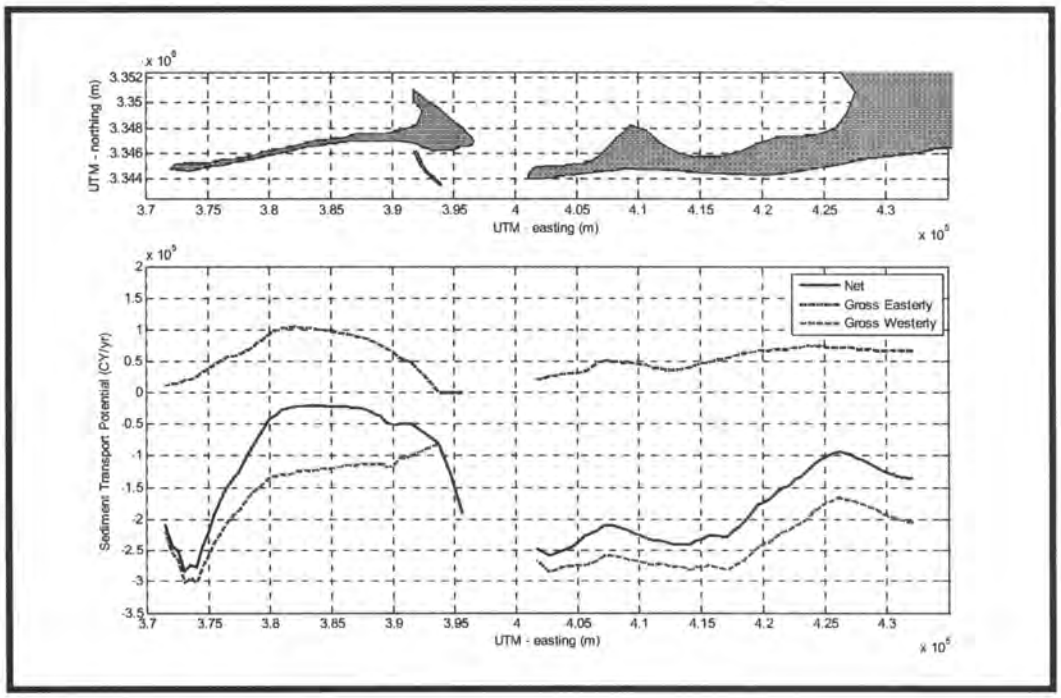

Figure 5-15. Longshore sediment transport potential along Dauphin Island and Morgan Peninsula. Net transport is indicated by a solid black line. Easterly transport is shown as dashed blue, and westerly transport is shown in dashed red.

A sensitivity analysis of model results illustrated that the most influential wave cases from the 20 year composite record (Cases 3, 4, and 5) were essentially shore-normal at breaking along the central portion of Dauphin Island. This is a result of wave refraction caused by nearshore bathymetry and shoreline orientation. As a result, sediment transport calculations were found to be extremely sensitive to wave angle

along this section of the shoreline. Therefore, a minor change in incident wave direction can alter the net direction of transport.

As discussed above, the wave direction reported in the WIS data was found to contain some uncertainty. The analysis discussed in Tracy (1999) revealed that average bounds on the 95% confidence interval were approximately ±8 deg. This uncertainty in the data used to drive the wave model, together with an understanding of the physical processes suggested that an adjustment to the nearshore wave angles may be warranted. Because the evaluation of Dauphin Island morphology indicates relatively strong east-to-west transport along the western two-thirds of the island, wave angles at breaking were adjusted to reflect observations in longshore sediment rates. A rotation of 3 deg to the west was required to reconcile trends in sediment transport prediction with our understanding of net physical processes on Dauphin Island. The 3 deg shift was applied to all wave cases for each of the three model domains. The results discussed below include this alteration of wave angle within the study region.

Overall trends indicate a dominance of west-directed transport. At the eastern edge of the calculation domain, around UTM 426,000 (approximately 15 miles east of Mobile Pass), westerly transport is about twice the rate of easterly transport, and the net value is approximately 125,000 cy/year to the west. The transport rate steadily increases from ~125,000 cy/year at UTM 426,000 to ~240,000 cy/year at UTM 416,000. This increase is due primarily to a gradual change in shoreline orientation, where dominant energy from the southeast arrives with an increasing angle to the shoreline and nearshore bathymetry contours. The western tip of Morgan Peninsula sees a relatively constant transport rate between 200,000 and 250,000 cy/year.

Directly west of Mobile Pass, the net longshore transport rate is approximately 100,000 to 150,000 cy/year to the west. Of note in this section is the absence of easterly transport. This is due to strong wave refraction over the ebb-tidal delta, which results in redirection of waves to the west, regardless of offshore direction. Transport rates decreased in the lee of Pelican Island due to decreased wave heights in this protected area. Central portions of Dauphin Island show transport in both directions to be in the range of 100,000 cy/year, with resulting net transport slightly biased to westerly transport at a rate of ~25,000 cy/year. As discussed earlier, sand transport predictions for this section of island are sensitive to incident wave direction due to shoreline orientation and wave refraction resulting from nearshore bathymetry. At the western end of Dauphin Island (approximately UTM 375,000), incident waves are increasingly directed to the west and the shore-normal angle is gradually shifting from southeast facing (perpendicular to the most energetic wave

conditions) to south facing. Both of these changes result in increased sand transport potential toward the western end of Dauphin Island. Transport rates increased from ~50,000 cy/year at UTM 380,000 to ~270,000 cy/year at UTM 374,000. At the western end of the island, transport rates dropped slightly towards 200,000 cy/year as a result of wave refraction over the shoals of Petit Bois Pass.

Hydrodynamic Modeling

Field Data Collection. Some recorded water levels and flow rates are required to calibrate hydrodynamic modeling. There are existing USACE tide recording stations in the region, each of which has been operational for various periods of time. Unfortunately, there are presently no verified tide recording stations in eastern Mississippi Sound. Together with Mobile Pass, Mississippi Sound serves to transmit water to and from Mobile Bay, and its functioning is important to understanding the hydrodynamics of the region.

Tide Data. To ensure proper data coverage for the modeling effort, a tide gauge was placed in Mississippi Sound in early November 2006. The tide gauge used for this deployment was a Brancker TGR-2050. The instrument was secured to a 10 ft long 2x4 wood beam which was attached to a day marker in the Sound using lag bolts. The instrument was placed as far into the water column as possible. Permission from the U.S. Coast Guard to attach the instrument to the navigational aid had been granted prior to the installation. Data sampling was set for 10-minute intervals, with each 10-minute observation resulting from an average of 16 1-sec pressure measurements. This instrument uses a strain gauge transducer to sense variations in pressure, with resolutions on the order of 1 cm head of water. The gauge was calibrated prior to installation to assure accuracy, and it returned 100% of the desired data.

Once data were downloaded from the instrument, pressure readings were corrected for variations in atmospheric pressure. Hourly atmospheric pressure readings were obtained from the Dauphin Island meteorological station, interpolated to 10-min intervals, and subtracted from the pressure readings. The readings were then converted from pressure units (psi) to head units (for example, feet of water above the tide gauge). After installation, staff from the Irvington Field Office of the USACE, Mobile District, surveyed the elevation of the 2x4 to provide a basis for vertical rectification of the water level. The result from this analysis was a time series record representing variations in water surface elevation in Mississippi Sound relative to NAVD88 (Figure 5-16).

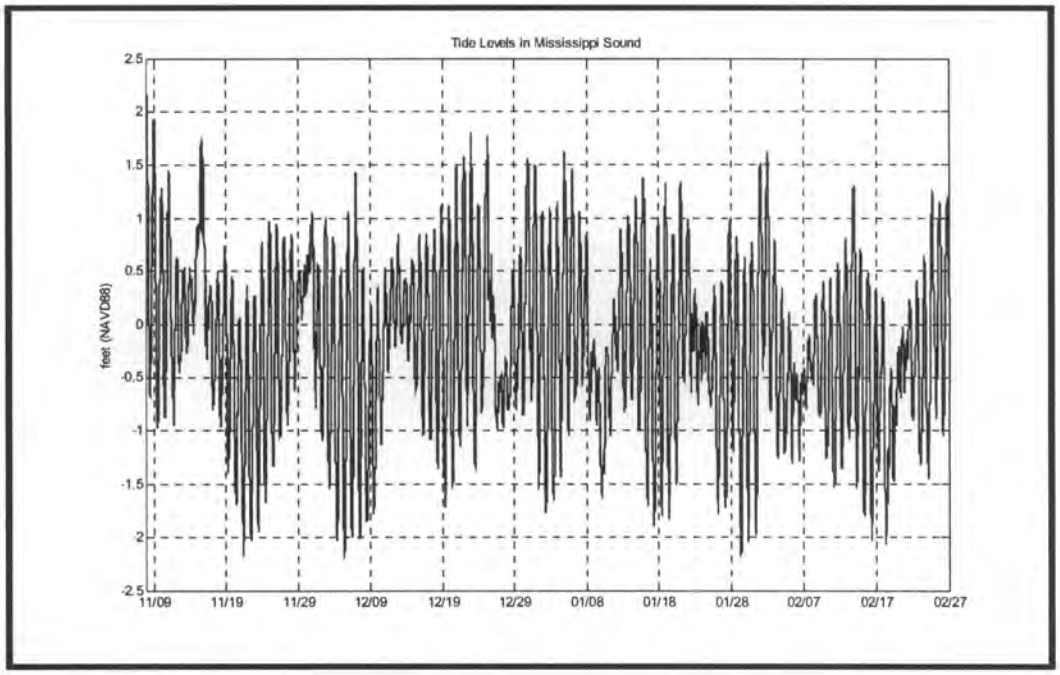

Figure 5-16. Tide data recorded in Mississippi Sound. Elevations are in feet NAVD 88.

Initial plans for field installation called for a 30-day deployment of the tide gauge, followed by a 2-day survey of tidal currents, and then recovery of the instrument. However, due to the pattern of winter weather in the region, the field schedule was delayed for months. The survey and recovery planned for mid-December was not completed until the end of February.

It should be noted that during field deployment of the Mississippi Sound gauge in November 2006, a second tide gauge was installed within Bon Secour Bay. It was also attached to a 2x4 wood beam which was secured to the outside of a day marker along the inter-coastal waterway. Upon arriving at the installation location in February for recovery, neither the 2x4 beam nor the instrument was found.

Tide data from the field deployment in Mississippi Sound, together with data from the Middle Bay Light station and the Exxon Well gauging station, provided excellent tidal information surrounding Mobile Pass. The location of these 3 stations is shown in Figure 5-17.

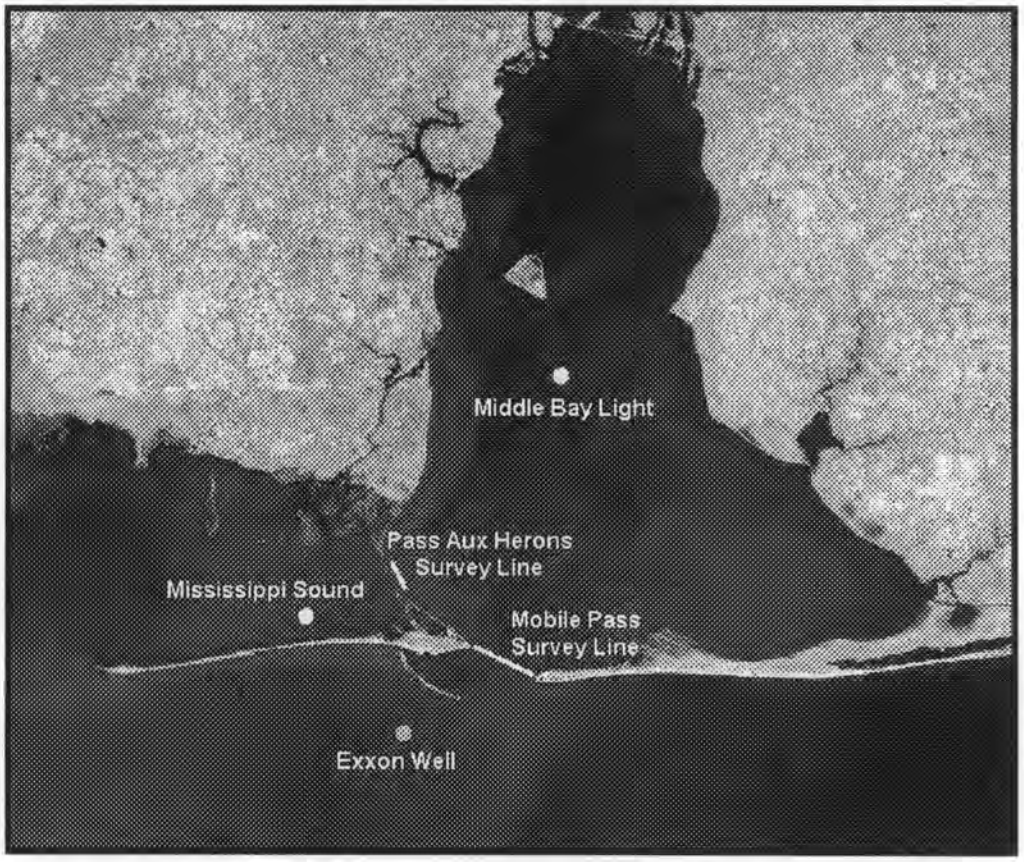

Figure 5-17. Three tide recording stations used to calibrate the hydrodynamic model. Two ADCP survey lines are shown in yellow.

ADCP Survey. In addition to the time series of water levels in the area, details of flow in and out of Mobile Bay were also integral for developing an understanding of the hydrodynamics in the area. A 2-day survey of tidal currents was undertaken to provide some understanding of flow patterns in the area. Figure 5-17 shows the location of the two survey lines.

Water velocity measurements were obtained with a BroadBand 1200-kHz Acoustic Doppler Current Profiler (ADCP) manufactured by RD Instruments (RDI). The ADCP was mounted to a specially constructed mast, which was rigidly attached to the rail of the survey vessel. The ADCP was oriented to measure downward into the water column, with the sensors located approximately 2 ft below the water surface. The mounting technique assured no flow disturbance due to vessel wake.

Geographic coordinates was recorded with a stand-alone global positioning system (GPS) relative to the 1984 World Geodetic System (WGS-84) datum. The GPS antenna was mounted at the top of the ADCP boom directly over the instrument.

Both ADCP and GPS data were recorded in WinRiver (®RD Instruments), an integrated ADCP and navigation software package running on a PC laptop computer, to provide an accurate position for each backscatter and velocity measurement. Data recording for each survey transect was started, ended, and recorded using the laptop and WinRiver to interface with the ADCP. Because the ADCP uses bottom tracking to correct real-time measurements, several potential error sources affecting the motion-corrected ADCP velocities are eliminated automatically. Fong and Monismith (2004) found this bottom tracking technique to yield a maximum error in measured velocity of less than 6%.

Current surveys of Mobile Pass and Pass aux Herons were performed on 26-27 February 2007, respectively. Because tides in the area are diurnal, a typical survey day of 12-14 hr recorded only a single stage of tide. In this case, both surveys captured the tail end of the ebbing tide, slack water, and then a majority of the flooding tide. The survey line for Mobile Pass ran from the eastern end on Dauphin Island to Mobile Point. The survey line across Pass aux Herons ran parallel to the causeway bridge on its east side. Figures 5-18 and 5-19 illustrate color contour plots of velocities during maximum flood conditions.

Figure 5-18 indicates an enormous volume of water moving through Mobile Pass during flood tide. Velocities of 5 ft/sec are observed to extend from near the surface to depths greater than 25 ft. A majority of flow is sharply contained within the navigational channel. The main channel carries 481,000 cfs which accounts for 76% of the total flow entering the inlet.

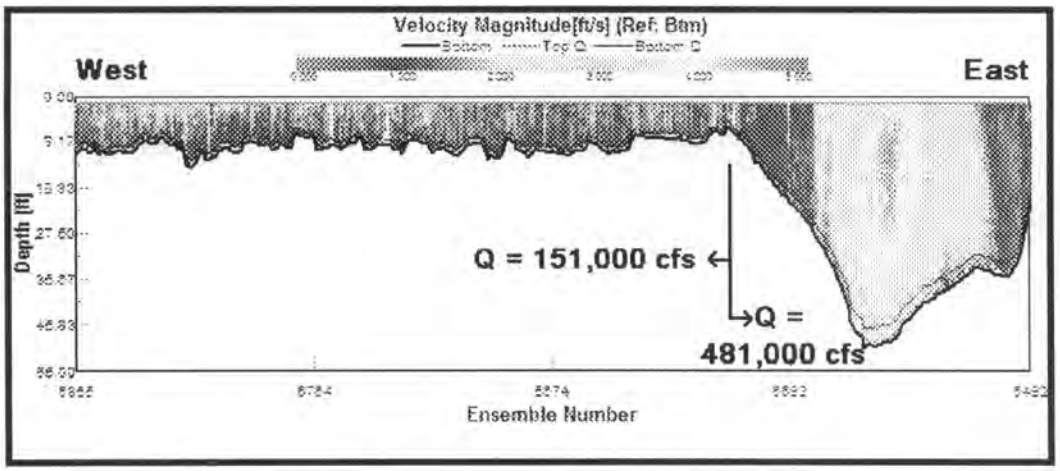

Figure 5-18. Color contour plot of velocities in Mobile Pass during maximum flood tide conditions.

Flows observed in Pass aux Herons (Figure 5-19) are notably smaller. The inter-coastal waterway channel at the right of the figure conveys a majority of the flow. A small unmarked channel approximately 1 mile north of the navigation channel also contributes.

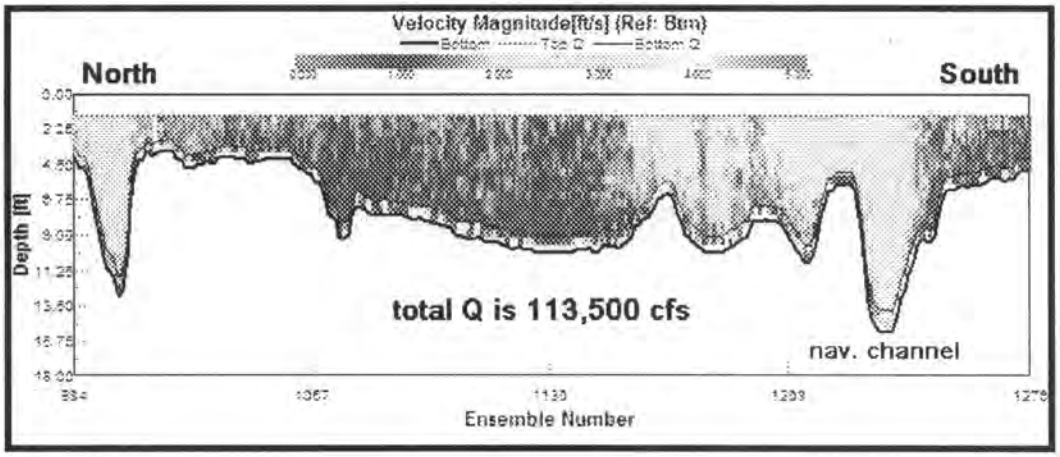

Figure 5-19. Color contour plot of velocities in Pass aux herons during maximum flood tide conditions.

A comparison of the two surveys shows that flow rates entering Mobile Pass on these flood tides was approximately 745,500 cfs, with Mobile Pass contributing 85% of the total and Pass aux Herons accounting for 15%. These quantities are consistent with flow partitioning reported by Isphording et al. (1996).

ADCIRC. A regional hydrodynamic model for the entire Gulf of Mexico was run, using the Advanced Circulation Model for Oceanic Coastal and Estuarine Waters (ADCIRC). ADCIRC is a two-dimensional, depth-integrated circulation model (Westerink et al., 1994). The model domain is described by a collection of finite elements which give the model excellent flexibility to cover both large domains as well as provide the required detail for areas where strong flow variations are expected. Computational features of ADCRIC include variable coriolis forcing, wetting and drying, choice of bottom stress model, and detailed user control over model output.

Model Domain. The ADCIRC model domain for the Gulf of Mexico is illustrated in Figure 5-20. Land boundaries are shown in brown, islands in green, and the open boundaries are in navy blue. The model was forced at 2 open boundaries. The first boundary runs across the Straight of Florida, between the Florida Keys and Cuba. The second open boundary runs from Belize (south of the

Yucatan Peninsula) north to the southern coast of eastern Cuba. The final model grid contained 58,685 nodes and 112,339 elements.

Boundary Conditions. ADCIRC allows various forcing options for driving flow in the model, including a time series of water-surface elevation, tidal constituents, a time series of flow rates, as well as wind stress and atmospheric pressure. For the current study, tidal constituent forcing was applied to the open boundaries, and tidal potential forcing was applied to the interior of the domain. Freshwater inflow at the north end of Mobile Bay was also included.

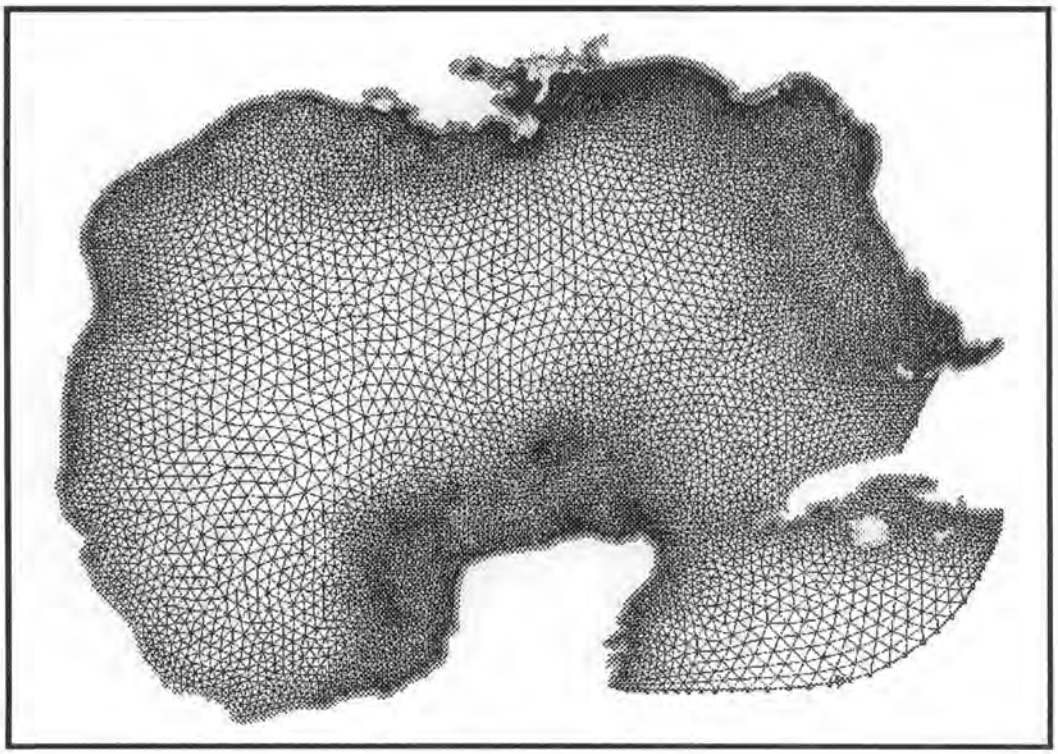

Figure 5-20. ADCIRC model domain for the Gulf of Mexico. The two open boundaries are shown in navy blue, land boundaries are in brown, and islands are in green.

The tidal constituent values for the 2 open boundaries were extracted from the existing Western North Atlantic, Gulf of Mexico, and Caribbean Sea Tidal Database (Mukai et al., 2001). This provided constituent data for the M2, S2, N2, K1, O1, Q1, P1, K2, M4 and M6 components of the tide.

Atmospheric pressure changes and local winds have a significant influence on water levels within the study area. The relatively shallow offshore shelf and shallow water within Mobile Bay suggest that atmospheric forcing can often result in changes in

water level that are similar in magnitude as astronomical tides. However, these atmospheric forcings were not included in the present study. The amount of data required to properly include these aspects into the modeling effort was beyond the scope of work.

Freshwater inflow for the Mobile and Tensaw Rivers was included at the northern extent of Mobile Bay. Flow rate data were taken from the USGS gauging stations for each river (USGS, 2007).

Model Calibration. The primary purpose for running the regional hydrodynamic model was to provide a time series of water surface elevation to serve as a boundary condition for detailed CMS-M2D morphology modeling. Field data used to evaluate model results were taken from the Middle Bay Light gauging station, tidal records from the Exxon Well offshore of Mobile Pass, and the tide gauge deployed in Mississippi Sound in support of this work. Model mesh and bathymetry, as well as the locations of field data stations, are shown in Figure 5-21.

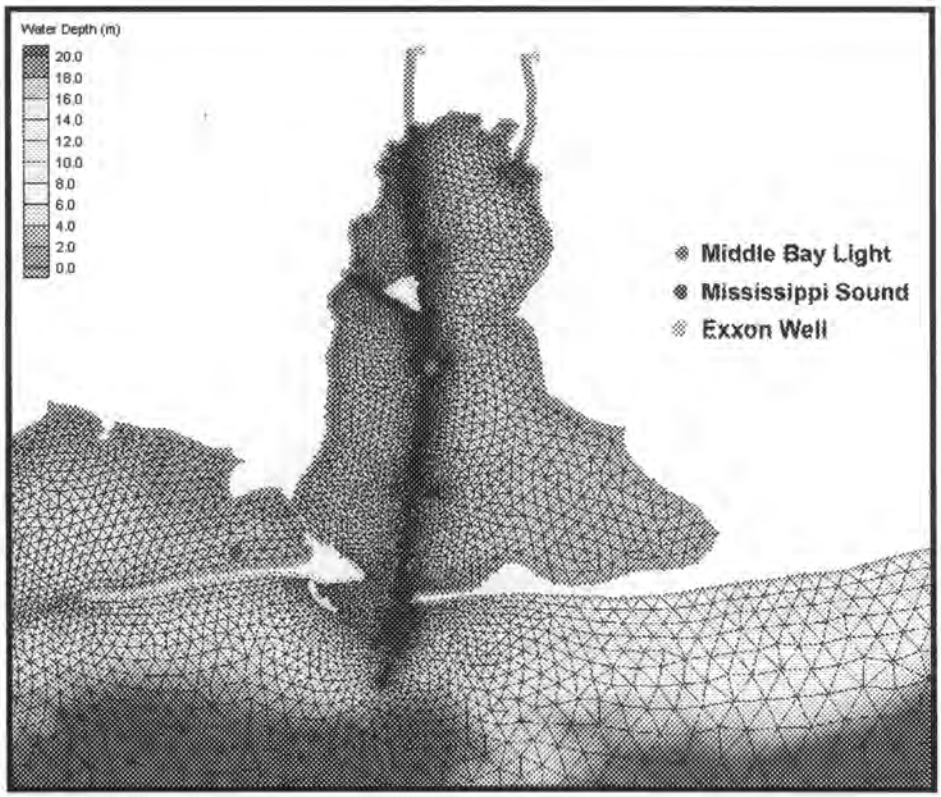

Figure 5-21. Detail of the ADCIRC domain focused on Mobile Bay and Mississippi Sound. Bathymetry contours are shown in color along with the model mesh for this region. Mobile and Tensaw River inflow portions of the mesh can be seen at the north end of Mobile Bay. Three tidal recording stations used to calibrate the model are also shown.

To limit the influence of the atmospheric signal in field data, the tidal record was searched for a period which had no storms and relatively low winds. Seeing as the field deployment was during the winter, such a period of time was difficult to identify. Ultimately the period from December 15 – 22, 2006 was chosen to evaluate the hydrodynamic model.

All runs commenced on December 12, providing 3 days of run time prior to the period of interest. Plots of recorded versus modeled water levels are shown in Figures 5-22, 5-23, and 5-24 for the Exxon Well, Mississippi Sound, and Middle Bay Light, respectively.

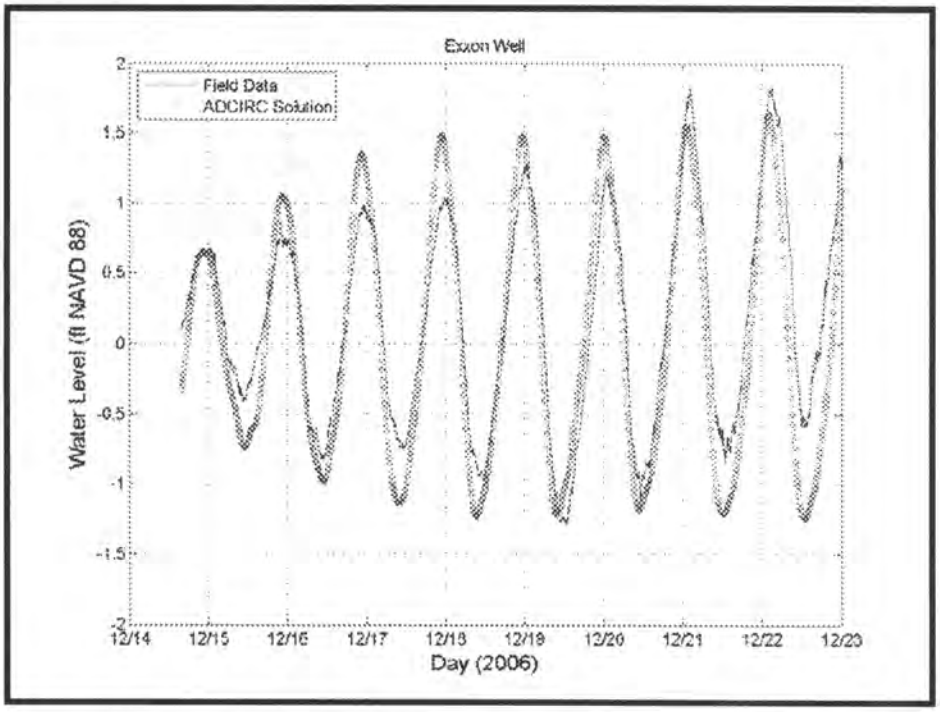

Figure 5-22. Comparison of modeled water levels with measured data for the Exxon Well, December 15, 2006 to December 23, 2006.

Results showed varying degrees of agreement between modeled and measured water levels. Model results offshore Mobile Pass at the Exxon Well (Figure 5-22) tend to show a slightly larger tide range than present in field data. The largest error was 6 inches on the high tide of December 17. Starting mid-day December 21, field data showed a departure from mean tide level of the previous week. This suggested that an atmospheric event was starting to have an influence on measured water levels, bringing them farther out of agreement with model results for those days. In general the phase is reproduced well. Model results lag field data by about 30 minutes.

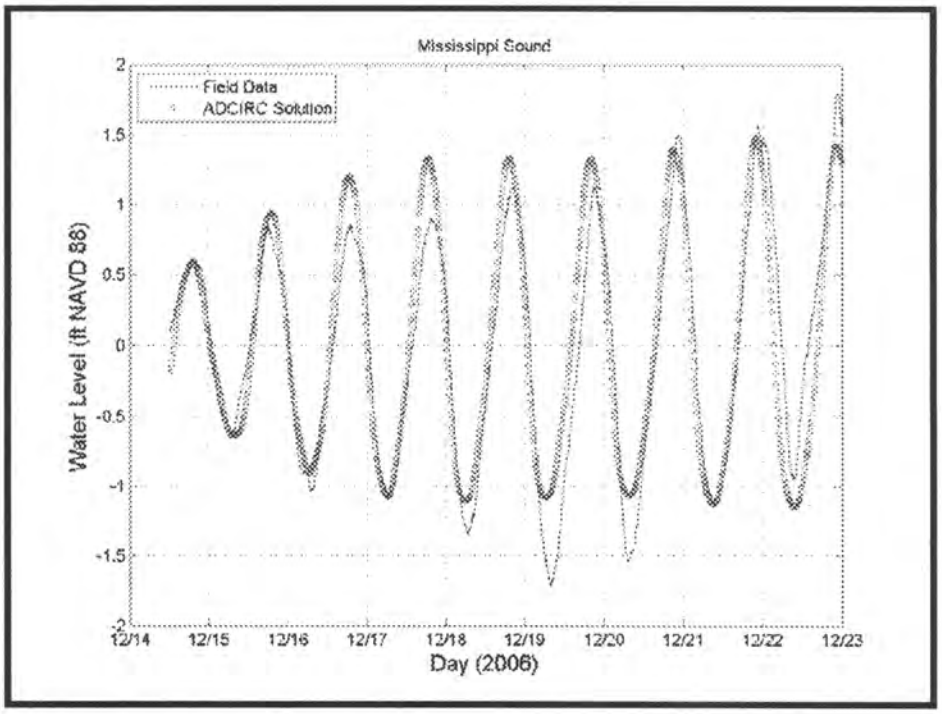

Figure 5-23. Comparison of modeled water levels with measured data for Mississippi Sound, December 15, 2006 to December 23, 2006.

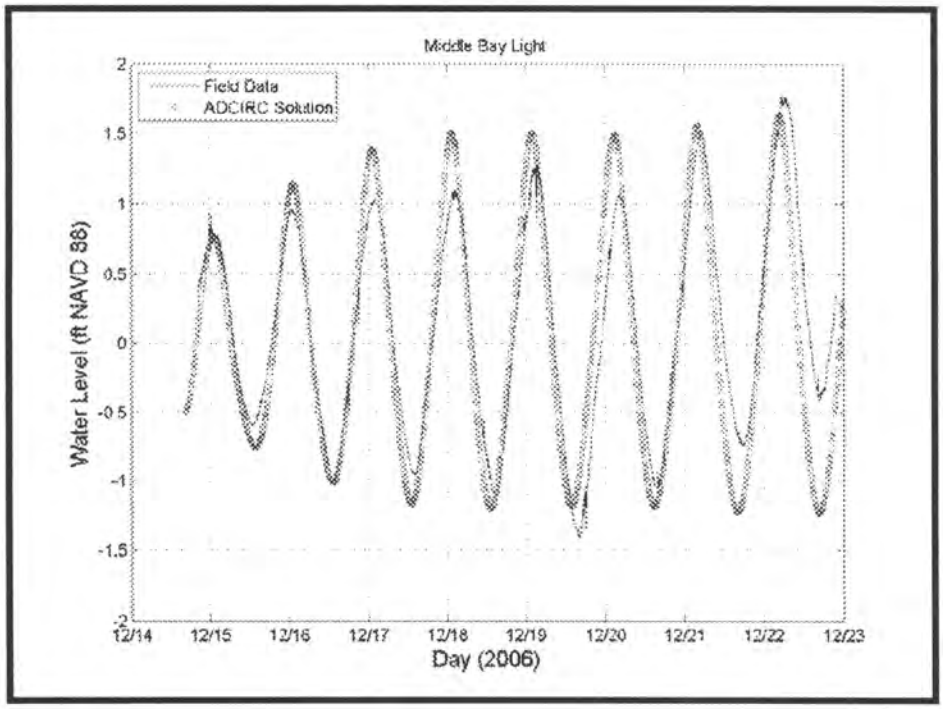

Figure 5-24. Comparison of modeled water levels with measured data for Middle Bay Light, December 15, 2006 to December 23, 2006.

Model results for Mississippi Sound (Figure 5-23) again over-predict high tide level on 17 December by 6 in. In addition, the model under predicts low tide on 19 December by about 1 ft. Tidal phase is again reasonably well predicted in the model solution. A trace of atmospheric influence raising mean water levels in the area is seen in field data for Mississippi Sound as well, although the influence is a bit smaller.

The comparison at Middle Bay Light (Figure 5-24) illustrated the same general trend of the model solution over predicting high tide levels around 17-18 December, with a maximum error of about 6 in. Tidal phase again closely predicted field data. The atmospheric event over the final two days of the record is recognized clearly in this set of data from inside Mobile Bay.

Although the agreement between model and field data is not perfect, trends in field data were reproduced for each recording station. These results are taken from a small portion of a model domain which spans over 600,000 square miles. The primary goal of this part of the modeling effort was to provide a reasonable hydrodynamic boundary condition with which to drive morphological modeling. In that regard, the effort can be considered successful.

General Circulation Patterns. In addition to providing a time series of water surface elevations for the study area, ADCIRC results also provided an understanding of regional flow patterns. To best compare model results with flow data recorded from the ADCP surveys, a separate ADCIRC run was performed to cover the survey days of 26-27 February 2007.

A plot of velocity contours and vectors at Mobile Pass for maximum flood tide during 26 February is shown in Figure 5-25. This result corresponds well with flows measured during this same time period of the ADCP survey (Figure 5-18). A majority of flow is conveyed by the navigation channel, and maximum velocities predicted (~ 5 ft/sec) are similar to those recorded by the ADCP. Velocities predicted by the model between the eastern tip of Dauphin Island and the navigation channel approach 3 ft/sec, while measured velocities for this area were closer to 1.5-2 ft/sec. The navigation channel contains strongest currents well inside Mobile Bay. Pelican Pass is subject to strong eastern flows, with velocities exceeding 3 ft/s. Flows predicted at Pass aux Herons are similar in magnitude to ADCP measurements, both falling around 2.5 ft/sec. ADCP data show the intracoastal waterway carrying much of the flow with low velocities on adjacent shallow channel margins. However, model calculations indicate flow evenly spread across Pass aux Herons. Increased mesh detail may have served to reproduce fine details of flow recorded by the ADCP.

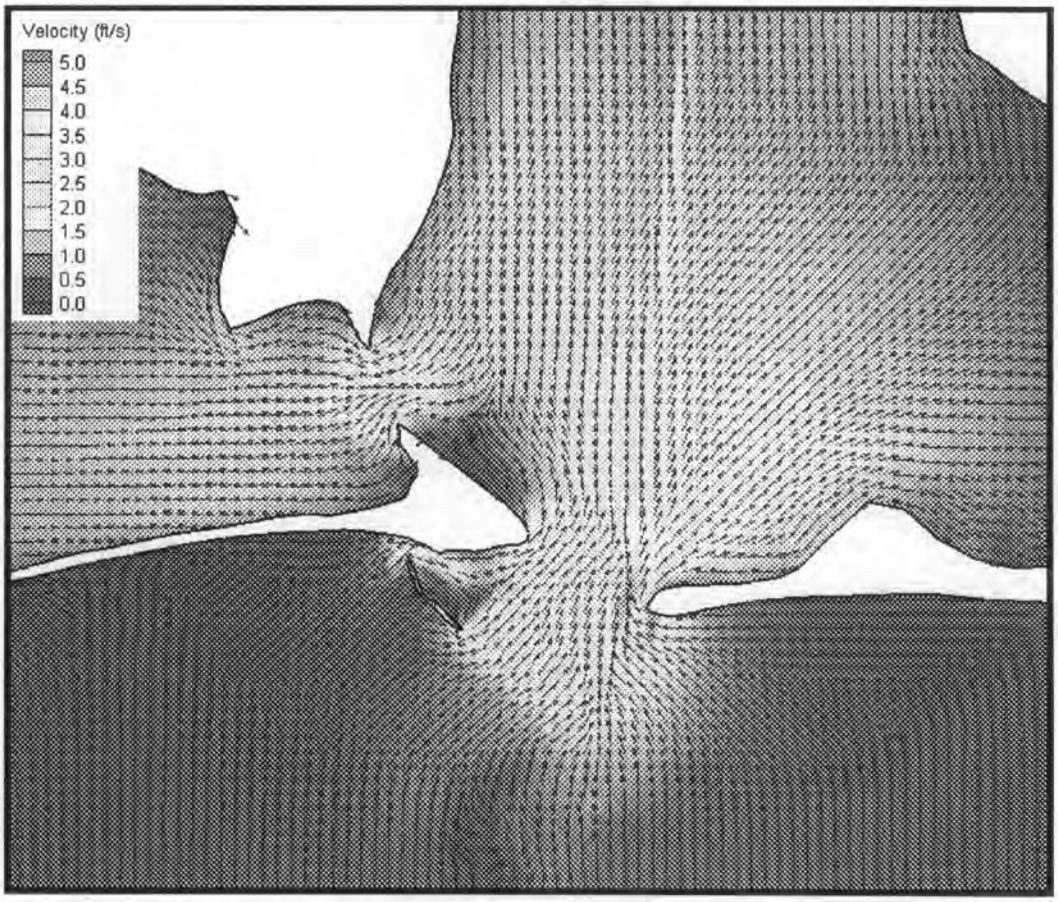

Figure 5-25. Velocity contours and vectors for maximum flooding tide at Mobile Pass February 26, 2007.

Maximum ebb-tidal conditions were not measured during the ADCP survey, so model results provide new insight here. Velocity contours and vectors at Mobile Pass for maximum ebb tide during February 26 are shown in Figure 5-26. A strong ebb-tidal jet is seen to extend offshore of Mobile Pass, with velocities greater than 2 ft/sec persisting more than 5 miles offshore. Pelican Pass carries a portion of the ebbing tide, but velocities are weaker than seen during the flood tide. This is to be expected as a flooding tide gathers water from all directions offshore of the inlet, while an ebbing tide is dominated by the ebb-tidal jet. A counter-clockwise gyre directly east of the navigation channel is seen outside the inlet, which persisted through the 4-5 hr of strongest ebb-tidal flow. Such a feature might serve to facilitate the growth of the eastern lobe of the ebb-tidal delta.

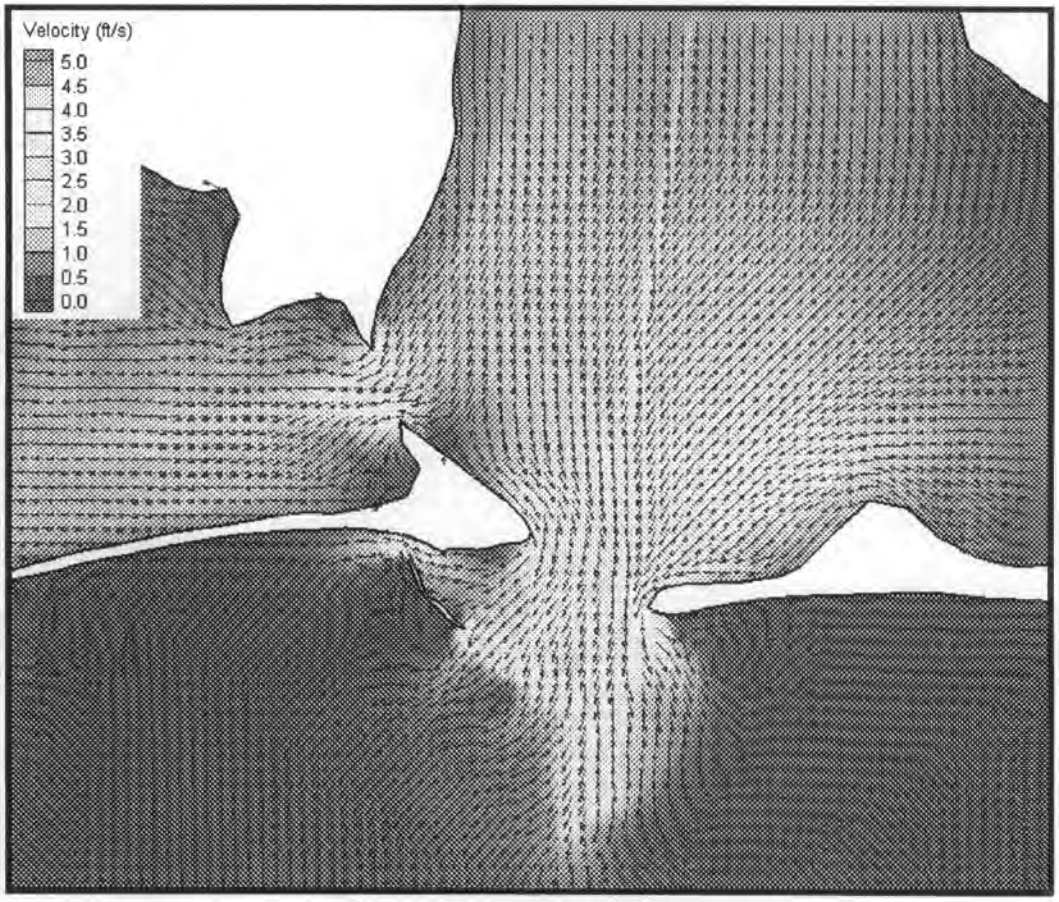

Figure 5-26. Velocity contours and vectors for maximum ebbing tide at Mobile Pass February 26, 2007.

Morphological Modeling

In addition to wave, sediment transport, and hydrodynamic modeling, morphological modeling of the ebb-shoal complex also was completed. Bathymetric change analysis presented in Chapter 4 is the definitive source for analyzing the complexities of the morphology change in and around Mobile Pass. However, it was anticipated that the numerical investigation could shed some light on the most likely pathways for sediment movement, as well as the relative magnitude of change under differing wave conditions.

CMS-M2D. CMS-M2D is a two-dimensional, depth-integrated, finite-difference hydrodynamic model. It also has the option of including morphology change estimates through the use of a sediment continuity equation for updating changes in bathymetry (Buttolph et al., 2006). Full coupling with an external wave model (STWAVE in this case) is possible, with the wave model passing radiation and shear

stresses to CMS-M2D. In return, hydrodynamic and morphology changes are passed back to the wave model.

Model Domain. Limits of the domain were chosen to encompass the ebb shoal and extend into Mobile Bay far enough to provide a well chosen boundary for hydrodynamics. In addition to these concerns, it is best practice for the coupled STWAVE and CMS-M2D runs for the hydrodynamic grid to lie completely within the wave grid. This prevents the need for CMS-M2D to extrapolate radiation and shear stresses past the boundaries of the wave model solution. In this case, the existing fine grid centered on Mobile Pass was used for efficiency. The final CMS-M2D domain is shown in Figure 5-27.

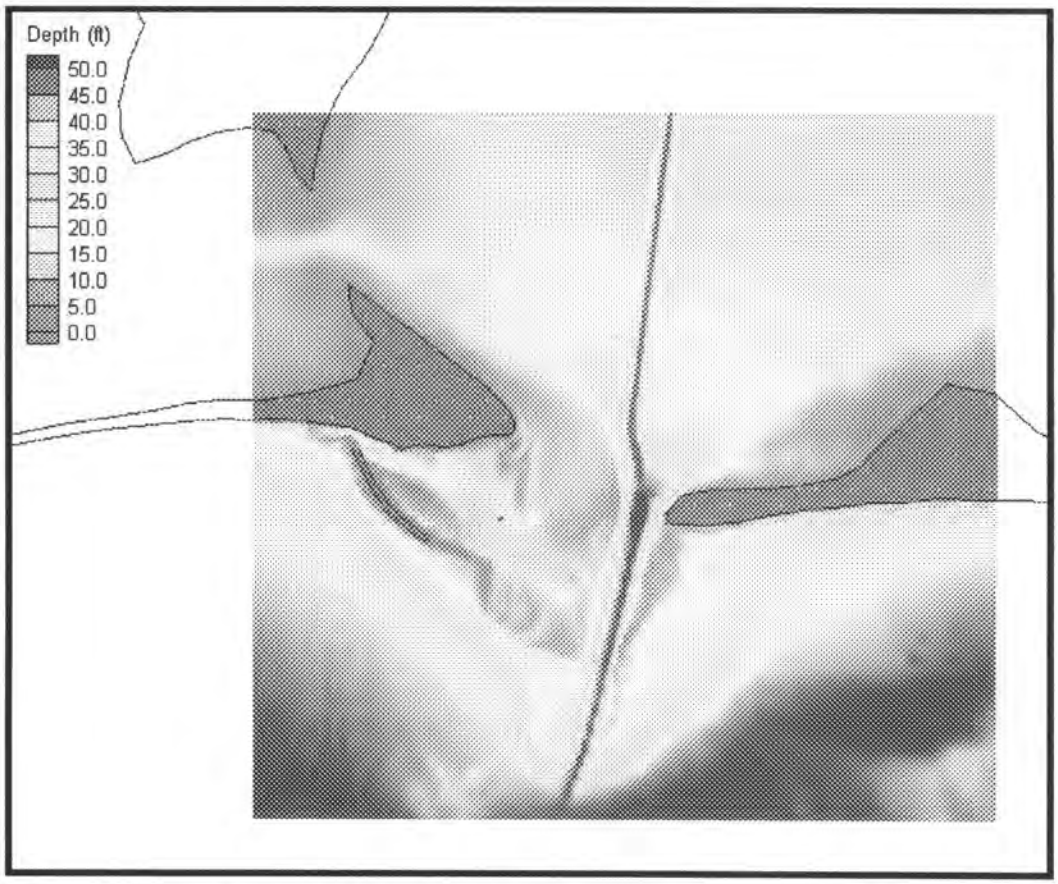

Figure 5-27. CMS-M2D model domain and bathymetry.

Boundary Conditions. The CMS-M2D model domain has three open boundaries. The hydrodynamic solution from ADCIRC was used to provide a time series of water levels along each open boundary. The 3-day period from 15-18 October2006 was used to drive hydrodynamics in the CMS-M2D simulations. This

period was chosen due to the moderate tidal range (1.5-2 ft) and considered representative for an average tidal condition.

Model Setup. With boundary conditions assigned, the remainder of model setup was concerned with properly choosing variables relevant to morphology predictions, as well as the coupling between STWAVE and CMS-M2D. A summary of model variables is shown in Table 5-3.

Table 5-3. Values for CMS-M2D model variables.

Variable	Setting
Hydrodynamic Time Step	3 sec
Transport Rate Time Step	2 min
Morphologic Time Step	30 min
Sediment Transport Formulation	Advection-diffusion
Mean Grain Size	0.25 mm
Interface with STWAVE every	2 hr

Morphological Model Results. It is understood that morphological predictions are useful only to reveal potential pathways for sediment movement and comparison of relative scales of change. Specific locations and values are not considered reliable. As such, results should not be considered quantitative predictions of change, but rather estimates for discussing morphology change on the ebb-tidal delta.

Initial model runs consisted of hydrodynamics only, where 3 days of average tidal conditions were run (Figure 5-28). As expected, there is little change associated with such a short time period and low energy conditions. Largest changes indicate movement of the east lobe of the ebb tidal delta near the shoreline from east-to-west. Deposition falls outside of the navigation channel. Net movement of the east lobe to the west is in keeping with observed morphology change and also with our understanding of nearshore flow regimes in the vicinity of tidal inlets. In addition, scouring of the navigational channel immediately west of Mobile Point is illustrated, an area which has typically not required maintenance dredging. There is also a small

signal of change at the offshore tip of Pelican Island, but no strong indication of transport direction is apparent.

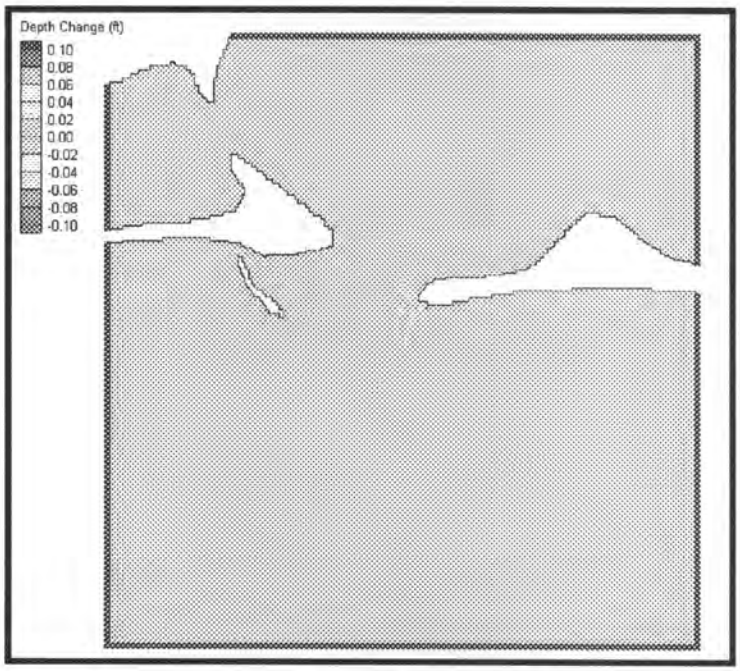

Figure 5-28. Bottom change results for 3 days of average tidal conditions only. Erosion is in yellow/red and accretion is in blue.

Case 2 consisted of the same 3 day tidal hydrodynamics, but with moderate wave energy (H_{mo} = 3.5 ft, T = 6 seconds) incident from the southeast. Results indicate migration of the east channel margin bar to the west (Figure 5-29). Change is much larger relative to the Case 1 results (note the change in scale of the color contours). Strongest change is along the offshore edge of the shoal, where wave breaking is strongest. Again, there is change along the shoal leading into Pelican Island, but these results show a clear trend of the shoal being pushed shoreward.

Figures 5-31 and 5-31 illustrate average transport vectors for Case 2 during maximum flood and ebb conditions, respectively. These plots are snapshots of a single time step extracted from the entire 3 day simulation. Each figure shows magnitude (color) and direction (arrow) of average transport (bed load and suspended load) calculated by CMS-M2D for the time step shown. Figure 5-30 shows clear trends in transport which mirror bottom change observed in Figure 5-29. On a flooding tide, waves and hydrodynamics are working to push material toward the inlet. Southeast of Pelican Island, transport is northward. Along the eastern

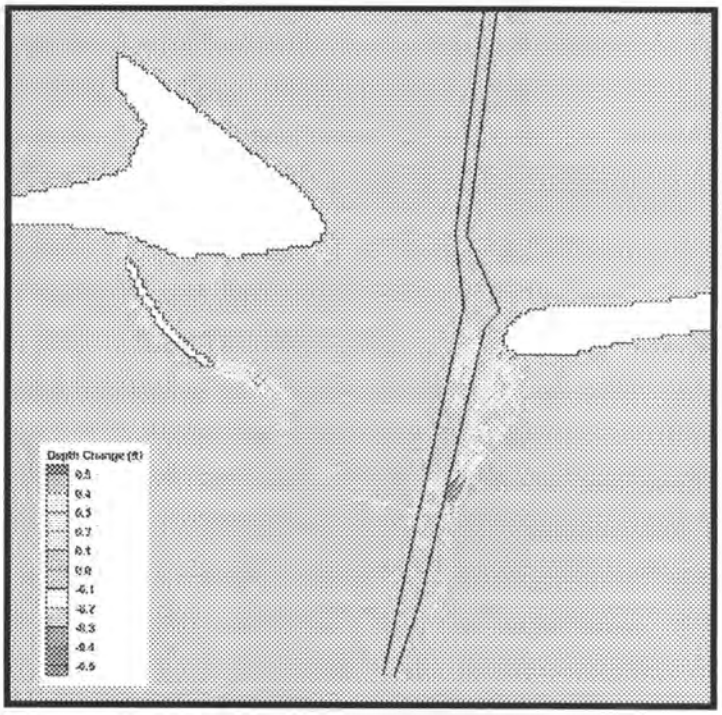

Figure 5-29. CMS-M2D bottom change results for 3 days of average tidal conditions under normal waves. Erosion is in yellow/red and accretion is in blue.

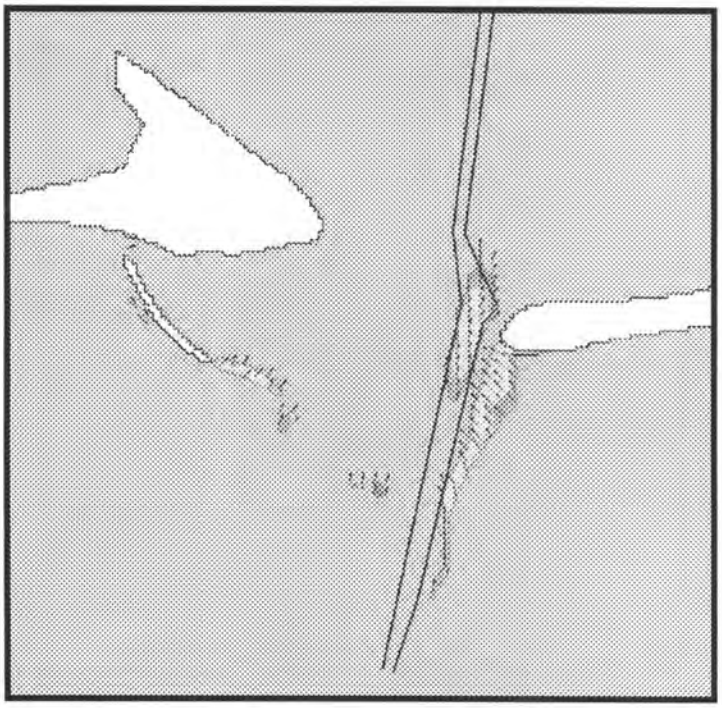

Figure 5-30. CMS-M2D average transport vectors for Case 2 during flood tide.

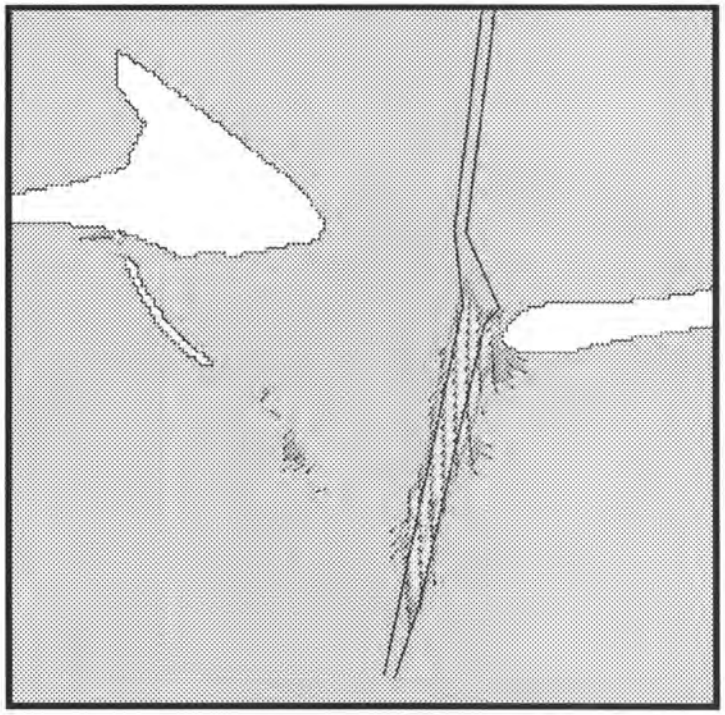

Figure 5-31. CMS-M2D average transport vectors for Case 2 during ebb tide.

channel margin bar, there is a well-defined area of east-directed transport that abruptly dissipates at the channel margin where deposition in bottom morphology is observed (see Figure 5-29). Flood tidal currents moving across the bar under breaking waves push sand from east to west towards the channel.

During ebbing tide (Figure 5-31), hydrodynamic forcing is directed offshore while wave energy is directing transport shoreward. This process results in most transport being confined to the navigation channel, where the currents are strongest, and only minor transport occurs on the shoals. Figure 5-31 illustrates conditions during maximum ebbing currents. Strong transport predicted in the navigation channel is short lived, which may be why only minor bottom change is reflected under these conditions.

Case 3 simulates a 3-day storm condition, with strong wave energy (H_{mo} = 10-15 ft, T = 9-13 sec) incident from the south and southeast. The tide signal is the same as other cases, but with a 3-ft surge added to water levels. As a result of the surge, Pelican Island became submerged during this simulation. Again, the east lobe is seen to migrate from east-to-west, with notable erosion along the outer fringe of the east lobe due to wave breaking farther seaward on the shoal (Figure 5-32). The outer edge of the western lobe is active for the first time, with the model indicating

shoreward migration for this area. Pelican Island shows erosion on the outer beach and deposition along the backshore, suggesting a trend of shoreward migration. There also is evidence of transport along the axis of Pelican Island, where change shows movement from southeast to northwest, towards the attachment area of Pelican Island to Dauphin Island.

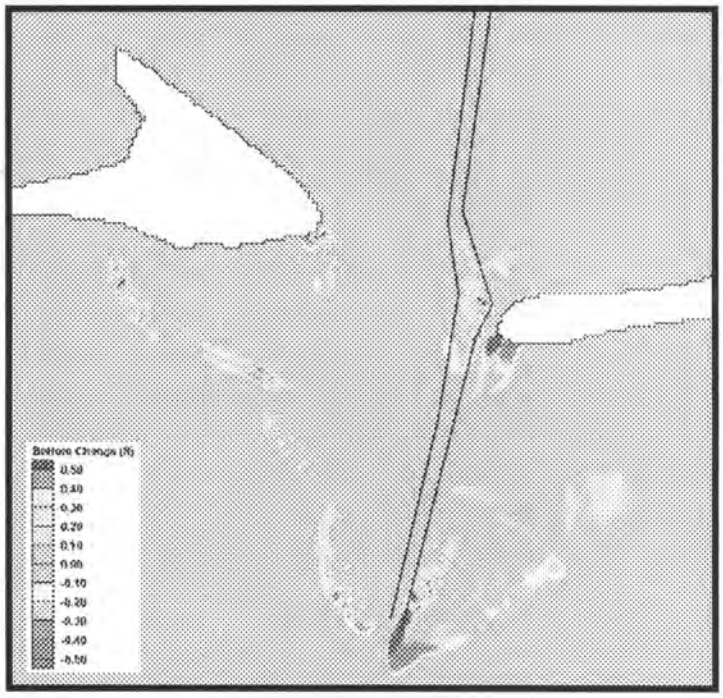

Figure 5-32. Bottom change results for 3 days of storm waves and a3-ft surge. Erosion is in yellow/red and accretion is in blue.

Transport vectors during flood tide (Figure 5-33) illustrate shoreward transport at the outer edges of the east and west lobes of the ebb-tidal delta. At Pelican Point (eastern Dauphin Island) and Mobile Point (western Morgan Peninsula), transport toward the inlet is indicative of changes predicted in the final bottom change plot (Figure 5-32). Both areas have relatively low wave energy, so observed transport can be attributed almost entirely to currents associated with maximum flood tide. Near Pelican Island, shoreward transport in the area immediately southeast of the island is dominant. Furthermore, northwest-directed transport along the seaward margin of Pelican Island indicates a primary direction of transport from the western lobe of the ebb-tidal delta to Dauphin Island. Both transport processes are illustrated in predicted bottom changes shown in Figure 5-32.

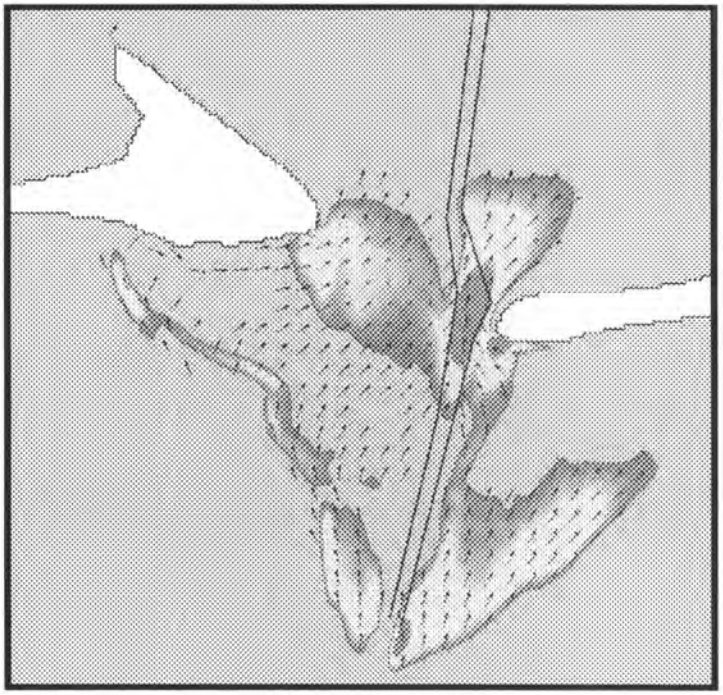

Figure 5-33. CMS-M2D average transport vectors for Case 3 during flood tide.

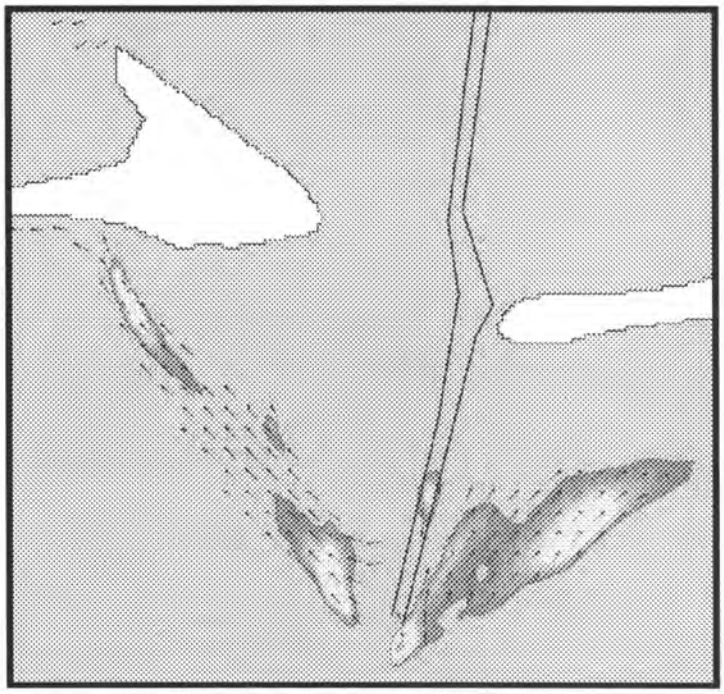

Figure 5-34. CMS-M2D average transport vectors for Case 3 during ebb tide.

During ebbing tide (Figure 5-34), observed transport is largely confined to the outer edges of the shoals on either side of the navigation channel. Ebb flow is confined to the navigation channel, and there is little wave energy across interior portions of the ebb-tidal delta due to wave breaking at the seaward margins. Along the western portion of the ebb shoal, there is a clear transport pathway from southeast to northwest toward Dauphin Island. With ebb currents confined to the navigation channel, waves are the dominant forcing mechanism along the east and west lobes of the shoal.

Summary of Numerical Modeling Results

Through the use of various numerical models, details of wave propagation, sediment transport potential, tidal hydraulics and morphology change in and around Mobile Pass have been analyzed.

Results from STWAVE simulations confirmed that the ebb-tidal delta dominates wave transformation in the area of Mobile Pass. Strong wave breaking and refraction across shoals were seen during energetic events. Pelican Island and surrounding shoals play an integral role in wave refraction and reduction of wave height in the lee of the island. Regardless of the details of the offshore wave conditions, refraction over the shoals southeast of Pelican Island was strong enough that all waves incident at the eastern tip of Dauphin Island were directed to the west.

STWAVE results were employed to calculate longshore sediment transport potential. These results showed a trend of net transport to the west across the entire study area. Transport along Morgan Peninsula increased from about 125,000 cy/year 15 miles east of Mobile Pass to 250,000 cy/year at Mobile Point. Transport along Dauphin Island is again directed to the west. Central portions of the island show significant transport in both directions, with a net transport of 25,000 cy/year directed to the west. For 3 miles of shoreline at the western tip of Dauphin Island, longshore transport showed a dramatic increase. The 25,000 cy/year simulated along the central portion of the island increased steadily to a rate 250,000 cy/year at the western end of the island.

ADCIRC modeling was performed to aid in understanding complex hydrodynamics of the inlet, as well as to provide boundary conditions for morphological modeling. Because of the complexities of tidal propagation in the Gulf of Mexico, and the lack of detailed field measurements outside of Mobile Bay, a regional model of the entire Gulf of Mexico was run. The model was given extra detail around Mobile Pass so that an accurate picture of flow in the area could be developed. Model results showed fair

comparison with tide gauge data in the area and were considered accurate enough to provide reasonable boundary conditions for morphological modeling.

CMS-M2D was used to investigate morphology change on the ebb-tidal delta. Results suggested that wave-driven transport dominated changes in bathymetry offshore Mobile Pass. Under storm conditions, transport from the western lobe of the ebb-tidal delta generally moved from the southeast to the northwest. This was particularly evident during ebbing tide. Although morphology change predictions were considered qualitative in nature, trends revealed from the modeling work closely simulated findings based on analysis of the historical bathymetric change discussed in Chapter 4.

6 Sediment Budget

Sediment budget determination for the coastal zone involves application of the principle of conservation of mass to littoral and offshore sediment (Bowen and Inman, 1966; Rosati and Kraus, 1999; Rosati, 2005). Development of a budget at Mobile Bay entrance and vicinity requires quantitative evaluation of various sediment sources to and losses from the study area, and a comparison of net gains or losses with observed rates of erosion or accretion. The USACE Sediment Budget Analysis System (SBAS; Rosati, 2005) was applied to display transport pathways and analyze sediment volume fluxes.

Originally, sediment erosion and accretion volumes were quantified for the period 1917/20 to 2002 by comparing (differencing) bathymetric survey data. However, the USACE 2002 bathymetry data were determined inadequate for computing a sediment budget because procedures associated with reference datum adjustments could not be verified accurately. This finding was identified during sediment budget formulation when change computations between 1917/20 and 2002 were determined to be abnormally large. Further analysis of the 2002 data set may yield appropriate datum adjustments, but this effort is beyond the scope of the present study.

For the period 1917/20 to 1984/87, twenty zones of erosion and accretion were identified throughout the sediment budget control area based on bathymetric change analysis. Overall, the entire ebb-tidal delta was net depositional. Beach and nearshore environments east of Mobile Pass were net erosional. One exception to this trend was the depositional zone adjacent to the jetties at Perdido Pass. Net west-directed transport deposits sand along the east side of the Pass, and sand dredged from the deposition basin at Perdido Pass was periodically bypassed to downdrift beaches west of the Pass, creating a region of net deposition.

Mobile Pass is an atypical navigation entrance in that jetties were not constructed to control channel shoaling and bar migration, even though a commercial navigation channel is maintained by dredging through the outer bar. The channel has always been a stable feature in that large shifts in shoal and channel geometry have not occurred historically. The modern channel occupies the general course of the ancient Mobile River valley when sea level was much lower than present (Boone, 1973; Smith, 1988; Hummell, 1990; Mars, 1992). Natural depths in the channel gorge are 55 to 60 ft, and flows through the Pass are sufficient to maintain channel depths. In fact, flows are so strong at Mobile Pass that hydrodynamic obstruction of net west-directed longshore currents east of the Pass produces an abrupt change in transport

direction at Mobile Point, forcing littoral sediment primarily south along the channel margin toward the outer part of the ebb-tidal delta. Todd (1968) termed this process dynamic diversion. Under this condition, shoaling through much of the channel is controlled by natural tidal currents. As such, only the seaward portion of the channel, across the outer bar, requires maintenance. Mobile Pass is an ideal entrance for commercial and recreational navigation.

Sediment Sources and Sinks

In recent geologic time, two primary sources of sediment have been available to form shoals on the ebb-tidal delta and beaches west of the Mobile Pass. Hummell (1990) suggested sediment transported out of Mobile Bay when sea level was lower created the foundation upon which the historical ebb-tidal delta has evolved. As sea level flooded the valley of the ancient Mobile River system, supply of sand-sized sediment to the coast diminished. The Mobile River delta was displaced farther inland and fine-grained sedimentation dominated infilling of Mobile Bay. The entrance channel occupied the ancient river valley and sand-sized sediment accumulated on the ebb-tidal delta by interaction of coastal and nearshore currents with cross-shore tidal flow at the entrance. Otvos (1973) suggested that ebb-tidal delta sands at Mobile entrance were derived primarily from Mobile Point and supplemented by sediment emerging from Mobile Bay.

Analysis of historical data from this study indicates that present-day sand supplied to the ebb-tidal delta is derived primarily from beach and nearshore sediment east of Mobile Pass (Stone et al, 2004). Only fine-grained material depositing along the outer margins of the ebb-tidal delta and west on the shelf fronting the Mississippi Sound barrier island system is derived from Mobile Bay. The coast and shelf east of Mobile Pass is sand rich from the 80-ft depth contour north into upland deposits (McBride and Byrnes, 1995); it is the primary source of sand for all beaches and tidal deltas west and into Mississippi.

Mobile Pass ebb-tidal delta also is a source of sediment for the barrier islands fronting Mississippi Sound. Barrier islands in this area historically have been growing and migrating to the west in the dominant direction of littoral transport (Byrnes et al., 1991; Morton, 2007). Inlets and their ebb-tidal deltas act as conduits for sand transport to the west. Islands become local sources of sediment as well, as sand is eroded from their eastern ends and transported to the west to be redeposited. This process is not occurring on Dauphin Island because the eastern end of the island is a relict late Pleistocene barrier ridge (Otvos, 1981). The stable ridge provides an area from which large volumes of littoral sand from the ebb-tidal delta can be

transported west, creating long and narrow sandy shoal platforms and islands off western Alabama and Mississippi (Otvos and Giardino, 2004). As such, Dauphin Island continues to extend to the west (sediment sink) as littoral sand is supplied to the beach via the ebb-tidal delta.

Storm overwash and island breaching have provided large sand volumes to backbarrier environments during landward migration of central Dauphin Island. As sand is transported across the island, the Gulf shoreline migrates to the north, apparently due to beach erosion. However, erosion implies that sand is permanently lost from the beach. Along central Dauphin Island, sand from the front side of the island often is recycled to the backside of the island as the island migrates landward (sand is not lost from the beach). This process is termed barrier rollover because the island migrates in a landward direction in response to storm processes. As such, the Gulf side of Dauphin Island can be considered a local source of sediment for landward island migration and lateral island growth.

Channel Shoaling Rates and Offshore Disposal

History of channel shoaling was discussed in Chapter 1 under Dredging and Placement History. Appendix B contains detailed information on new work and maintenance dredging quantities. Only maintenance dredging quantities can be used for estimating channel shoaling rates. Summarizing maintenance dredging data, one can derive an average shoaling rate for the outer bar channel for the period under which the sediment budget has been developed (1917/20 to 1984/87). Maintenance dredging records indicated that approximately 274,000 cy of sand was extracted from the channel each year between 1917 and 1987 and disposed of offshore. Most of this material was derived from the southern 1 to 2 miles of channel across the outer bar.

Although the exact location for disposal of dredged material from the outer bar is not known, bathymetric changes offshore of the outer bar indicated a large polygon of deposition just seaward and west of the navigation channel (Figure 6-1). This area appears to be the site of offshore dredged material disposal from the Mobile Pass Outer Bar. Prior to analyzing bathymetric changes in this area, it was not known whether dredged material deposited offshore was contributing to net sediment accumulation and transport on the ebb-tidal delta. The direct connection between the offshore disposal area and sand deposition and transport on the southwestern part of the ebb-tidal delta suggests that sediment exchange is active in this area. The mound of deposition to the west of the offshore disposal site is the Mobile Outer

Mound, a berm created by the USACE using about 17 million cy of dredged material from the Mobile Harbor dredging project.

New work and maintenance dredging records provided quantities of sediment dredged from the outer bar that were deposited offshore for the period 1917 to 1987. Summing these data provided an estimate of the quantity of sand dredged from the outer bar that was deposited offshore during this time. The annual maintenance dredging rate was about 274,000 cy, and the annual new work was about 75,000 cy, resulting in net deposition at the offshore site of about 349,000 cy/year. According to bathymetric change results, net sand accumulation at the offshore disposal site was determined to be about 191,000 cy/year. Therefore, the annual quantity of sand from the disposal site contributing to deposition on the western lobe of the outer bar between 1917/20 and 1984/87 was determined to be about 158,000 cy.

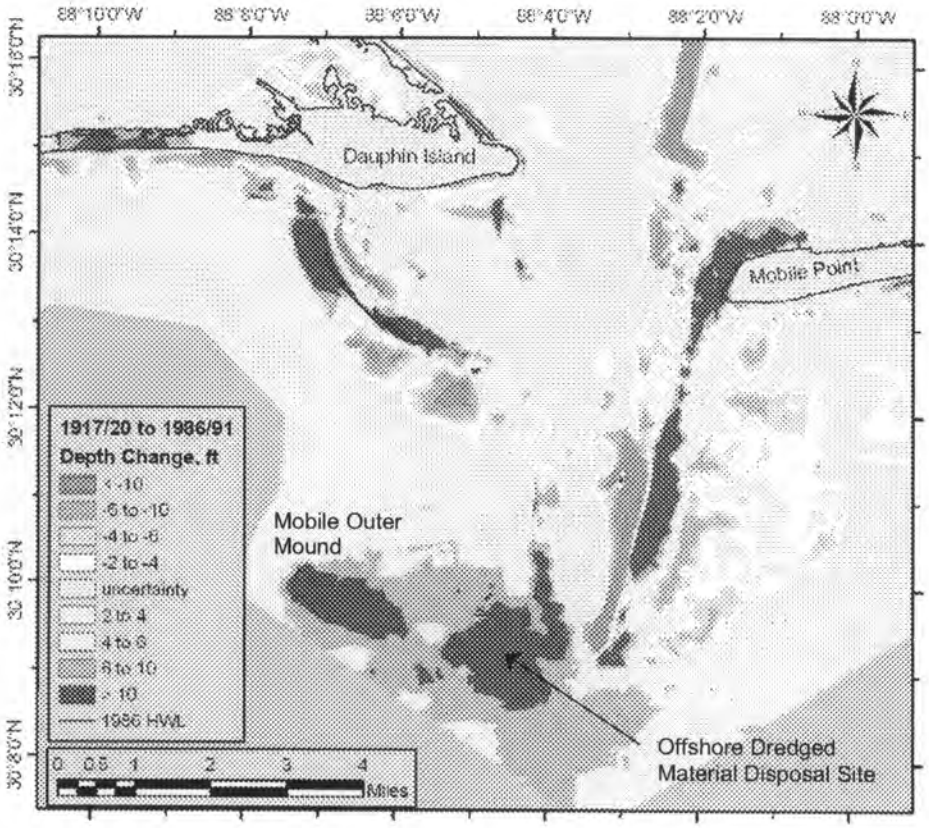

Figure 6-1. Location of offshore dredged material disposal site and the Mobile Outer Mound relative to deposition on the ebb-tidal delta.

Net Longshore Transport

In developing a sediment budget, sources and sinks for open boundaries within the sediment budget control area determine the reliability of the budget. Net littoral transport rates near the eastern boundary of the study area (Perdido Pass) were estimated by Walton (1973) at about 280,000 cy/year to the west. Basillie (1975) computed net west-directed transport at rates between 239,000 cy/year and 334,000 cy/year based upon wave observations for an area west of Pensacola, FL. Douglass (2001) estimated the annual net transport to be about 190,000 cy/year near Perdido Pass. When the USACE constructed two converging jetties at Perdido Pass in 1969, a 400,000 cy capacity deposition basin was built on the eastern side of the channel to capture sand transported over the weir section to limit channel shoaling. Dredging frequency for the basin was every two years, indicating that estimated net littoral drift to the west was about 200,000 cy/yr (Sargent, 1988). Within 2 years of construction, the basin was full and additional material was shoaling the navigation channel. Based on these data, net littoral transport at the eastern boundary of the sediment budget was estimated at 240,000 cy/yr.

Sediment Contribution from Mobile Bay

Fine-grained sediment transport from Mobile Bay to the Gulf has been documented based on photography and Landsat imagery, and discussed by numerous authors (e.g., Chermock, 1974; Hardin et al., 1976; Stumpf and Gelfenbaum, 1990). Using data reported by Hardin et al. (1976) for fine-grained sediment infilling of lower Mobile Bay, sediment transport seaward and to the west of the ebb-tidal delta was estimated at 337,000 cy/yr. Based on more recent discharge values for Mobile Pass, Isphording et al. (1996) estimated that about 420,000 cy of suspended sediment not retained in the lower Bay is transported to the Gulf of Mexico on an annual basis. Fine-grained sediment does not affect the sand budget along the beaches and on the ebb-tidal delta, but it is a component of the regional transport system and was included for completeness.

Net Transport Pathways and Quantities: 1917/20 to 1984/87

Net deposition and erosion throughout coastal Alabama for the period 1917/20 to 1984/87 were determined by differencing the 1917/20 and 1984/87 bathymetric surfaces to isolate polygons of erosion and deposition. This period encompassed a time of significant dredging activity in the outer bar channel. Figure 6-2 illustrates areas of net erosion and deposition (white numbers indicate quantities eroded or deposited in thousands of cubic yards on an annual basis within defined polygons)

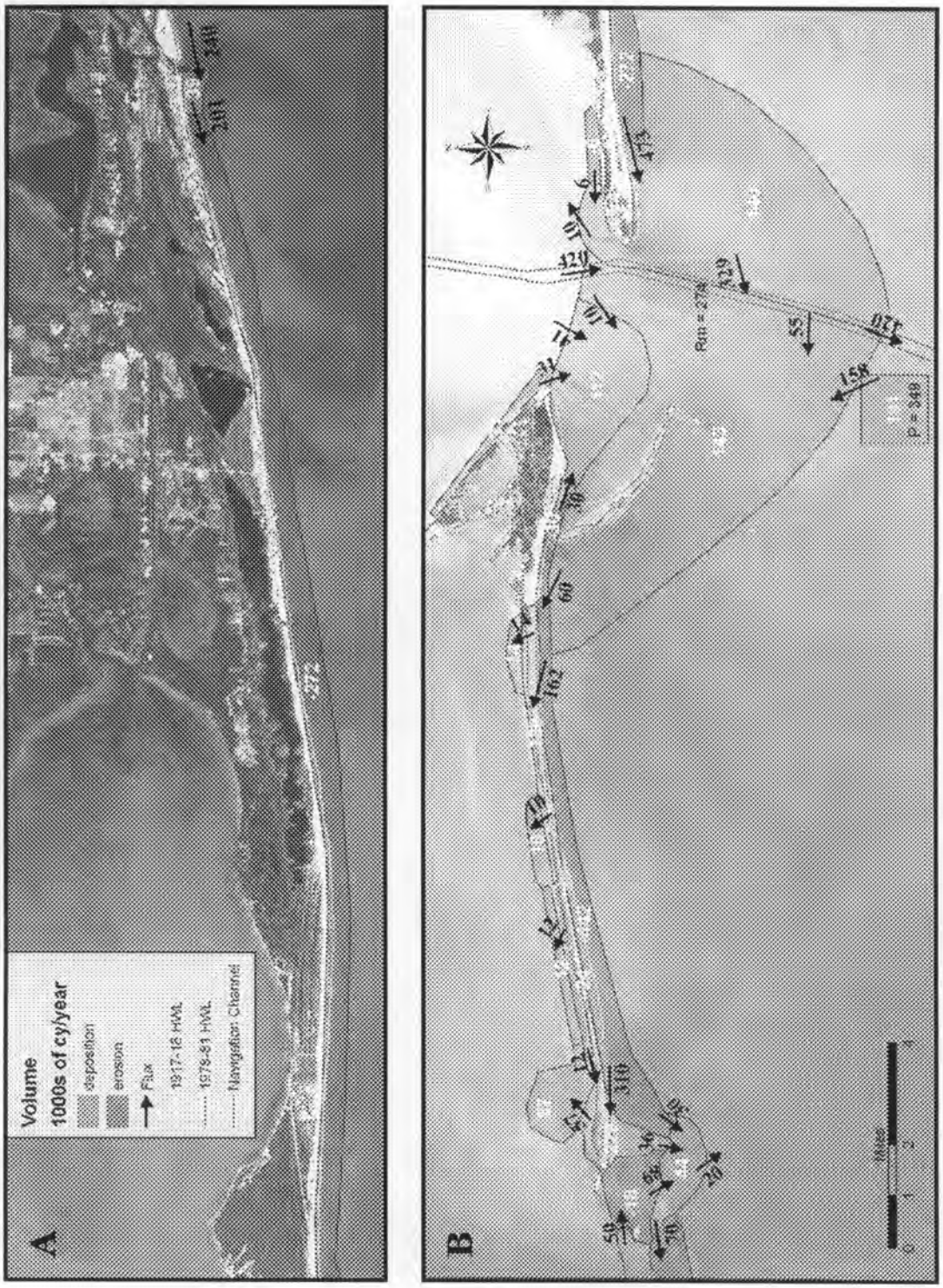

Figure 6-2. Sediment budget for the Alabama outer coast, 1917/20 to 1984/87. A: Alabama coast between Perdido Pass in the east and western Morgan Peninsula; B – Alabama coast between western Morgan Peninsula and eastern Petit Bois Island, MS. White numbers indicate quantities eroded or deposited in thousands of cubic yards on an annual basis within defined polygons, and black numbers associated with black arrows are sediment fluxes in thousands of cubic yards per year.

and associated sediment fluxes (black numbers associated with black arrows in thousands of cubic yards per year) in coastal Alabama.

Starting east of Perdido Pass, net littoral transport at the eastern boundary was estimated by Basillie (1975) to be about 240,000 cy/year. Because net sand deposition was recorded just west of Perdido Pass (39,000 cy/year), the flux of sand from this point west was estimated at 201,000 cy/year (Figure 6-2A). Net erosion along the shoreline, and particularly in the nearshore, was dominant for most of the Gulf shore fronting Morgan Peninsula until encountering Mobile Pass and its ebb-tidal delta. At this point, sand available to the transport system had increased in proportion to net erosion documented via bathymetric change analysis. As such, by the time sand began depositing along Mobile Point and the eastern side of the ebb-tidal delta, sand flux was approximately 473,000 cy/year. The bay side of Mobile Point indicated net erosion as well, which contributed another 6,000 cy/year to the ebb-tidal delta.

Net sediment accumulation dominated sedimentation trends on the eastern lobe of the ebb-tidal delta, adding 140,000 cy/year to shoals on the eastern side of the channel (Figure 6-2B). Bathymetric change results illustrated that most deposition was associated with channel infilling as the channel migrated to the west during this time (Figure 6-1). Sediment deposition at Mobile Point and inside the Bay illustrated the northern extent of channel infilling as the channel margin bar evolved in direct response to strong tidal currents exiting and entering the Bay and their interaction with west-directed sediment transport. Erosion on eastern shoals of the ebb-tidal delta contributed to channel margin sedimentation as well.

Although significant net deposition was computed east of the channel, large quantities of sand were transported to and across the channel to the western lobe of the ebb-tidal delta. Approximately 329,000 cy/year of sand was transported west, 274,000 cy/year of which were dredged from the outer bar channel and deposited at the offshore disposal site (shown as R_m=274 on Figure 6-2B). The remaining 55,000 cy/year bypassed the channel to the west as described in Chapter 4. Disposal of new work and maintenance dredging material from the outer bar at the offshore disposal site was approximately 349,000 cy/year for the period of record (shown as P=349 on Figure 6-2B). Of this quantity, it was estimated that 158,000 cy/year was transported north and west onto the western lobe of the ebb-tidal delta.

Stumpf and Gelfenbaum (1990) and Isphording et al. (1996) indicate that fine-grained material exiting lower Mobile Bay contributes to deposition on the shelf seaward and west of Mobile Pass. Based on discharge values for Mobile Pass, it was

estimated that about 420,000 cy/year of suspended sediment exits the bay and deposits on the shelf outside the study area.

Net deposition west of the channel on the outer portion of the delta amounted to about 143,000 cy/year. Growth of Pelican Island during this time was extensive, and sand bypassing to Dauphin Island provided needed sediment for closing breaches caused by the July 1916 hurricane and expanding the island westward. Approximately 60,000 cy of sand was bypassed to Dauphin Island on an annual basis between 1917/20 and 1984/87, of which 162,000 cy/year was needed to restore the island (138,000 cy/year) and account for washover deposition behind the island (24,000 cy/year). There is evidence in the historical record that flooding currents in Pelican Pass are sufficiently competent to deposit sand along the shoreline and nearshore of Pelican Bay. As such, 30,000 cy/year of sand was directed toward Pelican Bay to account for this process. Hydrodynamic modeling results presented in Chapter 5 confirm that flooding tides to the east through Pelican Pass are stronger than ebbing tides to the west. Another 31,000 cy/year of sand was transported southeast from Little Dauphin Island, predominantly during ebbing tide, and deposited in Pelican Bay as shoals south of eastern Dauphin Island (see Figure 6-1). An additional 41,000 cy of sand was needed on an annual basis from the large shoal fronting Little Dauphin Island to balance net deposition in Pelican Bay of 112,000 cy/year.

Net transport to the west along western Dauphin Island was driven primarily by beach and nearshore erosion along central and western portions of the island that supplied approximately 310,000 cy/year of sand to lengthen Dauphin Island to the west. Of this sediment flux, about 229,000 cy/year was required for island expansion to the west and growth of the ebb-tidal delta at Petit Bois Pass. Approximately 70,000 cy/year was transported to the western side of the pass, where beach erosion and barrier island washover supplied sand to backbarrier shoals and downdrift beaches along Petit Bois Island. Cycling of sand at Petit Bois Pass is complex, but overall net transport pathways and quantities are controlled by recorded patterns of net geomorphic change.

Inlet Reservoir Model

The Inlet Reservoir Model (Kraus, 2000) is a time-dependant model for predicting inlet morphology based on equilibrium volumes and transport rates. With equilibrium volumes and transport rates assigned for an inlet system, the model produces a time-dependant sediment budget based on feature volumes, transport rates, and longshore sediment transport predictions at study area boundaries.

The Reservoir model calls upon five assumptions (Bodge and Rosati, 2003):

- The volume of sand within the study area is conserved.
- Morphological forms and sediment pathways can be identified and preserve their identity while they evolve.
- Changes in morphological forms are relatively smooth.
- Material composing the ebb-tidal shoal is predominately transported to and from the shoal through longshore sediment transport.

Furthermore, to achieve an analytical solution to the sediment balance between morphological features, a linear rate of bypassing for a given feature is assigned such that

$$FlowRateOut = FlowRateIn\left(\frac{CurrentVolume}{EquilibriumVolume}\right)$$

Kraus (2000) and Bodge and Rosati (2003) offer a more thorough discussion of model formulations and theoretical underpinnings.

Inlet Reservoir Model at Mobile Pass. The values from the final sediment budget were applied to a simplified account of Mobile Pass as shown in Figure 6-3. Morphological features included in the model were the east and west lobes of the ebb-tidal delta, an area to represent offshore disposal, and the navigation channel.

Sediment pathways are simplified such that all sediment arriving from the east (Q Left In) is passed into the east lobe of the ebb-tidal delta. The volume not retained by the east lobe is passed into the navigation channel. The navigation channel is represented so no volume remains in the channel. Sediment transported into the navigation channel was either passed into the offshore disposal site (to represent channel dredging) or onto the west lobe of the ebb-tidal delta. The west lobe received material from the navigation channel directly, as well as from the disposal site. The west lobe retains volume as prescribed by model and passes the excess downdrift in the direction of Q Left Out.

Given that a working sediment budget has been established, equilibrium volumes for the east and west lobes of the ebb-tidal delta could be calculated directly and input to the Inlet Reservoir Model. The model was run for the period 1917/20 to 1984/87. Volumes for east and west lobes of the ebb-tidal delta were taken directly from Table 3-5, using the values reported for the 1917/20 year and the 30-ft depth contour. The

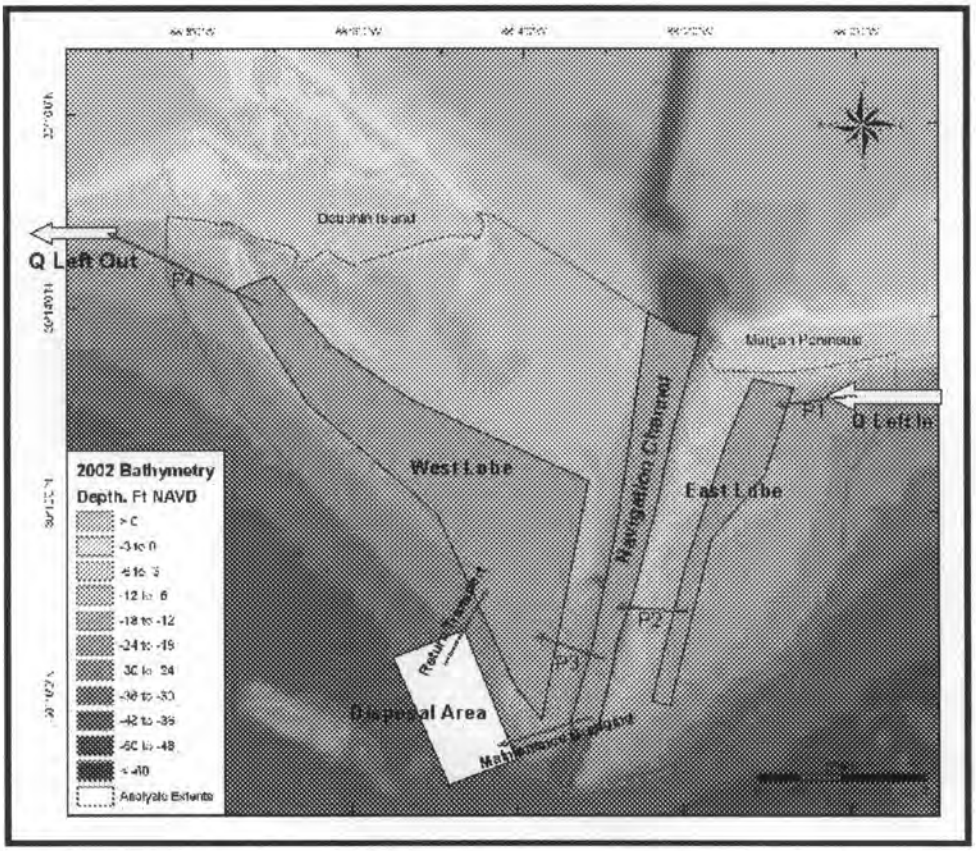

Figure 6-3. The Inlet Reservoir Model domain and component features for Mobile Pass.

Table 6-1. Input variables for the Inlet Reservoir Model.

	Starting Volume (cy)	Equilibrium Volume (cy)	Transport Rate (cy/year)	Coupling Coefficient
East Lobe	112,394,000	151,588,000	--	--
Navigation Channel	100,000	100,000	--	--
Disposal Area	9,500,000	20,984,000	--	--
West Lobe	311,003,000	1,504,606,000	--	--
Q Left In	--	--	473,000	--
P1	--	--	--	1.0
P2	--	--	--	1.0
P3	--	--	--	0.17
Maintenance Dredging	--	--	--	0.83
Return Transport	--	--	--	1.0
P4	--	--	--	1.0

30-ft depth contour was chosen as it better represents the active region of transport on the ebb-tidal delta. Table 6-1 shows input values for the final model run. The coupling coefficient listed for pathways controls the distribution of material leaving a given area.

In general, volumes associated with the navigation channel are irrelevant to the final result, as long as initial and equilibrium volumes are the same so that all material passed into the polygon is passed through pathways P3 and Maintenance Dredging. Similarly, the initial volume chosen for the disposal area is not exact. Instead, the ratio between initial and equilibrium volumes is the critical parameter. This ratio determines the amount of material leaving the disposal area through the return transport pathway.

Figure 6-4 illustrates predicted volumes by time for east and west lobes of the ebb-tidal delta compared with volumes calculated from bathymetry data. In both cases, predicted curves are flat, which is expected because the inlet has been active for thousands of years and these data consider only the past 70 years of evolution. In

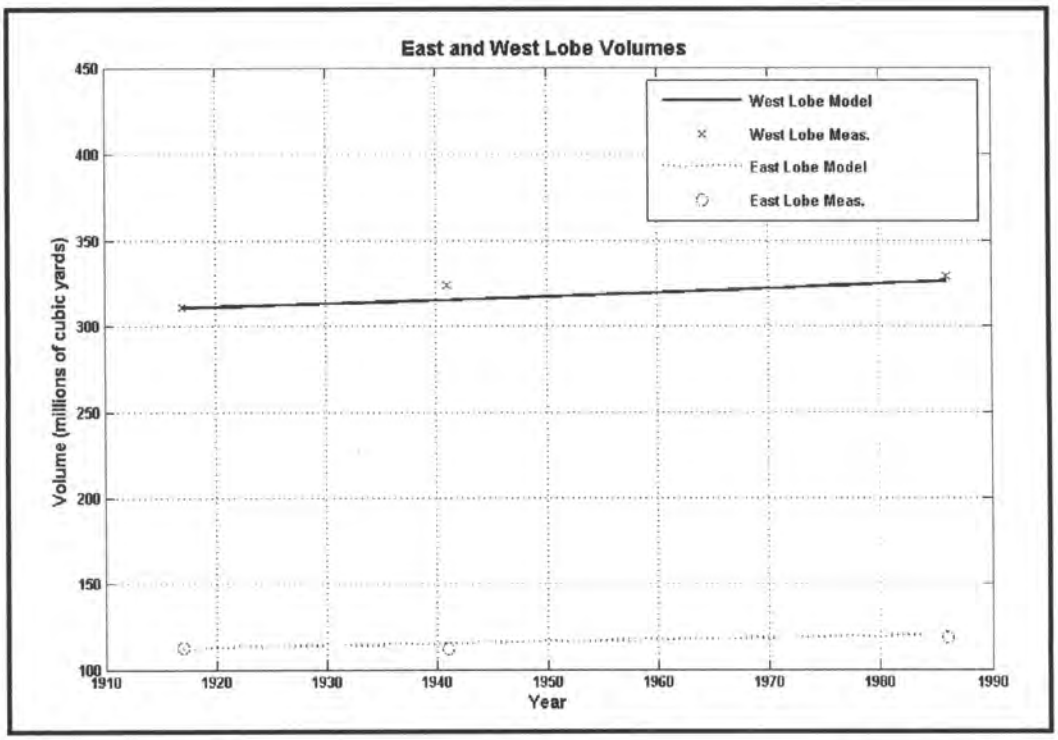

Figure 6-4. Modeled versus measured volume change on the east and west lobes of the ebb-tidal delta, 1917/18 to 1984/87.

addition, the flow rate out of the model, reported as Q Left Out, increased slowly from 40,000 cy/year in 1917 to 77,000 cy/year in 1987, which is in close agreement with the sediment budget estimation of 60,000 cy/year between 1917/20 and 1984/87.

The value of the Inlet Reservoir Model is with establishing bounds on volumes and growth rates for various morphological features for a given inlet. In addition, it can help display the estimated growth of various features during evolution of the inlet. Because Mobile Pass and the ebb-tidal delta are so complex and mature, results from the model are somewhat redundant relative to the sediment budget. The model does provide an estimate of equilibrium shoal volumes, which is something other work does not. However, the change rate, transport rates, and volume changes are all better described within the original sediment budget based on bathymetric change analysis. A further concern with application of the Inlet Reservoir Model is that the role of storms is so dominant, that the model assumption of smooth change to morphological features is violated.

7 Changes Resulting from Channel Dredging

The primary purpose of this study was to evaluate the impact of construction and maintenance dredging for the Federal navigation project in Mobile Outer Bar Channel on shoreline response along Dauphin Island and shoal evolution on the Mobile Pass ebb-tidal delta. A number of previous studies have expressed concern regarding the effect engineering activities may have had on beach changes. Specifically, the USACE Beach Erosion Control and Hurricane Protection report for Mobile County, Alabama (1978) stated

> "The principal causes of shore erosion along the westernmost 11 miles of Dauphin Island are attributable to rise in sea level and maintenance dredging of the Mobile Bay entrance channel."

Douglass (1994) discussed the annual rate of sand removal from the Mobile Outer Bar between 1974 and 1989 and stated

> "Almost all of this sediment has been removed from the littoral system of coastal Alabama to deepwater disposal sites."
>
> "The littoral system of Dauphin Island and Sand Island has probably not received any littoral drift from the east of Mobile Pass in fifty years."
>
> "In essence, because of dredging practices, Mobile Pass has probably functioned as a sink for sand moving along the coast this century. Assuming that all of the sediment dredged from the outer bar came from the littoral system, the efficiency of the sink has been much greater than 100% relative to the flowrate of sand along the coast."

Although neither study relied on a detailed evaluation of historical dredging records for the outer bar channel or a quantitative comparison of historical shoreline and bathymetry surveys for documenting historical sediment transport pathways and net rates of change across the ebb-tidal delta and along the shoreline of Dauphin Island, qualitative connections between channel dredging and beach erosion along Dauphin Island were asserted. Douglass (1994, p. 327) recognized this shortfall when stating "A comprehensive study that conclusively correlates the changes in the shoals and erosional-depositional patterns on Dauphin Island with the dredging history and storm and wave climate record was beyond the scope of this study".

The working hypothesis tested in the present study was that historical construction and channel maintenance dredging in the Mobile Outer Bar Channel have resulted in adverse changes to the western lobe of the ebb-tidal delta and the beach along

Dauphin Island west of Pelican Island. Ebb-shoal changes and shoreline response relative to storm and normal forces, and dredging in the outer bar channel, were evaluated to determine the extent to which beach erosion along Dauphin Island could be attributed to USACE channel construction and maintenance dredging operations.

Minimum Measurable Quantity

Early in the project, one of the tasks requested by the ITRT involved documenting uncertainty related to shoreline position, bathymetry, and numerical simulations of flow and sediment transport to gauge the significance of change rates and transport values for quantifying the potential impact of dredging activities at Mobile Pass on adjacent shorelines. The methods used to document uncertainty with shoreline and bathymetry data were presented in Chapters 2 and 3 and discussed in Byrnes et al. (2002) and Baker and Byrnes (2004). A so-called minimum measurable longshore transport quantity was derived based on our analyses and presented to the ITRT for evaluation in January 2007. The following is a summary of the analysis.

All survey data sets contain some amount of inherent uncertainty associated with data acquisition and compilation procedures. It is important to quantify limitations in survey measurements and document potential systematic errors that can be eliminated during quality control procedures (Byrnes et al., 2002). Substantial effort was spent ensuring that any systematic errors were eliminated from all data sets prior to change analysis. As such, measurement errors associated with present and past surveys are considered random. Because random errors are considered equally distributed, they can be neglected relative to change calculations. This leaves data density as the primary factor for determining the reliability of erosion and accretion quantities associated with change surfaces.

Interpolation between measured points always includes uncertainty associated with terrain irregularity and data density. The density of bathymetry data, survey line orientation, and the magnitude and frequency of terrain irregularities are the most important factors influencing uncertainties in volume change calculations between two bathymetric surfaces (Byrnes et al., 2002; Baker and Byrnes, 2004). Volume uncertainty relative to terrain irregularities and data density can be determined by comparing surface characteristics at adjacent survey lines. Large variations in depth between survey lines (i.e., few data points describing variable bathymetry) will result in large uncertainty calculations between lines. Additionally, surveys with track lines oriented parallel to major geomorphic features can result in large uncertainty calculations between lines. This computation provides the best estimate of

uncertainty for gauging the significance of volume change calculations between two surfaces.

Uncertainty estimates were calculated for the 1917/18, 1960/61, 1982/92, and 2001/2002 bathymetric surfaces using the methods outlined in Byrnes et al. (2002). Multiple sets of line pairs were compared for each time period to represent terrain variability. Line pairs were chosen that would accurately reflect track line spacing for each survey and irregularity of prominent geomorphic features in the region. Lines were established for each time period to overlay survey lines for that year. Bathymetry data were extracted along each line to calculate variations in elevation between line pairs. Depths were extracted at 10-ft intervals, and the absolute value of differences was averaged to calculate potential uncertainty for each line pair.

Results of uncertainty calculations are summarized in Table 7-1. Estimates were generated for each bathymetric surface, with particular emphasis on the ebb–tidal delta of each data set. As expected, areas with greatest uncertainty were associated with channel and ebb shoal features. To identify potential uncertainty related to sediment transport calculations, a separate calculation was made for the channel/ebb-tidal delta area. Potential elevation uncertainty ranged from ±0.54 to ±1.30 ft for calculations made across the entire surface to ±1.88 to ±2.59 ft for the channel/ebb shoal areas. Combining this information to judge the impact of potential uncertainties associated with volume change calculations derived from these surfaces resulted in root-mean-square variations shown in Table 7-2.

Table 7-1. Potential uncertainty for bathymetric surfaces from western Dauphin Island to Perdido Pass, AL.

	Entire Surface (ft)	Ebb-Tidal Delta/Channel (ft)
1917/20	±0.84	±1.88
1960/61	±1.02	±2.30
1982/92	±0.54	±1.43
2001/2002	±1.30	±2.59

Table 7-2. Maximum root-mean-square (RMS) potential uncertainty for bathymetric change data from western Dauphin Island to Perdido Pass, AL.

	1960/61	1982/92	2001/2002
1917/20	±1.32[1] (±2.97[2])	±0.99 (±2.36)	±1.55 (±3.20)
1960/61		±1.15 (±2.71)	±1.65 (±3.46)
1982/92			±1.41 (±2.96)

[1]Entire Surface, [2]Ebb-Tidal Delta/Channel

Applying these limits to the area of sand accumulation along the western end of Dauphin Island as the island expanded to the west in response to dominant westward longshore transport (Figures 7-1 and 7-2), a range in potential uncertainty can be determined relative to the area of accumulation. The sand accumulation rate in Table 7-3 can be directly associated with the net longshore sand transport rate for the ocean fronting portion of Dauphin Island. As such, potential uncertainty calculations can be determined relative to net transport rates, providing an estimate of the minimum measurable quantity for this area. For long-term data comparisons (e.g., 1917/20 to 2001/2002), potential volume uncertainty, calculated using the ebb-tidal delta/channel elevation uncertainty estimates, ranged from ±43,500 to ±70,000 cy/yr (Table 7-4). Using the entire shelf surface elevation uncertainty estimates, potential volume uncertainty ranged from ±18,500 to ±34,000 cy/yr. Because net transport estimates were calculated for an inlet region, the minimum measurable quantity range was estimated at ±43,500 to ±70,000 cy/yr, or about 25 to 30% of calculated net longshore sand transport rates (RMS depth uncertainty in Table 7-2 times the corresponding polygon surface area in Table 7-3).

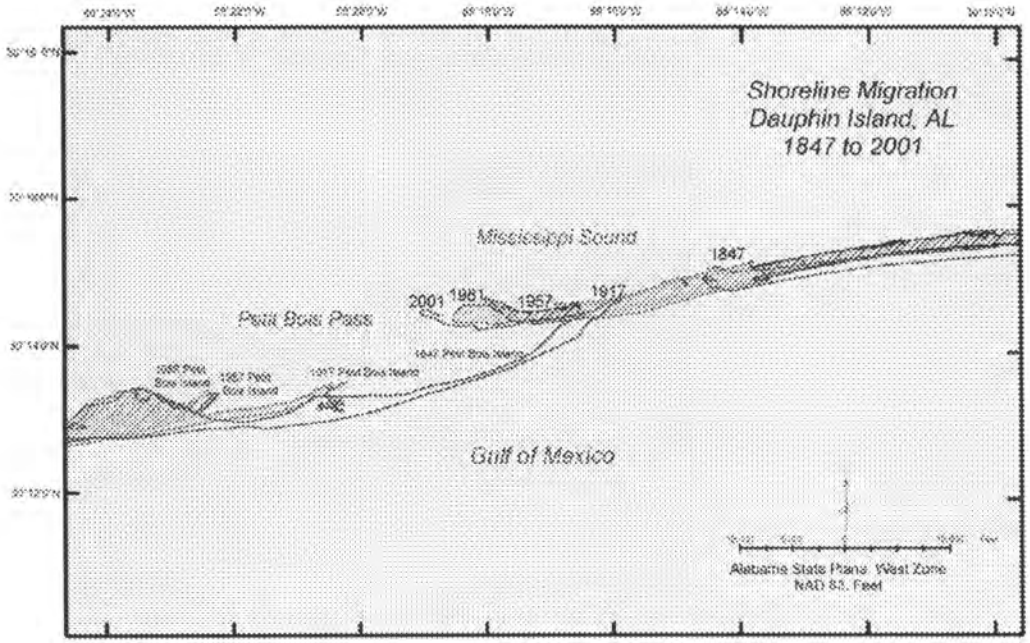

Figure 7-1. Historical shoreline position at the western end of Dauphin Island, 1847/67 to 2001/2002.

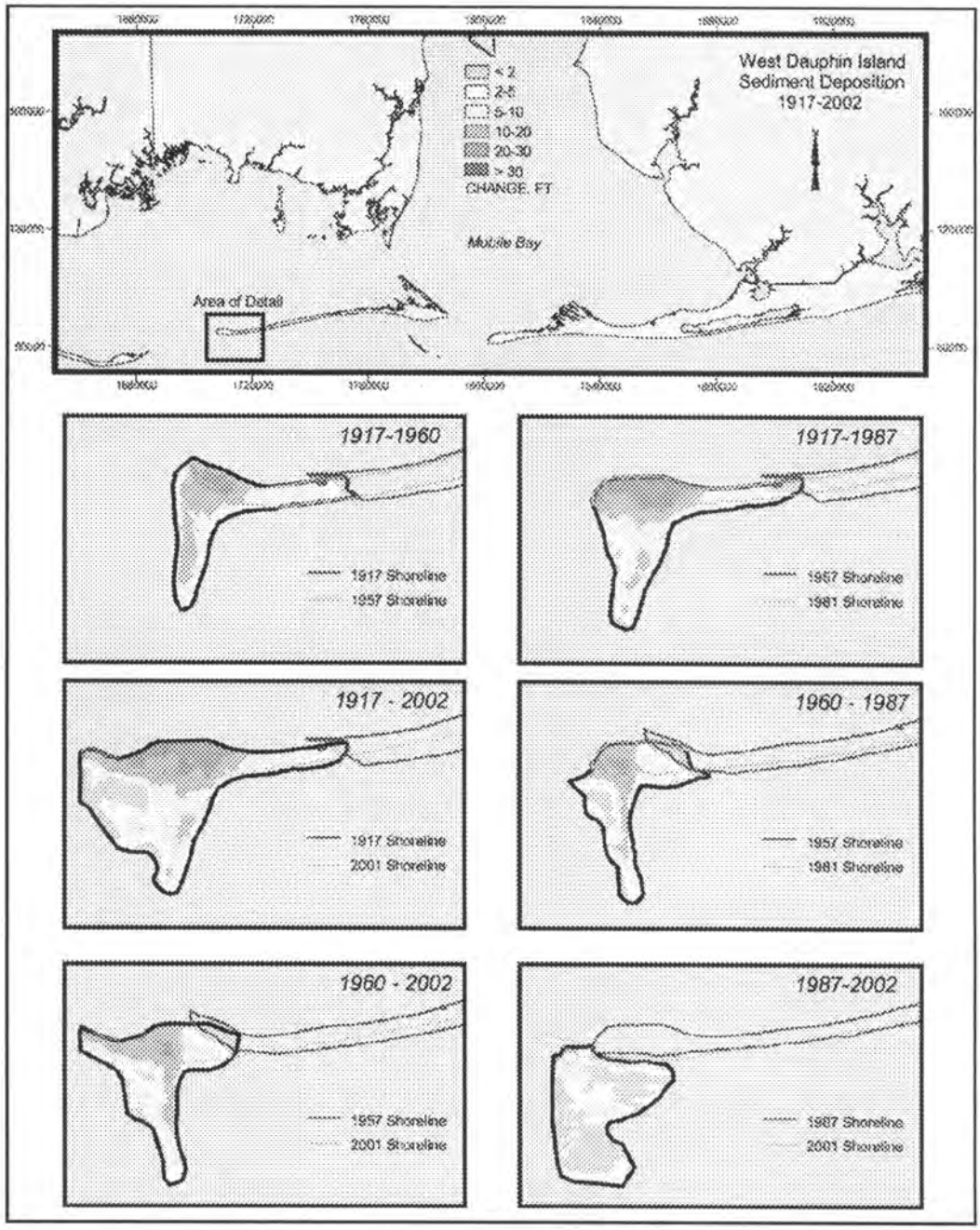

Figure 7-2. Sediment accumulation at the western end of Dauphin Island, 1917/20 to 2001/2002.

Table 7-3. Sediment accumulation at the western end of Dauphin Island in response to net westward longshore sand transport (accumulation polygons illustrated in Figure 7-2).

	1960/61	1982/92	2001/2002
1917/20	230,370[1]	195,704	202,697
	3,042,330[2]	3,853,774	5,580,772
1960/61		268,704	236,802
		2,699,775	3,422,885
1982/92			196,412
			3,321,997

[1] Accumulation Volume (cy/year); [2] Accumulation area (sq yd)

Table 7-4. Maximum potential volume uncertainty for bathymetric change data from western Dauphin Island, AL.

	1960/61	1982/92	2001/2002
1917/20	±30,500 (±68,500)	±18,500 (±43,500)	±34,000 (±70,000)
1960/61		±40,000 (±94,000)	±46,000 (±96,500)
1982/92			±104,000 (±218,000)

[1]Entire Surface, [2]Ebb-Tidal Delta/Channel

Local Changes

After compiling and analyzing at least 50 to 100 historical shoreline and bathymetry data sets, over a century of documentation regarding construction and maintenance dredging history for the channel across the Mobile Outer Bar, detailed histories of tropical cyclones in the northern Gulf of Mexico, and coastal processes data sets in support of numerical modeling, sediment transport and morphology changes at the shoreline and on the Mobile Pass ebb-tidal delta were documented within the context of data coverage and measurement uncertainty. Local changes resulting from navigation channel dredging involved direct removal of sediment from the outer bar to depths at least twice that of the shallowest point across the bar prior to dredging. Channel location has been fixed at its westernmost position since the mid-1800s. Natural westward migration of the channel controlled its current location.

Maintenance dredging captured a substantial quantity of littoral sand from east of the entrance, but a time series of bathymetric changes for the ebb-tidal delta indicated that sand bypassing from east-to-west remained active as channel construction and maintenance occurred. For most of the historical record, sand dredged from the outer bar channel was deposited offshore at a site just west of the navigation channel. Water depths in the area are between 30 and 40 ft, and bathymetric change surfaces indicate that sand from this offshore disposal site is

supplying sediment to the southwestern end of the ebb-tidal delta. Overall, large volumes of sand are being transported onto the western lobe of the inlet shoals, resulting in net deposition in this area and sufficient transport to Dauphin Island to mend storm-related breaches and washover surge channels. This process is supported by numerical modeling results documenting transport pathways and sedimentation patterns consistent with historical trends (see Figures 5-32 through 5-34). Furthermore, sand supply is so robust that island expansion to the west has continued at a relatively consistent rate with or without channel dredging.

Shoal migration and growth on the western lobe of the ebb-tidal delta is controlled by storm frequency and magnitude, and the availability of sand from the eastern side of the channel. Sand transported from east of Mobile Pass has resulted in net deposition on both lobes of the ebb-tidal delta prior to and after dredging commenced. Although storm impacts on sedimentation trends were indicated in a few of the change data sets, recovery to normal depositional patterns was rapid. Overall, there appears to be no measurable negative local impacts to the ebb-tidal delta or Dauphin Island associated with channel dredging.

Regional Changes

Regional changes prior to channel dredging were consistent with those identified after dredging commenced. As stated above, natural channel migration controlled channel location and may have been instrumental in promoting sand bypassing just south of Sand Island Lighthouse where the channel offset formed during westward migration in the early to mid-1900s. The capacity of this inlet system to continue bypassing sand from east-to-west during channel development and maintenance attests to the quantity of material available for transport. Furthermore, because dredged material from the channel appears to have been placed within the active transport system offshore and west of the channel between the 30- and 40-ft depth contours, onshore transport of sand by wave-generated currents during storms is able to supply dredged material to the ebb-tidal delta. Again, transport and bottom change simulations support this finding (see Figures 5-32 through 5-34).

Without the existence of these transport processes, it is difficult to envision how such large quantities of sand could be depositing on both lobes of the ebb-tidal delta, along the shoreline of Dauphin Island to close breaches and add elevation to low-relief washover deposits, and to promote continued growth of Dauphin Island to the west. Similar to local change, there appears to be no measurable negative regional impacts to the ebb-tidal delta or Dauphin Island associated with channel dredging across the Mobile Pass Outer Bar.

8 Conclusions and Recommendations

Sediment erosion, transport, and deposition in coastal Alabama is controlled by storm wave and current processes that produce net littoral transport to the west. The east-to-west gradient in transport is so dominant that minor reversals are not evident in shoreline, bathymetry, or photographic data sets. Effectively, net and gross transport are nearly equal. This bias in transport makes determination of net transport pathways and quantities relatively straightforward.

Historical shoreline and bathymetry data; dredging records; tropical cyclone records; coastal process data sets; and wave, current, and morphologic change modeling results were analyzed to evaluate the potential impact of channel dredging across the Mobile Pass Outer Bar Channel on erosion processes along Dauphin Island and on the ebb-tidal delta west of the navigation channel. In addition, transport pathways and quantities derived during the time of major dredging activities were evaluated in light of natural sand bypassing and shoal development and migration on the Mobile Pass ebb-tidal delta.

Analysis of shoreline position change between 1847/48 and 2006 revealed a common link associated with geomorphic evolution of Dauphin Island. Major changes in island configuration west of Pelican Island were always associated with hurricanes or tropical storms. Every breach recorded along central Dauphin Island (starting in 1853) was connected with a specific storm (or series of storms). Furthermore, all breaches filled within a relatively short post-storm recovery period (decade or so). The breach initiated by Hurricane *Ivan* (2004) and expanded during Hurricane *Katrina* (2005) still exists, but May 2007 photography indicates the breach is gradually closing. The net result of storm overwash and breaching is rapid landward movement (not net erosion) of the Gulf and Sound shorelines. This process, called barrier island rollover, allows the low-profile portion of the barrier island to maintain its integrity at a landward location after major storms.

The primary requirement for breach closure and island recovery is a constant supply of sand updrift of the damaged island. If sufficient sand quantities were not being supplied to the island throughout the historical record, storm breaches along central Dauphin Island would be difficult to fill and beaches would not recover very rapidly. Furthermore, island growth to the west has lengthened the island approximately 5.2 miles since 1847/48, 2.9 miles of which occurred since 1917/20 (the period of major dredging activity in the outer bar channel). Sand transport from Pelican Island and

the west lobe of the ebb-tidal delta had to be maintained throughout the period of channel dredging to repair storm damage and promote island growth.

Analysis of bathymetry data at and adjacent to the Mobile Pass ebb-tidal delta indicated the same response as shoreline data. Pelican and Sand Islands are emergent features that have formed, migrated, and eroded in response to storms and post-storm processes. In addition to creating a 5-mile breach along central Dauphin Island, the July 1916 hurricane degraded most of the shoals and islands on the ebb-tidal delta. Only a small portion of Pelican Island remained above water after the storm. However, shoals and islands on the west lobe of the delta continued to grow and migrate to the northwest between 1917/20 and 1986/2002 (periodically disrupted by hurricanes). By 2002, approximately 85 years after major dredging commenced, Pelican Island had expanded to its greatest extent since 1908. This is the same period under which breach infilling and westward island growth were occurring on Dauphin Island. A simple sand balance evaluation requires that east-to-west sand transport across the channel, on to the ebb-tidal delta, and northwest to Dauphin Island be maintained to produce net deposition on the delta, breach closure, and island expansion along the barrier island west of Pelican Island.

Bathymetric change analysis indicates consistent deposition for the entire ebb-tidal delta prior to and after channel dredging, except for two periods where the end dates were close to major storms. The magnitude of deposition on the delta prior to channel dredging was similar to net deposition recorded during major dredging activities. The observation that net deposition is the trend on the ebb-tidal delta and on Dauphin Island during channel dredging indicates the requirement for an external source of sand and active transport processes to redistribute the sand. If the channel were a long-term total littoral barrier and maintenance dredging and offshore placement were removing sediment from the active transport system, one would expect the rate of sand volume change on the west lobe of the ebb-tidal delta to decrease, not increase. In turn, if sand transport to Dauphin Island were not consistent with pre-dredging quantities, one would not expect storm breaches on the island to recover concomitant with rapid island growth to the west.

Wave, hydrodynamic, and sediment transport modeling were conducted to provide a process link to morphologic response. Wave modeling results illustrated a trend of net transport to the west throughout the study area, consistent with all morphology change analyses. Maximum transport magnitudes occurred near Mobile Point and western Dauphin Island. Morphologic modeling, which includes wave and current modeling, indicated wave-driven transport dominates changes to bathymetry on the Mobile Pass ebb-tidal delta. Under average tide and wave conditions, predicted

bottom changes documented the pattern of channel margin deposition and bypassing to the western lobe of the ebb-tidal delta illustrated in historical bathymetric change results. During storms, sediment from most locations on the ebb-tidal delta, on both sides of the navigation channel, generally moved to the north-northwest.

Patterns of bathymetric change illustrated in Figure 4-10 are well-described by modeling results. Seafloor changes on the outer margins of the ebb-tidal delta reflect sand movement under storm conditions (see Figures 5-32 to 5-34), and depositional patterns near the latitude of Sand Island Lighthouse reflect transport dynamics associated with average tide and wave conditions (see Figures 5-29 to 2-31). The link between historical sand bypassing discussed in Chapter 4 and the dominant processes responsible for patterns of deposition are well-documented when comparing wave-current simulations and bathymetric change results. Although morphology change predictions are qualitative in nature, the trends revealed from modeling are consistent with and confirm findings based on analysis of historical bathymetry data.

A sediment budget was developed to link all data sets analyzed. Shoreline and bathymetry change provided transport volumes along the shore and on the ebb-tidal delta. Dredging data also were incorporated in the analysis. Net transport from east-to-west was dominant in all parts of the system. Net deposition over the entire ebb-tidal delta required substantial transport quantities from the east. The flux of sediment from the Morgan Peninsula Gulf beach and nearshore to the east side of the ebb-tidal delta was estimated at 473,000 cy annually, 55,000 cy/year of which bypass the channel to the west (274,000 cy/year was dredged from the channel). Bathymetric change analysis identified the general location of the offshore disposal site west of the channel mouth, and there appears to be a direct connection between deposition on the western side of the outer bar and the offshore disposal site. Wave and tide simulations indicated that the disposal site was located in the area of north-northwest transport illustrated for storm conditions (see Figure 5-33 and 5-34). After calculating sediment accumulation at the disposal site between 1917/20 and 1986, it was determined that approximately 158,000 cy/year was supplied to the western lobe of the delta. Accounting for net deposition on the western lobe of the delta, approximately 60,000 cy/year was provided to Dauphin Island to nourish and expand the island to the west. These volumes were required to recreate changes recorded between 1917/20 and 1984/87.

Overall, net sediment transport from east-to-west between 1917/20 and 1984/87 has been supplying sand quantities necessary to produce net deposition on the islands and shoals of the ebb-tidal delta, infill and nourish storm breaches and washover

surge channels on Dauphin Island, and promote growth of western end of the island, even though channel dredging has been active. Based on all of this information, there appears to be no measurable negative impacts associated with historical channel dredging across the Mobile Pass Outer Bar.

According to dredging records, disposal procedures in recent years have been to place as much of the sand dredged from the outer bar channel as possible in the SIBUA (beneficial sand disposal area; see Figure 1-23). Because there is no guarantee that sand bypassing and transport from the historical offshore disposal site will continue at rates shown in the sediment budget, it is recommended that procedures followed in recent years for disposal of bar channel sand in the SIBUA be continued for the life of the project.

9 References

Anders, F.J. and M.R. Byrnes, 1991. Accuracy of shoreline change rates as determined from maps and aerial photographs. Shore and Beach, 59(1): 17-26.

ARCE, 1896-1990. Improvement of Rivers and Harbors: Mobile Outer Bar and Mobile Harbor. Annual Reports of the Corps of Engineers, Washington, DC.

Battjes, J.A. and J.P. Janssen, 1978. Energy loss and set-up due to breaking of random waves. Proc. 23rd Int. Conf. Coastal Engineering, ASCE, pp. 569-587.

Baker, J.L. and M.R. Byrnes, 2004. Appendix F: Shoreline and Bathymetry Data. In: Kraus, N.C. and H.T. Arden (editors), North Jetty Performance and Entrance Channel Maintenance, Grays Harbor, Washington. Technical Report ERDC/CHL TR-03-12, US Army Engineer Research and Development Center, Vicksburg, MS.

Balsillie, J.H., 1975. Analysis and Interpretation of Littoral Environment Observation (LEO) and Profile Data Along the Western Panhandle Coast of Florida. USAE Waterways Experiment Station, Coastal Engineering Research Center, Technical Memorandum 49, 104 p.

Bearden, B.L. and R.L. Hummell, 1990. Geomorphology of Coastal Sand Dunes, Morgan Peninsula, Baldwin County, Alabama. Geological Survey of Alabama Circular 150, 71 pp.

Bedford, K.W., and J. Lee, 1994. Near-bottom sediment response to combined wave-current conditions, Mobile Bay, Gulf of Mexico. Journal of Geophysical Research, 16: 161-177.

Bentley, S.J., Y. Furukawa, and W.C. Vaughan, 2000. Record of event sedimentation in Mississippi Sound. Gulf Coast Association of Geological Societies Transactions, 50: 715-723.

Bentley, S.J., T.R. Keen, C.A. Blain, and W.C. Vaughan, 2002. The origin and preservation of a major hurricane event bed in the northern Gulf of Mexico: Hurricane Camille, 1969. Marine Geology, 186: 423-446.

Blake, E.S., E.N. Rappaport, and C.W. Landsea, 2007. The Deadliest, Costliest, and Most Intense United States Tropical Cyclones from 1851 to 2006 (and Other Frequently Requested Hurricane Facts). NOAA Technical Memorandum NWS TPC-5, National Hurricane Center, Miami, FL, 45 p.

Blanton, J.O., 1994. U.S. Southeast Continental Shelf Inner Shelf Processes Relevant to the Northeast Gulf of Mexico Inner Shelf. Proceedings of the Northeast Gulf of Mexico Physical Oceanography Workshop, U.S. Department of the Interior, Minerals Management Service, OCS Study 94-0044.

Bodge, K.R. and J.D. Rosati, 2003. Sediment Management at Inlets. In: Donald L. Ward (Ed.), Coastal Engineering Manual, Part V, Coastal Project Planning and Design, Chapter V-6, Engineer Manual 1110-2-1100, U.S. Army Corps of Engineers, Washington, DC.

Boone, P., 1973. Depositional systems of the Alabama, Mississippi, and western Florida coastal zone. Gulf Coast Association of Geological Societies Transactions, 23: 266-277.

Bossak, B.H., 2003. Early 19th Century U.S. Hurricanes: A GIS Tool and Climate Analysis. PhD Dissertation, Florida State University, Tallahassee, FL, 100 p.

Bossak, B.H. and J.B. Elsner, 2004. Plotting early nineteenth-century hurricane information. EOS, 85(20): 199.

Bowen, A. J. and D.L. Inman, 1966. Budget of Littoral Sands in the Vicinity of Port Arguello, California. Technical Memorandum No. 19, U.S. Army Engineer Waterways Experiment Station, Coastal Engineering Research Center, Vicksburg, MS.

Bruun, P., 1962. Sea level rise as a cause of shore erosion. American Society of Civil Engineers Proceedings, Journal Waterways and Harbors Division, 88: 33-74.

Bruun, P., 1983. Review of conditions for uses of the Bruun Rule of erosion. Coastal Engineering, 7: 77-89.

Bruun, P., 1988. The Bruun Rule of erosion by sea-level rise: a discussion of large-scale two- and three-dimensional usages. Journal of Coastal Research, 4(4): 627-648.

Buttolph, A. M., C.W. Reed, N.C. Kraus, N. Ono, M. Larson, B. Camenen, H. Hanson, T. Wamsley, and A.K. Zundel, 2006. Two-Dimensional Depth-Averaged Circulation Model CMS-M2D: Version 3.0, Report 2, Sediment Transport and Morphology Change. Technical Report ERDC/CHL-TR-06-7, US Army Engineer Research and Development Center, Coastal and Hydraulics Laboratory, Vicksburg, Mississippi.

Byrnes, M.R. and K.J. Gingerich, 1987. Cross-island profile response to Hurricane Gloria. In: N.C. Kraus (editor), Proceedings Coastal Sediments '87, American Society of Civil Engineers, New York, NY, p. 1486-1502.

Byrnes, M.R. and M.W. Hiland, 1995. Large-scale sediment transport patterns on the continental shelf and influence on shoreline response: St. Andrew Sound, Georgia to Nassau Sound, Florida, U.S.A. In: J.H. List and J.H.J. Terwindt (editors), Large-Scale Coastal Behavior. Marine Geology, 126: 19-43.

Byrnes, M.R. and R.A. McBride, 1996. Northeast Gulf of Mexico hard mineral resources study. Proceeding of the 15th Annual Information Transfer Meeting, U.S. Department of the Interior, Minerals Management Service, New Orleans, LA, pp. 481-486.

Byrnes, M.R. and J.L. Baker, 2003. Chapter 3: Inlet and Nearshore Morphodynamics. In: Kraus, N.C. and H.T. Arden (Editors), North Jetty Performance and Entrance Navigation Channel Maintenance, Grays Harbor, Washington, Volume I: Main Text. ERDC/CHL TR-03-12, Coastal and Hydraulics Laboratory, U.S. Army Engineer Research and Development Center, Vicksburg, MS, pp. 67-136.

Byrnes, M.R., J.L. Baker, and F. Li, 2002. Quantifying potential measurement errors and uncertainties associated with bathymetric change analysis. ERDC/CHL CHETN-IV-50, Coastal and Hydraulics Laboratory, U.S. Army Engineer Research and Development Center, Vicksburg, MS, 17 p.

Byrnes, M.R., S.F. Griffee, and H.R. Moritz, 2007. Engineering activities influencing historical sediment transport pathways at the Columbia River Mouth, WA/OR. In: N.C. Kraus and J.D. Rosati (editors), Proceedings Coastal Sediments '07, American Society of Civil Engineers, Reston, VA, pp. 1754-1767.

Byrnes, M.R., R.A. McBride, S. Penland, M.W. Hiland, and K.A. Westphal, 1991. Historical changes in shoreline position along the Mississippi Sound barrier islands. In: Coastal Depositional Systems in the Gulf of Mexico: Quaternary Framework and Environmental Issues, GCS-SEPM 12th Annual Research Conference, pp. 43-55.

Byrnes, M.R., R.M. Hammer, B.A. Vittor, J.S. Ramsey, D.B. Snyder, K.F. Bosma, J.D. Wood, T.D. Thibaut, and N.W. Phillips, 1999. Environmental Study of Identified Sand Resource Areas Offshore Alabama: Volume I: Main Text, Volume II: Appendices. U.S. Department of the Interior, Minerals Management Service, International Activities and Marine Minerals Division (INTERMAR), Herndon, VA. OCS Report MMS 99-0052, 326 pp. + 132 pp. appendices.

Chermock, R.L., P.A. Boone, and R.L. Lipp, 1974. The Environment of Offshore and Estuarine Alabama. Geological Survey of Alabama Information Series 51, 135 pp.

Cipriani, L.E. and G.W. Stone, 2001. Net longshore sediment transport and textural changes in beach sediments along the southwest Alabama and Mississippi barrier islands, USA. Journal of Coastal Research, 17(2):443-458.

Clarke, A.J., 1994. Overview of the Physical Oceanography of the Florida Shelf in the Study Region. Proceedings of the Northeast Gulf of Mexico Physical Oceanography Workshop, U.S. Department of the Interior, Minerals Management Service, OCS Study 94-0044.

Crowell, M., S.P. Leatherman, and M.K. Buckley, 1991. Historical shoreline change: error analysis and mapping accuracy. Journal of Coastal Research, 7(3): 839-852.

Davies, D.J. and R.L. Hummell, 1994. Lithofacies evolution from transgressive to highstand systems tracts, Holocene of the Alabama coastal zone. Gulf Coast Association of Geological Societies Transactions, 44: 145-153.

Dean, R.G. and M. Perlin, 1977. Coastal engineering study of Ocean City Inlet, Maryland. Proceedings Coastal Sediment '77, Charleston, South Carolina, p. 520-542.

Dolan, R.B. and P.J. Godfrey, 1973. Effects of Hurricane Ginger on the barrier islands of North Carolina. Bulletin Geological Society America, 84: 1329-1334.

Douglass, S.L., 1991. Summary of Existing Coastal Engineering Data for Dauphin Island, Alabama. College of Engineering Report No. 91-1, University of South Alabama, Mobile, AL, 39 pp.

Douglass, S.L., 1994. Beach erosion and deposition on Dauphin Island, Alabama, U.S.A. Journal of Coastal Research, 10(2): 306-328.

Douglass, S.L., 2001. "State-of-the-beaches" of Alabama: 2001. Report to Alabama Department of Economic and Community Affairs, 27 pp.

Douglass, S.L. and D.R. Haubner, 1992. Coastal Processes of Dauphin Island, Alabama. College of Engineering Report No. 92-1, University of South Alabama, Mobile, AL, 90 p. plus Appendices.

Douglass, S.L., D.T. Resio, and E.B. Hands, 1995. Impact of Near-Bottom Currents on Dredged Material Mounds Near Mobile Bay. Technical Report DRP-95-6, U.S. Army Engineers Waterways Experiment Station, Dredged Material Research Program, Vicksburg, MS.

Douglass, S.L. and A.E. Browder, 2005. Hurricane Ivan's impacts on the Alabama coast. Shore and Beach, 73(2/3): 71-78.

Doyle, L.J. and T.N. Sparks, 1980. Sediments of the Mississippi, Alabama, and Florida (MAFLA) Continental Shelf. Journal of Sedimentary Petrology, 50(3): 905-915.

Dunn, G.E. and B.I. Miller, 1964. Atlantic Hurricanes. Louisiana State University Press, Baton Rouge, LA, 377 p.

Ellis, M.Y., 1978. Coastal Mapping Handbook. U.S. Department of the Interior, Geological Survey, U.S. Department of Commerce, National Ocean Service, U.S. Government Printing Office, Washington, D.C., 199 pp.

Escoffier, F.F., 1958. Harrison County (Mississippi) artificial beach. American Society of Civil Engineers Transactions, 123: 817-823.

Fisher J.S. and D.K. Stauble, 1977. Impact of Hurricane Belle on Assateague Island washover. Geology, 5: 765-768.

Fong, D.A. and S.G. Monismith, 2004. Evaluation of the accuracy of a ship-mounted, bottom-tracking ADCP in a near-shore coastal flow. Journal of Atmospheric and Oceanic Technology, **21**: 1121–1128.

Foxgrover, A.C., S.A. Higgins, M.K. Ingraca, B.E. Jaffe, and R.E. Smith, 2004. Deposition, Erosion, and Bathymetric Changes in South San Francisco Bay: 1858-1983. USGS Open-File Report 2004-1192, U.S. Geological Survey, Reston, VA.

Froede, C.R., Jr., 2006a. A Hurricane Fredric-generated storm-surge deposit exposed along a surf-zone foredune scarp on Dauphin Island, Alabama, USA. Journal of Coastal Research, 22(2): 371-376.

Froede, C.R., Jr., 2006b. The impact of Hurricane Ivan (September 16, 2004) made across Dauphin Island, Alabama. Journal of Coastal Research, 22(3): 561-573.

Garcia, A. W., 1977. Dauphin Island Littoral Transport Calculations. U.S. Army Engineer Waterways Experiment Station, Hydraulics Laboratory, Vicksburg, MS, Miscellaneous Paper H-77-11, 12 pp.

Gelfenbaum, G. and R.P Stumpf, 1993. Observations of currents and density structure across a buoyant plume front. Estuaries, 16(1): 40-52.

Goda, Y., 1985. Random Seas and Design of Maritime Structures. University of Tokyo Press, Tokyo, Japan.

Graumann, A., T. Houston, J. Lawrimore, D. Levinson, N. Lott, S. McCown, S. Stephens, and D. Wuertz, 2005. *Hurricane Katrina – A Climatological Perspective.* NOAA National Climate Data Center, U.S. Department of Commerce, Asheville, NC, 27 p.

Guidroz, W.S., K.R. Poole, G.W. Stone, D. Dartez, and L.G. Pong, 2007. Contrasting sediment transport along the southwestern Louisiana and upper Texas shorelines: Impacts from Hurricane Rita, 2005. Shore and Beach, 75(1): 57-64.

Hands, E.B., 1991. Wide-area monitoring of Alabama berms. Marine Technology Society Conference, New Orleans, LA, p. 98-105.

Hands, E.B., 1992. Monitoring of Alabama Berms. Technical Note DRP-1-08, UASE Waterways Experiment Station, Dredging Research Program, Vicksburg, MS, 14 p.

Hands, E.B., 1994. Shoreward Movement and Other 5-yr Changes at the Sand Island Berms, Alabama. In: Proceeding of the 15th Western Dredging Association Conference, College Station, TX, pp. 223-235.

Hands, E.B. and M.C. Allison, 1991. Mound migration in deeper water and methods of categorizing active and stable depths. In: N.C. Kraus, K.J. Gingerich, and D.L. Kriebel (editors), Coastal Sediments '91, American Society of Civil Engineers, New York, NY, pp. 1985-1999.

Hardin, J.D., C.D. Sapp, J.L. Emplaincourt, and K.E. Richter, 1976. Shoreline and Bathymetric Changes in the Coastal Area of Alabama: A Remote Sensing Approach. Geological Survey of Alabama Information Series 50, 125 pp.

Harris, D.L., 1981. Tides and Tidal Datums in the United States. Special Report No. 7, U.S. Army Coastal Engineering Research Center, Fort Belvoir, VA, 382 p.

Hayes, M.O., 1967. Hurricanes as Geologic Agents: Case Studies of Hurricane Carla, 1961, and Cindy, 1963. Texas Bureau of Economic Geology, Report of Investigation 61, 54 p.

Hess, K.W., 2004. Tidal datums and tidal coordination. In: Byrnes, M.R., M. Crowell, and C. Fowler (editors), Shoreline Mapping and Change Analysis: Technical Considerations and Management Implications. Journal of Coastal Research, Special Issue 38, pp. 33-43.

Hicks, S.D., 1981. Tidal datums and their uses – A summary. Shore and Beach, 53(1): 27-32.

Hubbard, D.K., G.F. Oertel, and D. Nummedal, 1979. The role of waves and tidal currents in the development of tidal-inlet sedimentary structures and sand body geometry examples from North Carolina, South Carolina, and Georgia. Journal of Sedimentary Petrology, 49(4): 1073-1092.

Hubertz, J.M., R.M. Brooks, W.A. Brandon, and B.A. Tracy, 1993. Hindcast Wave Information for the U.S. Atlantic Coast. WIS Report 30, U.S. Army Engineer Waterways

Experiment Station, Coastal Engineering Research Center, Wave Information Study, Vicksburg, MS.

Hummell, R.L., 1990. Main Pass and the Ebb-Tidal Delta of Mobile Bay, Alabama. Geological Survey of Alabama Circular 146, 45 pp.

Hummell, R.L., 1996. Holocene Geologic History of the West Alabama Inner Continental Shelf, Alabama. Geological Survey of Alabama Circular 189, 131 pp.

Hummell, R.L. and S.J. Parker, 1995. Holocene Geologic History of Mobile Bay, Alabama. Geological Survey of Alabama Circular 186, 96 pp.

Hummell, R.L. and W.E. Smith, 1995. Geologic and Environmental Characterization and Near-term Lease Potential of an Offshore Sand Resource Site for Use in Beach Nourishment Projects on Dauphin Island, Alabama. Final Report, Prepared by the Geological Survey of Alabama in fulfillment of U.S. Department of the Interior, Minerals Management Service Cooperative Agreement No. 14-35-0001-30725, 165 pp.

Hummell, R.L. and W.E. Smith, 1996. Geologic Resource Delineation and Hydrographic Characterization of an Offshore Sand Resource Site for Use in Beach Nourishment Projects on Dauphin Island, Alabama. Final Report, Prepared by the Geological Survey of Alabama in cooperation with the Department of Geology, University of Alabama in fulfillment of U.S. Department of the Interior, Minerals Management Service Cooperative Agreement No. 14-35-0001-30781, 169 pp.

Isphording, W.C. and G.C. Flowers, 1987. Mobile Bay: The right estuary in the wrong place. In: T.A. Lowrey (editor), Symposium on the Natural Resources of the Mobile Bay Estuary, Mississippi-Alabama Sea Grant Consortium, MASGP-87-007, p. 165-174.

Isphording, W.C. and F.D. Imsand, 1991. Cyclonic events and sedimentation in the Gulf of Mexico. In: N.C. Kraus, K.J. Gingerich, and D.L. Kriebel (editors), Coastal Sediments '91, American Society of Civil Engineers, New York, NY, pp. 1122-1136.

Isphording, W.C., F.D. Imsand, and R.B. Jackson, 1996. Fluvial sediment characteristics of the Mobile River delta. Gulf Coast Association of Geological Societies Transactions, 46: 185-191.

Jarrell, J.D., P.J. Hebert, and B.M. Mayfield, 1992. Hurricane Experience Levels of Coastal County Populations - Texas to Maine. NOAA Technical Memorandum NWS-NHC-46, 152 p.

Jarvinen, B.R., C.J. Neumann, and A.S. Davis, 1984. A Tropical Cyclone Data Tape for the North Atlantic Basin, 1886-1983: Contents, Limitations, and Uses. NOAA Technical Memorandum NWS-NHC-22, 21 p.

Kamphuis, J.W., 1990. Alongshore sediment transport rate. Proceedings 22nd Coastal Engineering Conference, ASCE, New York.

Kinoshita, K. and M. Noble, 1995. Current Data from the Northern Gulf of Mexico. Open File Report 95-633, U.S. Department of the Interior, U.S. Geological Survey.

Kraus, N.C., 2000. Reservoir model of ebb-tidal shoal evolution and sand bypassing. Journal of Waterway, Port, Coastal, and Ocean Engineering, 126(3): 305-313.

Kraus, N.C., C.C. Ebbesmeyer, and O.P. Smith., 1991. Introduction to the Mobile, Alabama, Field Data Collection Project. In N.C. Kraus (editor), Mobile, Alabama, Field Data Collection Project, 18 August – 2 September 1989: Report 1, Technical Report DRP-91-3, USAE Waterways Experiment Station, CERC, Vicksburg, MS, p. 7-52.

Lamb, G.M., 1987. Erosion downdrift from tidal passes in Alabama and the Florida Panhandle. Bulletin of the Association of Engineering Geologists, 24: 359-362.

Larson, M. and N.C. Kraus, 1995. Prediction of cross-shore sediment transport at different temporal and spatial scales. In: J.H. List and J.H.J. Terwindt (editors), Large-Scale Coastal Behavior. Marine Geology, 126: 111-127.

Lee, W., 1998. Sand Island Lighthouse Chronicles. Beacon Publishing, Theodore, AL, 89 p.

Lewis, J.K. and R.O. Reid, 1985. Local wind forcing of a coastal sea at subinertial frequencies. Journal of Geophysical Research, 90: 934-944.

Ludlum, D.M., 1963. Early American Hurricanes: 1492 to 1870. American Meteorological Society, 198 p.

Ludwick, J.C., 1964. Sediments in Northeastern Gulf of Mexico. In: R.L. Miller (ed.), Papers in Marine Geology, Macmillan Co., New York, NY, pp. 204-238.

Marmer, H.A., 1951. Tidal Datum Planes. Special Publication No. 135, NOAA National Ocean Service, U.S. Coast and Geodetic Survey, U.S. Government Printing Office, Washington, D.C., 142 p.

Mars, J.C., A.W. Shultz, and W.W. Schroeder, 1992. Stratigraphy and Holocene evolution of Mobile Bay in southwestern Alabama. Gulf Coast Association of Geological Societies Transactions, 42: 529-542.

McBride, R.A., 1997. Synthesis of Hard Mineral Resources of the Florida Panhandle Shelf: Spatial Distribution and Subsurface Evaluation. Final Report, U.S. Department of the Interior, Minerals Management Service, Contract No. 1435-01-96-CT-30812, 5 p. + 727 p. appendix.

McBride, R.A. and M.R. Byrnes, 1995. Surficial sediments and morphology of the southwestern Alabama/western Florida panhandle coast and shelf. Gulf Coast Association of Geological Societies Transactions, 45: 393-404.

McBride, R.A., L.C. Anderson, A. Tudoran, and H.H. Roberts, 1999. Holocene stratigraphic architecture of a sand-rich shelf and the origin of linear shoals: northeastern Gulf of Mexico. In: Bergman, K.M. and Snedden, J.W. (editors), Isolated Shallow Marine Sand Bodies; Sequences, Stratigraphic Analysis, and Sedimentologic Interpretation. SEPM Special Publication 64, p. 95-126.

McBride, R.A., M.R. Byrnes, S. Penland, D.L. Pope, and J.L. Kindinger, 1991. Geomorphic History, Geologic Framework, and Hard Mineral Resources of the Petit Bois Pass Area, Mississippi-Alabama. In: Coastal Depositional Systems in the Gulf of Mexico: Quaternary Framework and Environmental Issues, GCS-SEPM 12th Annual Research Conference, pp. 116-127.

McGehee D., J.P. McKinney, W.E. Grogg, and E.B. Hands, 1994. Monitoring of Waves and Currents at the Dredged Material Mounds Offshore of Mobile Bay, Alabama. Technical Report DRP-94-4, U.S. Army Engineer Waterways Experiment Station, Dredged Material Research Program, Vicksburg, MS.

Meyer, T.H., D.R. Roman, and D.B. Zilkoski, 2004. What does height really mean? Part I: Introduction. Surveying and Land Information Science, 64(4): 223-233.

Morang, A. and L. Parson, 2002. Coastal Morphodynamics. In: A. Morang (editor), Part IV, Coastal Geology, Chapter IV-3. Engineer Manual 1110-2-1100, U.S. Army Engineer Research and Development Center, Vicksburg, MS.

Morton, R.A., 2007. Historical Changes in the Mississippi-Alabama Barrier Islands and the Roles of Extreme Storms, Seal Level, and Human Activities. U.S. Geological Survey Open File Report 2007-1161, Coastal and Marine Geology Program, St. Petersburg, FL, 38 p.

Mukai, A. Y., J.J. Westerink, R.A. Luettich, and D.J. Mark, 2001. East Coast 2001, A Tidal Constituent Database for the Western North Atlantic, Gulf of Mexico and Caribbean Sea. U.S. Army Engineer Research and Development Center, Vicksburg, MS.

Murray, S.P., 1970. Bottom currents near the coast during hurricane Camille. Journal of Geophysical Research, 75(24): 4579-4582.

Nichols R.L. and A.F. Marston, 1939. Shoreline changes in Rhode Island produced by hurricane of September 21, 1938. Bulletin Geological Society America, 50: 241-246.

NOAA, 2001. Tidal Datums and Their Applications. NOAA Special Publication NOS CO-OPS 1, U.S. Department of Commerce, National Oceanic and Atmospheric Administration, Silver Spring, MD, 112 p.

NOAA, 2003. Computational Techniques for Tidal Datums Handbook. NOAA Special Publication NOS CO-OPS 2, U.S. Department of Commerce, National Oceanic and Atmospheric Administration, Silver Spring, MD, 98 p.

Nummedal, D., S. Penland, R. Gerdes, W. Schramm, J. Kahn, and H. Roberts, 1980. Geologic response to hurricane impact on low-profile Gulf Coast barriers. Gulf Coast Association of Geological Societies Transactions, 30: 183-195.

Otvos, E.G., 1973. Sedimentology. In: J.Y. Christmas (editor), Cooperative Gulf of Mexico Estuarine Inventory Study, Mississippi. Gulf Coast Research Laboratory, Ocean Springs, MS, Project 2-25-R, p. 123-139.

Otvos, E.G, 1979. Barrier island evolution and history of migration, north-central Gulf Coast. In: S.P. Leatherman (ed.), Barrier Islands, Academic Press, New York, NY, pp. 291-319.

Otvos, E.G., 1981. Barrier island formation through nearshore aggradation – stratigraphic and field evidence. Marine Geology, 43: 195-243.

Otvos, E.G., 2006. Discussion of : Froede, C.R., Jr., 2006. The impact the Hurricane Ivan (September 16, 2006) made across Dauphin Island, Alabama. *Journal of Coastal Research*, 22(2), 561-573. Journal of Coastal Research, 22(6): 1585-1588.

Otvos, E.G. and Giardino, M.J., 2004. Interlinked barrier chain and delta lobe development, northern Gulf of Mexico. Sedimentary Geology, 169: 47-73.

Parker, S.J., 1990. Assessment of Nonhydrocarbon Mineral Resources in the Exclusive Economic Zone Offshore Alabama. Geological Survey of Alabama Circular 147, 73 pp.

Parker, S.J., A.W. Shultz, and W.W. Schroeder, 1992. Sediment Characteristics and Seafloor Topography of a Palimset Shelf, Mississippi-Alabama Continental Shelf. In: Quaternary Coasts of the United States: Lacustrine and Marine Systems. SEPM Special Publication 48, pp. 243-251.

Parker, S.J., D.J. Davies, and W.E. Smith, 1997. Geologic, Economic, and Environmental Characterization of Selected Near-term Leasable Offshore Sand Deposits and Competing Onshore Sources for Beach Nourishment. Geologic Survey of Alabama, Environmental Geology Division, Tuscaloosa, AL. Circular 190, 173 pp. + app.

Parker, S.J., D.J. Davies, W.E. Smith, T.G. Crawford, and R. Kelly, 1993. Geological, Economic, and Environmental Characterization of Selected Near-term Leasable Offshore Sand Deposits and Competing Onshore Sources for Beach Nourishment. Final Report. Prepared by the Geological Survey of Alabama in fulfillment of U.S. Department of the Interior, Minerals Management Service Cooperative Agreement No. 14-35-0001-30630, 223 pp.

Petrie, G., 1991. Modelling, interpolation and contouring procedures. In: Petrie, G. and Kennie, T.J.M. (editors), Terrain Modelling in Surveying and Civil Engineering, McGraw-Hill, Inc., New York, NY, p. 112-127.

Pilkey, O.H., R.S. Young, S.R. Riggs, A.W. Smith, H. Wu, and W.D. Pilkey, 1993. The concept of shoreface profile of equilibrium: a critical review. Journal of Coastal Research, 9: 255-278.

Reid, R.O., 1994. Preliminary Results of LATEX Relevant to the Proposed Study. Proceedings of the Northeast Gulf of Mexico Physical Oceanography Workshop, U.S. Department of the Interior, Minerals Management Service OCS Study 94-0044.

Resio, D.T., and B.A. Tracy, 1983. A Numerical Model for Wind-Wave Prediction in Deepwater. WIS Report 12, U.S. Army Engineer Waterways Experiment Station, Coastal Engineering Research Center, Wave Information Study, Vicksburg, MS.

Rosati, J.D., 2005. Concepts in sediment budgets. Journal of Coastal Research, 21(2): 307-322.

Rosati, J. D. and N.C. Kraus, 1999. Formulation of Sediment Budgets at Inlets. Coastal Engineering Technical Note CETN-IV-15 (Revised August 1999), U.S. Army Engineer Research and Development Center, Vicksburg, MS.

Sallenger, A.H., C.W. Wright, and J. Lillycrop, 2005. Coastal impacts of the 2004 hurricanes measured with airborne Lidar: initial results. Shore and Beach, 73(2/3): 10-15.

Sanchez, T.A. and S.L. Douglass, 1994. Alabama Shoreline Change Rates: 1970 – 1993. Final Report for the Coastal Programs Office, Alabama Department of Economic and community Affairs, Montgomery, AL, 16 p. plus Appendices.

Sapp, C.D., J.G. Emplaincourt, and J.D. Hardin, 1975. Remote sensing of shoreline dynamics, Mobile Bay area, 1900-1975. Gulf Coast Association of Geological Societies Transactions, 25: 153-167.

Sargent, F.E., 1988. Case Histories of Corps Breakwater and Jetty Structures, Report 2, South Atlantic Division, Perdido Pass Jetties. Technical Report REMR-CO-3, USAE Waterways Experiment Station, Coastal Engineering Research Center, Vicksburg, MS, p. 100-104.

Sawyer, W.B., C. Vaughan, D. Lavoie, Y. Furukawa, N. Carnaggio, J. Maclean, and E. Populis, 2001. Northern Gulf Littoral Initiative (NGLI), Geology and Physical Properties of Marine Sediments in the N.E. Gulf of Mexico: Data Repoort. Naval Oceanographic Office, Stennis Space Center, MS, 12 p.

Schramm, W.E., S. Penland, R.G. Gerdes, and D. Nummedal, 1980. Effects of Hurricane Fredric on Dauphin Island, Alabama. Shore and Beach, 48(3): 20-25.

Schroeder, W.W. and W. Wiseman, 1985. An analysis of the winds *1974-1984) and sea level elevations (1973-1983) in coastal Alabama. Mississippi-Alabama Sea Grant Publication MASGP-84-024.

Schroeder, W.W., S.P Dinnel, F.J. Kelly, W.J. Wiseman, 1994. Overview of the Physical Oceanography of the Louisiana-Mississippi-Alabama Continental Shelf. Proceedings of the Northeast Gulf of Mexico Physical Oceanography Workshop, U.S. Department of the Interior, Minerals Management Service OCS Study 94-0044.

Scott, A.J., R.A. Hoover, and J.H. McGowen, 1969. Effects of Hurricane Beulah, 1967 on Texas coastal lagoons and barriers. In: A.A Castanaras and F.B. Phleger (editors), Lagunas Costeras, un Simposio, pp. 221-236.

Seim, H. E., B. Kjerfve, and J.E. Sneed, 1987. Tides of Mississippi Sound and the adjacent continental shelf. Estuarine, Coastal and Shelf Science, 25: 143-156.

Shalowitz, A.L., 1964. Shoreline and Sea Boundaries, Volume 2. U.S. Department of Commerce Publication 10-1, U.S. Coast and Geodetic Survey, U.S. Government Printing Office, Washington, DC, 420 pp.

Sherrill, C.O., 1913. Mobile Harbor, AL. Professional Memoirs, Corps of Engineers, United States Army and Engineer Department at Large, Washington, DC, Vol. V, No. 19, p. 1-27.

Smith, J.M., D.T. Resio, and A.K. Zundel, 1999. STWAVE: Steady-State Spectral Wave Model. Instructional Report CHL-99-1, U.S. Army Engineering Waterways Experiment Station, Vicksburg, MS.

Smith, W.E., 1981. Geologic Features and Erosion Control in Alabama Gulf Coastal Area. Geological Survey of Alabama Information Series 57, 57 pp.

Smith, W.E., 1988. Geomorphology of the Mobile Delta. Alabama Geological Survey Bulletin 132, 133 p.

Smith, W.E., 1990. Regimes contributory to progressive loss of Alabama coastal shoreline and wetlands. Gulf Coast Association of Geological Societies Transactions, 40: 793-796.

Stone, G.W. and P. Wang, 1999. The importance of cyclogenesis on the short-term evolution of Gulf Coast barriers. Gulf Coast Association of Geological Societies Transactions, 49: 478-486.

Stone, G.W., F.W. Stapor, J.P. May, and J.P. Morgan, 1992. Multiple sediment sources and a cellular, non-integrated, longshore drift system: northwest Florida and southeast Alabama coast, USA. Marine Geology, 105: 141-154.

Stone, G.W., B. Liu, D.A. Pepper, and P. Wang, 2004. The importance of extratropical and tropical cyclones on the short-term evolution of barrier islands along the northern Gulf of Mexico, USA. Marine Geology, 210: 63-78.

Stumpf, R.P., and G. Gelfenbaum, 1990. Effects of high river discharge on suspended sediments in Mobile Bay, Alabama. EOS, 71: 1,406-1,407.

Stumpf, R.P., G. Gelfenbaum, J.R. Pennock, 1993. Wind and tidal forcing of a buoyant plume, Mobile Bay, Alabama. Continental Shelf Research, 13(11): 1281-1301.

Swift, D.J.P. and A.W. Niedoroda, 1985. Fluid and Sediment Dynamics on Continental Shelves. In: Tillman, R.W., D.J.P. Swift, and R.G. Walker (editors), Shelf Sands and Sandstone Reservoirs, SEPM Short Course No. 13, Tulsa, OK, pp. 47-133.

Tannehill, I.R., 1956. Hurricanes, their nature and history. Princeton University Press, 308 p.

Todd, T.W., 1968. Dynamic diversion: influence of longshore current-tidal flow interaction on chenier and barrier island plains. Journal of Sedimentary Petrology, 38: 734-746.

Tracy, B. A., 1999. Directional Characteristics of the 1990-1999 Wave Information Studies. Gulf of Mexico Hindcast. Ft. Belvoir, Defense Technical Information Center. http://handle.dtic.mil/100.2/ADA423403.

Tracy, B.A. and A. Cialone, 2004. Comparison Of Gulf Of Mexico Wave Information Studies (WIS) 2-G Hindcast With 3-G Hindcasting. Engineer Research and Development Center, Coastal and Hydraulics Laboratory, Waterways Experiment Station, Vicksburg, Mississippi, USA.

USACE, 1955. Perdido Pass (Alabama Point) Alabama Beach Erosion Control Study. U.S. Army Corps of Engineers, Mobile District, Mobile, AL.

USACE, 1978. Feasibility Report for Beach Erosion Control and Hurricane Protection, Mobile County, Alabama (Including Dauphin Island). U.S. Army Corps of Engineers, Mobile District, Mobile, AL, 142 pp. plus Attachments.

USACE, 1984. Exploration and Production of Hydrocarbon Resources in Coastal Alabama and Mississippi. U.S. Army Corps of Engineers, Mobile District, Mobile, AL, 615 pp.

USGS, 2007. Real-Time Water Data for the Nation. US Geological Survey Station 02471019, Tensaw River near Mount Vernon, AL and USGS Station 02470629, Mobile River at River Mile 31 at Bucks, AL. http://waterdata.usgs.gov/usa/nwis/uv?

Walton, T. L., 1974. Calculation of Littoral Drift Roses for the Alabama and Mississippi Gulf Coastline. Coastal and Oceanographic Engineering Department, University of Florida, Gainesville, FL, UFL/COEL-74-023, 26 p.

Westerink, J.J., C.A. Blain, R.A. Luettich, and N.W. Scheffner, 1994. ADCIRC: An Advanced Three-Dimensional Circulation Model for Shelves, Coasts and Estuaries; Report 2: Users Manual for ADCIRC-2DDI. Dredging Research Program Technical Report, U.S. Army Engineers Waterways Experiment Station, Vicksburg, MS., 156 pp.

Wilson, W.K., 1951. Beach erosion problems in the Mobile District. Shore and Beach, 19(2): 8-10.

Wiseman, W.J., W.W. Schroeder, and S.P. Dinnel, 1988. Shelf-estuarine water exchanges between the Gulf of Mexico and Mobile Bay, Alabama. American Fisheries Society Symposium, 3: 1-8.

Report Appendices

Appendix A

Gulf and Atlantic Hurricane Tracks: 1851 to 2005; Category 3 or Stronger

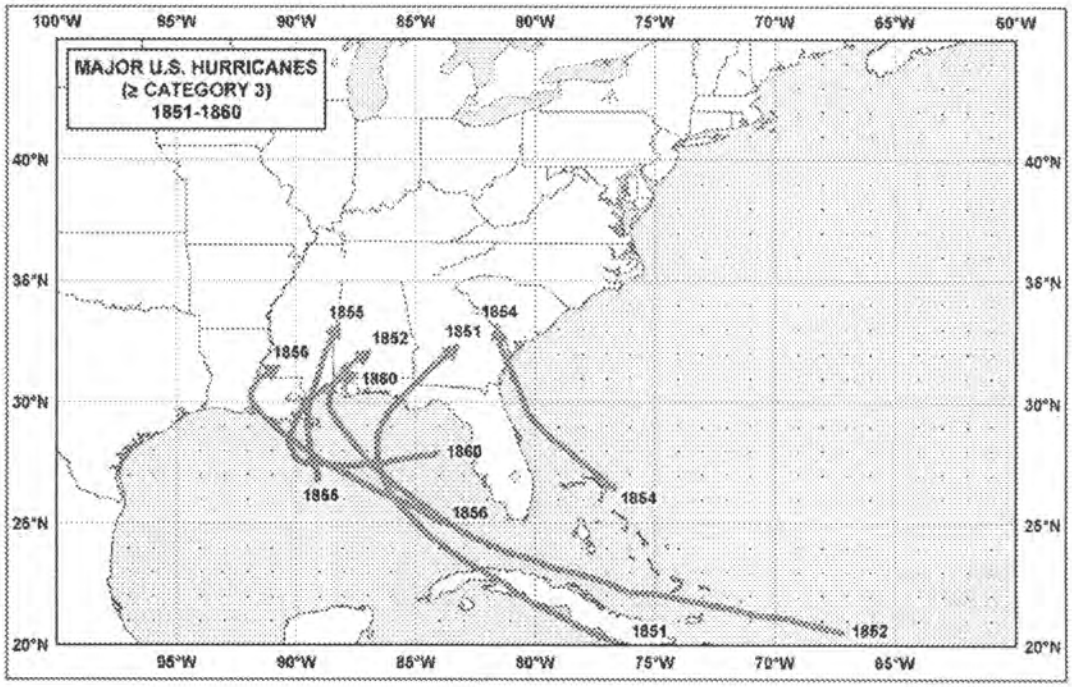

Figure A1. Hurricanes stronger than or equal to category 3 for the Gulf and Atlantic coasts – 1851 to 1860 (Blake et al., 2005).

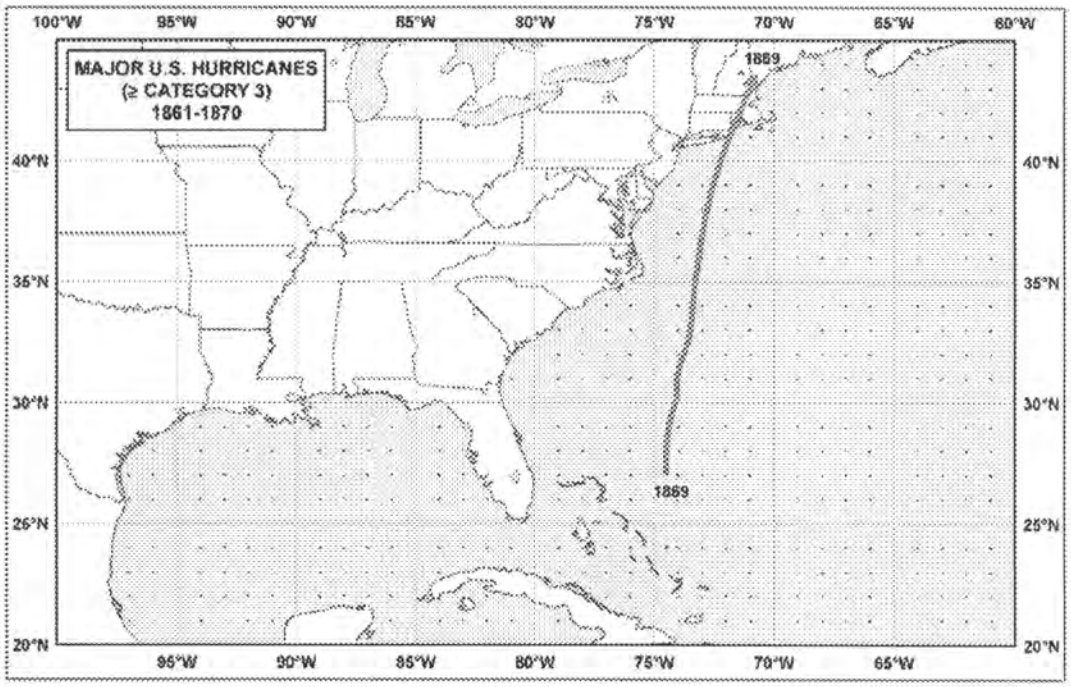

Figure A2. Hurricanes stronger than or equal to category 3 for the Gulf and Atlantic coasts – 1861 to 1870 (Blake et al., 2005).

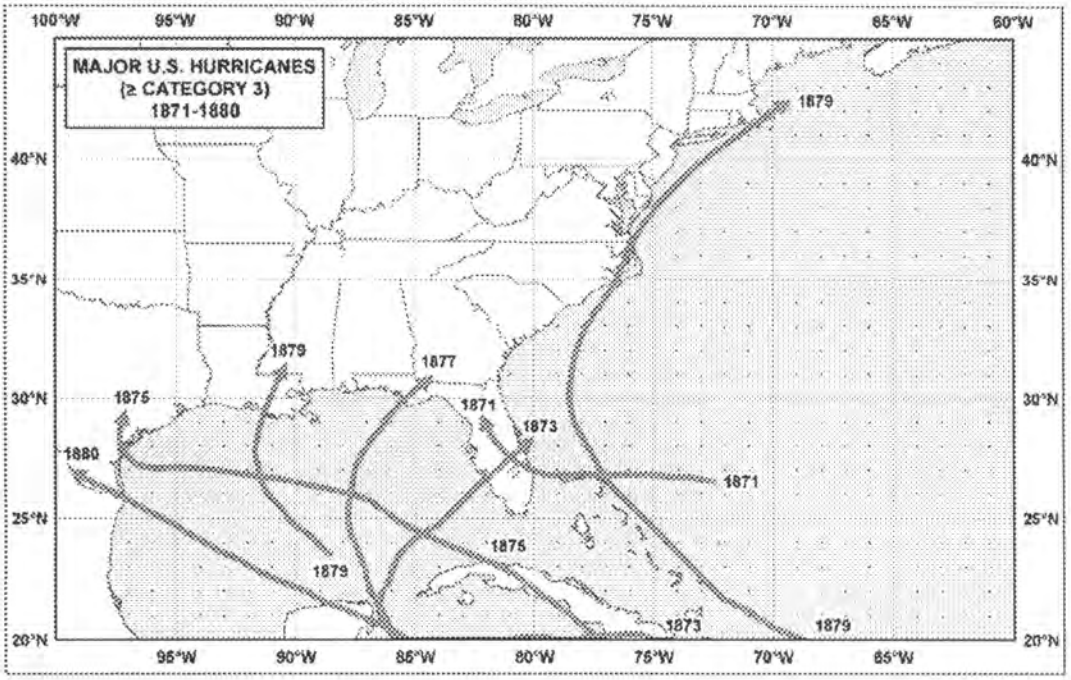

Figure A3. Hurricanes stronger than or equal to category 3 for the Gulf and Atlantic coasts – 1871 to 1880 (Blake et al., 2005).

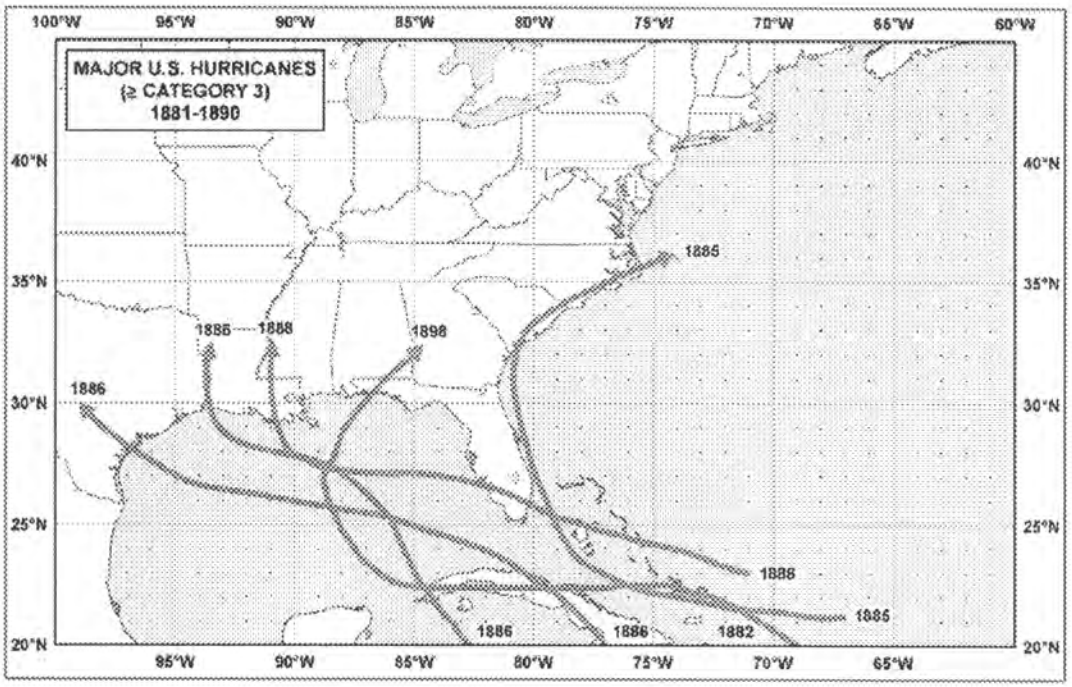

Figure A4. Hurricanes stronger than or equal to category 3 for the Gulf and Atlantic coasts – 1881 to 1890 (Blake et al., 2005).

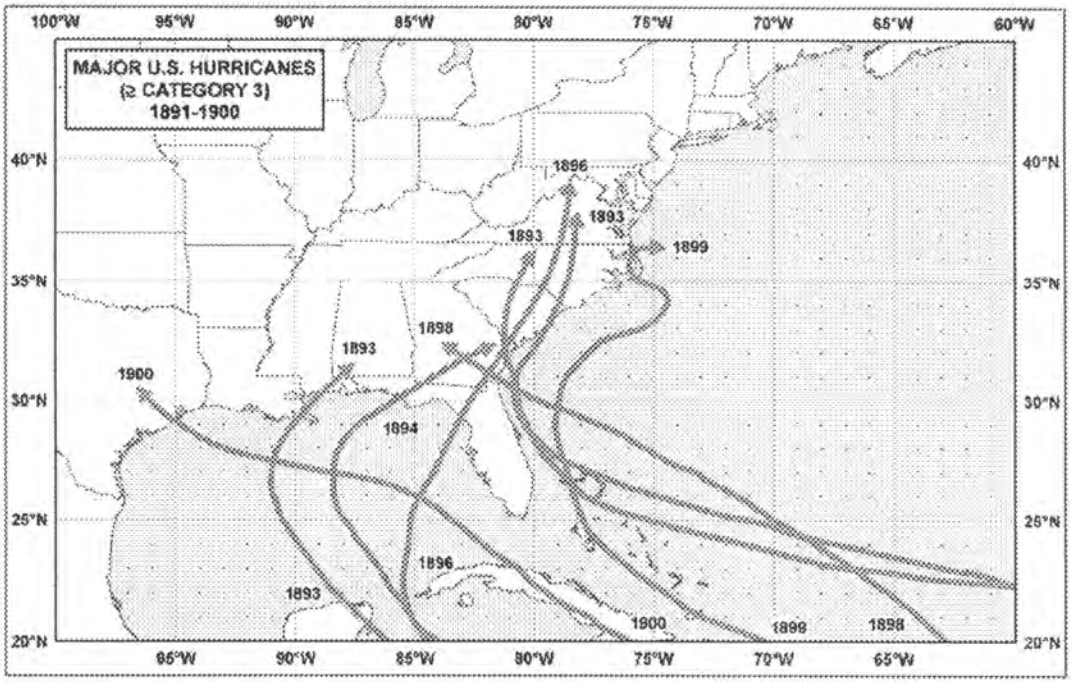

Figure A5. Hurricanes stronger than or equal to category 3 for the Gulf and Atlantic coasts – 1891 to 1900 (Blake et al., 2005).

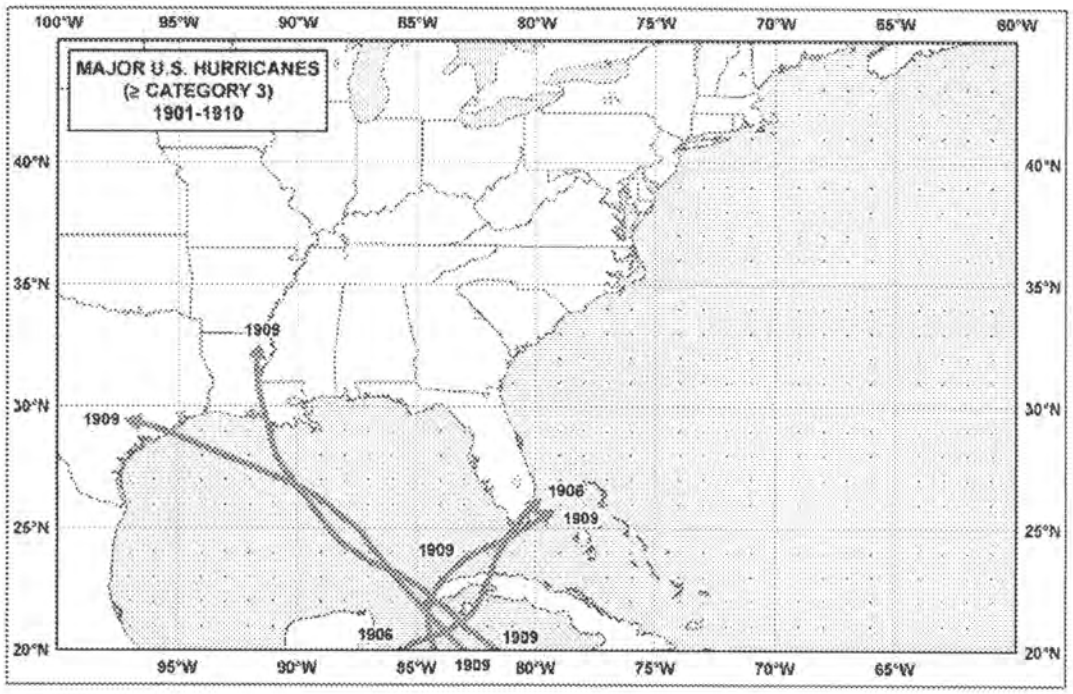

Figure A6. Hurricanes stronger than or equal to category 3 for the Gulf and Atlantic coasts – 1901 to 1910 (Blake et al., 2005).

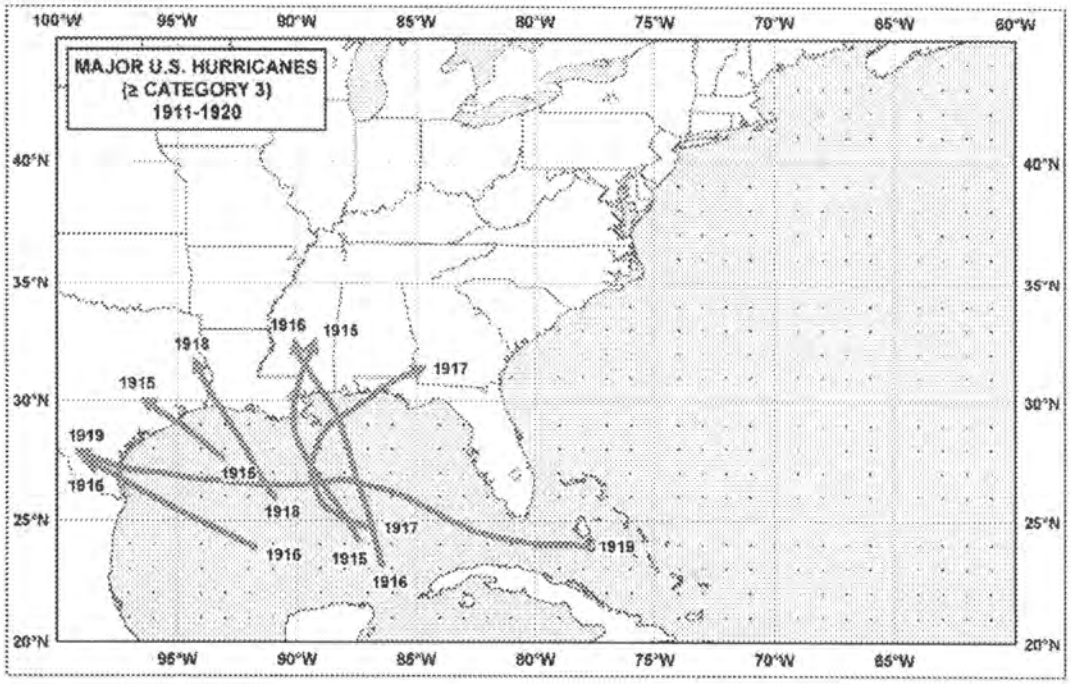

Figure A7. Hurricanes stronger than or equal to category 3 for the Gulf and Atlantic coasts – 1911 to 1920 (Blake et al., 2005).

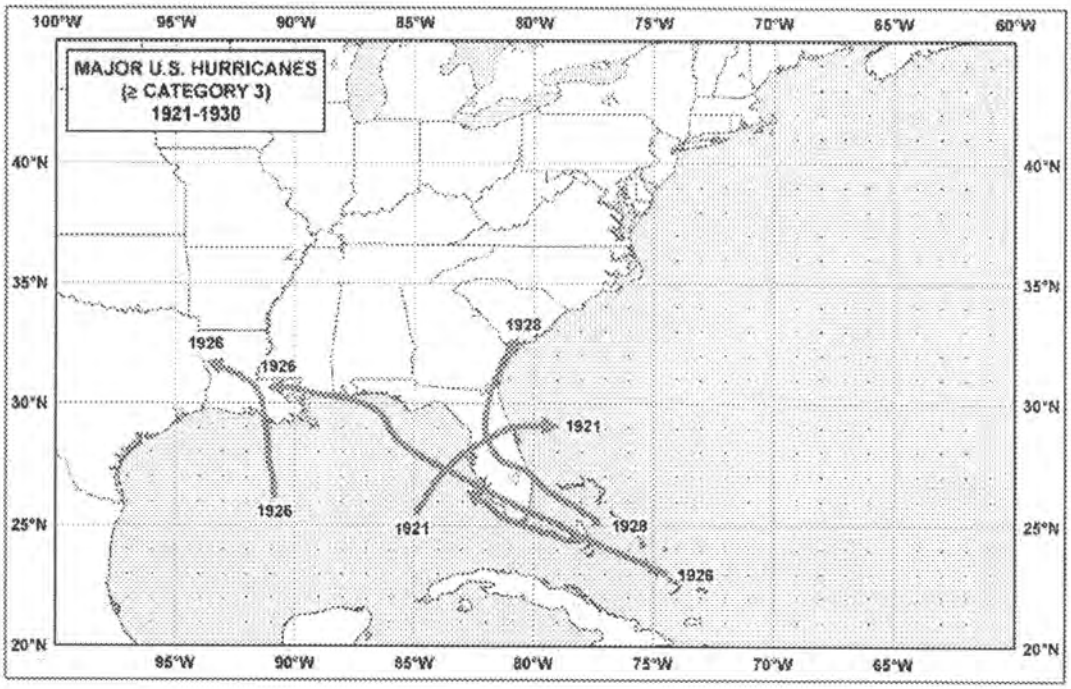

Figure A8. Hurricanes stronger than or equal to category 3 for the Gulf and Atlantic coasts – 1921 to 1930 (Blake et al., 2005).

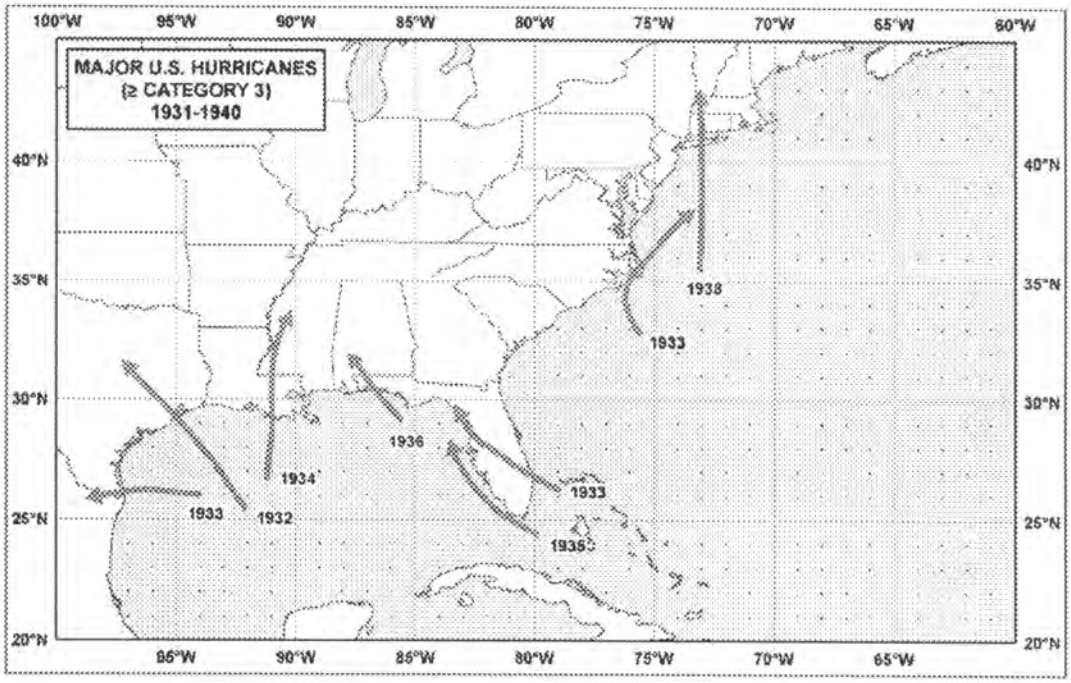

Figure A9. Hurricanes stronger than or equal to category 3 for the Gulf and Atlantic coasts – 1931 to 1940 (Blake et al., 2005).

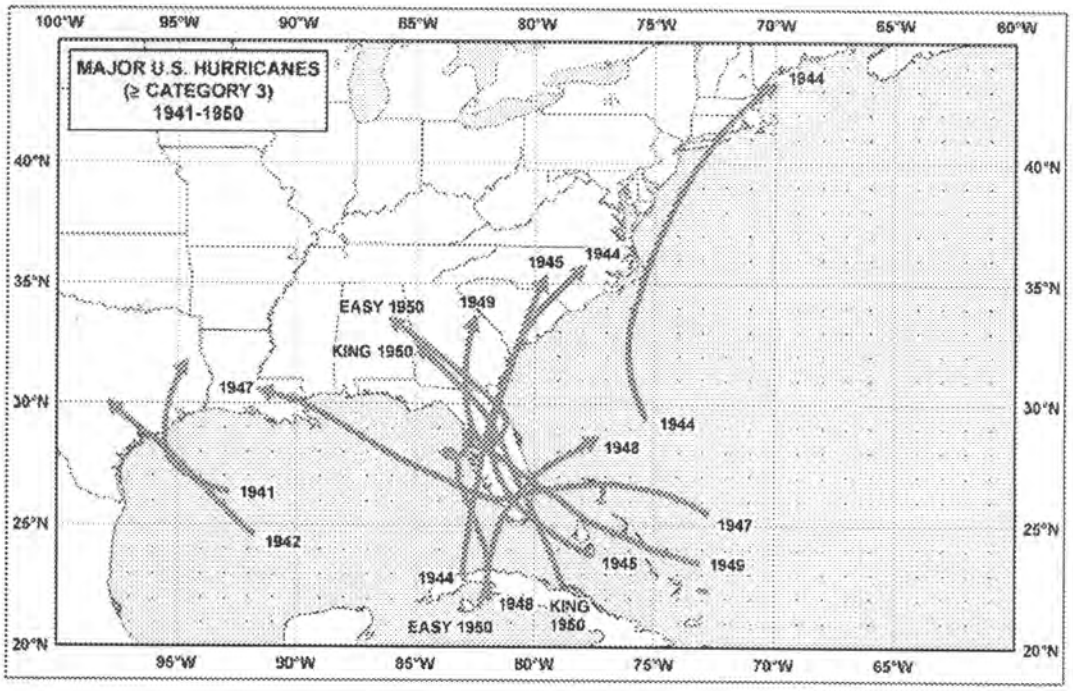

Figure A10. Hurricanes stronger than or equal to category 3 for the Gulf and Atlantic coasts – 1941 to 1950 (Blake et al., 2005).

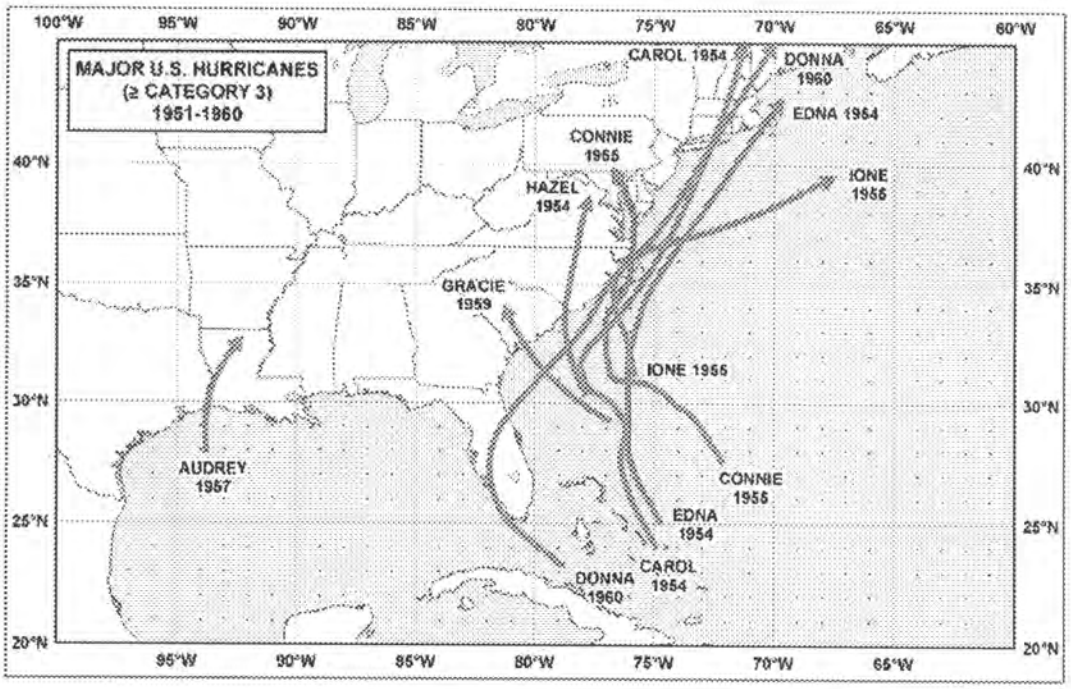

Figure A11. Hurricanes stronger than or equal to category 3 for the Gulf and Atlantic coasts – 1951 to 1960 (Blake et al., 2005).

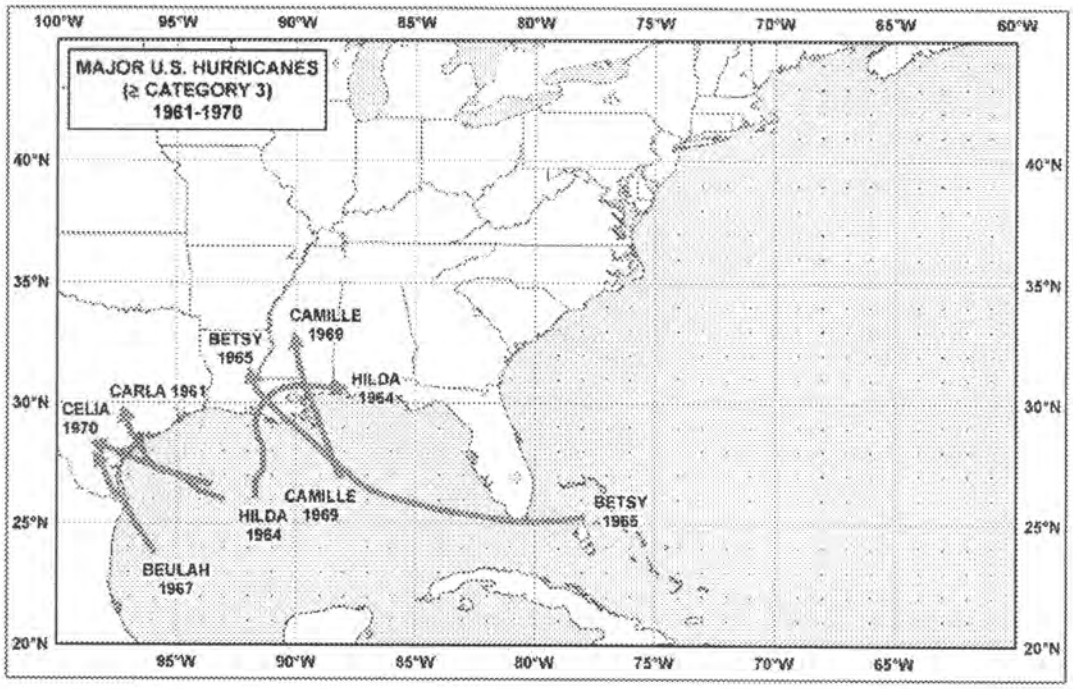

Figure A12.Hurricanes stronger than or equal to category 3 for the Gulf and Atlantic coasts – 1961 to 1970 (Blake et al., 2005).

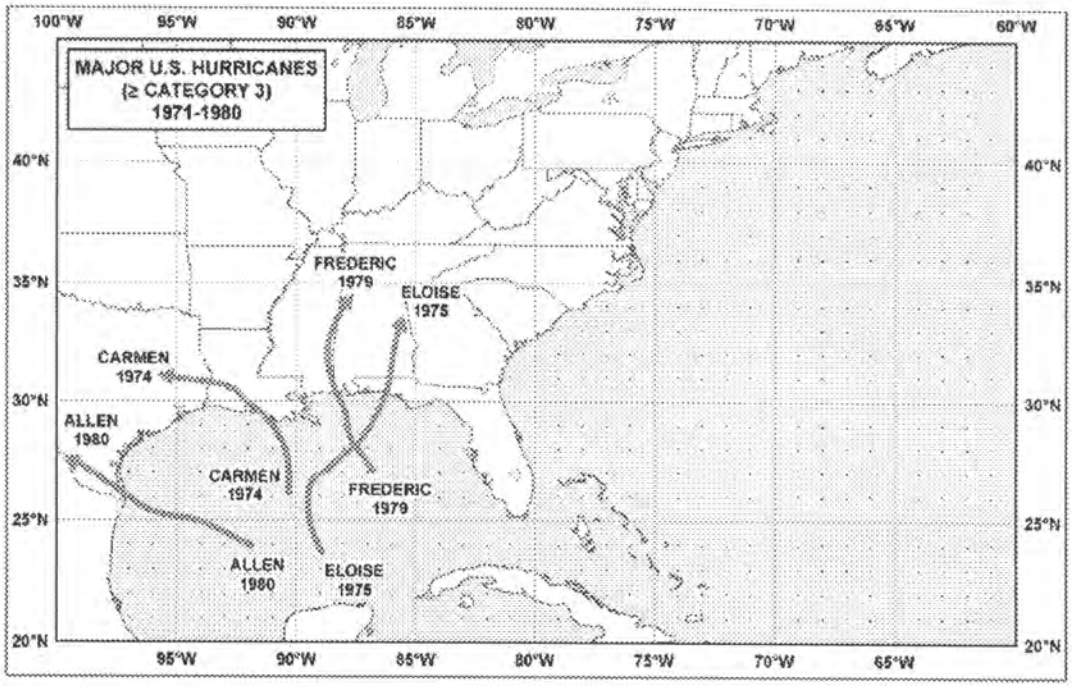

Figure A13.Hurricanes stronger than or equal to category 3 for the Gulf and Atlantic coasts – 1971 to 1980 (Blake et al., 2005).

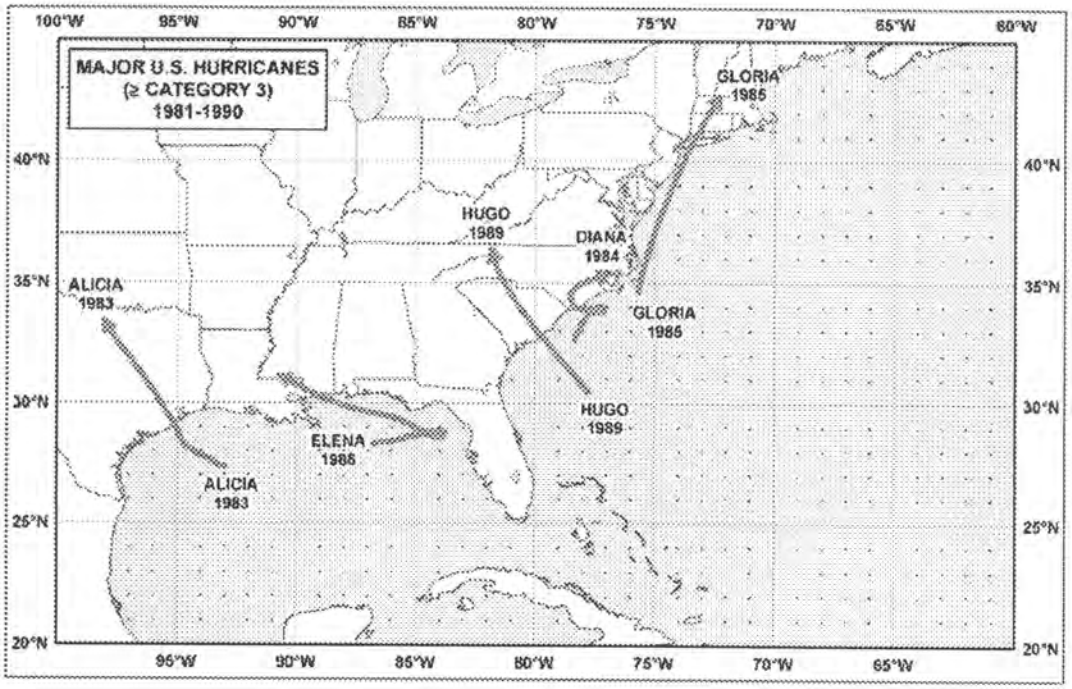

Figure A14. Hurricanes stronger than or equal to category 3 for the Gulf and Atlantic coasts – 1981 to 1990 (Blake et al., 2005).

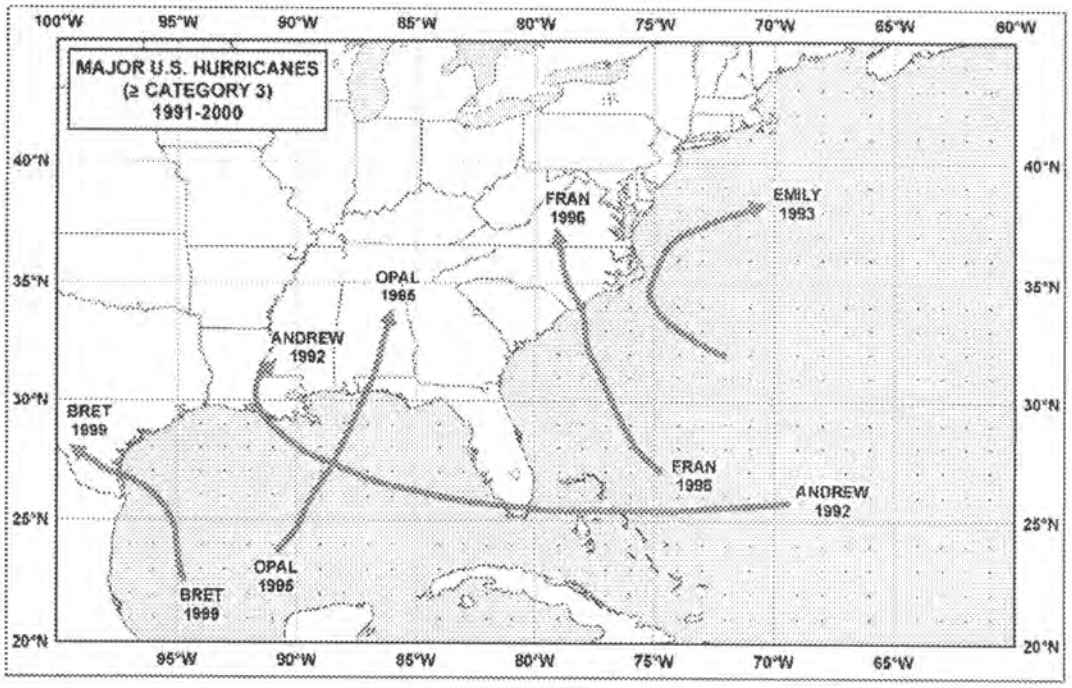

Figure A15. Hurricanes stronger than or equal to category 3 for the Gulf and Atlantic coasts – 1991 to 2000 (Blake et al., 2005).

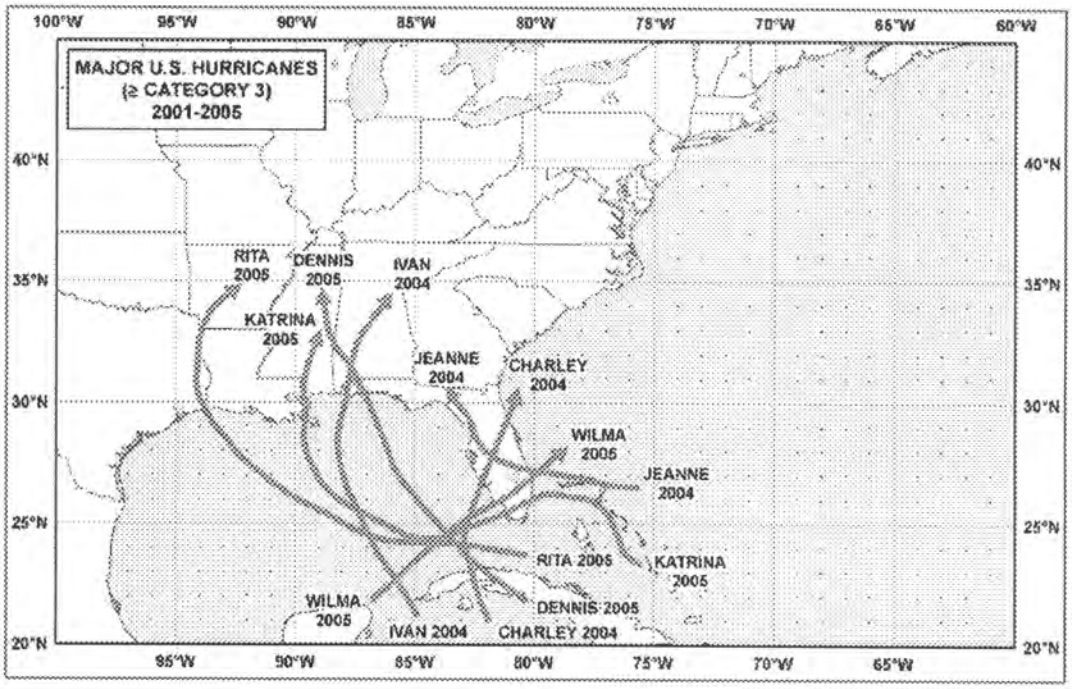

Figure A16. Hurricanes stronger than or equal to category 3 for the Gulf and Atlantic coasts – 2000 to 2005 (Blake et al., 2005).

Appendix B

Dredging History for the Mobile Outer Bar: 1902 to 2006

Dredging History for the Mobile Outer Bar: 1902 to 2006					
Date	**Authority**	**Description**	**New Work (cy)**	**Maintenance (cy)**	**Source**
June 30, 1896		"... in Pickett's History of Alabama it is stated that on February 18, 1702, Iberville found 20 feet over the outer bar."			ARCE, 1896; p. 1426
April 1902		"... detailed survey, including triangulation, to determine the present condition of the ship channel within the limits of the project ..."			ARCE, 1902; p. 1282
June 13, 1902	River and Harbor Act	"... the Secretary of War may, in his discretion, expend a sum not to exceed fifty thousand dollars in deepening and widening the channel through the outer bar near Fort Morgan." The original condition of the channel was a minimum usable depth of 23 ft MLW over a distance of about 0.5 mile across the bar.			ARCE, 1902; p. 1282
June 30, 1903		"The work of widening and deepening the channel through the outer bar near Fort Morgan ... has not yet commenced as suitable plant for this work could not be obtained."			ARCE, 1903; p. 1238
August 22, 1903		Contract signed between Mr. Rittenhouse Moore (Mobile, AL; the only bidder) and the District to dredge the outer bar channel near Fort Morgan at a rate of 30 cents per cubic yard bin measurement.			ARCE, 1904; p. 1805
October 2, 1903		Work commenced on deepening and widening the channel through the outer bar near Fort Morgan.			ARCE, 1904; p. 1805
November 10, 1903		Contractor's dredge *Jumbo* sank and proved a total loss.			ARCE, 1904; p. 1805
May 16 to June 30, 1904		Dredging commenced and by June 30, a minimum depth on the lighthouse range through the channel to be improved was 25 ft; dredged material was placed in deep water in the Gulf of Mexico.	100,433		ARCE, 1904; p. 1805
July 1 to 20, 1904		Dredging continued through the Mobile bar channel which resulted in a 225- to 250-ft wide channel with a minimum depth of 27 ft.	43,697		ARCE, 1905; p. 1399
March 3, 1905	River and Harbor Act	Made a separate project of the Mobile bar work.			ARCE, 1905; p. 1399
June 15, 1905		Proposals for deepening and widening the existing channel through the Mobile Outer Bar to 30 ft deep and 300 ft wide were opened; awarded to Southern Dredging Company.			ARCE, 1905; p. 1399
August 23, 1905 to May 12, 1906		Dredging operations continued when weather would permit, securing a channel 27- to 30-ft deep with a width 250 to 275 ft.	144,412		ARCE, 1906; p. 1271
July 1, 1906 to June 30, 1907		No dredging work was completed during this fiscal year. "The storm of September, 1906, changed the configuration of the bottom at the entrance to Mobile Bay, but seems not to have affected materially the depth of the dredged channel.			ARCE, 1907; p. 1371
July 1, 1907 to June 30, 1908		The U.S. dredge *Charleston* was dredging the channel most of the year. Most of the bar channel was deepened to 30 ft or more.	185,683		ARCE, 1908; p. 1427
July 1, 1908 to June 30, 1909		Maximum channel depth at the beginning of the year was about 27.5 ft – shoals were in the channel. The dredge *Charleston* removed shoals from the channel and increased the depth to between 30 and 35 ft. Dredged volume missing from Annual Report; value derived from dredged totals listed in the table on page 5 of Professional Memoirs, Corps of Engineers, v. 5, no. 19, January-February, 1913.		198,279	ARCE, 1909; p. 1412
July, 1909 and January 25 to April 20, 1910		The dredge *Charleston* removed shoals that formed in the dredged channel to maintain a project channel depth of 30 ft.		121,640	ARCE, 1910; p. 1559
August 9 to 24, 1910		The dredge *Charleston* worked in the outer bar channel removing shoals from the previously dredge channel and deepening unfinished parts.		32,184	ARCE, 1911; p. 1701
April 22 to June 30, 1912		The dredge *Charleston* worked in the outer bar channel removing shoals from the previously dredge channel.		63,852	ARCE, 1912; p. 1921
July 1, 1912 to June 30, 1913		The U.S. dredge *Charleston* worked on the Mobile Bar Channel during the entire fiscal year when weather permitted. Maintenance work accounted for about 34% of total dredging.		113,772	ARCE, 1913; p. 2142
July 1, 1912 to June 30, 1913		The total amount of sand removed from the channel was 332,190 cy, which involved 218,418 cy of new work to relocate the channel 700 ft west of its previous location. "This change was necessitated by the fact that the channel was naturally shifting in this direction and shoals were forming from the east more rapidly than the dredge could remove them."	218,418		ARCE, 1913; p. 2142
July 10 to October 31, 1913		Dredging work resulted in the completion of the channel through the Mobile Outer Bar to its full project dimensions (30 ft deep and 300 ft wide).	94,661		ARCE, 1914; p. 2187
May 16, 1904 to October 13, 1913	**1905 River and Harbor Act**	**Total dredging upon completion of a channel through the Mobile Outer Bar to a depth of 30 ft MLW and a width of 300 ft.**	**787,304**	**529,727**	
December 31, 1914 to January 30, 1915		The U.S. dredge *Caucus* (rented from the Montgomery, AL District) work on the Mobile Bar to remove all shoals from the channel.		58,418	ARCE, 1915; p. 2530

Dredging History for the Mobile Outer Bar: 1902 to 2006					
Date	**Authority**	**Description**	**New Work (cy)**	**Maintenance (cy)**	**Source**
July 1, 1915 to June 30, 1916		No dredging was done in the Mobile Outer Bar channel during the fiscal year.			ARCE, 1916; p. 2381
July 1, 1916 to June 30, 1917		The channel across the bar was maintained by dredging between the 30-ft contours at the outer and inner end of the bar. Under ordinary conditions, mean tide range over the bar was 1.1 ft; extreme tide rage was 3.4 ft.		144,099	ARCE, 1917; p. 833
August 8, 1917	River and Harbor Act	New project dimension approved for the Mobile Outer Bar channel include 33 ft deep at MLW and 450 ft wide for a length of about 1 mile, connecting the 33-ft contours south and north of the bar.			ARCE, 1917; p. 833
July 1, 1917 to June 30, 1918		All work was for maintenance of dimensions of the previous project (30-ft deep by 300-ft wide channel). "The channel across the bar was maintained by dredging between the 30-ft contours at the outer and inner end of the bar."		177,925	ARCE, 1918; p. 866
July 1, 1918 to June 30, 1919		All work was for maintenance of dimensions of the previous project (30-ft deep by 300-ft wide channel). "No new work has been done on Mobile Bar under the existing project ..."		143,746	ARCE, 1919; p. 913
September 29, 1919 to June 30, 1920		The U.S. dredge *Charleston* was used for new and maintenance work in the bar channel. Work on the new outer bar project dimension was initiated on October 13, 1919.	201,368	4,521	ARCE, 1920; p. 2356
December 4, 1919		New Mobile Outer Bar channel location approved.			ARCE, 1921; p. 883
July 1, 1920 to June 30 1921		New work consisted of relocating the existing bar channel.	188,971		ARCE, 1921; p. 882
July 1, 1921 to June 30, 1922		Maintenance work along the Mobile Outer Bar Channel focused on maintaining a channel depth of 30 ft MLW.		60,041	ARCE, 1922; p. 908
July 1, 1922 to June 30, 1923		For new work in the Outer Bar Channel, "... an average depth of 32 feet has been obtained over the project width of 450 feet and the project depth of 33 feet over about one-half the project width along the center line of the channel."	310,989	62,486	ARCE, 1923; p. 785-786
July 1, 1923 to June 30, 1924		New work in the Outer Bar Channel resulted in completion of the channel to project dimensions (33-ft MLW depth and 450-ft wide). Work completed by the U.S. dredge *Charleston*.	377,098		ARCE, 1924; p. 780-781
July 1, 1924 to June 30, 1925		"In the Outer Bar Channel the project dimensions have been obtained." No dredging was done in the Mobile Outer Bar channel during the fiscal year.			ARCE, 1925; p. 762-763
May 16, 1904 to June 30, 1925	**1917 River and Harbor Act**	**Total dredging upon completion of a channel through the Mobile Outer Bar to a depth of 33 ft MLW and a width of 450 ft.**	**1,865,730**	**1,180,963**	
July 1, 1925 to June 30, 1926		The seagoing dredge *Benyaurd* was operated 1¼ months in the Mobile Outer Bar Channel to restore project depth and width.		398,680	ARCE, 1926; p. 769
July 1, 1926 to June 30, 1927		No dredging was done in the Mobile Outer Bar channel during the fiscal year.			ARCE, 1927; p. 798
July 1, 1927 to June 30, 1928		No distinction was made between total maintenance dredging for the entire channel and dredging in the Outer Bar Channel. As such, the reported maintenance dredging quantity for the Outer Bar Channel was estimated based on the previous quantity (for a 2 year period) reported in 1926.		199,340	ARCE, 1928; p. 833
July 1, 1928 to June 30, 1929		No dredging was done in the Mobile Outer Bar channel during the fiscal year.			ARCE, 1929; p. 835
July 1, 1929 to June 30, 1930		No dredging was done in the Mobile Outer Bar channel during the fiscal year.			ARCE, 1930; p. 903
July 3, 1930	River and Harbor Act	New project "... provides for a channel across the Mobile Bar 36 feet deep at mean low water and 450 feet wide, and about 1 mile long, connecting the 36-foot contours south and north of the bar ..."			ARCE, 1931; p. 900
July 1, 1930 to June 30, 1931		Dredging was completed in the channel to maintain existing project dimensions (33-ft deep channel, 450-ft wide) and begin work on the new project. No distinction was made between maintenance dredging and new work; however, the statement "work remaining to be done to complete the project is the dredging of the Outer Bar Channel to a width of 450 feet and depth of 36 feet" suggests that new work was started. As such, previous maintenance dredging quantities were used to estimate new versus maintenance dredging volumes for FY1931. Dredging was completed by the U.S. hopper dredge *Benyuard*.	347,741	598,020	ARCE, 1931; p. 901-902
July 1, 1931 to June 30, 1932		No dredging was done in the Mobile Outer Bar channel during the fiscal year.			ARCE, 1932; p. 802-803
July 1, 1932 to June 30, 1933		No dredging was done in the Mobile Outer Bar channel during the fiscal year.			ARCE, 1933; p. 482-483
May 7 to June 30, 1934		The U.S hopper dredge *Benyuard* dredged the Outer Bar Channel to a controlling depth of 34 ft. No distinction between new work and maintenance dredging was made,		816,571	ARCE, 1934; p. 565

Dredging History for the Mobile Outer Bar: 1902 to 2006					
Date	**Authority**	**Description**	**New Work (cy)**	**Maintenance (cy)**	**Source**
		except to state that the channel is now 1 ft deeper than the previous project depth. As such, all dredged sediment was considered maintenance, although some of it would have been new work. Work remaining to complete the project consisted of dredging the Outer Bar Channel to a width of 450 ft and a depth of 36 ft MLW.			
July 16 to August 3, 1934		The U.S hopper dredge *Benyuard* dredged the Outer Bar Channel to a depth of 36 ft MLW and a width of 450 ft. All dredging was new work. The 1930 River and Harbor Act Outer Bar Channel project dimensions were completed. As of June 30, 1935, the channel controlling depth was 36 ft MLW.	337,430		ARCE, 1935; p. 657
May 16, 1904 to June 30, 1935	**1930 River and Harbor Act**	**Total dredging upon completion of a channel through the Mobile Outer Bar to a depth of 36 ft MLW and a width of 450 ft.**	**2,550,901**	**3,193,574**	
October 21 to December 6, 1935		The U.S hopper dredge *Benyuard* dredged the Outer Bar Channel to maintain a controlling depth of 36 ft MLW and a width of 450 ft. All dredging was maintenance work.		690,196	ARCE, 1936; p. 637
July 1, 1936 to June 30, 1937		No dredging was done in the Mobile Outer Bar channel during the fiscal year.			ARCE, 1937; p. 678
August 5-13, September 18-29, October 1-13, 1937		The U.S hopper dredge *Benyuard* dredged the Outer Bar Channel to maintain a controlling depth of 36 ft MLW and a width of 450 ft. All dredging was maintenance work.		451,085	ARCE, 1938; p. 720
May 27 to June 27, 1939		The U.S hopper dredge *Manhattan* dredged the Outer Bar Channel to maintain a controlling depth of 36 ft MLW and a width of 450 ft. All dredging was maintenance work.		455,062	ARCE, 1939; p. 797
August 10 to September 8, 1939		The U.S hopper dredge *Benyuard* dredged the Outer Bar Channel to maintain a controlling depth of 36 ft MLW and a width of 450 ft. All dredging was maintenance work.		335,816	ARCE, 1940; p. 790
August 23 to October 15, 1940		The U.S hopper dredge *Benyuard* dredged the Outer Bar Channel to maintain a controlling depth of 36 ft MLW and a width of 450 ft. All dredging was maintenance work.		600,656	ARCE, 1941; p. 754
August 7 to September 7, 1941		The U.S hopper dredge *Benyuard* dredged the Outer Bar Channel to maintain a controlling depth of 36 ft MLW and a width of 450 ft. All dredging was maintenance work.		350,067	ARCE, 1942; p. 667
May 29 to June 30, 1943		The U.S hopper dredge *Benyuard* dredged the Outer Bar Channel to maintain a controlling depth of 36 ft MLW and a width of 450 ft. All dredging was maintenance work.		386,634	ARCE, 1943; p. 599
July 1, 1943 to June 30, 1944		No dredging was done in the Mobile Outer Bar Channel during the fiscal year.			ARCE, 1944; p. 586
December 27, 1944 to January 28, 1945		The U.S hopper dredge *Benyuard* dredged the Outer Bar Channel to maintain a controlling depth of 36 ft MLW and a width of 450 ft. All dredging was maintenance work.		226,000	ARCE, 1945; p. 826
July 1, 1945 to June 30, 1946		No dredging was done in the Mobile Outer Bar Channel during the fiscal year.			ARCE, 1946; p. 891
July 1, 1946 to June 30, 1947		No dredging was done in the Mobile Outer Bar Channel during the fiscal year.			ARCE, 1947; p. 874
December 26, 1947 to February 7, 1948		The U.S hopper dredge *Lyman* dredged the Outer Bar Channel to maintain a controlling depth of 36 ft MLW and a width of 450 ft. All dredging was maintenance work.		385,200	ARCE, 1948; p. 969-970
June 16-19, 1949		The U.S hopper dredge *Langfitt* dredged a small portion of the Outer Bar Channel. The controlling depth throughout the channel as of June 1949 was 35 ft MLW. All dredging was maintenance work.		78,361	ARCE, 1949; p. 872
April 30 to June 10, 1950		The U.S hopper dredge *Hyde* dredged the Outer Bar Channel to maintain a controlling depth of 36 ft MLW and a width of 450 ft. The controlling depth throughout the channel as of May 1950 was 36 ft MLW. All dredging was maintenance work.		475,004	ARCE, 1950; p. 880-881
July 1, 1950 to June 30, 1951		No dredging was done in the Mobile Outer Bar Channel during the fiscal year.			ARCE, 1951; p. 713
May 16-29, 1952		The U.S hopper dredge *Gerig* dredged the Outer Bar Channel to maintain a controlling depth of 36 ft MLW and a width of 450 ft. As of June 1952, only the controlling depth on the east side of the channel was shallower than 36 ft MLW. All dredging was maintenance work.		345,773	ARCE, 1952; p. 671-672
July 31, 1952		Chief of Engineers recommended modification of the existing project to enlarge the Mobile Bar Channel to a depth of 42 ft MLW and a width of 600 ft.			ARCE, 1953; p. 628
July 1, 1952 to June 30, 1953		No dredging was done in the Mobile Outer Bar Channel during the fiscal year. By June 1953, all parts of the channel had controlling depths of between 35- and 36-ft MLW, except the eastern section of the outer channel, which had a controlling depth of 29 ft.			ARCE, 1953; p. 628-629
July 1, 1953 to June 30, 1954		No dredging was completed for the Mobile Outer Bar Channel during the fiscal year.			ARCE, 1954; p. 430

Dredging History for the Mobile Outer Bar: 1902 to 2006					
Date	**Authority**	**Description**	**New Work (cy)**	**Maintenance (cy)**	**Source**
September 3, 1954	River and Harbor Act	Authorized deepening of the project to 42-ft MLW and widening the channel to 600 ft.			ARCE, 1955; p. 423
July 1, 1954 to June 30, 1955		No dredging was completed for the Mobile Outer Bar Channel during the fiscal year. Channel controlling depths reported in March 1955 indicated a shoaled channel that was 31 ft deep in the southwestern quarter, 26-ft deep in the southeaster quarter, 34-ft deep in the northwestern quarter , and 35.5-ft deep in the northeastern quarter.			ARCE, 1955; p. 423-424
September 26 – October 13, 1955		The U.S hopper dredge *Langfitt* dredged the Outer Bar Channel for a relatively short period of time. As of October 1955, the controlling depth in the channel was 36 ft MLW. All dredging was maintenance work.		495,452	ARCE, 1956; p. 547
July 15-18, 1956		The U.S hopper dredge *Langfitt* dredged the Outer Bar Channel to previous project dimensions (36-ft deep, 450-ft wide). All dredging was maintenance work.		135,606	ARCE, 1957; p. 545
July 5 – September 15, 1956		The U.S hopper dredge *Langfitt* dredged the Outer Bar Channel to a controlling depth of 38 ft MLW. This was the initial phase of development for the 42-ft deep by 600-ft wide authorized project.	1,204,526		ARCE, 1957; p. 545
July 1, 1957 to June 30, 1958		No dredging was completed for the Mobile Outer Bar Channel during the fiscal year.			ARCE, 1958; p. 495
July 1, 1958 to June 30, 1959		No dredging was completed for the Mobile Outer Bar Channel during the fiscal year.			ARCE, 1959; p. 522
July 1, 1959 to June 30, 1960		No dredging was completed for the Mobile Outer Bar Channel during the fiscal year.			ARCE, 1960; p. 509
July 1, 1960 to June 30, 1961		No dredging was completed for the Mobile Outer Bar Channel during the fiscal year.			ARCE, 1961; p. 558
April 21 – May 10, 1962		The U.S hopper dredge *Gerig* dredged the Outer Bar Channel to a controlling depth of 38 ft MLW. No new work was done on the 42-ft deep by 600-ft wide authorized project.		533,875	ARCE, 1962; p. 569-570
July 1, 1962 to June 30, 1963		No dredging was completed for the Mobile Outer Bar Channel during the fiscal year.			ARCE, 1963; p. 505
July 1, 1963 to June 30, 1964		No dredging was completed for the Mobile Outer Bar Channel during the fiscal year.			ARCE, 1964; p. 469
October 24 – December 10, 1964		The U.S hopper dredge *Harding* dredged the Outer Bar Channel toward completion of the authorized 42-ft deep by 600-ft wide channel.	1,381,500		ARCE, 1965; p. 460
June 30, 1965		The U.S hopper dredge *Gerig* operated in the Outer Bar Channel toward completion of the authorized project.	13,271		ARCE, 1965; p. 460
July 1-30, 1965		The U.S hopper dredge *Gerig* operated in the Outer Bar Channel completing the authorized project to a depth of 42 ft and a width of 600 ft.	911,581		ARCE, 1966; p. 497
May 16, 1904 to July 30, 1965	**1954 River and Harbor Act**	**Total dredging upon completion of a channel through the Mobile Outer Bar to a depth of 42 ft MLW and a width of 600 ft.**	**6,061,779**	**9,138,361**	
November 18 - December 1, 1966		The U.S hopper dredge *Gerig* operated in the Mobile Outer Bar Channel maintaining the authorized project to a depth of 42 ft and a width of 600 ft.		272,439	ARCE, 1967; p. 487
April 1-10, 1968		The U.S hopper dredge *Langfitt* operated in the Mobile Outer Bar Channel maintaining the authorized project to a depth of 42 ft and a width of 600 ft.		192,857	ARCE, 1968; p. 373
December 28, 1968 – January 4, 1969		The U.S hopper dredge *Langfitt* operated in the Mobile Outer Bar Channel maintaining the authorized project to a depth of 42 ft and a width of 600 ft.		174,953	ARCE, 1969; p. 356
January 13 – February 4, 1970		The U.S hopper dredge *Langfitt* operated in the Mobile Outer Bar Channel maintaining the authorized project to a depth of 42 ft and a width of 600 ft.		361,815	ARCE, 1970; p. 341
October 19 – November 2, 1970 and January 23 – February 10, 1971		The U.S hopper dredge *Langfitt* operated in the Mobile Outer Bar Channel maintaining the authorized project to a depth of 42 ft and a width of 600 ft.		827,388	ARCE, 1971; p. 10-11
June 14 - 30, 1972		The U.S hopper dredge *McFarland* operated in the Mobile Outer Bar Channel maintaining the authorized project to a depth of 42 ft and a width of 600 ft.		262,450	ARCE, 1972; p. 10-11
July 1, 1972 to June 30, 1973		No dredging was completed for the Mobile Outer Bar Channel during the fiscal year.			ARCE, 1973; p.10-11
July 1, 1973 to June 30, 1974		No dredging was completed for the Mobile Outer Bar Channel during the fiscal year.			ARCE, 1974; p. 10-9
July 16-31, 1974		The U.S hopper dredge *Gerig* operated in the Mobile Outer Bar Channel maintaining the authorized project to a depth of 42 ft and a width of 600 ft.		349,260	Mobile District O&M

Dredging History for the Mobile Outer Bar: 1902 to 2006					
Date	**Authority**	**Description**	**New Work (cy)**	**Maintenance (cy)**	**Source**
February 16-28, 1975		The U.S hopper dredge *Gerig* operated in the Mobile Outer Bar Channel maintaining the authorized project to a depth of 42 ft and a width of 600 ft.		982,829	Mobile District O&M
May 3 - June 14, 1976		The U.S hopper dredge *Gerig* operated in the Mobile Outer Bar Channel maintaining the authorized project to a depth of 42 ft and a width of 600 ft.		1,364,113	Mobile District O&M
May 17 to June 14, 1977		The U.S hopper dredge *McFarland* dredged sediment from the Mobile Outer and Inner Bar Channel maintaining the authorized project to a depth of 42 ft and a width of 600 ft.		1,272,432	ARCE, 1977; p. 10-11; Mobile District O&M
July 1, 1977 to June 30, 1978		No dredging was completed for the Mobile Outer Bar Channel during the fiscal year.			ARCE, 1978; p. 10-11
July 1, 1978 to June 30, 1979		No dredging was completed for the Mobile Outer Bar Channel during the fiscal year.			ARCE, 1979; p. 10-12
October 15-27, 1979		The U.S hopper dredge *Langfitt* operated in the Mobile Outer Bar Channel maintaining the authorized project to a depth of 42 ft and a width of 600 ft.		707,142	Mobile District O&M
March 10-24, 1980		U.S. hopper dredges *Essayons* and *Goethals* operated in the Mobile Outer Bar Channel maintaining the authorized project to a depth of 42 ft and a width of 600 ft.		190,300	Mobile District O&M
October 15 – December 17, 1980		Contractor's hopper dredge *Buster Bean* operated in the Mobile Outer Bar Channel maintaining the authorized project to a depth of 42 ft and a width of 600 ft.		939,037	ARCE, 1981; p. 10-11
January 26 to February 8, 1981		The U.S hopper dredge *Langfitt* operated in the Mobile Outer Bar Channel maintaining the authorized project to a depth of 42 ft and a width of 600 ft.		610,623	Mobile District O&M
December 11, 1982 to January 7, 1983		Contractor's dredge *Mermentau* operated in the Mobile Outer Bar Channel maintaining the authorized project to a depth of 42 ft and a width of 600 ft.		312,408	Mobile District O&M
January 1-23, 1984		Contractor's dredge *Atchafalaya* operated in the Mobile Outer Bar Channel maintaining the authorized project to a depth of 42 ft and a width of 600 ft.		218,672	Mobile District O&M
October 22-November 1, 1984		Contractor's dredge *Eagle* operated in the Mobile Outer Bar Channel maintaining the authorized project to a depth of 42 ft and a width of 600 ft.		340,935	Mobile District O&M
August 15, 1985	Supplemental Appropriations Act	Deepen and widen Mobile Outer Bar Channel to 57 feet deep and 700 feet wide for a distance of approximately 7.4 miles. A General Design Memorandum was approved at Division level modifying for project dimensions.			ARCE, 1985; Table 10-B and p. 10-9
August 20 to October 8, 1985		Contractor's dredge *Sugar Island* operated in the Mobile Outer Bar Channel maintaining the authorized project to a depth of 42 ft and a width of 600 ft. Hurricane *Elena* caused significant channel shoaling on Mobile Outer Bar that was handled through emergency procurement.		1,386,536	Mobile District O&M
January 6 – February 24, 1987		Contractor's dredges *Atchafalaya* and *Mermentau* operated in the Mobile Outer Bar Channel maintaining the authorized project to a depth of 46 ft and a width of 600 ft. **All material disposed on the nearshore feeder berm.**		656,089	Mobile District O&M
October 1, 1987 to September 30, 1988		Although the authorized project is for construction of a 57-ft deep x 700-ft wide channel across the outer bar, the plan for improvement consists of deepening the channel from 42 feet to 47 feet for a distance of about 6.1 miles from the Gulf of Mexico to Mobile Bay.			ARCE, 1988; p.10-10
February 7, 1989 to May 8, 1990		Contractor's dredges *Sugar Island* operated in the Mobile Outer Bar Channel creating new authorized project dimensions of 47 ft deep by 600 ft wide of a distance of about 1.5 miles across Mobile Outer Bar.	1,911,284		ARCE, 1990; p. 10-10; Mobile District O&M
February 23, 1989 to April 16, 1990		Contractor's dredges *Manhattan Island* operated in the Mobile Outer Bar Channel creating new authorized project dimensions of 47 ft deep by 600 ft wide of a distance of about 1.5 miles across Mobile Outer Bar.	4,844,068		Mobile District O&M
May 16, 1904 to April 16, 1990		**Total dredging upon completion of a channel through the Mobile Outer Bar to a depth of 47 ft MLW and a width of 600 ft.**	**12,817,131**	**20,560,639**	
October 1, 1990 to September 30, 1991		No dredging was completed for the Mobile Outer Bar Channel during the fiscal year.			Mobile District O&M
August 13 - September 2, 1992		Contractor's dredges *Ouachita* operated in the Mobile Outer Bar Channel maintaining the authorized project dimensions of 47 ft deep by 600 ft wide.		466,607	Mobile District O&M
October 1, 1992 to September 30, 1993		No dredging was completed for the Mobile Outer Bar Channel during the fiscal year.			Mobile District O&M

Dredging History for the Mobile Outer Bar: 1902 to 2006					
Date	**Authority**	**Description**	**New Work (cy)**	**Maintenance (cy)**	**Source**
October 1, 1993 to September 30, 1994		No dredging was completed for the Mobile Outer Bar Channel during the fiscal year.			Mobile District O&M
October 1, 1995 to September 30, 1995		No dredging was completed for the Mobile Outer Bar Channel during the fiscal year.			Mobile District O&M
November 17 to December 16, 1995		Contractor's dredges *Eagle I* operated in the Mobile Outer Bar Channel maintaining the authorized project dimensions of 47 ft deep by 600 ft wide.		621,172	Mobile District O&M
August 8 – 20, 1997		Contractor's dredges *Padre Island* operated in the Mobile Outer Bar Channel maintaining the authorized project dimensions of 47 ft deep by 600 ft wide.		238,256	Mobile District O&M
September 4 – October 2, 1997		Contractor's dredges *Eagle I* operated in the Mobile Outer Bar Channel maintaining the authorized project dimensions of 47 ft deep by 600 ft wide.		292,200	Mobile District O&M
December 16 – 25, 1997		Contractor's dredges *Columbus* operated in the Mobile Outer Bar Channel maintaining the authorized project dimensions of 47 ft deep by 600 ft wide.		180,540	Mobile District O&M
September 21 – October 9, 1998		Contractor's dredges *Eagle* operated in the Mobile Outer Bar Channel maintaining the authorized project dimensions of 47 ft deep by 600 ft wide.		443,761	Mobile District O&M
October 9 – 28, 1998		The U.S hopper dredge *Wheeler* dredged sediment on an emergency basis from the Mobile Outer and Inner Bar Channel to maintain the authorized project to a depth of 47 ft and a width of 600 ft. Hurricane *Georges* caused significant channel shoaling on the Mobile Outer Bar.		836,054	Mobile District O&M
August 26 to September 22, 1999		Contractor's dredges *Columbus and Atchafalaya* operated in the Mobile Outer Bar Channel maintaining the authorized project dimensions of 47 ft deep by 600 ft wide. **54,600 cy placed in the nearshore disposal area.**		125,580	Mobile District O&M
May 3 to September 29, 1999		Contractor's dredge *Newport* operated in the Mobile Outer Bar Channel creating new authorized project dimensions of 49 ft deep by 600 ft wide. **Placed in the Sand Island Beneficial Use Area.**	3,061,598		Mobile District O&M
May 16, 1904 to September 29, 1999		**Total dredging upon completion of a channel through the Mobile Outer Bar to a depth of 49 ft MLW and a width of 600 ft.**	**15,878,729**	**23,764,809**	
July 13-26, 2000		Contractor's dredge *Stuyvesant* operated in the Mobile Outer Bar Channel maintaining the authorized project dimensions of 49-ft deep by 600-ft wide.		758,280	Mobile District O&M
March 27 - May 10, 2002		Contractor's dredge *Atchafalaya* operated in the Mobile Outer Bar Channel maintaining the authorized project dimensions of 49-ft deep by 600-ft wide. **Placed in the Sand Island Beneficial Use Area (SIBUA).**		92,820	Mobile District O&M
June 1-24, 2004		Contractor's dredge *Atchafalaya* operated in the Mobile Outer Bar Channel maintaining the authorized project dimensions of 49-ft deep by 600-ft wide. **Placed in SIBUA.**		230,110	Mobile District O&M
October 2 - November 14, 2004		Contractor's dredge *Dodge Island* operated in the Mobile Outer Bar Channel maintaining the authorized project dimensions of 49-ft deep by 600-ft wide. **Placed in SIBUA.**		1,184,817	Mobile District O&M
October 26, 2004 - January 13, 2005		Contractor's dredge *Padre Island* operated in the Mobile Outer Bar Channel maintaining the authorized project dimensions of 49-ft deep by 600-ft wide. **Placed in SIBUA and Sand Island Lighthouse disposal area.**		1,808,765	Mobile District O&M
April 28 to June 11, 2006		Contractor's dredge *Atchafalaya* operated in the Mobile Outer Bar Channel maintaining the authorized project dimensions of 49-ft deep by 600-ft wide. **Placed in SIBUA.**		487,975	Mobile District O&M
1904 to 2006		**Total dredging in the Mobile Outer Bar Channel**	**15,878,729**	**28,327,576 (277,721 cy/yr)**	
1904 to 2006		**Dredged Material placed in nearshore disposal areas.**	**3,061,598**	**4,515,176**	
1904 to 2006		**Dredged Material placed offshore.**	**12,817,131**	**23,812,400**	

Appendix C

Historical Shoreline Position Change for Dauphin Island: 1847 to 2006

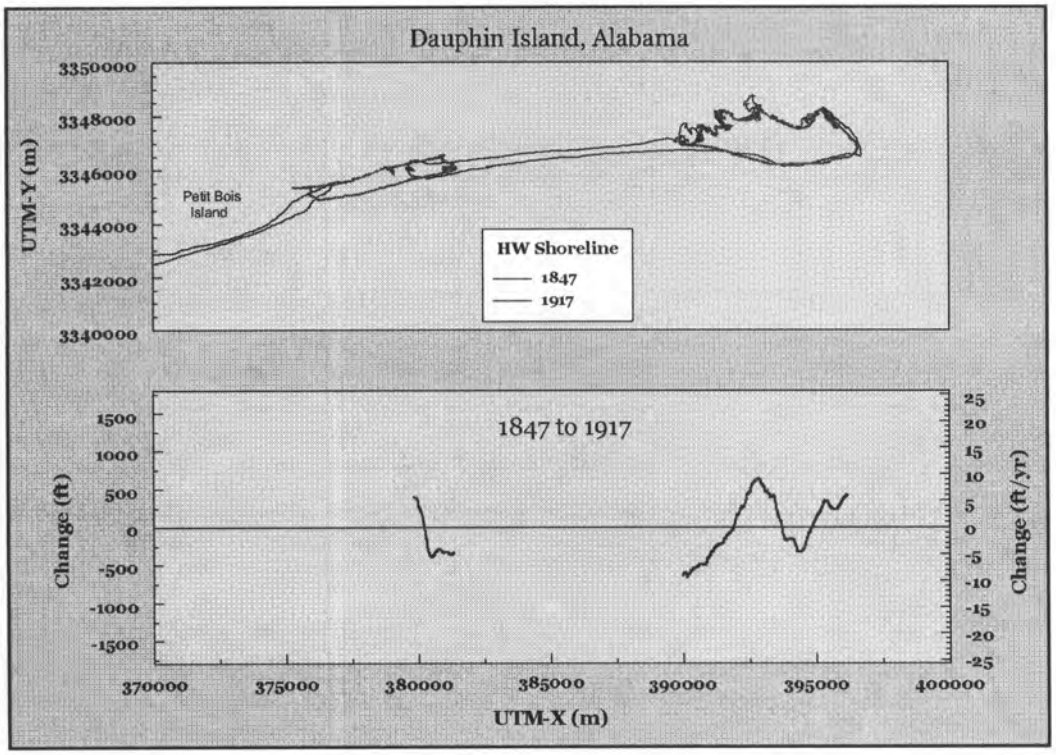

Figure C1. Historical shoreline position change, Dauphin Island, Alabama: 1847 to 1917.

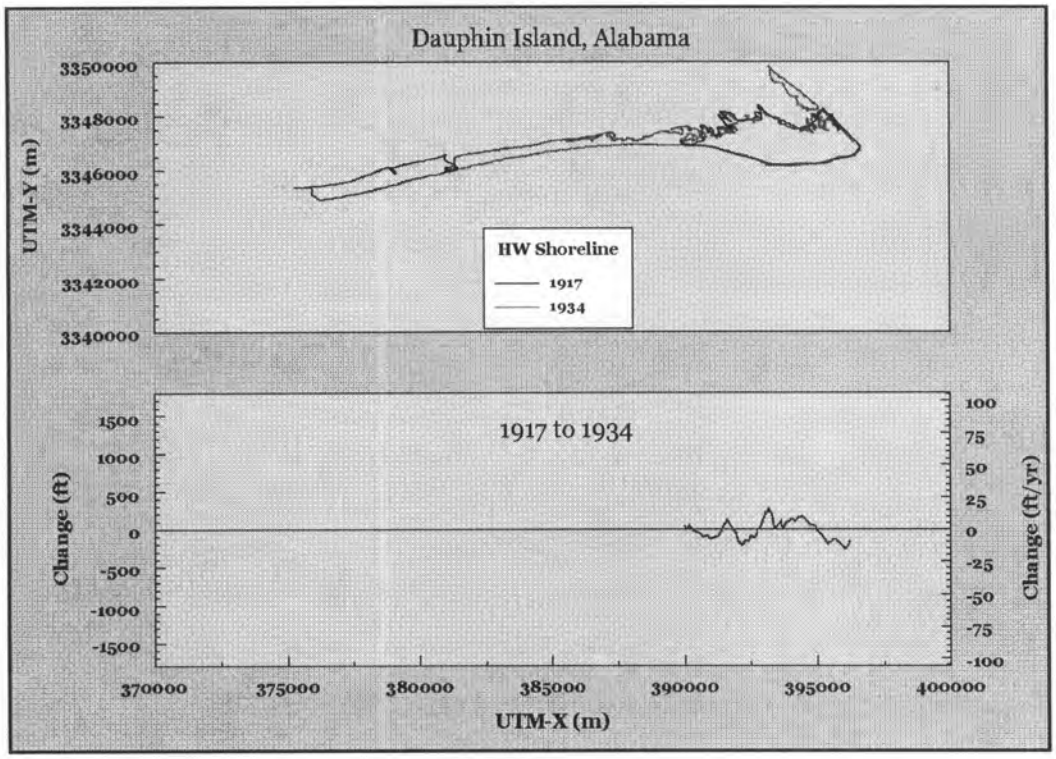

Figure C2. Historical shoreline position change, Dauphin Island, Alabama: 1917 to 1934.

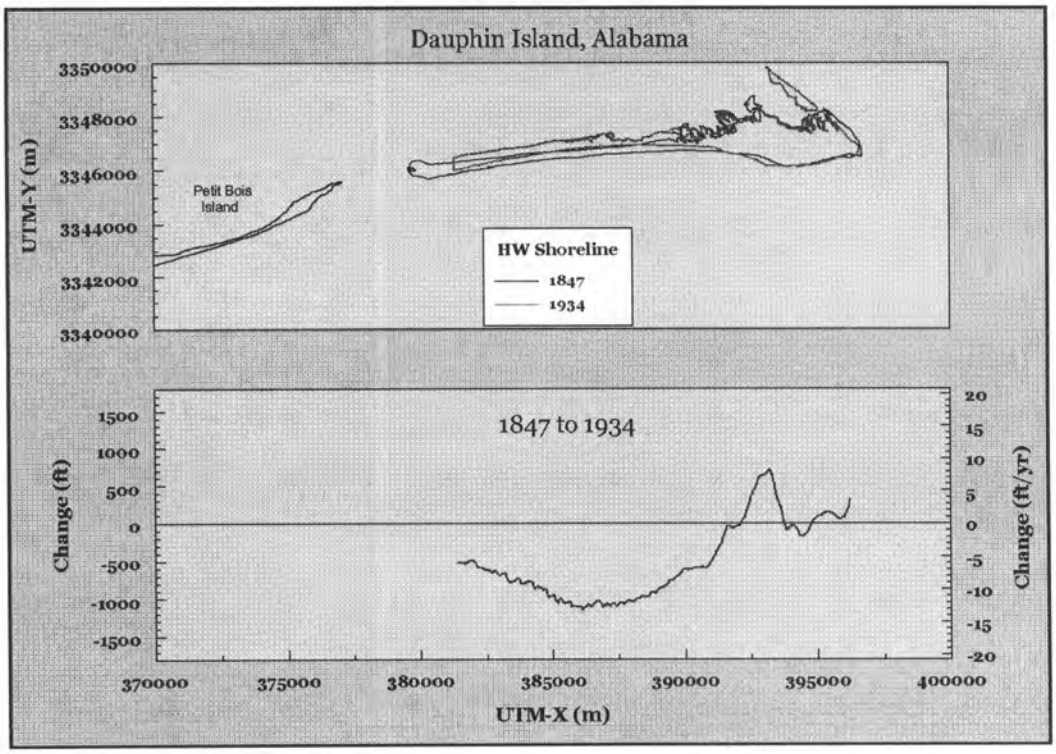

Figure C3. Historical shoreline position change, Dauphin Island, Alabama: 1847 to 1934.

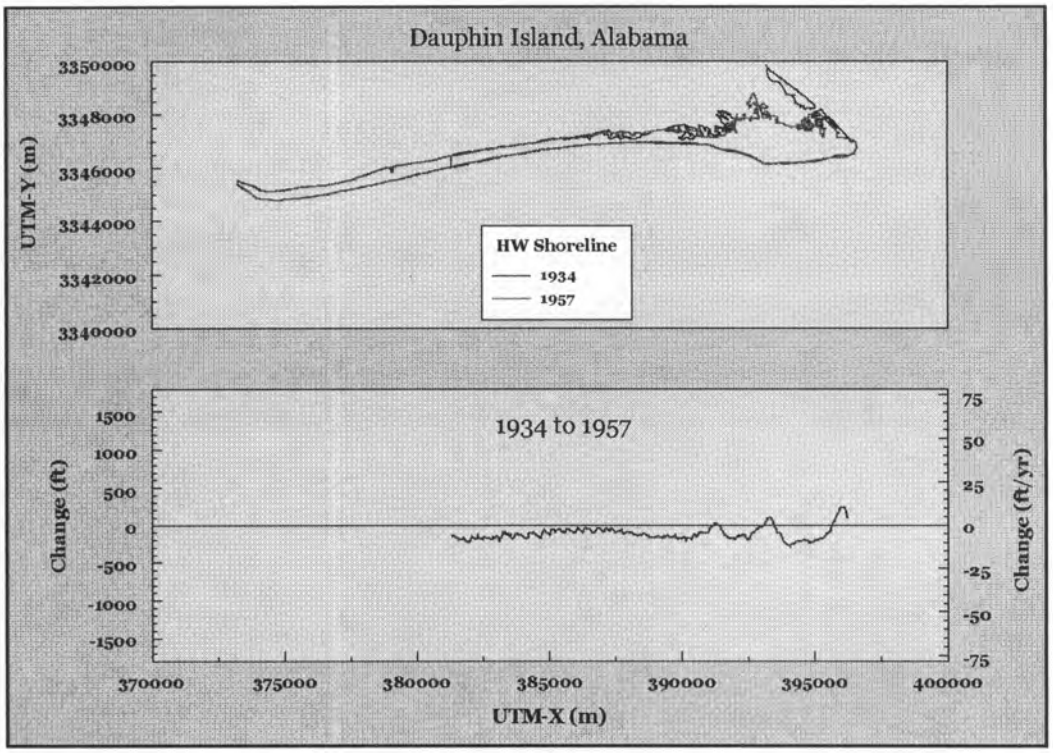

Figure C4. Historical shoreline position change, Dauphin Island, Alabama: 1934 to 1957.

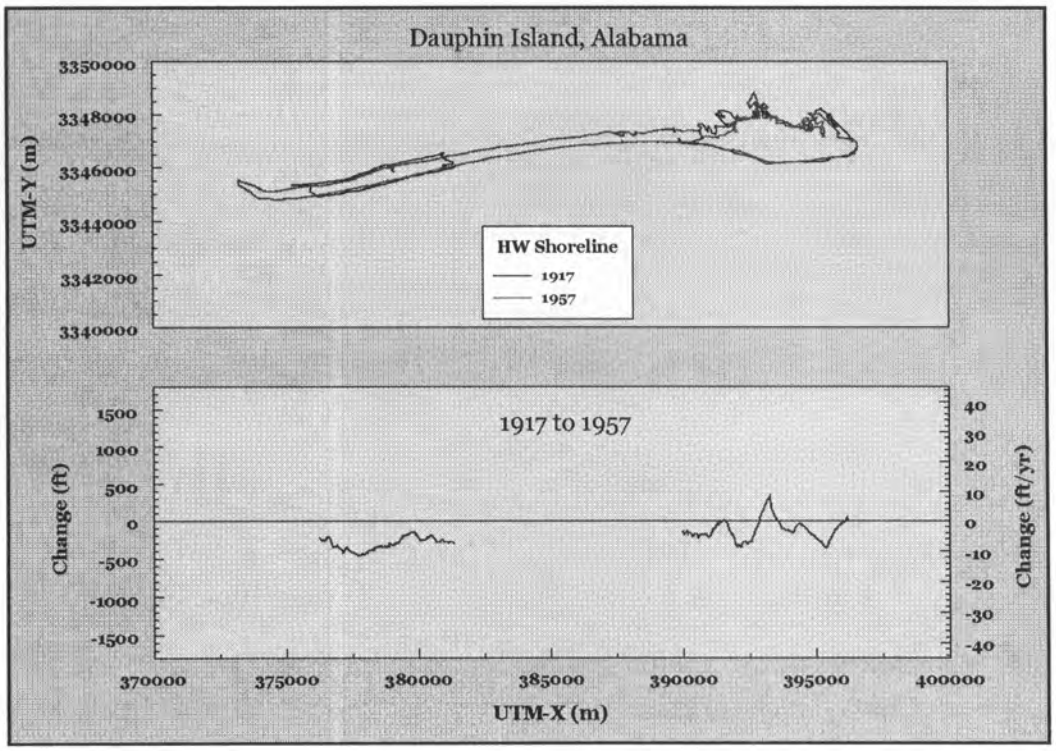

Figure C5. Historical shoreline position change, Dauphin Island, Alabama: 1917 to 1957.

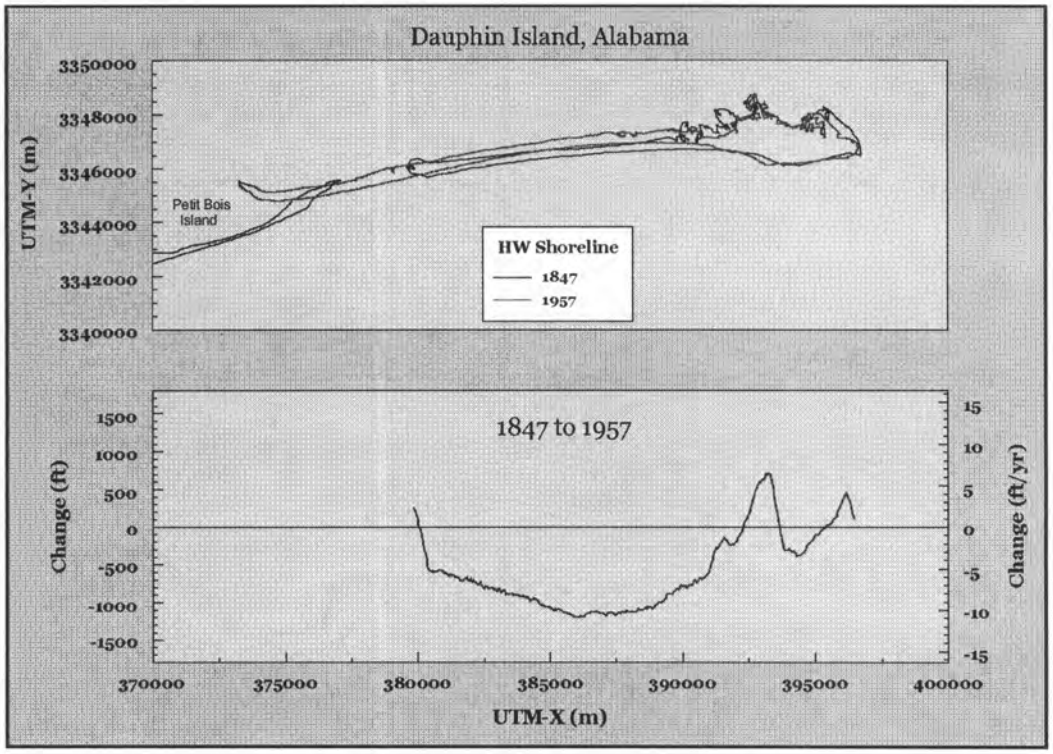

Figure C6. Historical shoreline position change, Dauphin Island, Alabama: 1847 to 1957.

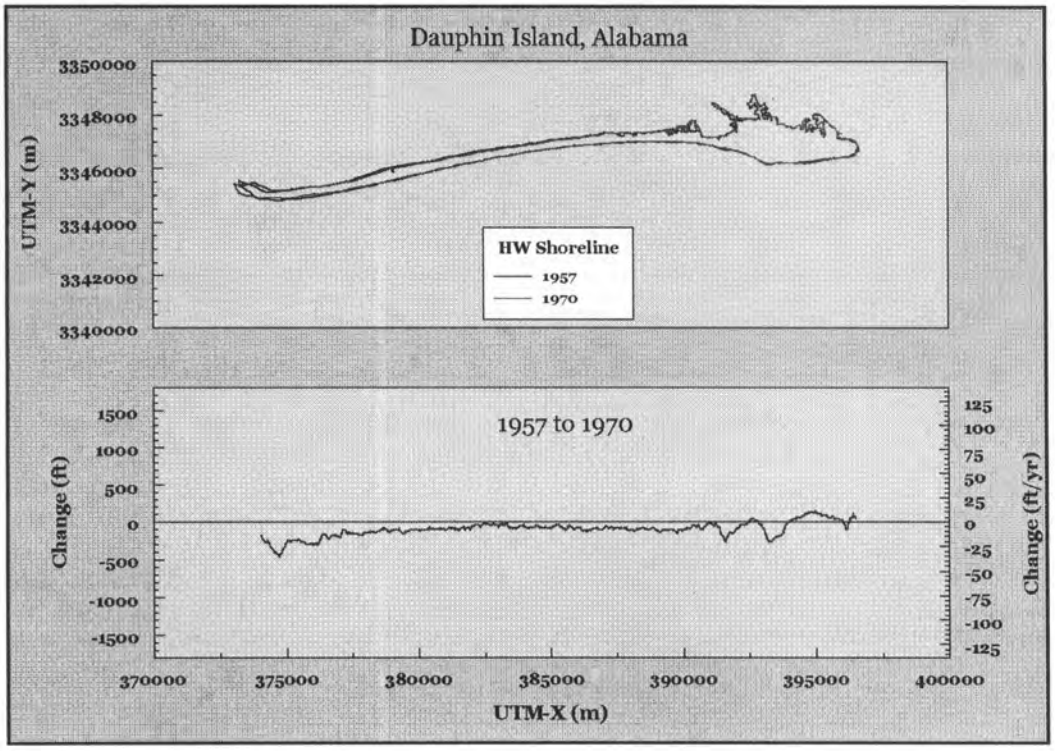

Figure C7. Historical shoreline position change, Dauphin Island, Alabama: 1957 to 1970.

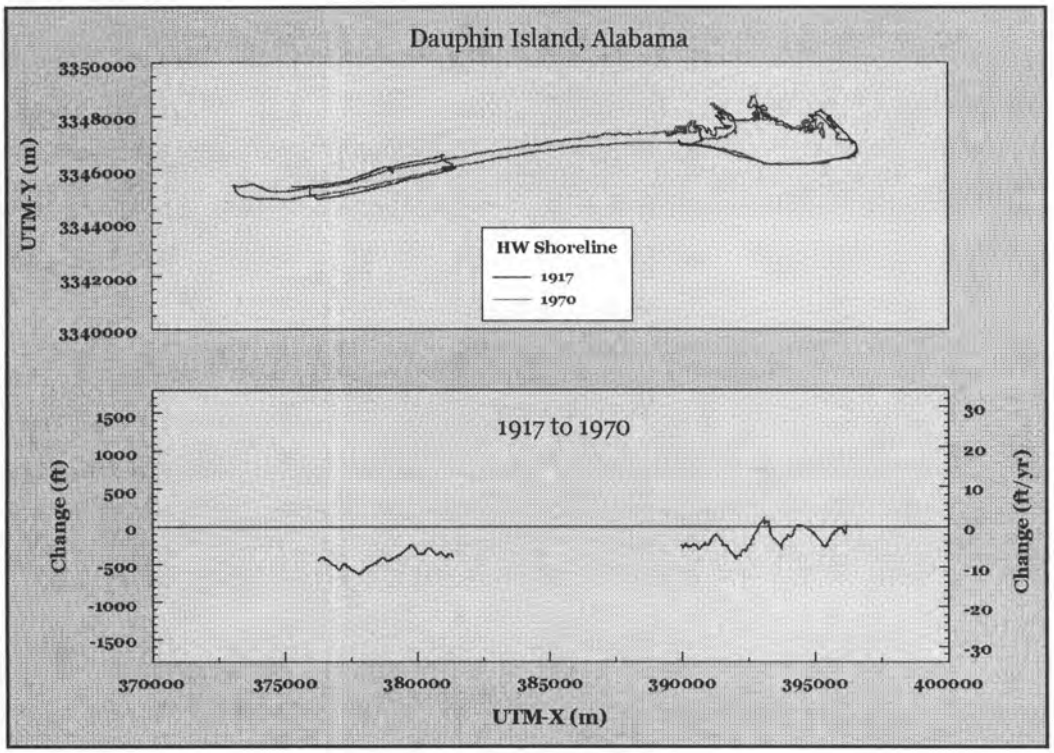

Figure C8. Historical shoreline position change, Dauphin Island, Alabama: 1917 to 1970.

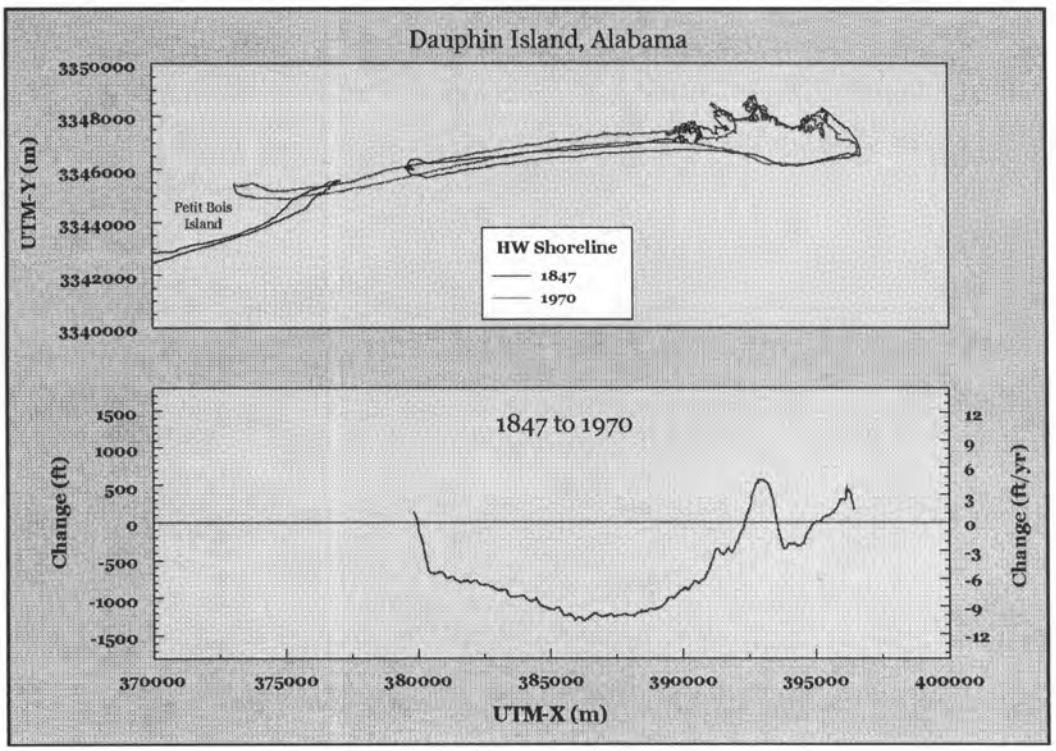

Figure C9. Historical shoreline position change, Dauphin Island, Alabama: 1847 to 1970.

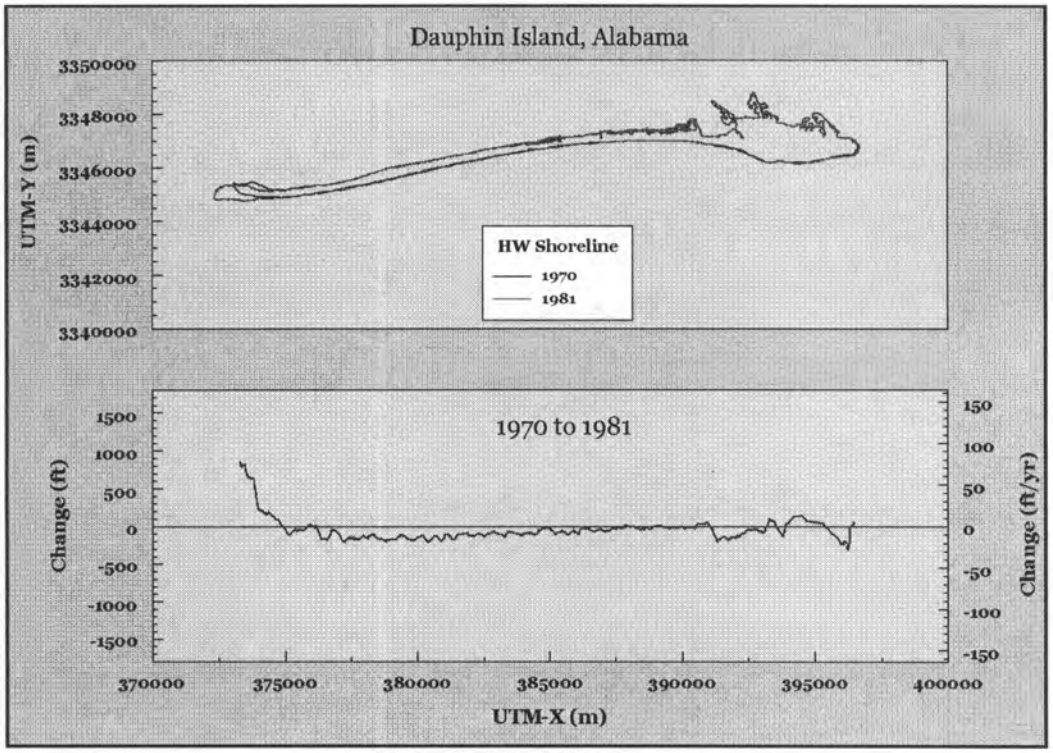

Figure C10. Historical shoreline position change, Dauphin Island, Alabama: 1970 to 1981.

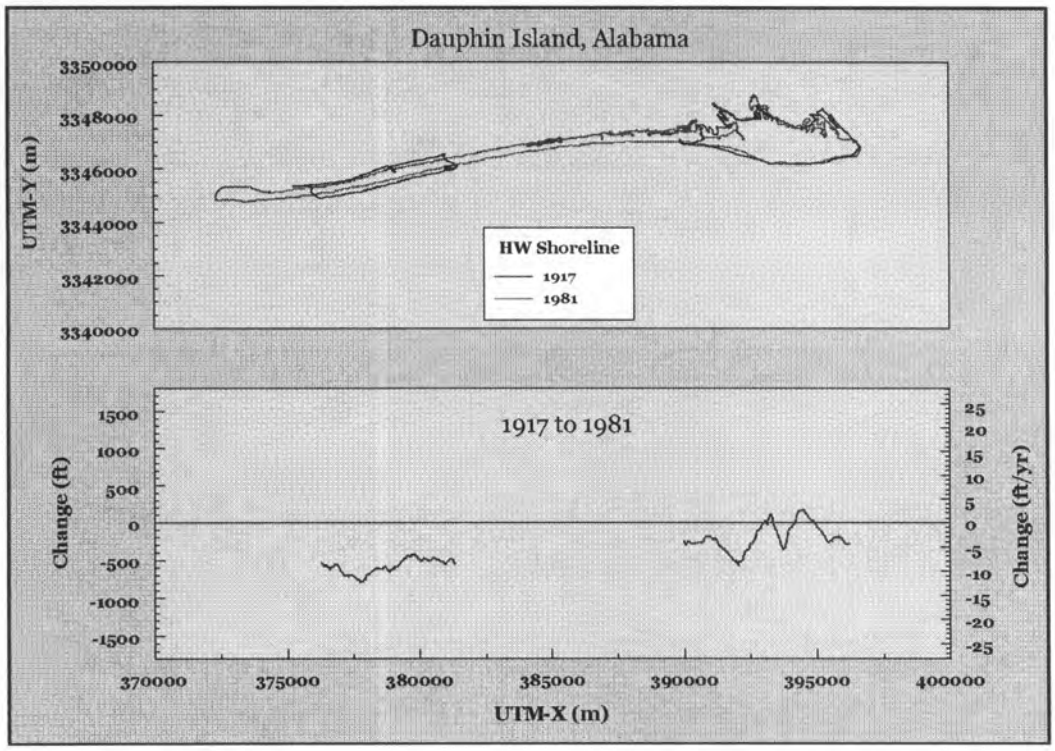

Figure C11. Historical shoreline position change, Dauphin Island, Alabama: 1917 to 1981.

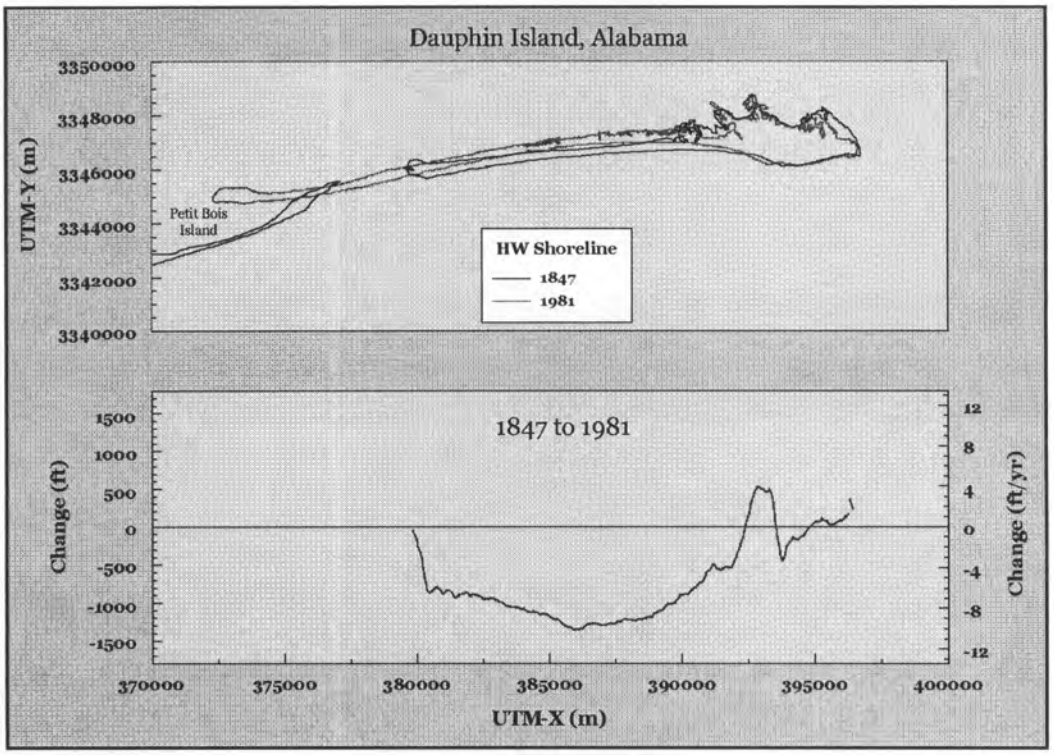

Figure C12. Historical shoreline position change, Dauphin Island, Alabama: 1847 to 1981.

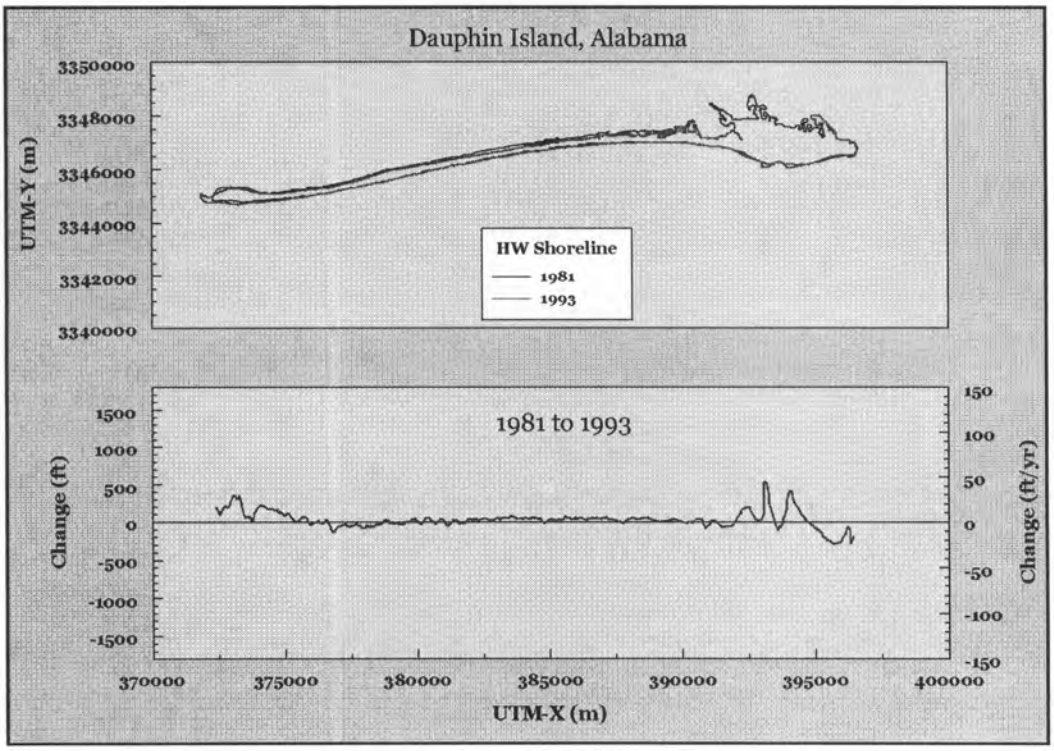

Figure C13. Historical shoreline position change, Dauphin Island, Alabama: 1981 to 1993.

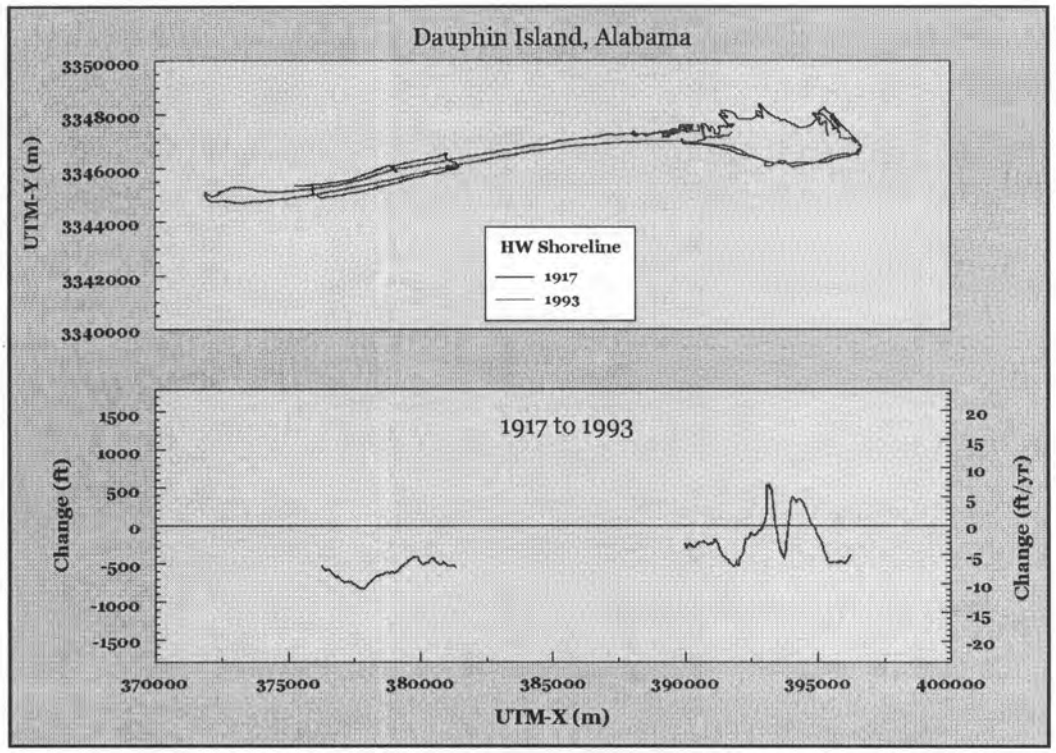

Figure C14. Historical shoreline position change, Dauphin Island, Alabama: 1917 to 1993.

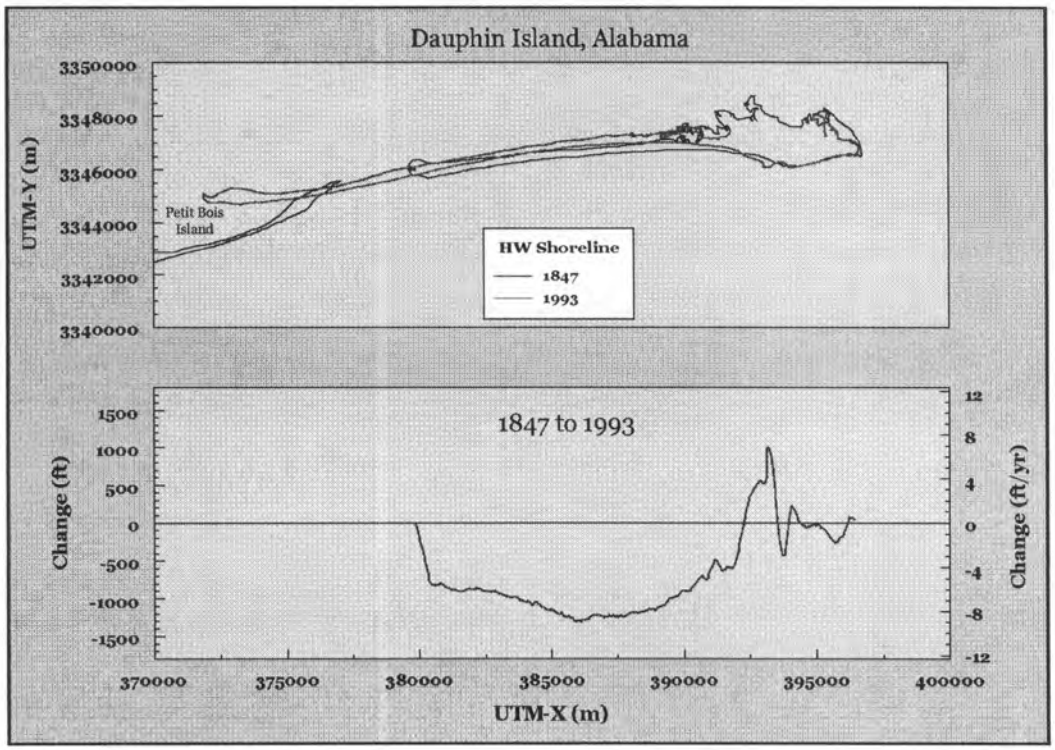

Figure C15. Historical shoreline position change, Dauphin Island, Alabama: 1847 to 1993.

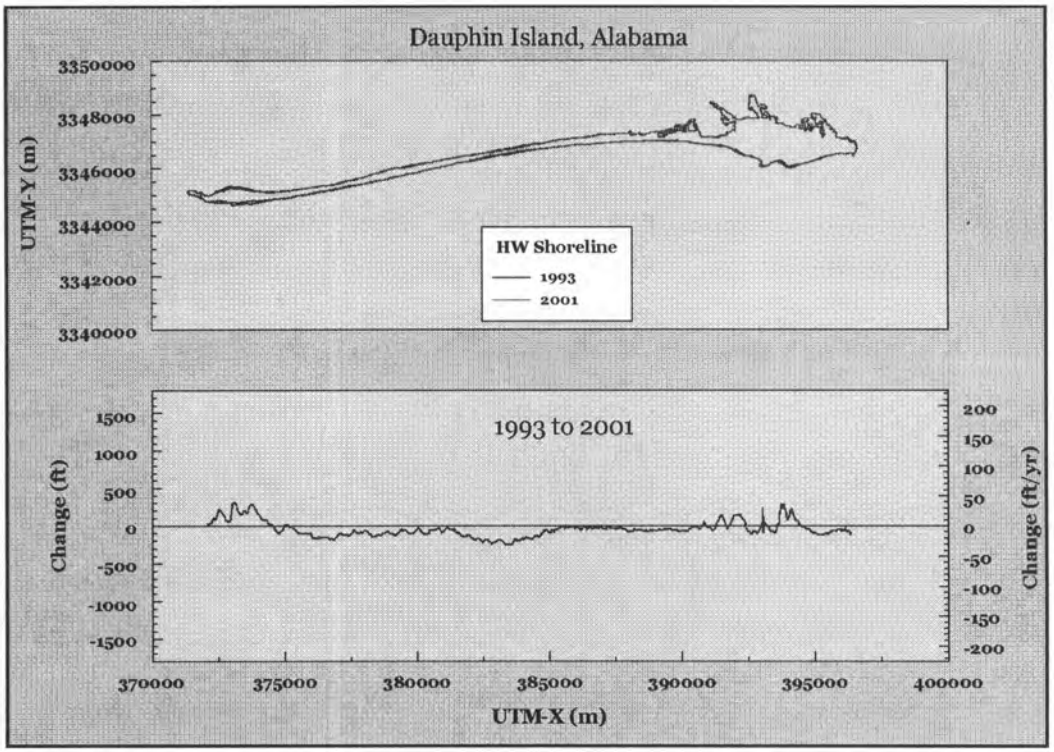

Figure C16. Historical shoreline position change, Dauphin Island, Alabama: 1993 to 2001.

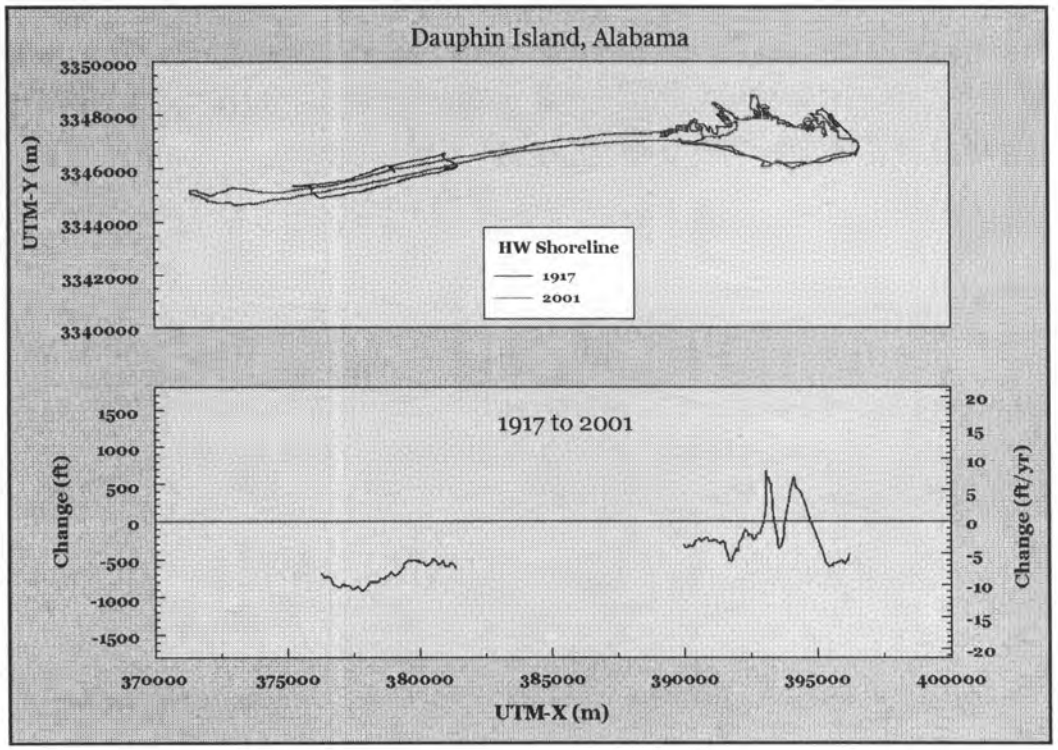

Figure C17. Historical shoreline position change, Dauphin Island, Alabama: 1917 to 2001.

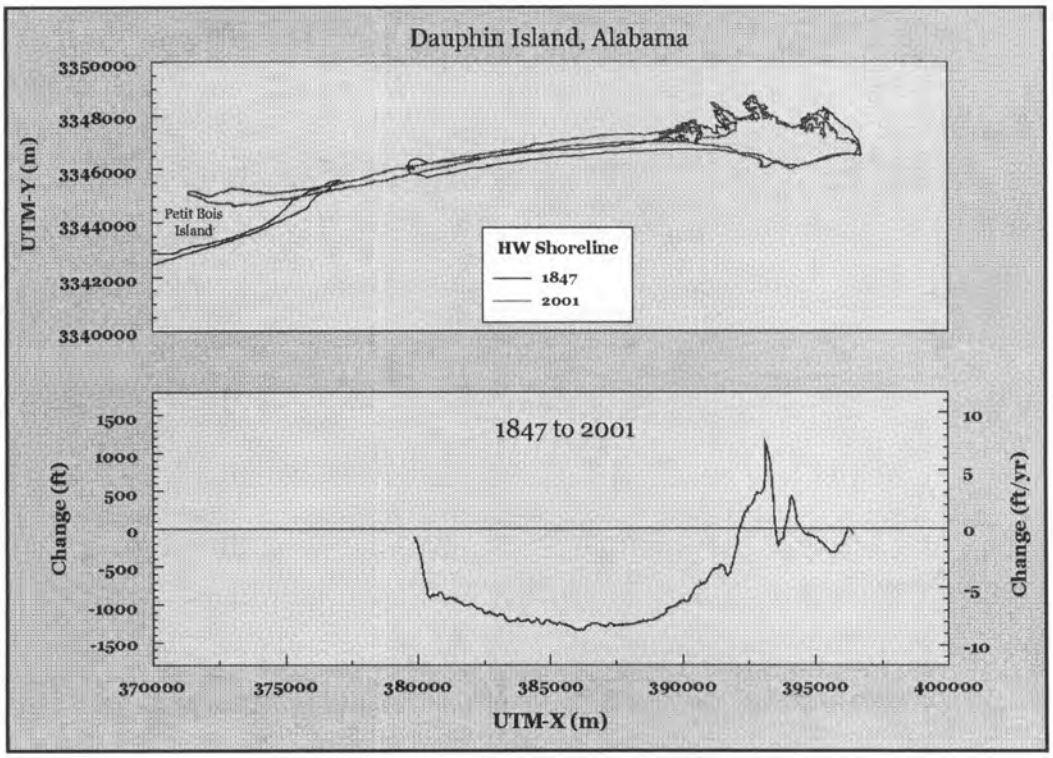

Figure C18. Historical shoreline position change, Dauphin Island, Alabama: 1847 to 2001.

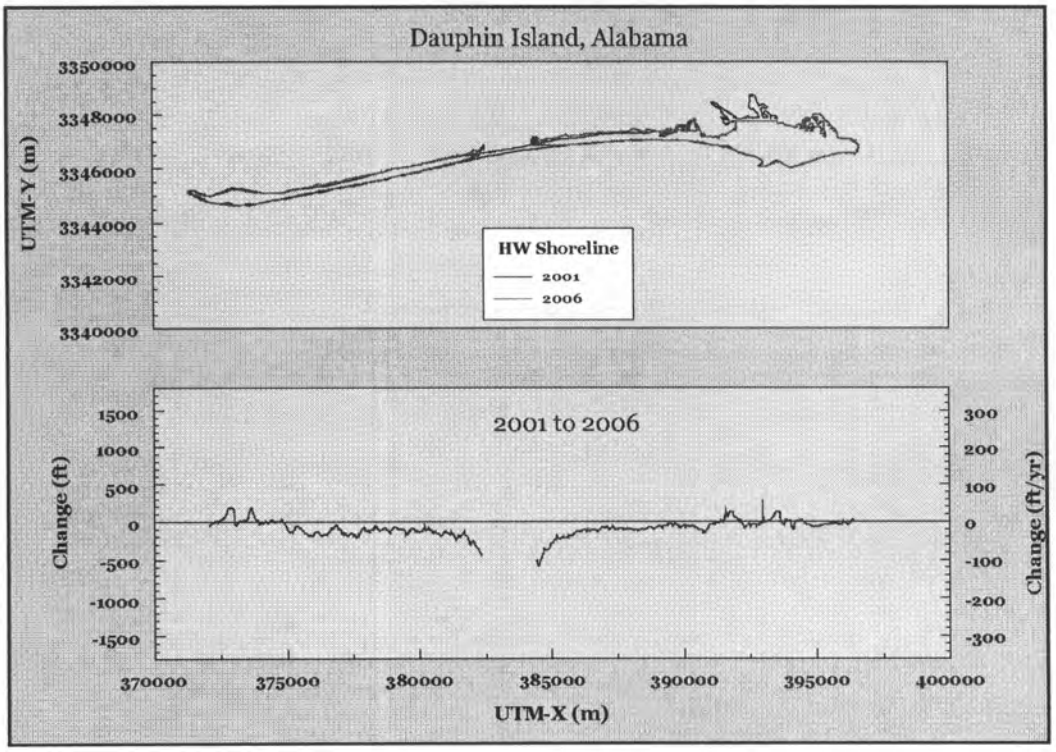

Figure C19. Historical shoreline position change, Dauphin Island, Alabama: 2001 to 2006.

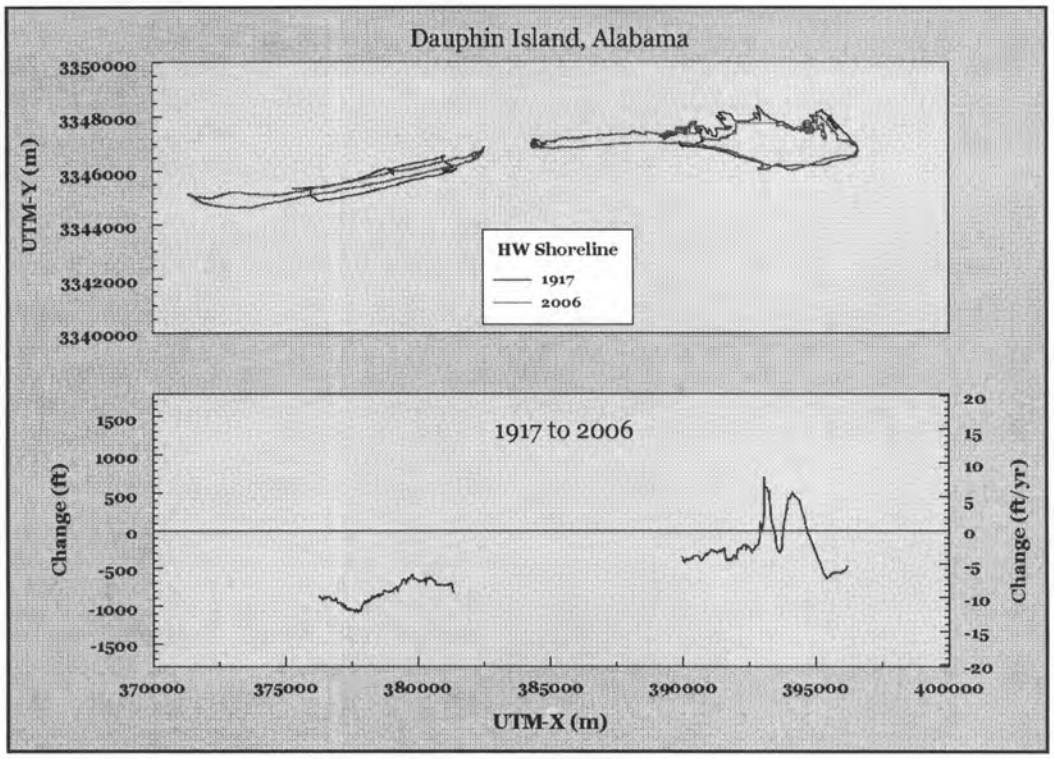

Figure C20. Historical shoreline position change, Dauphin Island, Alabama: 1917 to 2006.

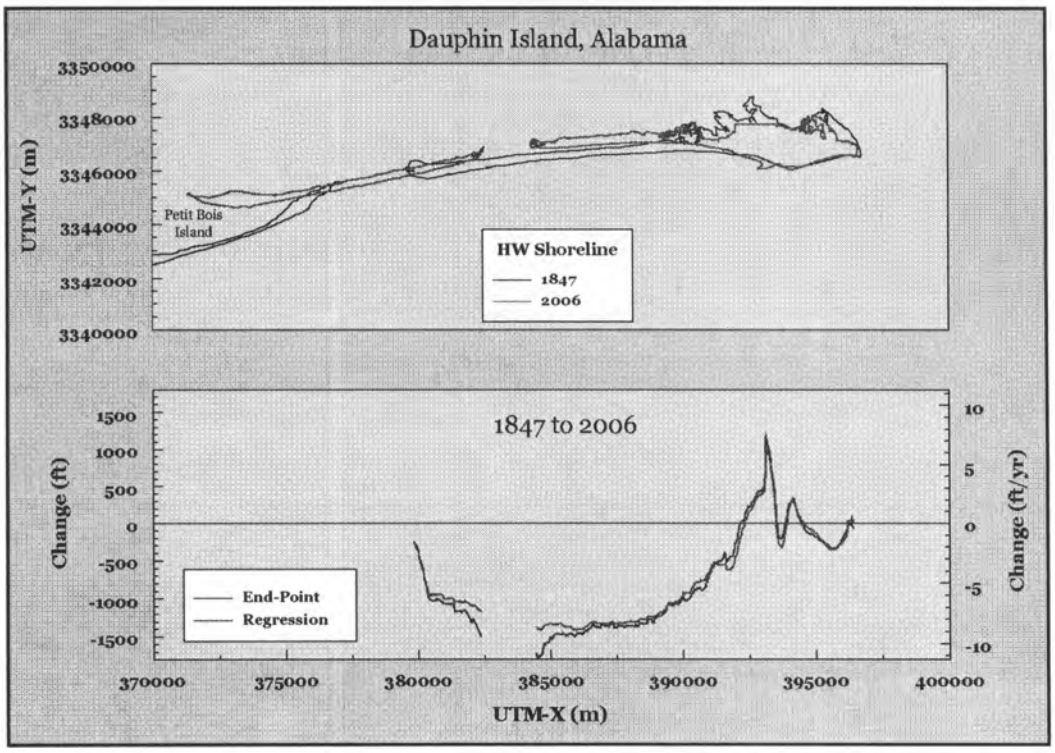

Figure C21. Historical shoreline position change, Dauphin Island, Alabama: 1847 to 2006.

Appendix D

Historical Shoreline Position Change Perdido Pass to Mobile Point: 1847 to 2006

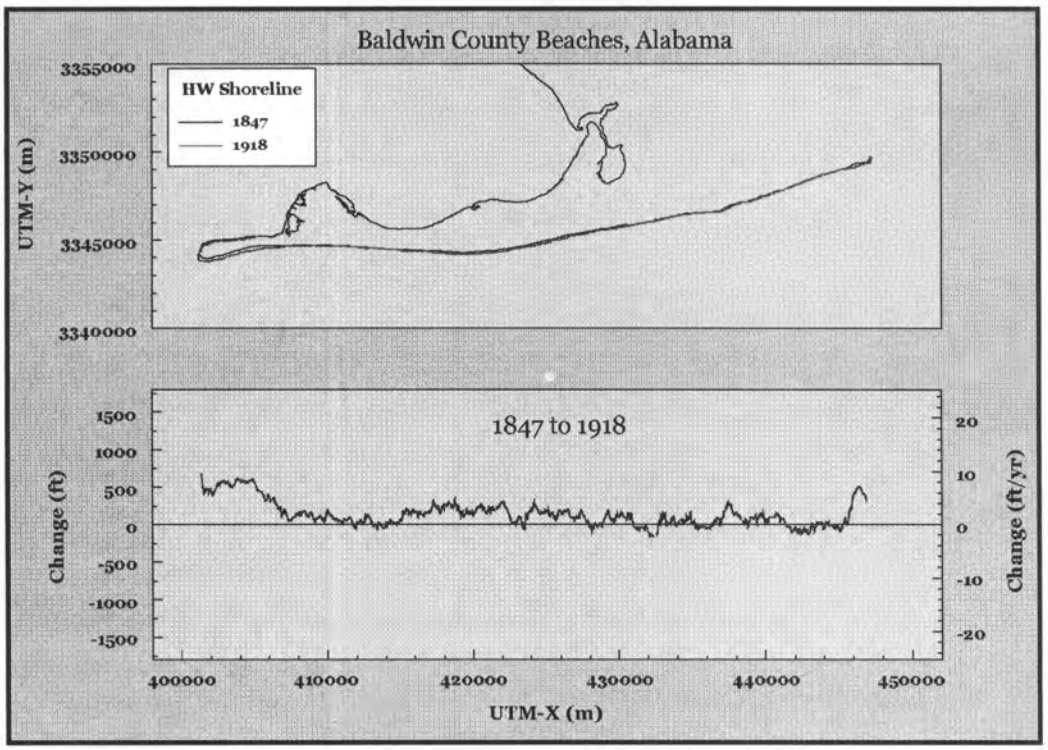

Figure D1. Historical shoreline position change, Perdido Pass to Mobile Point, Alabama: 1847 to 1918.

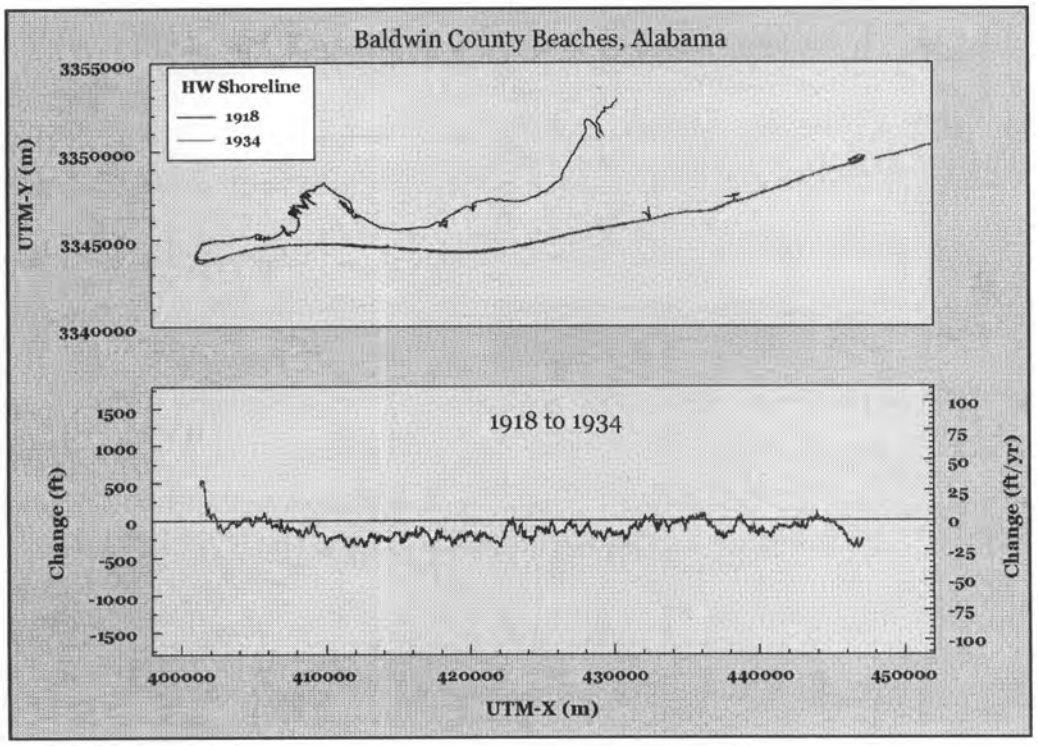

Figure D2. Historical shoreline position change, Perdido Pass to Mobile Point, Alabama: 1918 to 1934.

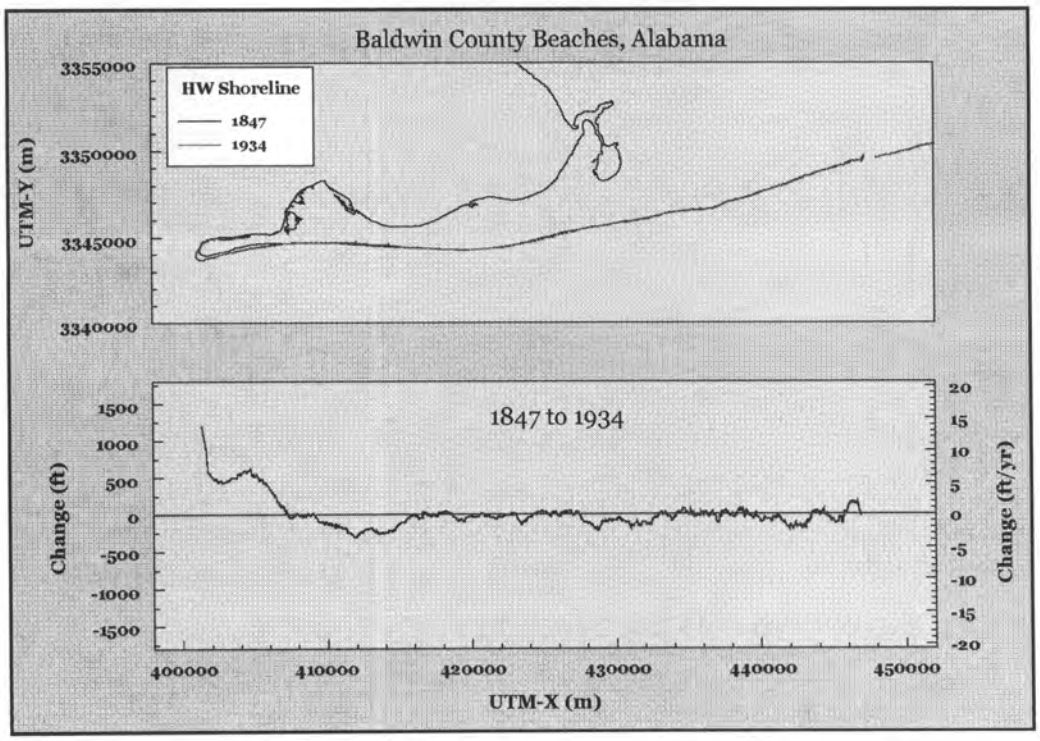

Figure D3. Historical shoreline position change, Perdido Pass to Mobile Point, Alabama: 1847 to 1934.

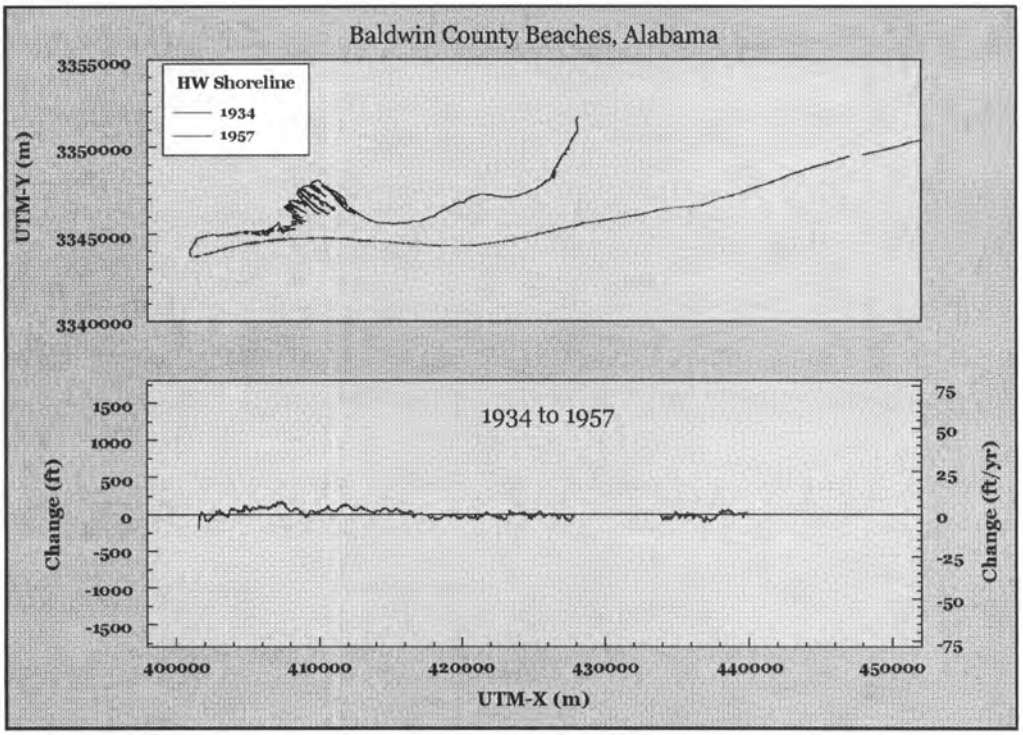

Figure D4. Historical shoreline position change, Perdido Pass to Mobile Point, Alabama: 1934 to 1957.

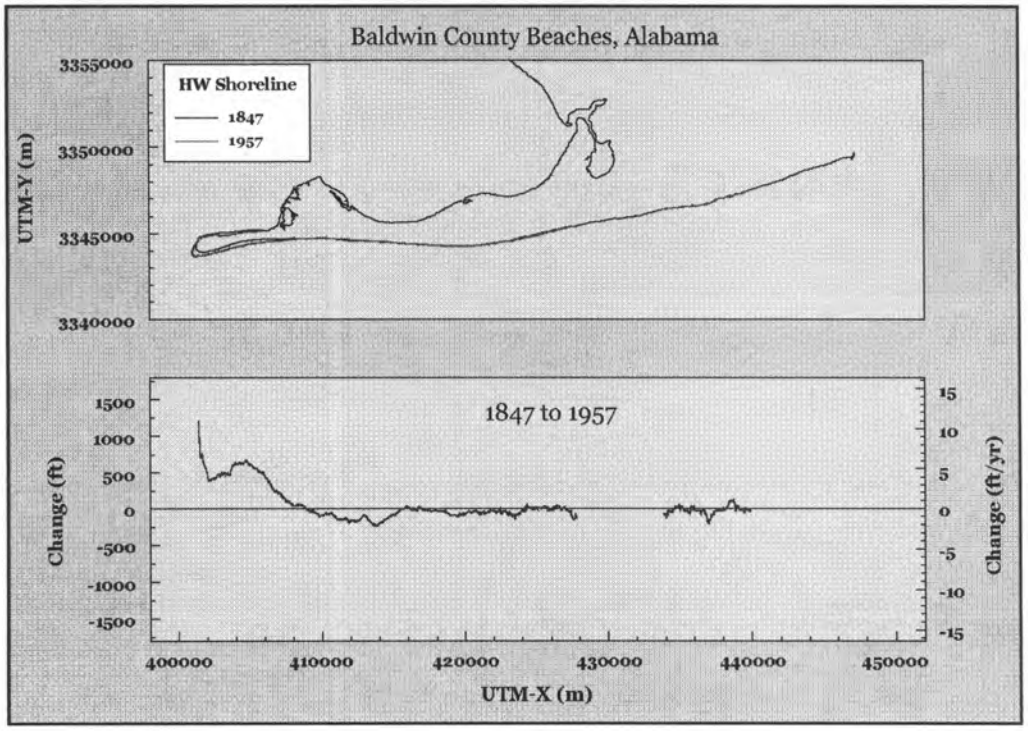

Figure D5. Historical shoreline position change, Perdido Pass to Mobile Point, Alabama: 1847 to 1957.

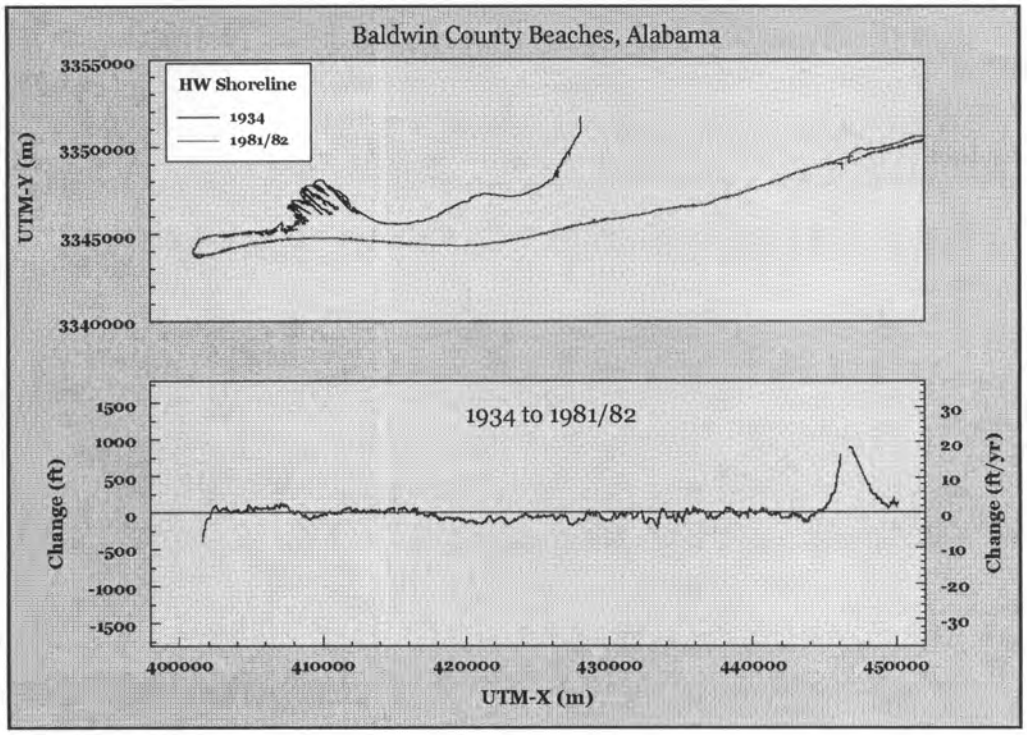

Figure D6. Historical shoreline position change, Perdido Pass to Mobile Point, Alabama: 1934 to 1981/82.

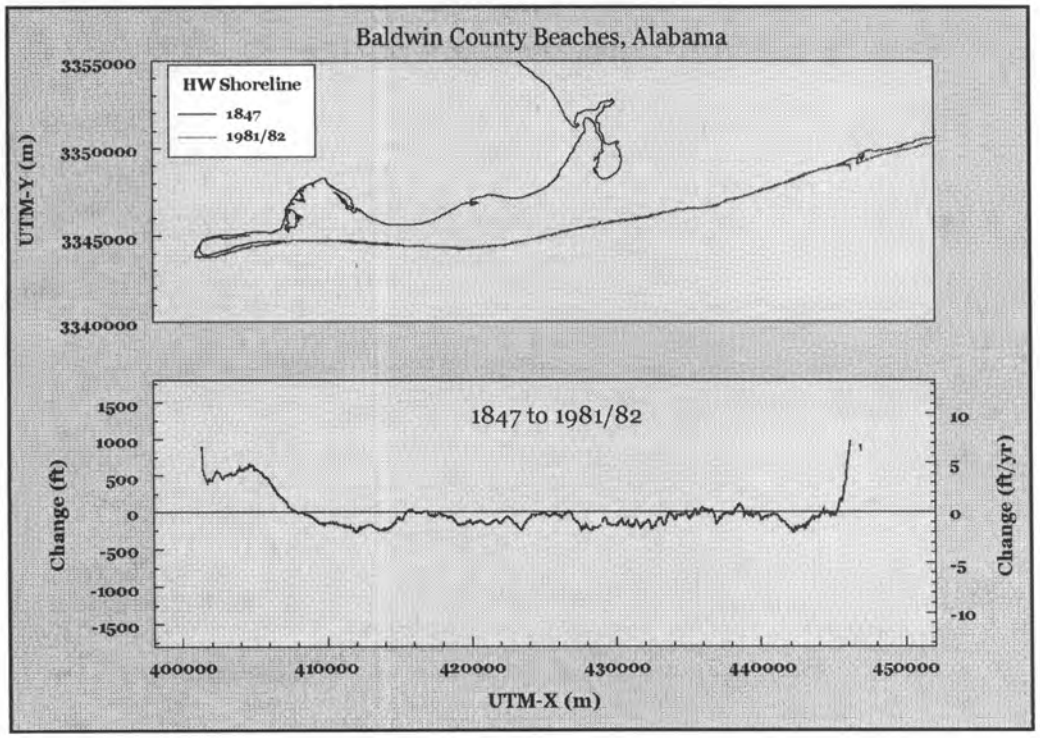

Figure D7. Historical shoreline position change, Perdido Pass to Mobile Point, Alabama: 1847 to 1981/82.

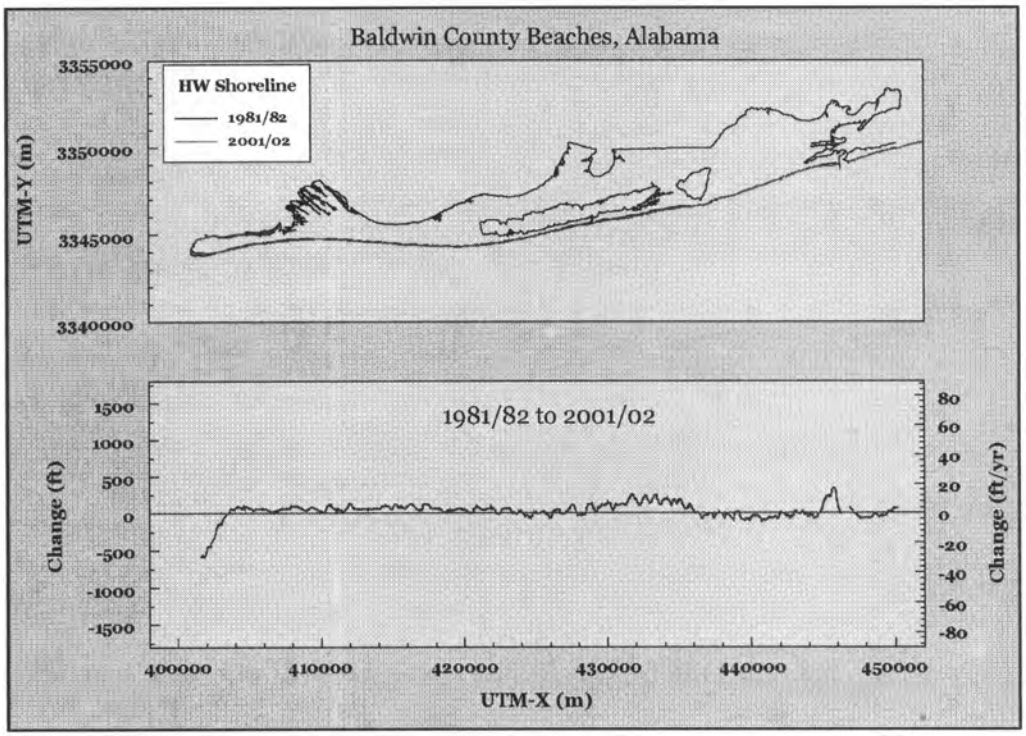

Figure D8. Historical shoreline position change, Perdido Pass to Mobile Point, Alabama: 1981/82 to 2001/02.

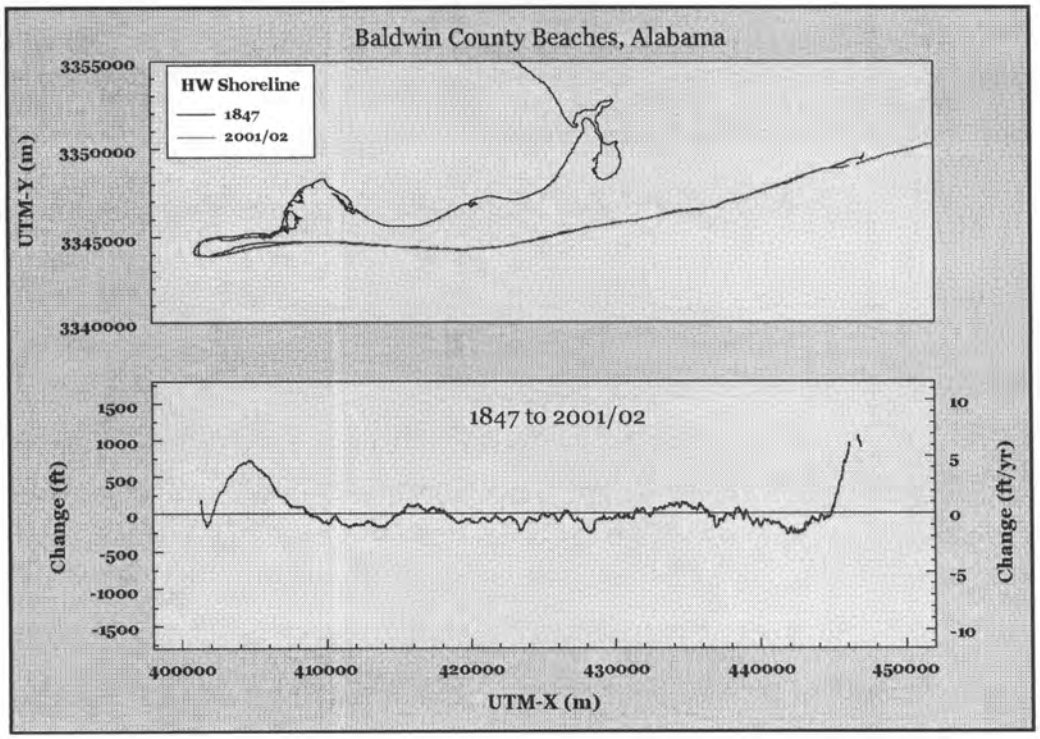

Figure D9. Historical shoreline position change, Perdido Pass to Mobile Point, Alabama: 1847 to 2001/02.

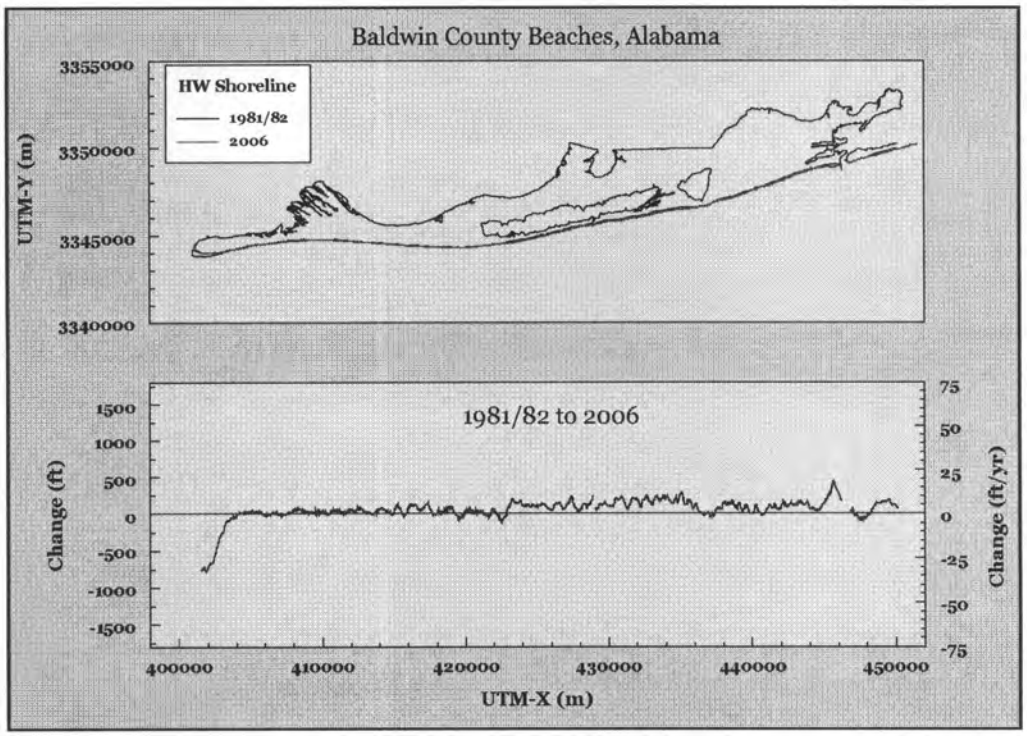

Figure D10. Historical shoreline position change, Perdido Pass to Mobile Point, Alabama: 1981/82 to 2006.

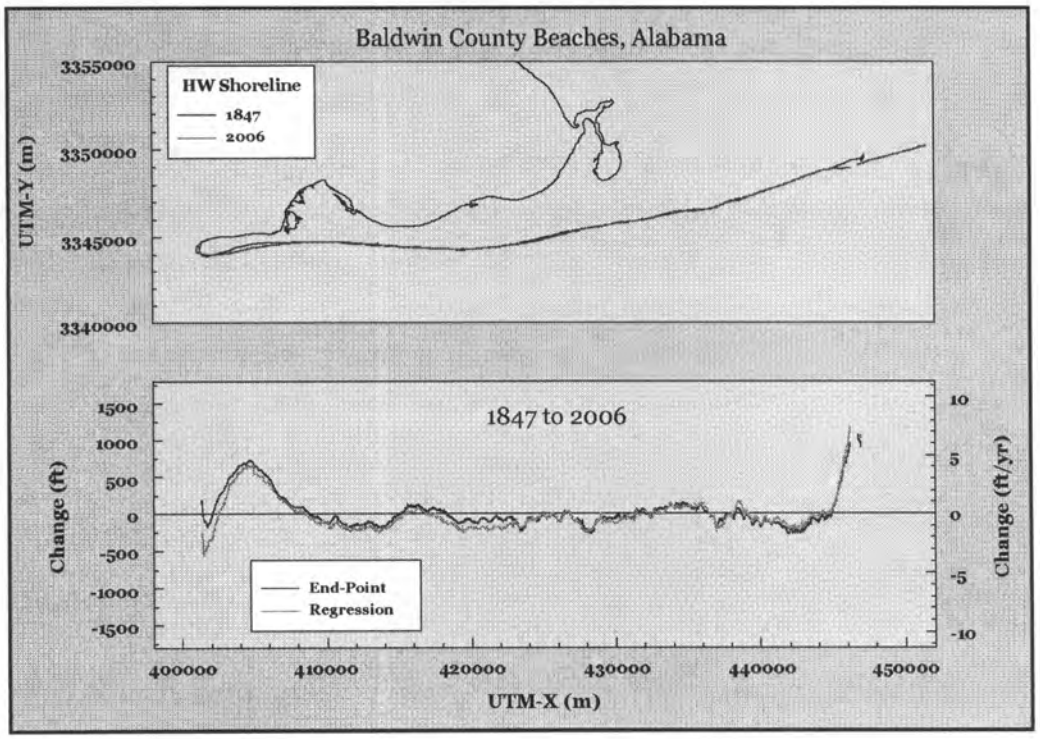

Figure D11. Historical shoreline position change, Perdido Pass to Mobile Point, Alabama: 1847 to 2006.

Appendix E

Shoreline and Bathymetry Data Extents

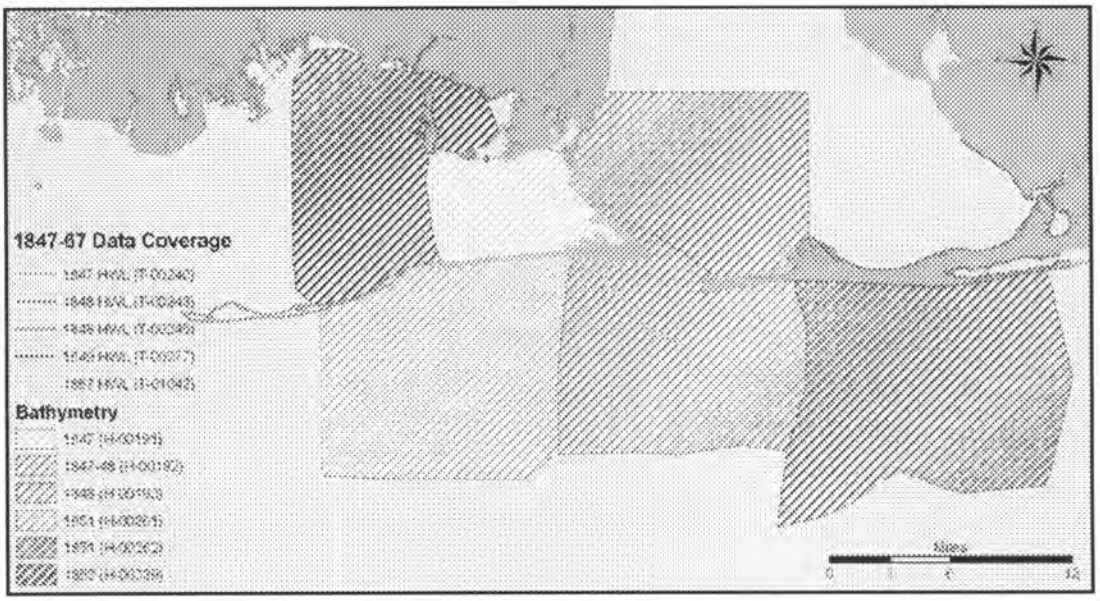

Figure E1. Bathymetry and high-water shoreline data coverage – 1847/52.

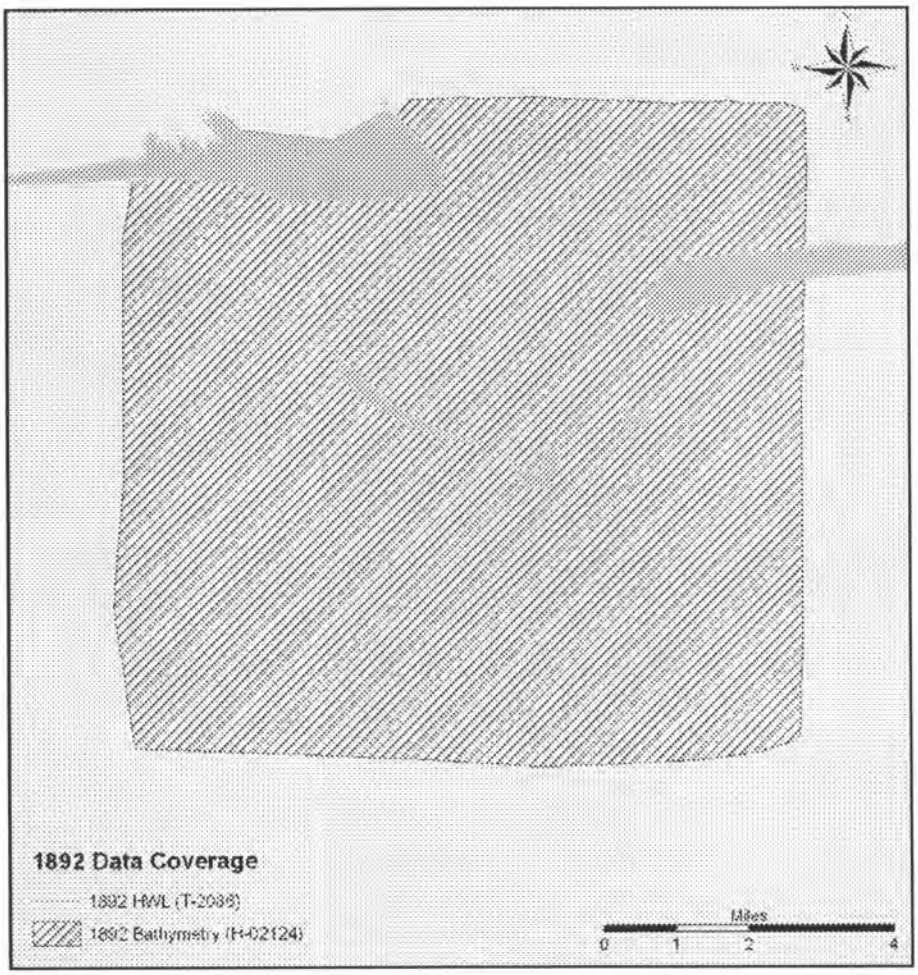

Figure E2. Bathymetry and high-water shoreline data coverage – 1892.

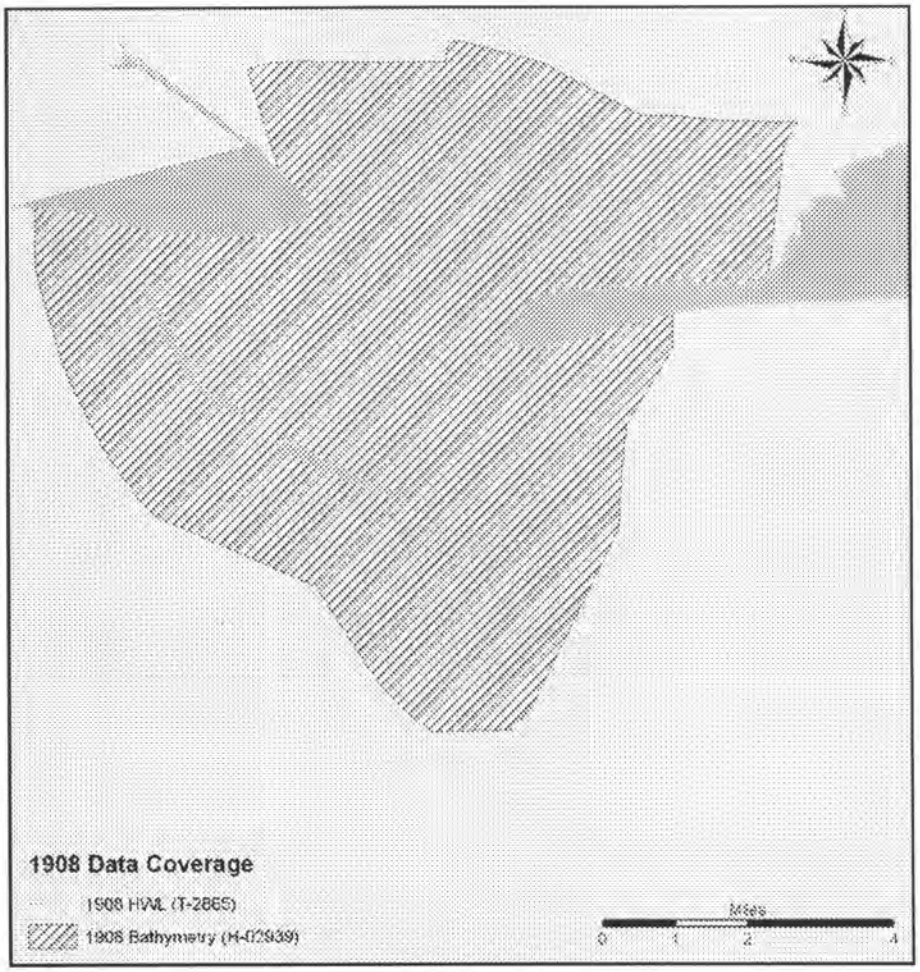

Figure E3. Bathymetry and high-water shoreline data coverage – 1908.

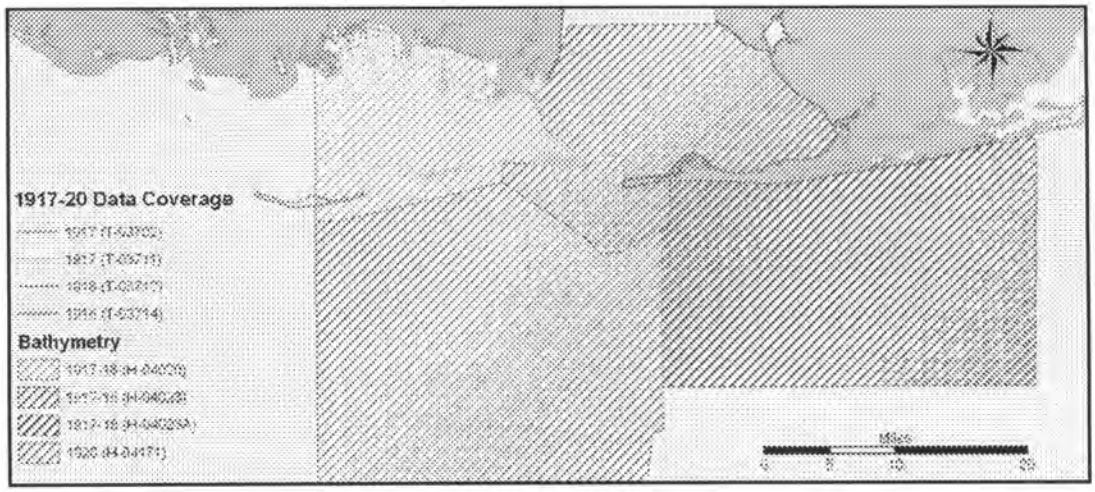

Figure E4. Bathymetry and high-water shoreline data coverage – 1917/20.

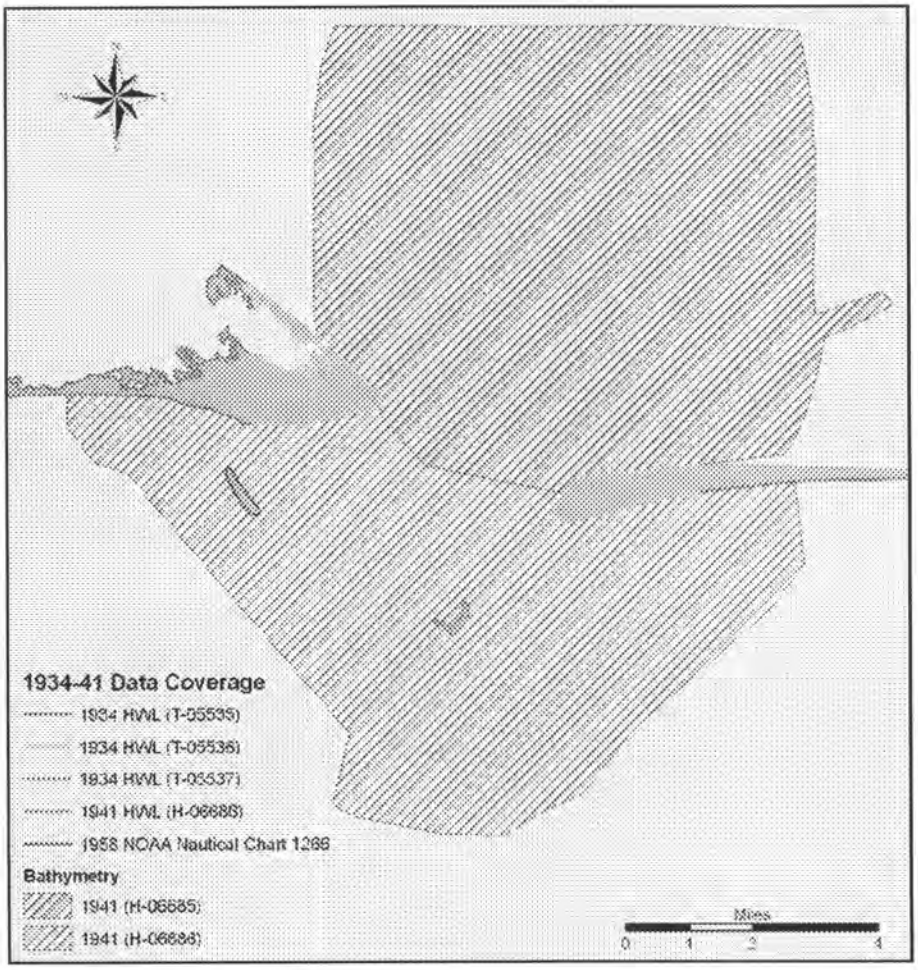

Figure E5. Bathymetry and high-water shoreline data coverage – 1941.

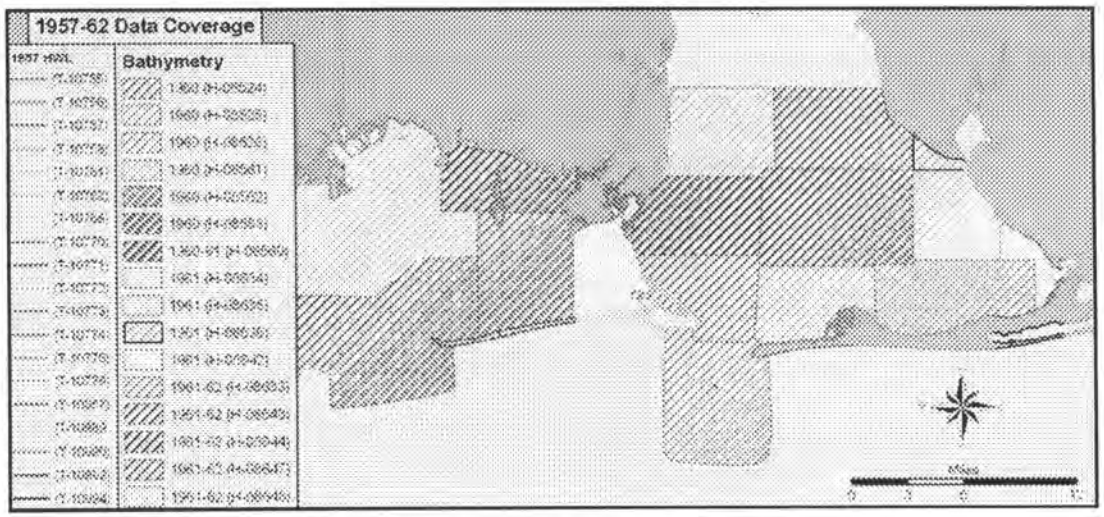

Figure E6. Bathymetry and high-water shoreline data coverage – 1957/62.

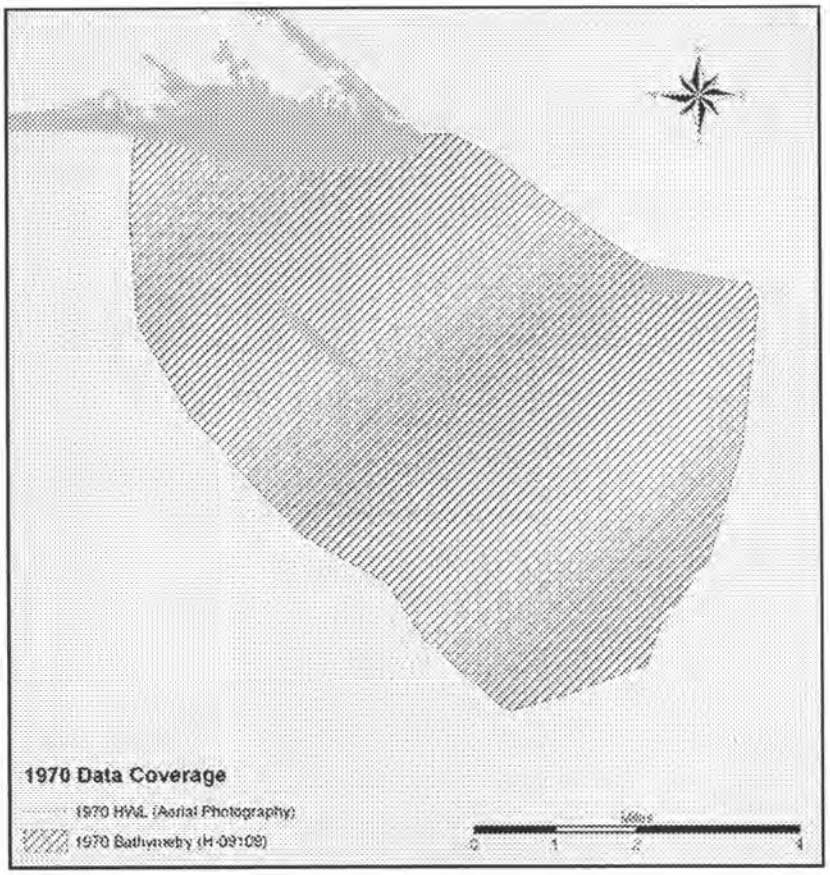

Figure E7. Bathymetry and high-water shoreline data coverage – 1970.

Figure E8. Bathymetry and high-water shoreline data coverage – 1978/88.

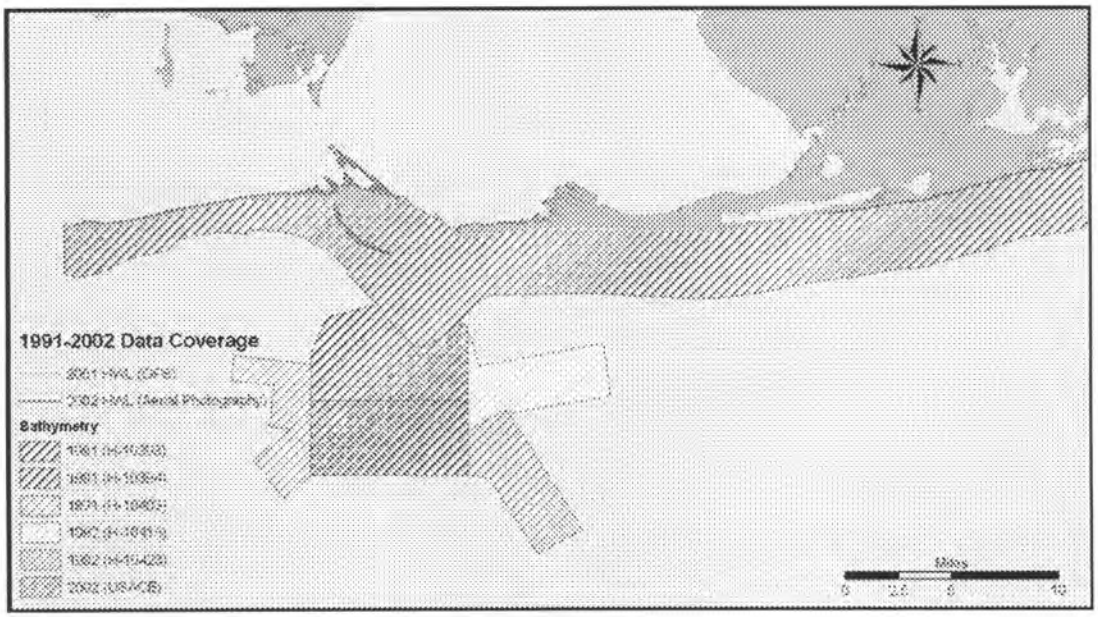

Figure E9. Bathymetry and high-water shoreline data coverage – 1991/2002.

Appendix F

Ebb-Tidal Delta Volume Calculation Extents

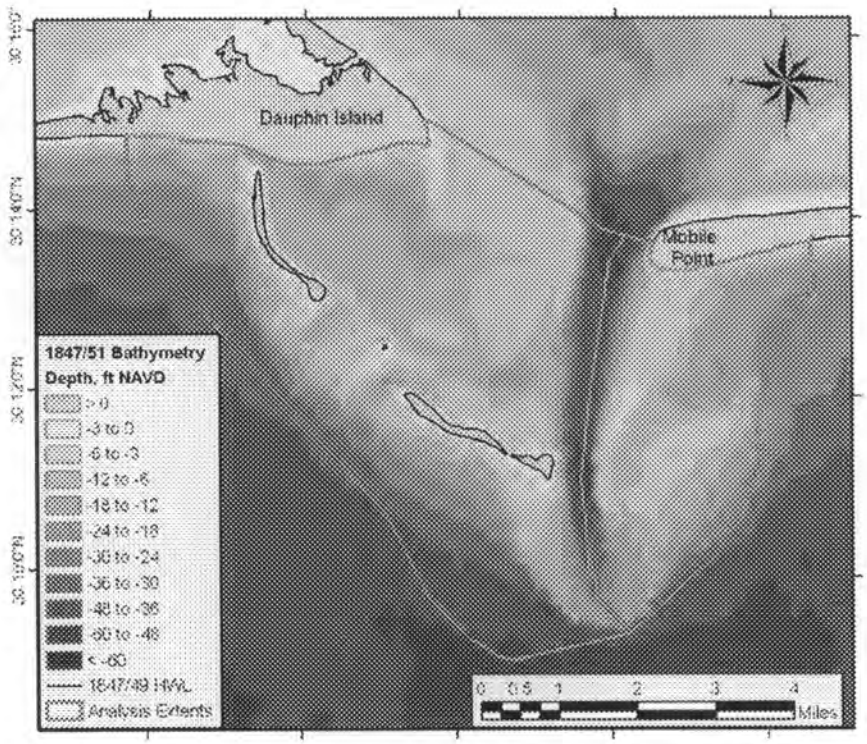

Figure F1. Analysis extent for calculating sand volume above the 30-ft depth contour – 1847/48.

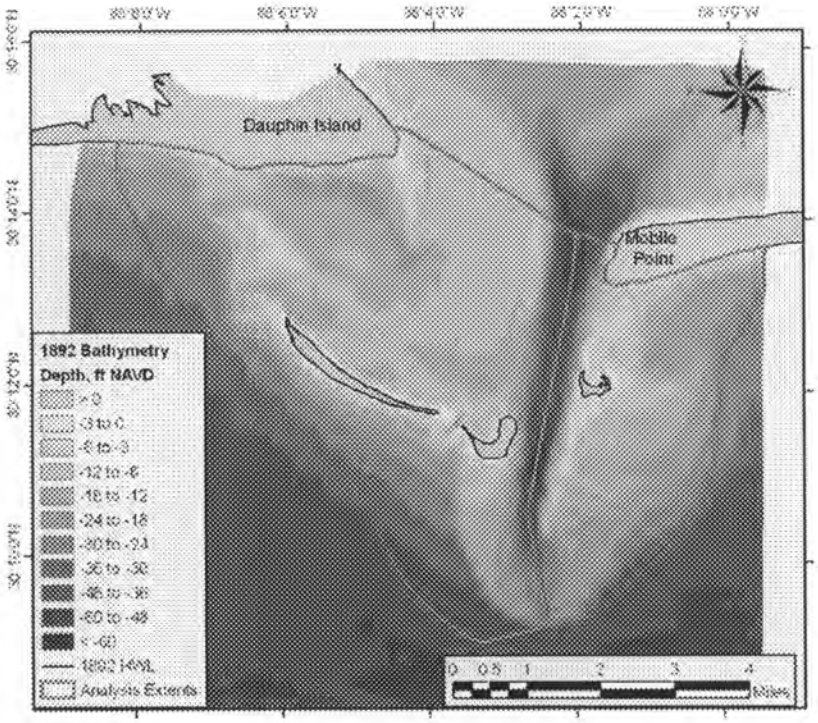

Figure F2. Analysis extent for calculating sand volume above the 30-ft depth contour – 1892.

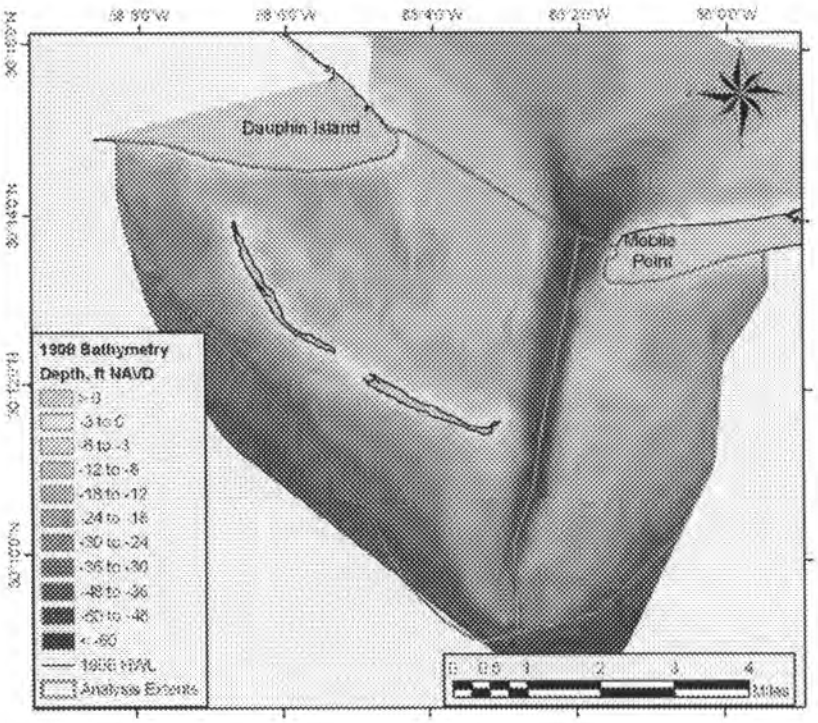

Figure F3. Analysis extent for calculating sand volume above the 30-ft depth contour – 1908.

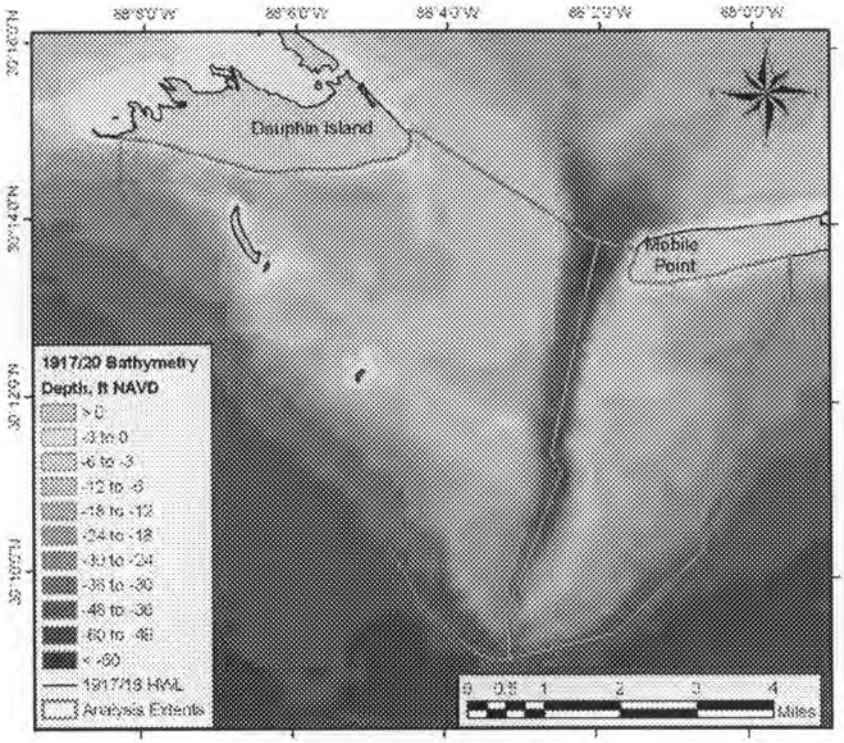

Figure F4. Analysis extent for calculating sand volume above the 30-ft depth contour – 1917/20.

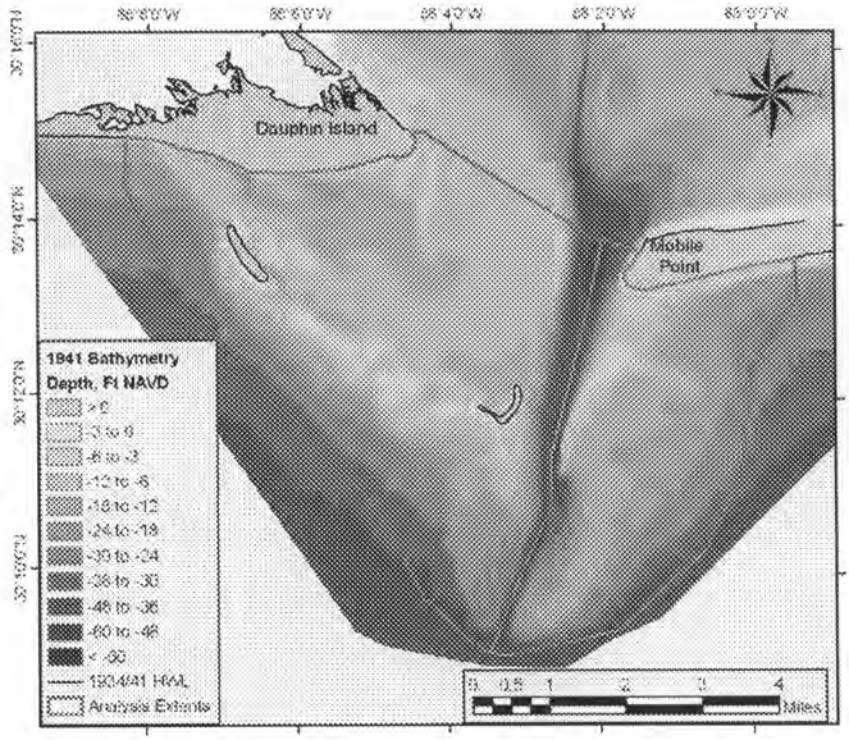

Figure F5. Analysis extent for calculating sand volume above the 30-ft depth contour – 1941.

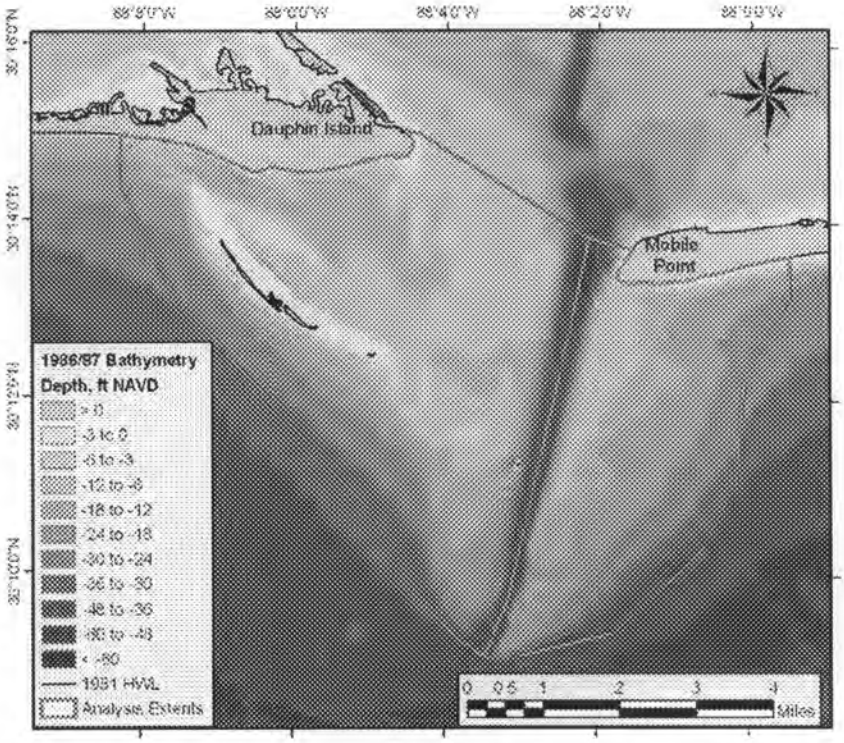

Figure F6. Analysis extent for calculating sand volume above the 30-ft depth contour – 1986/87.

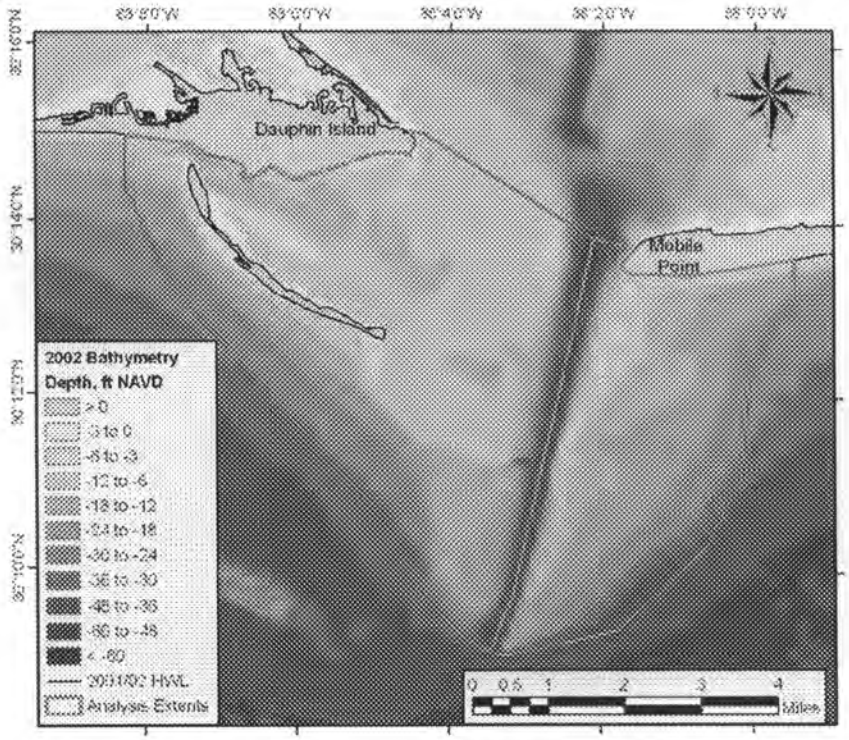

Figure F7. Analysis extent for calculating sand volume above the 30-ft depth contour – 2002.

Appendix G

Bathymetric Change Volume Calculation Extents for Mobile Ebb-Tidal Delta

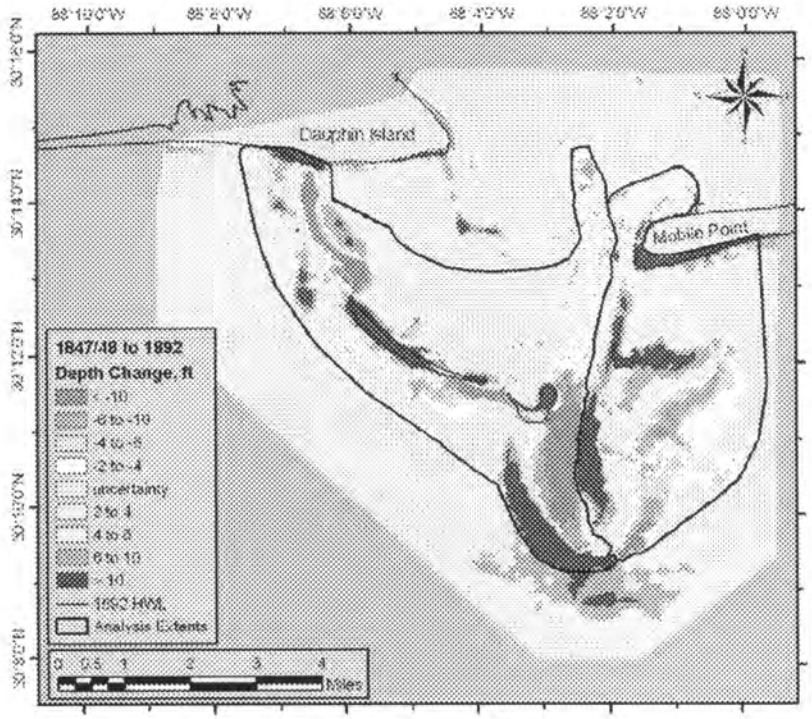

Figure G1. Analysis extent for calculating sand volume change – 1847/48 to 1892.

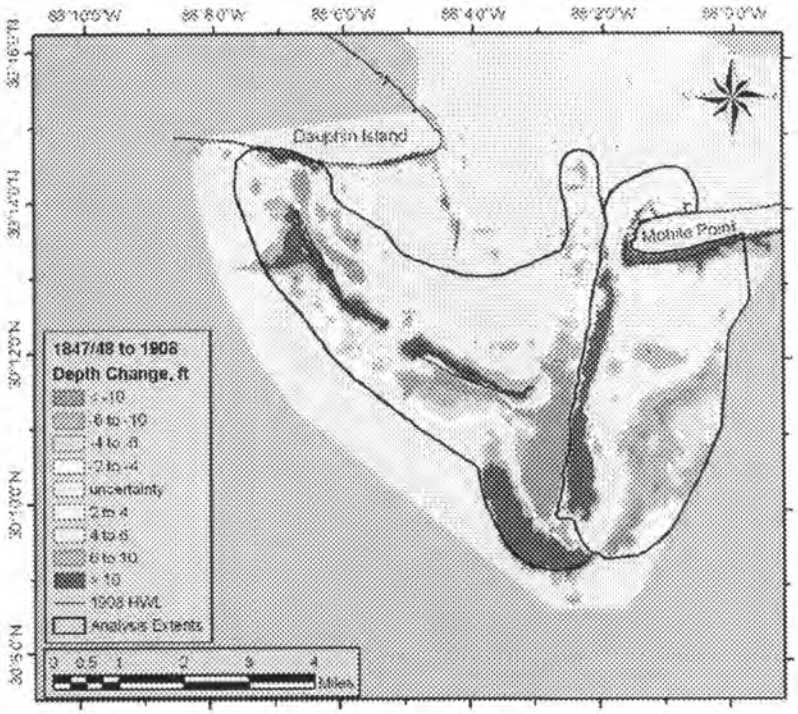

Figure G2. Analysis extent for calculating sand volume change – 1847/48 to 1908.

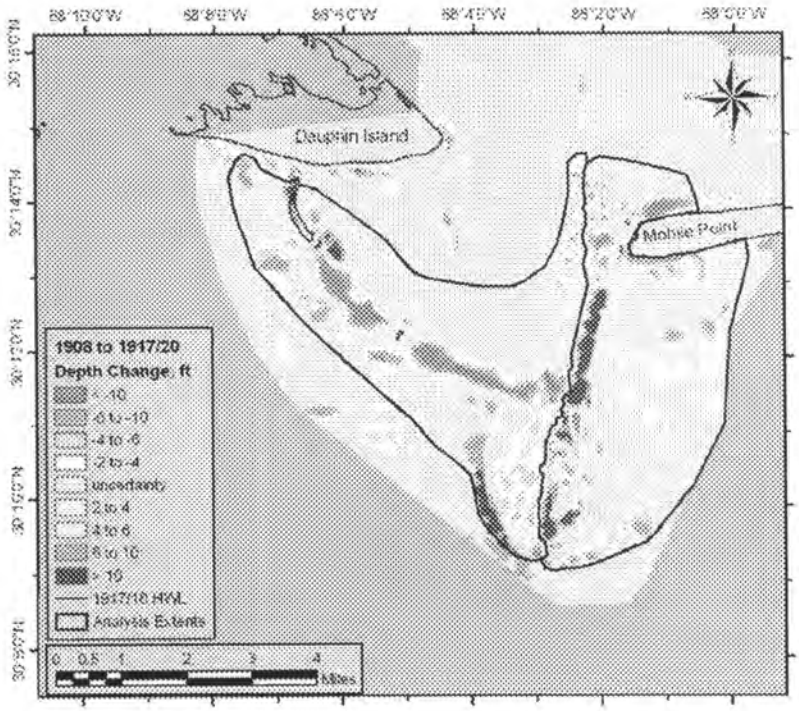

Figure G3. Analysis extent for calculating sand volume change – 1908 to 1917/20.

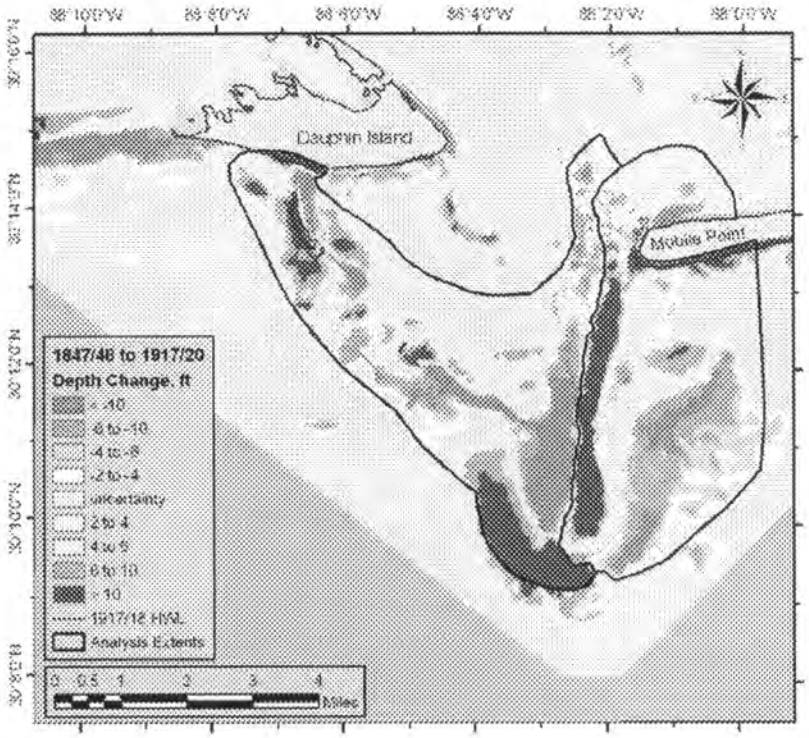

Figure G4. Analysis extent for calculating sand volume change – 1847/48 to 1917/20.

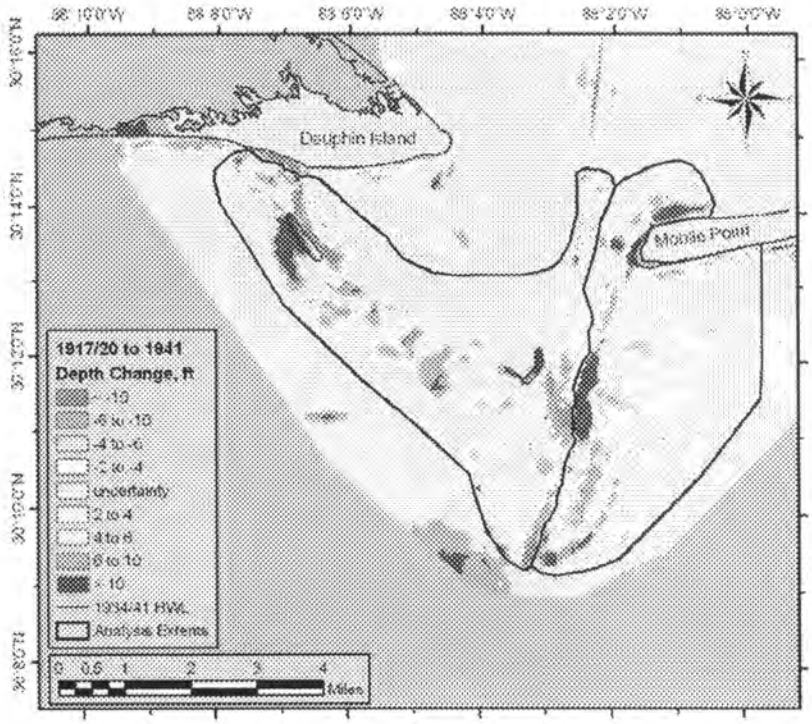

Figure G5. Analysis extent for calculating sand volume change – 1917/20 to 1941.

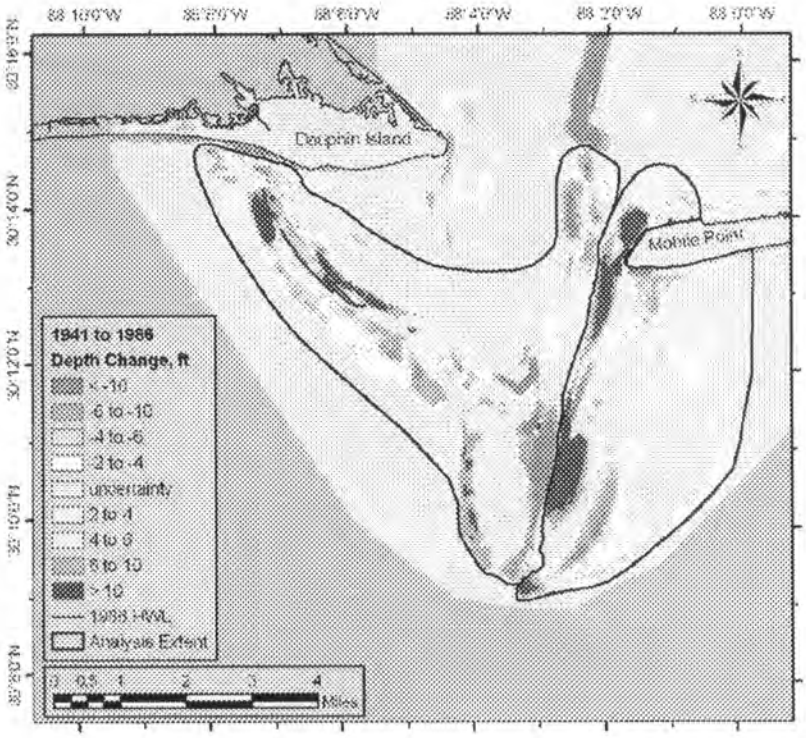

Figure G6. Analysis extent for calculating sand volume change – 1941 to 1986.

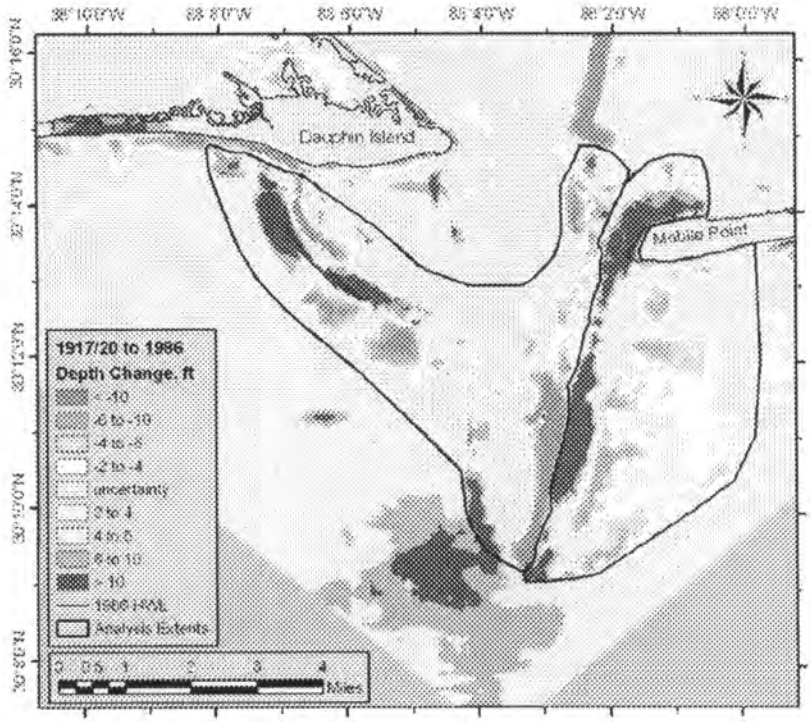

Figure G7. Analysis extent for calculating sand volume change – 1917/20 to 1986.

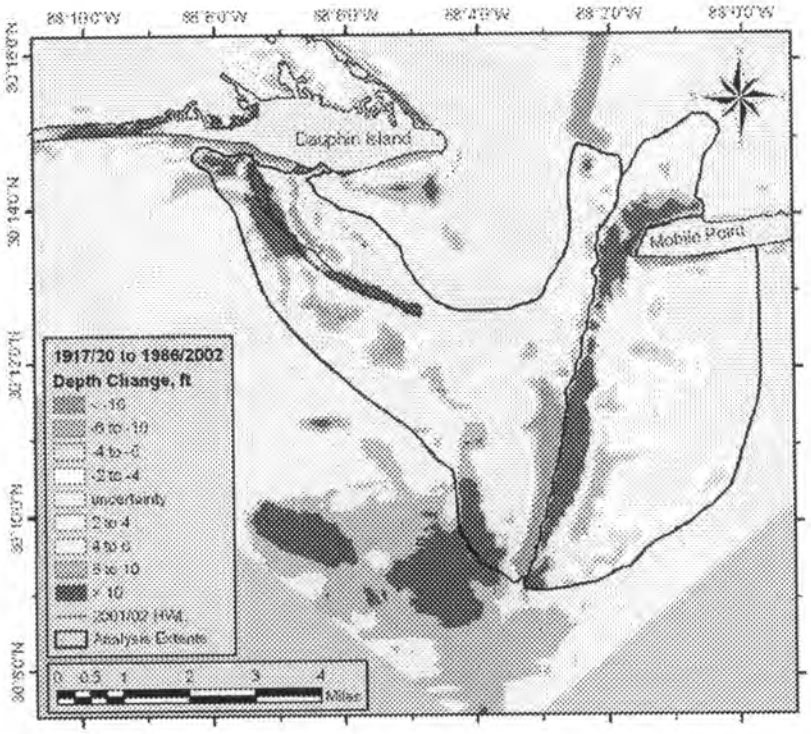

Figure G8. Analysis extent for calculating sand volume change – 1917/20 to 2002.

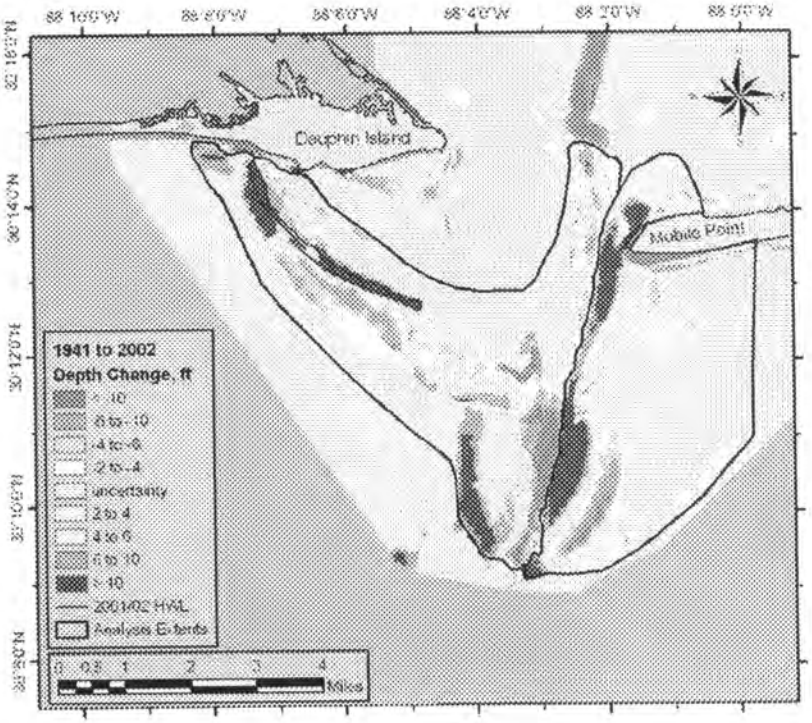

Figure G9. Analysis extent for calculating sand volume change – 1941 to 2002.

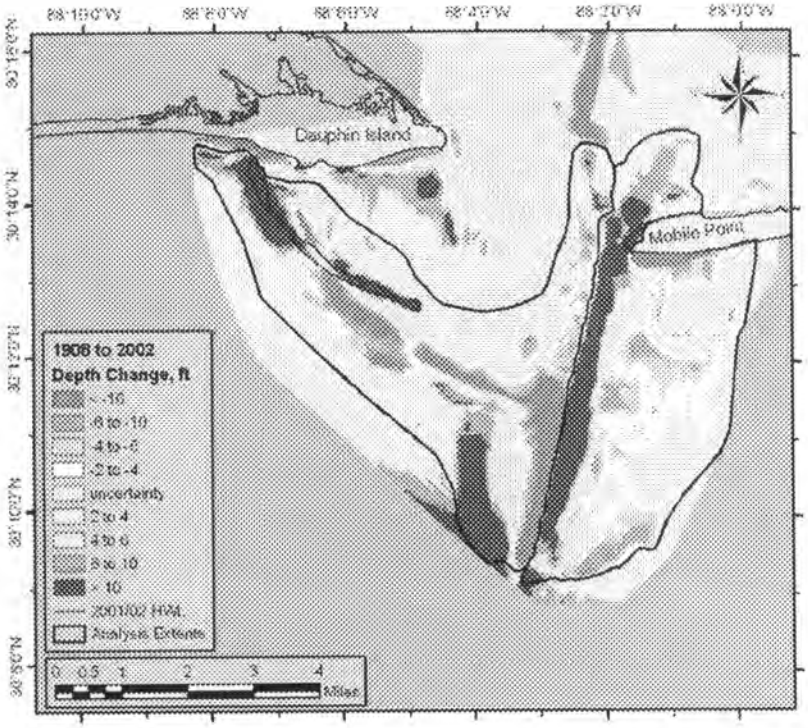

Figure G10. Analysis extent for calculating sand volume change – 1908 to 2002.

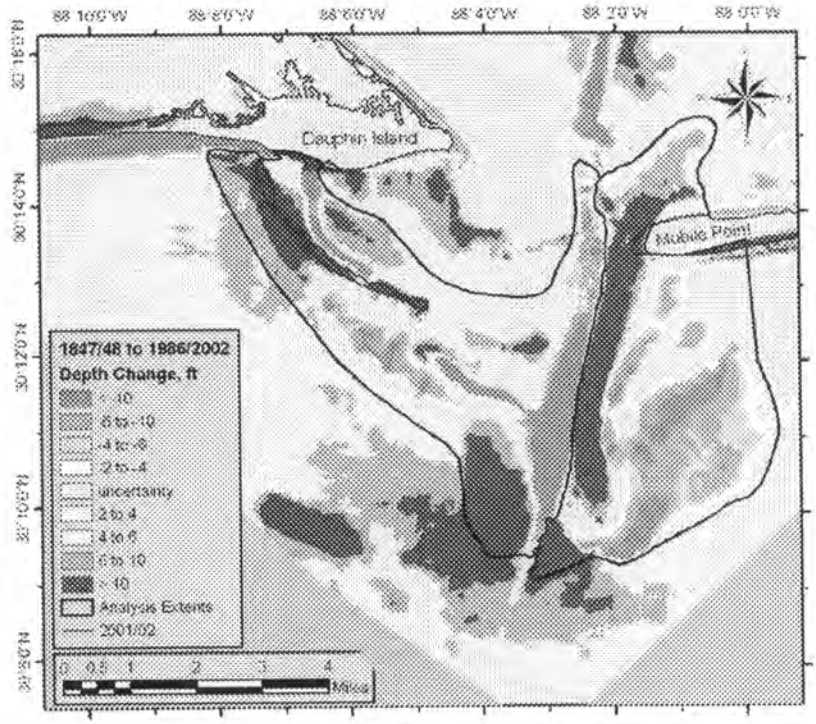

Figure G11. Analysis extent for calculating sand volume change – 1847/48 to 2002.

Appendix H

STWAVE Modeling Results

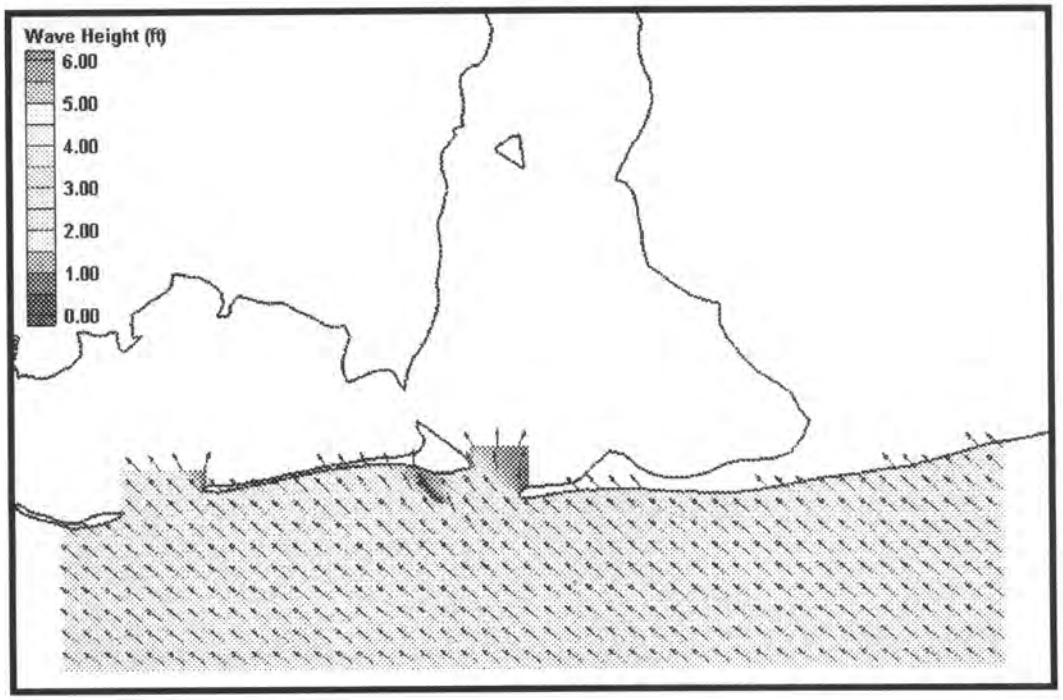

Figure H1. Coarse grid (200m x 200m) wave results for Case 1. Wave heights are shown by color while wave direction is indicated by the arrow direction.

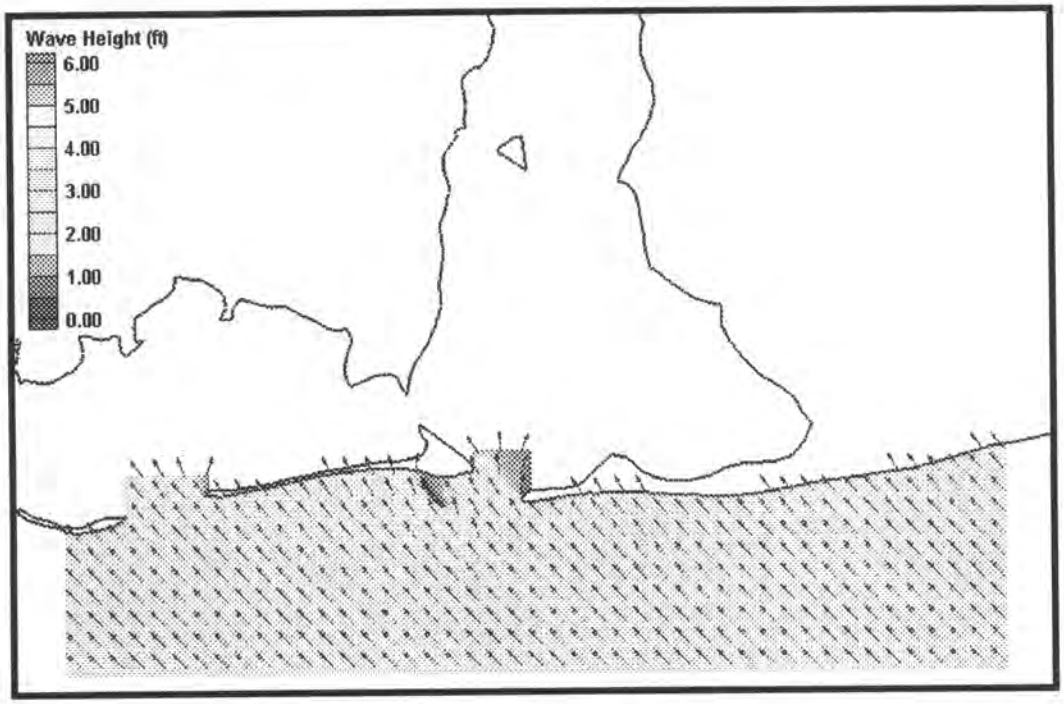

Figure H2. Coarse grid (200m x 200m) wave results for Case 2. Wave heights are shown by color while wave direction is indicated by the arrow direction.

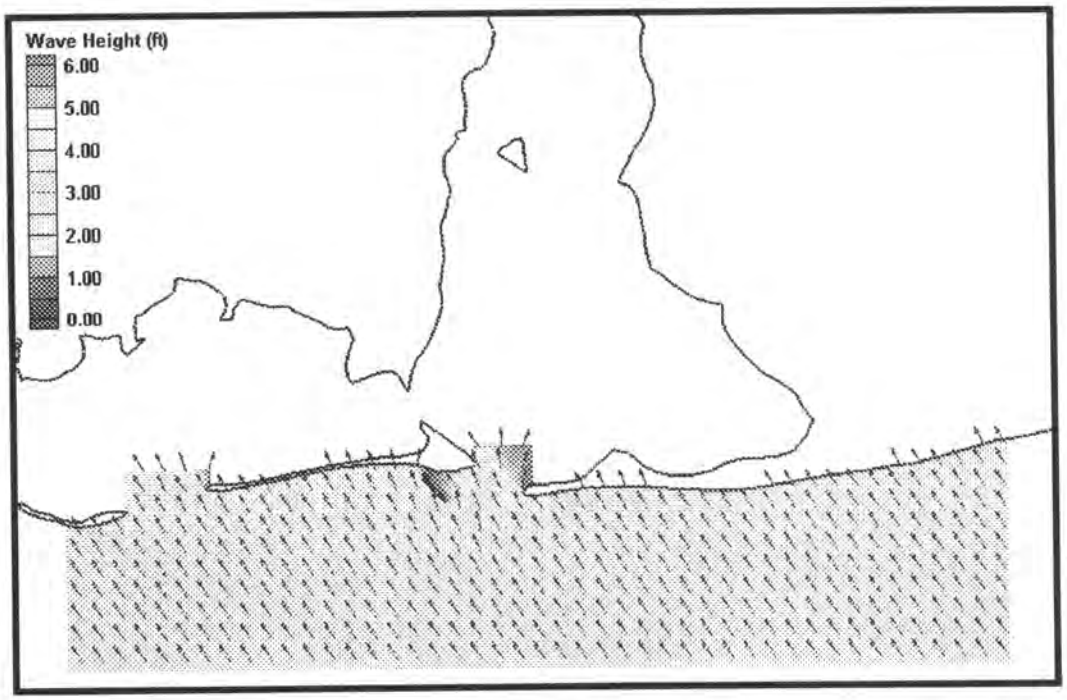

Figure H3. Coarse grid (200m x 200m) wave results for Case 3. Wave heights are shown by color while wave direction is indicated by the arrow direction.

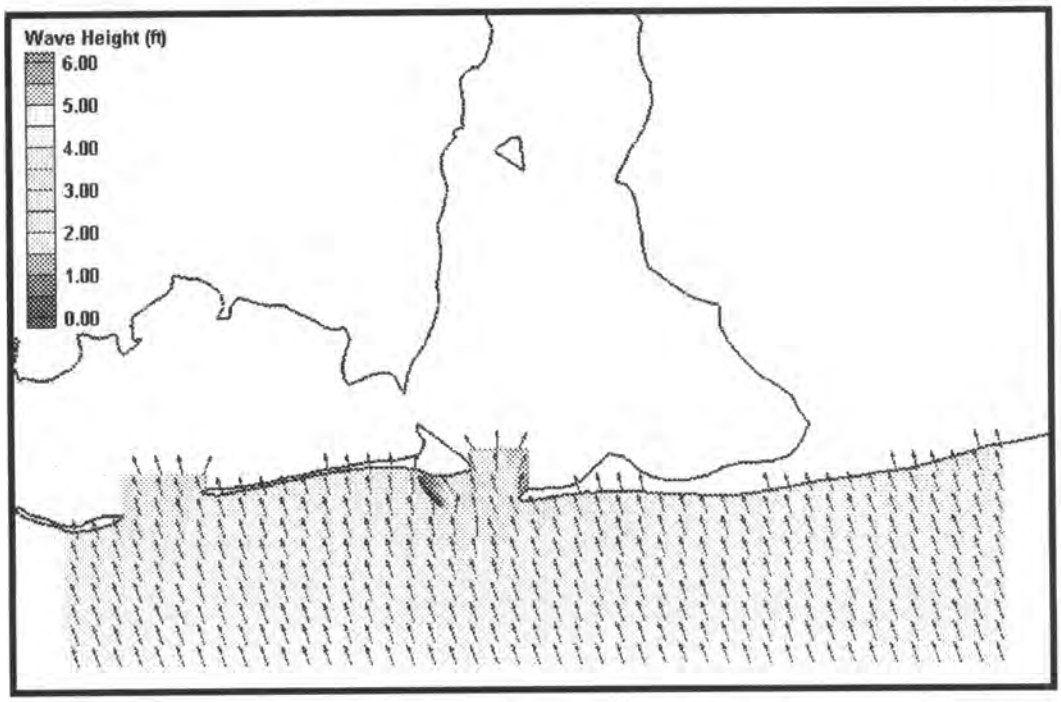

Figure H4. Coarse grid (200m x 200m) wave results for Case 4. Wave heights are shown by color while wave direction is indicated by the arrow direction.

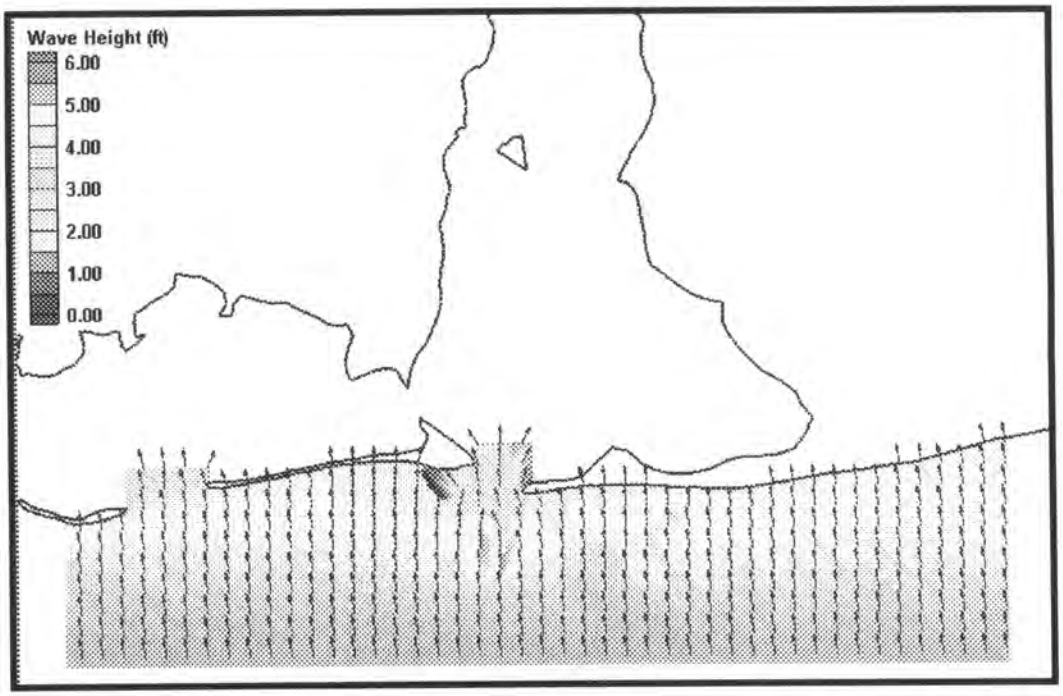

Figure H5. Coarse grid (200m x 200m) wave results for Case 5. Wave heights are shown by color while wave direction is indicated by the arrow direction.

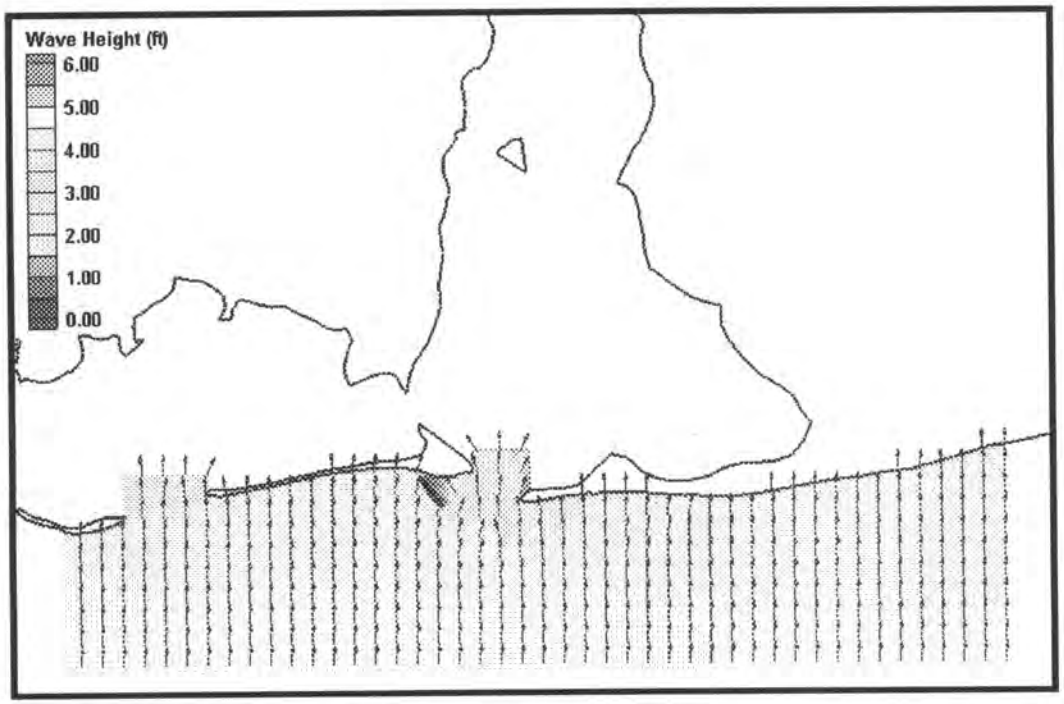

Figure H6. Coarse grid (200m x 200m) wave results for Case 6. Wave heights are shown by color while wave direction is indicated by the arrow direction.

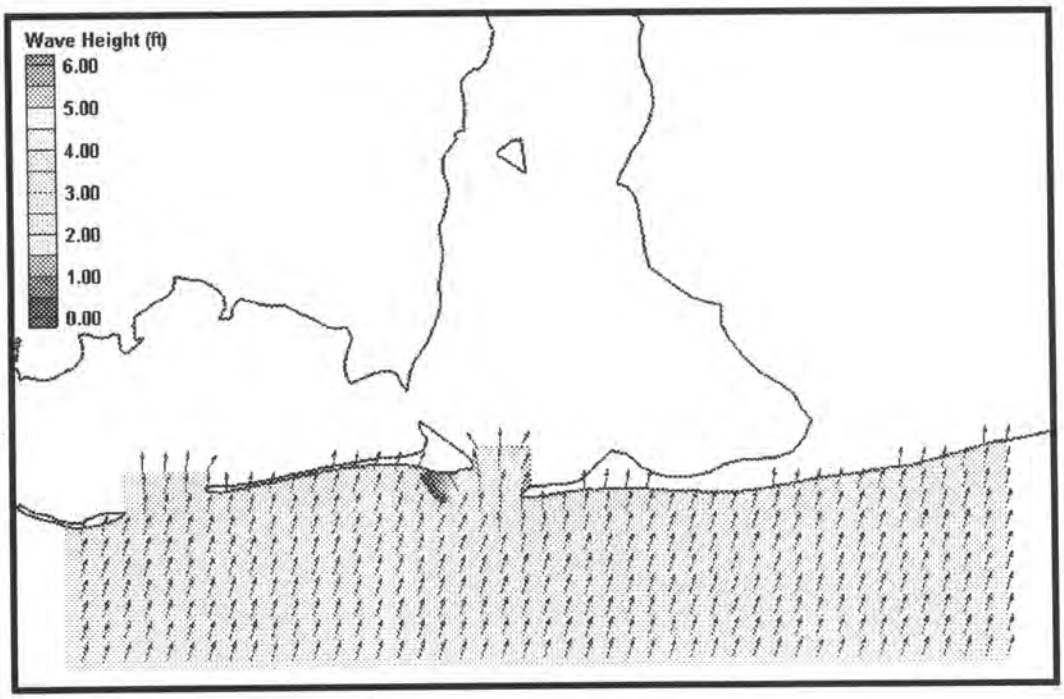

Figure H7. Coarse grid (200m x 200m) wave results for Case 7. Wave heights are shown by color while wave direction is indicated by the arrow direction.

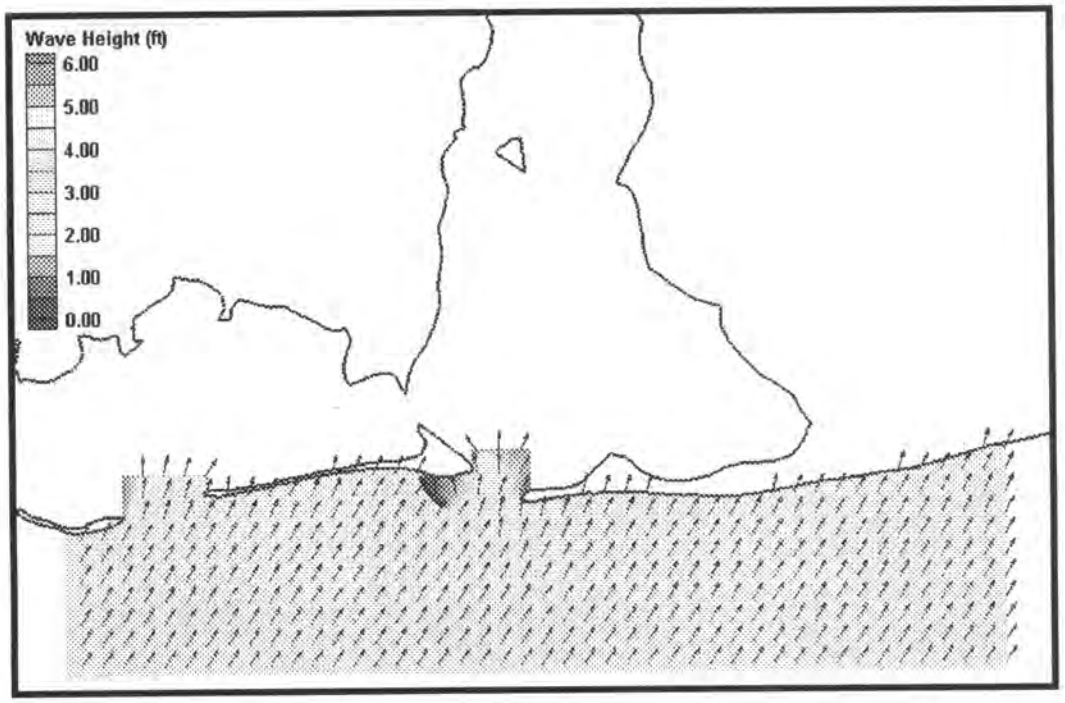

Figure H8. Coarse grid (200m x 200m) wave results for Case 8. Wave heights are shown by color while wave direction is indicated by the arrow direction.

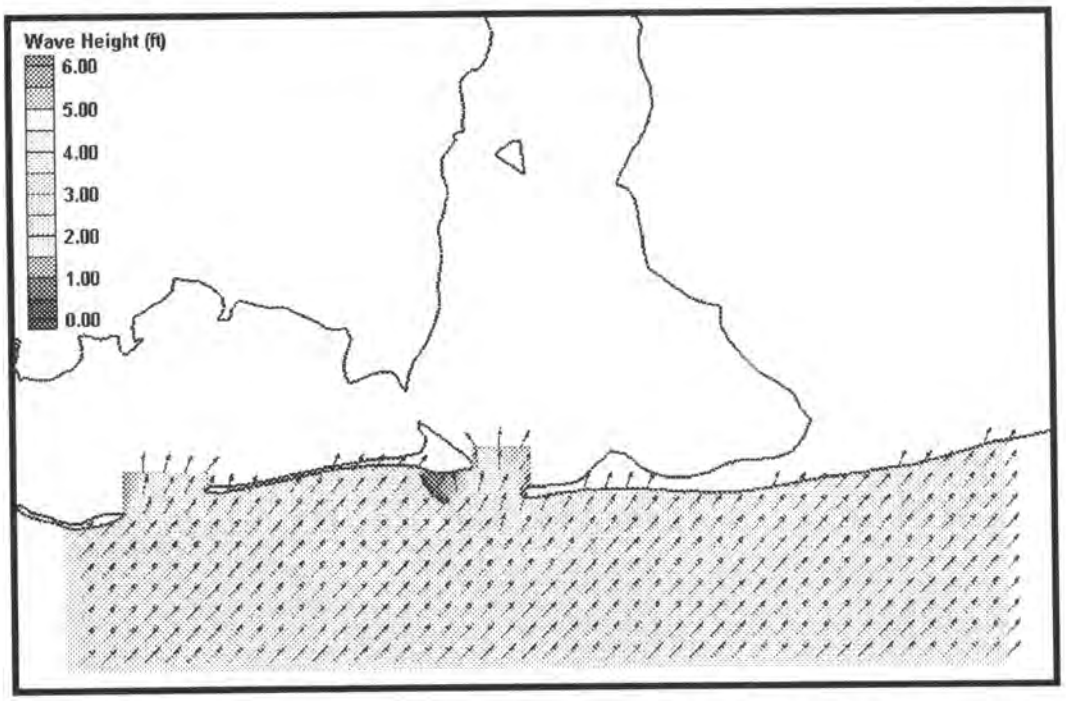

Figure H9. Coarse grid (200m x 200m) wave results for Case 9. Wave heights are shown by color while wave direction is indicated by the arrow direction.

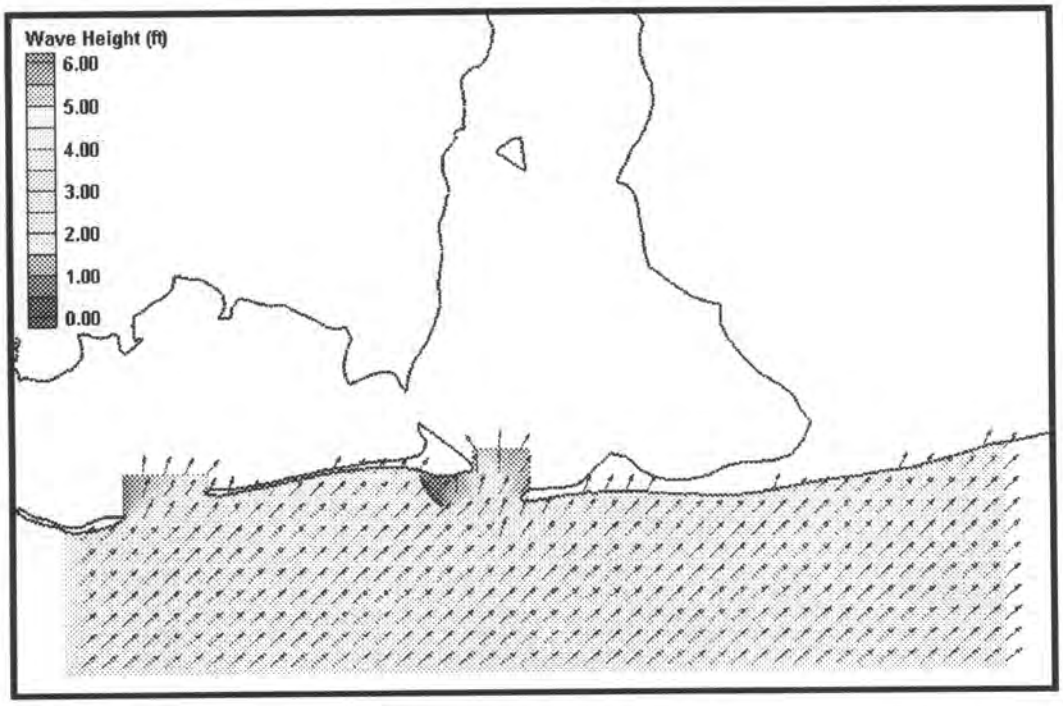

Figure H10. Coarse grid (200m x 200m) wave results for Case 10. Wave heights are shown by color while wave direction is indicated by the arrow direction.

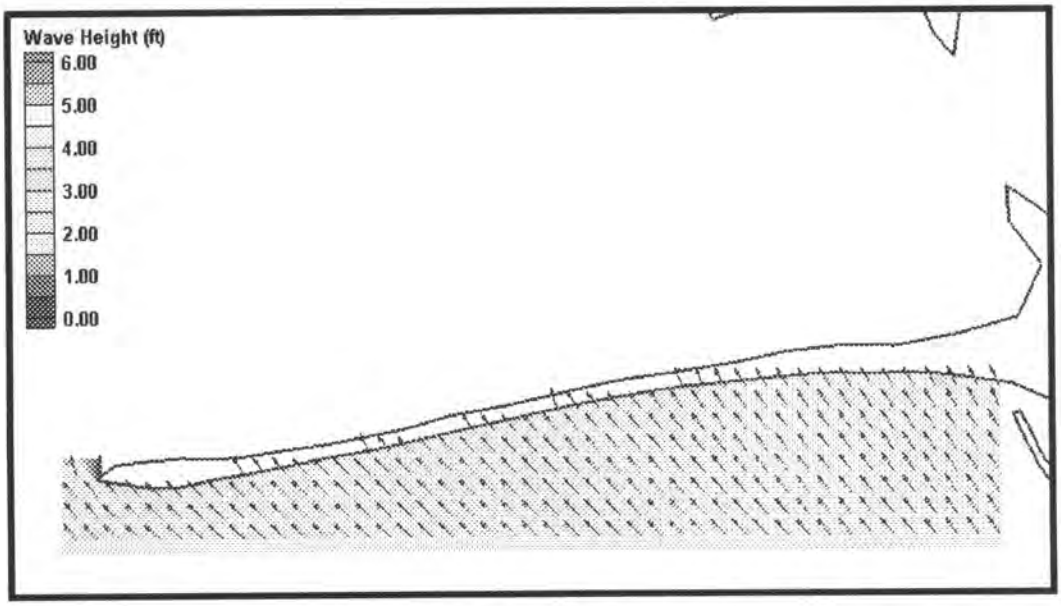

Figure H11. Fine grid (25m x 25m) wave results for Case 1, Dauphin Island. Wave heights are shown by color while wave direction is indicated by the arrow direction.

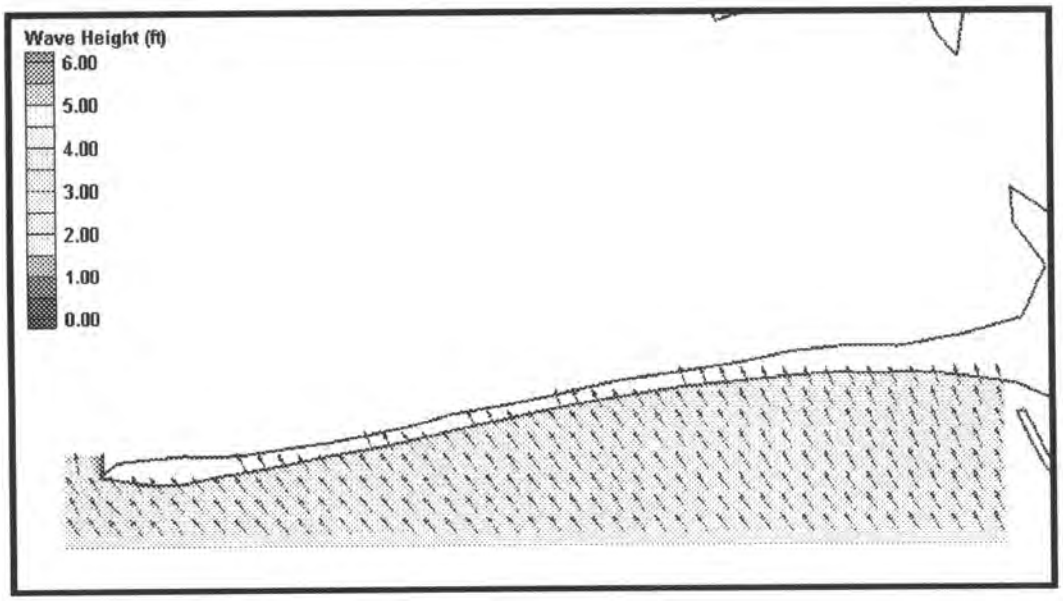

Figure H12. Fine grid (25m x 25m) wave results for Case 2, Dauphin Island. Wave heights are shown by color while wave direction is indicated by the arrow direction.

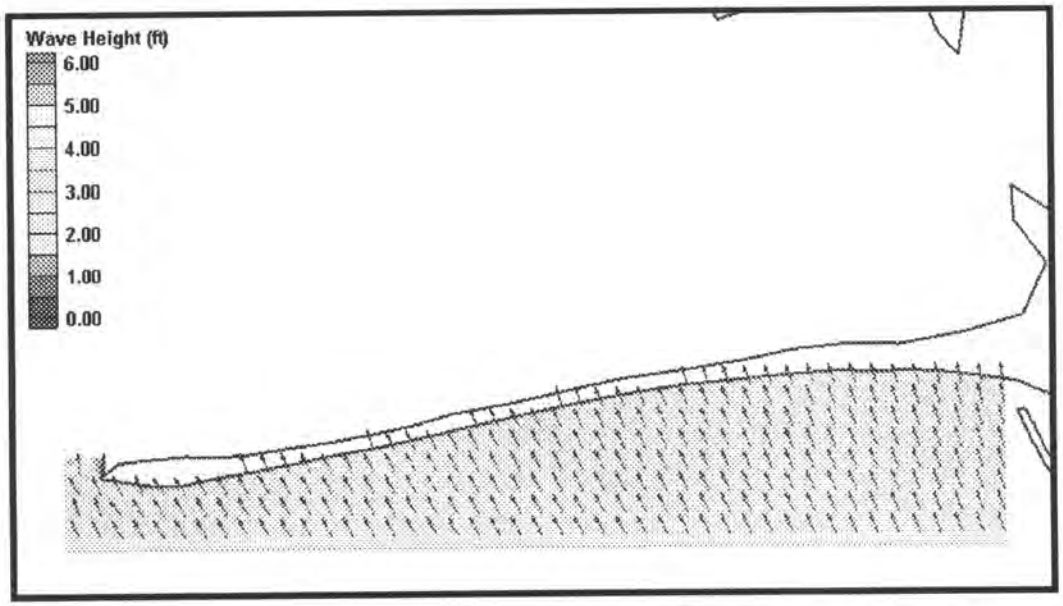

Figure H13. Fine grid (25m x 25m) wave results for Case 3, Dauphin Island. Wave heights are shown by color while wave direction is indicated by the arrow direction.

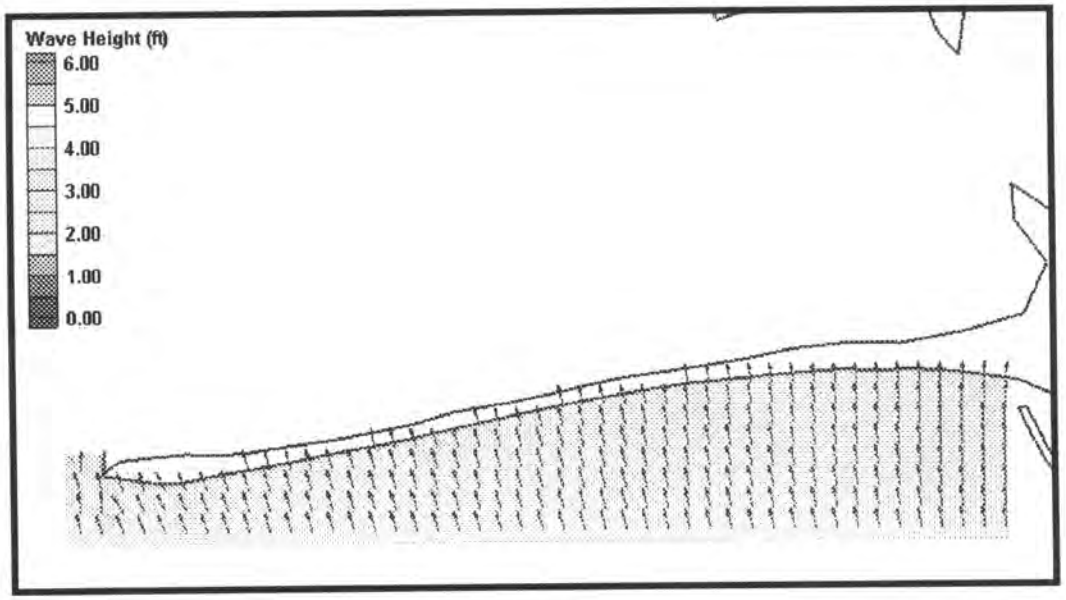

Figure H14. Fine grid (25m x 25m) wave results for Case 4, Dauphin Island. Wave heights are shown by color while wave direction is indicated by the arrow direction.

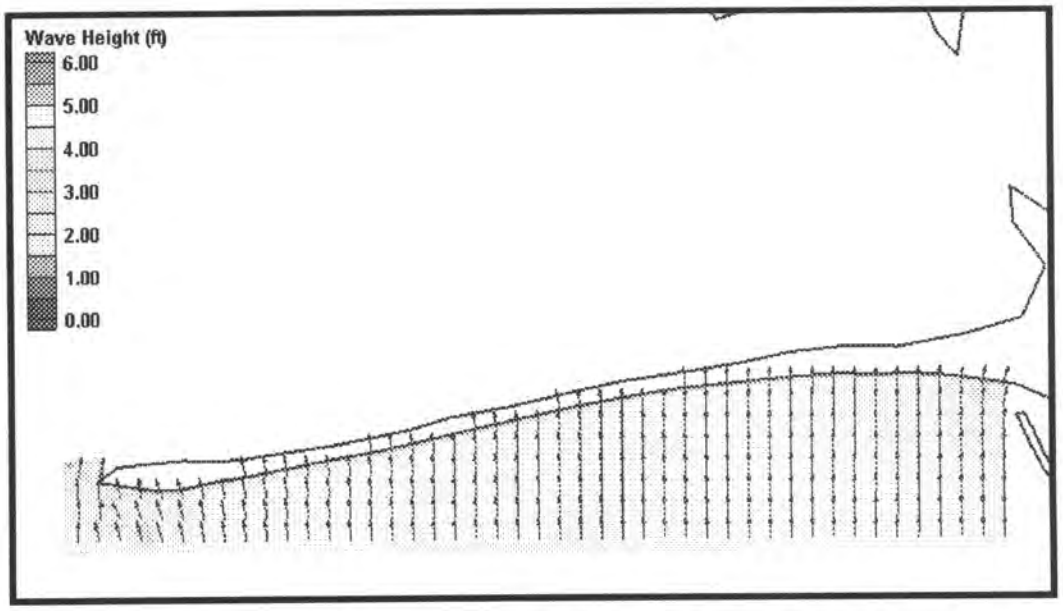

Figure H15. Fine grid (25m x 25m) wave results for Case 5, Dauphin Island. Wave heights are shown by color while wave direction is indicated by the arrow direction.

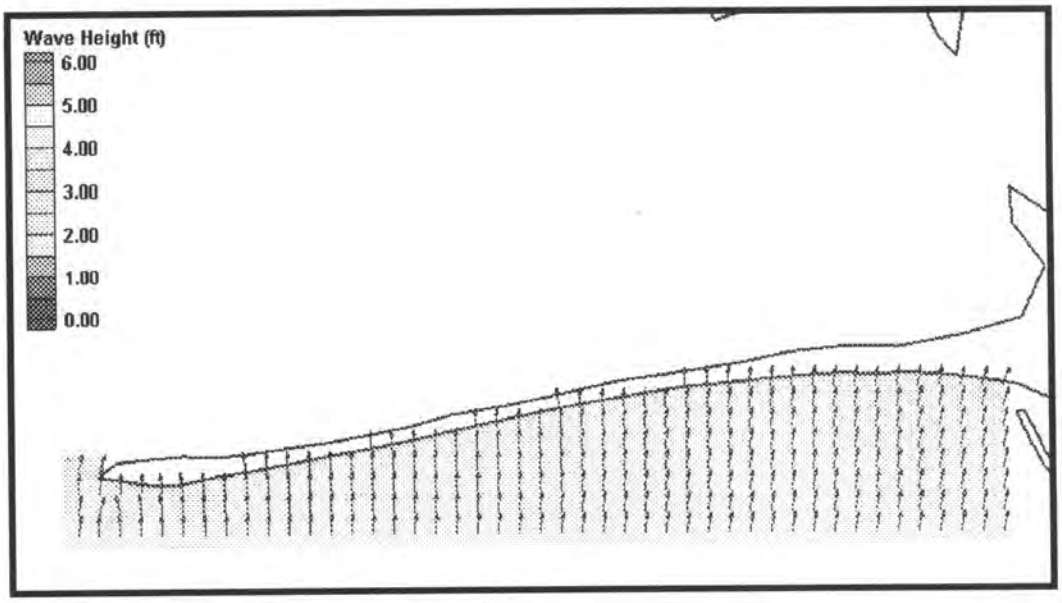

Figure H16. Fine grid (25m x 25m) wave results for Case 6, Dauphin Island. Wave heights are shown by color while wave direction is indicated by the arrow direction.

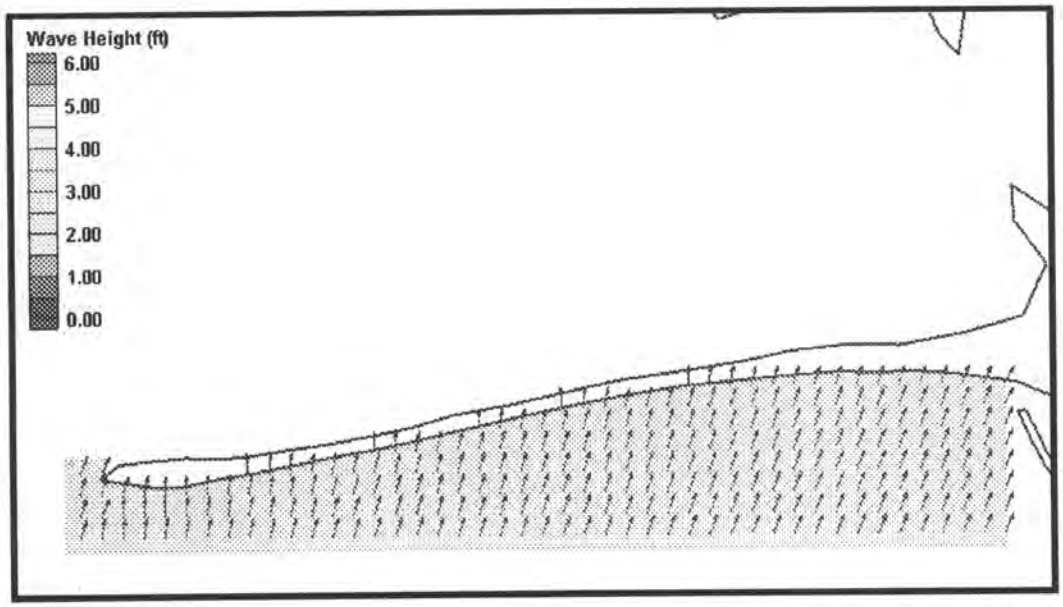

Figure H17. Fine grid (25m x 25m) wave results for Case 7, Dauphin Island. Wave heights are shown by color while wave direction is indicated by the arrow direction.

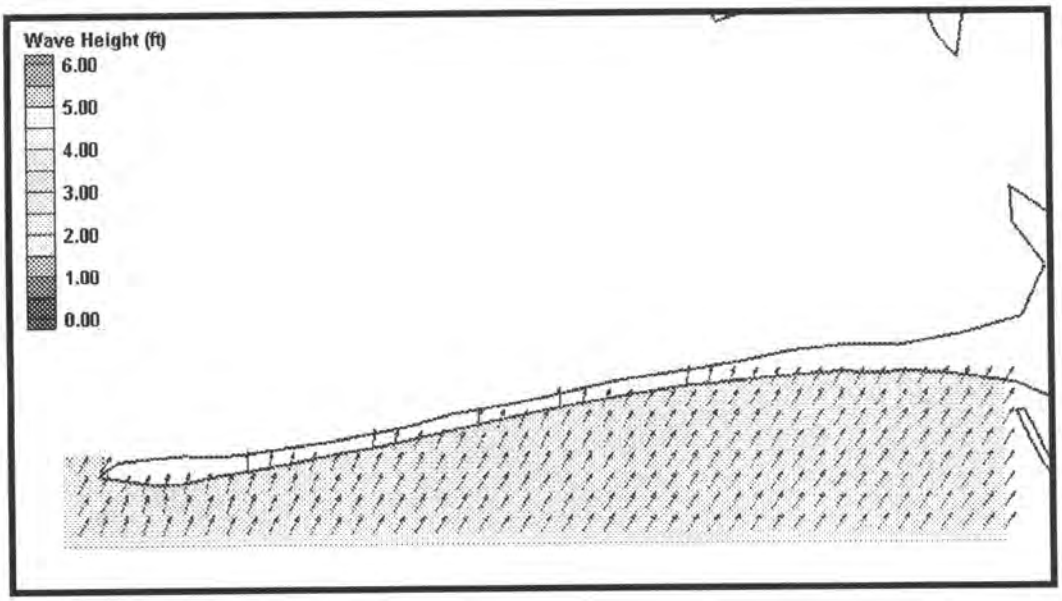

Figure H18. Fine grid (25m x 25m) wave results for Case 8, Dauphin Island. Wave heights are shown by color while wave direction is indicated by the arrow direction.

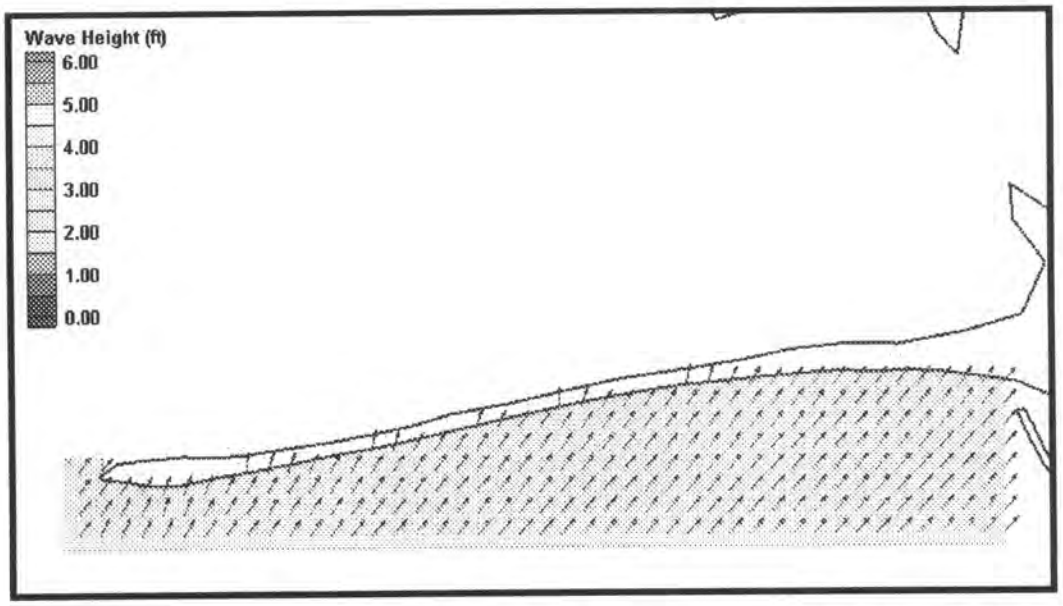

Figure H19. Fine grid (25m x 25m) wave results for Case 9, Dauphin Island. Wave heights are shown by color while wave direction is indicated by the arrow direction.

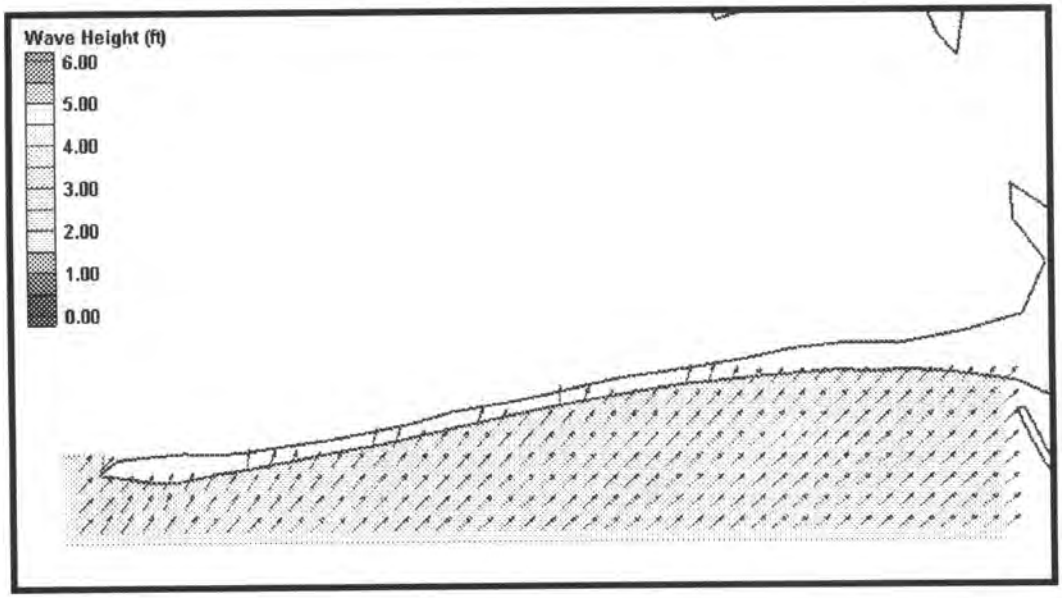

Figure H20. Fine grid (25m x 25m) wave results for Case 10, Dauphin Island. Wave heights are shown by color while wave direction is indicated by the arrow direction.

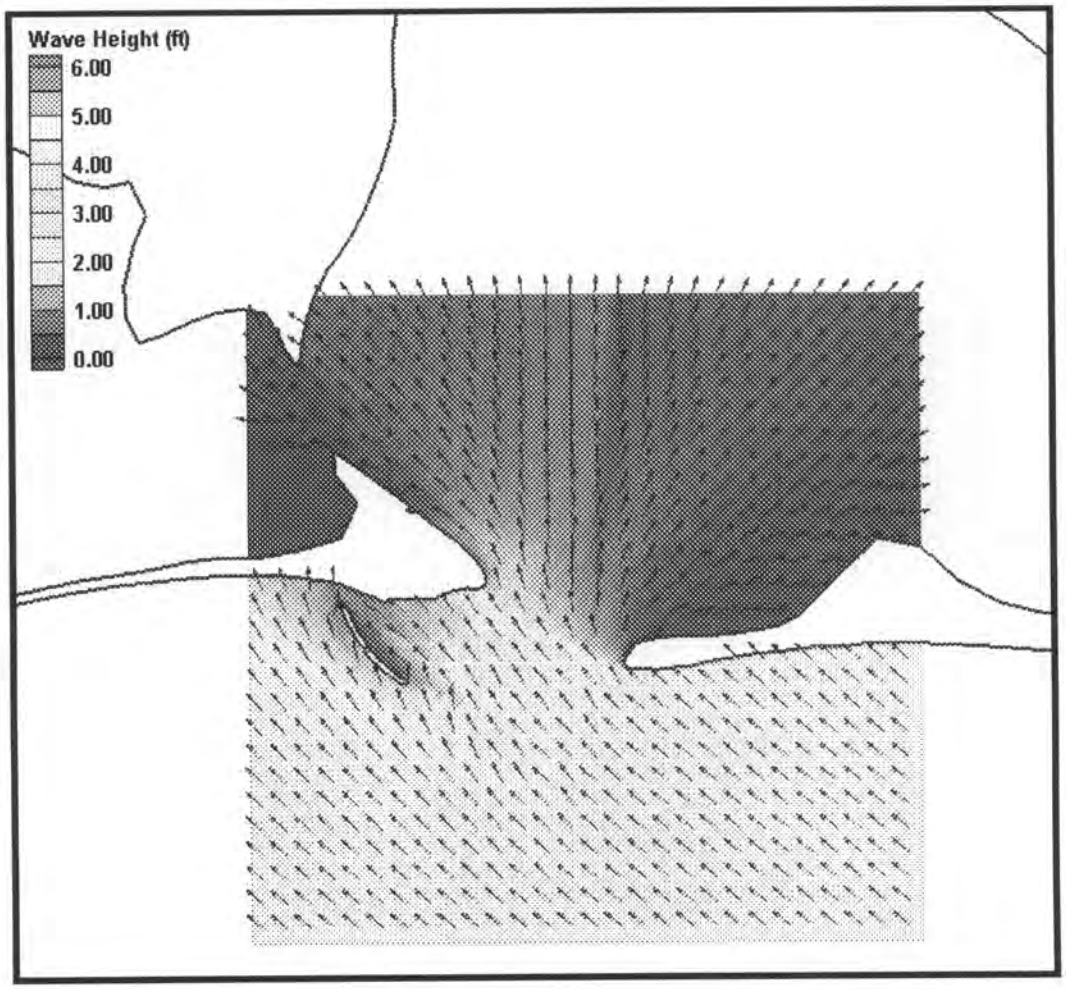

Figure H21. Fine grid (50m x 50m) wave results for Case 1, Mobile Pass. Wave heights are shown by color while wave direction is indicated by the arrow direction.

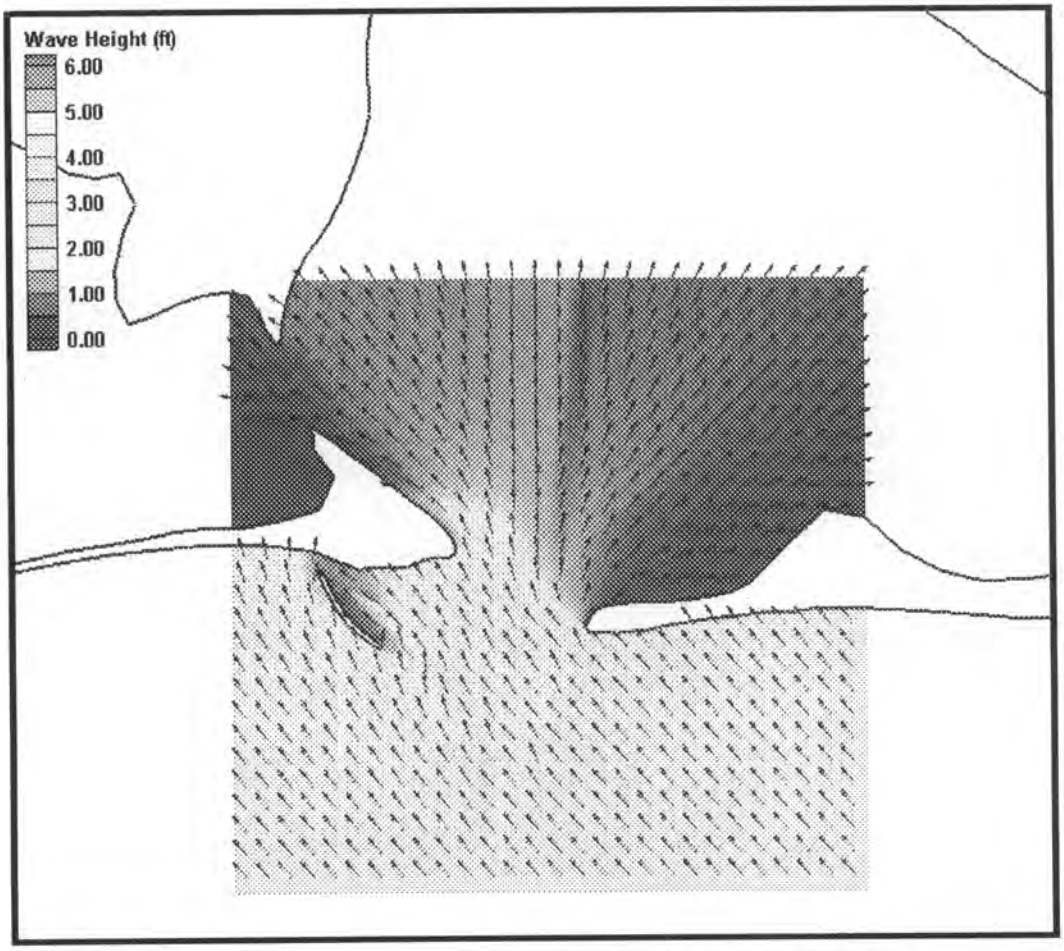

Figure H22. Fine grid (50m x 50m) wave results for Case 2, Mobile Pass. Wave heights are shown by color while wave direction is indicated by the arrow direction.

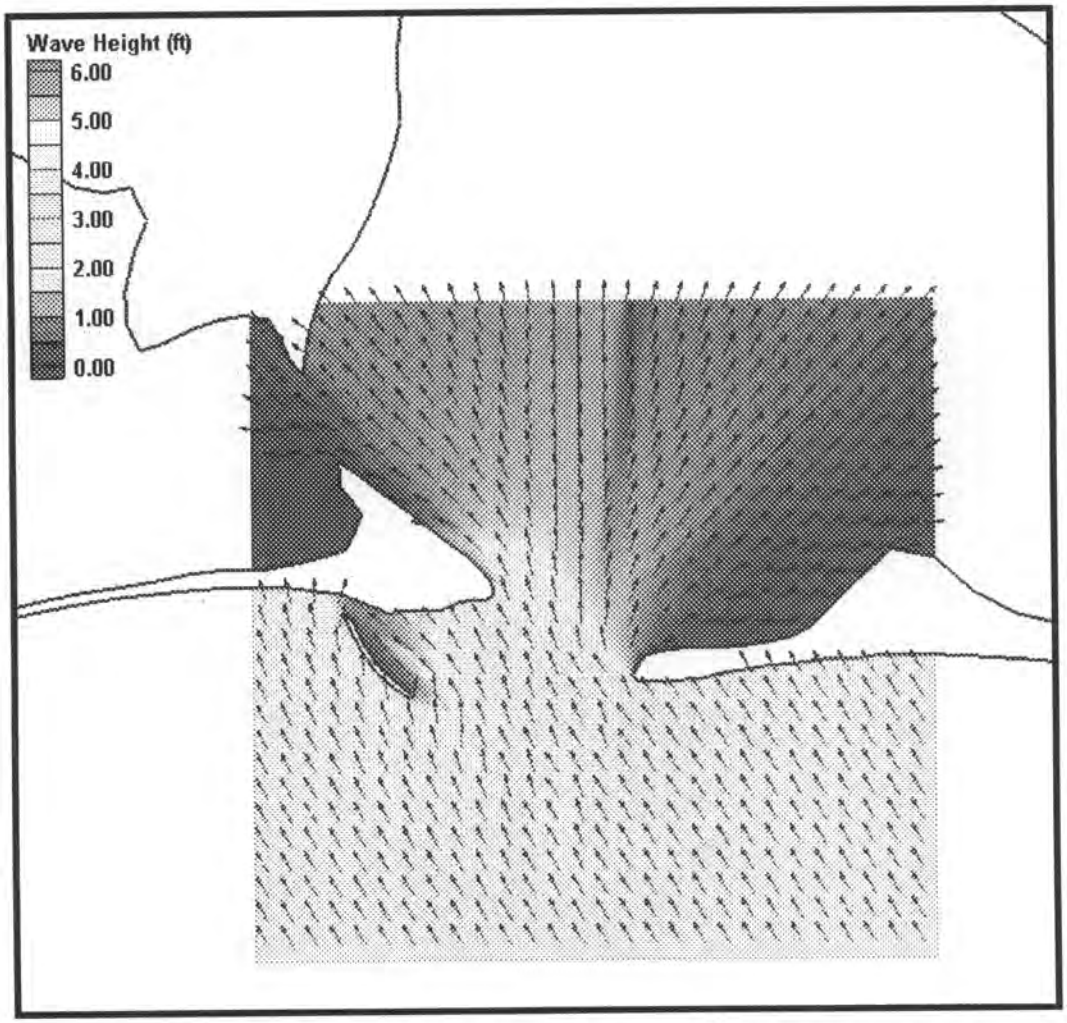

Figure H23. Fine grid (50m x 50m) wave results for Case 3, Mobile Pass. Wave heights are shown by color while wave direction is indicated by the arrow direction.

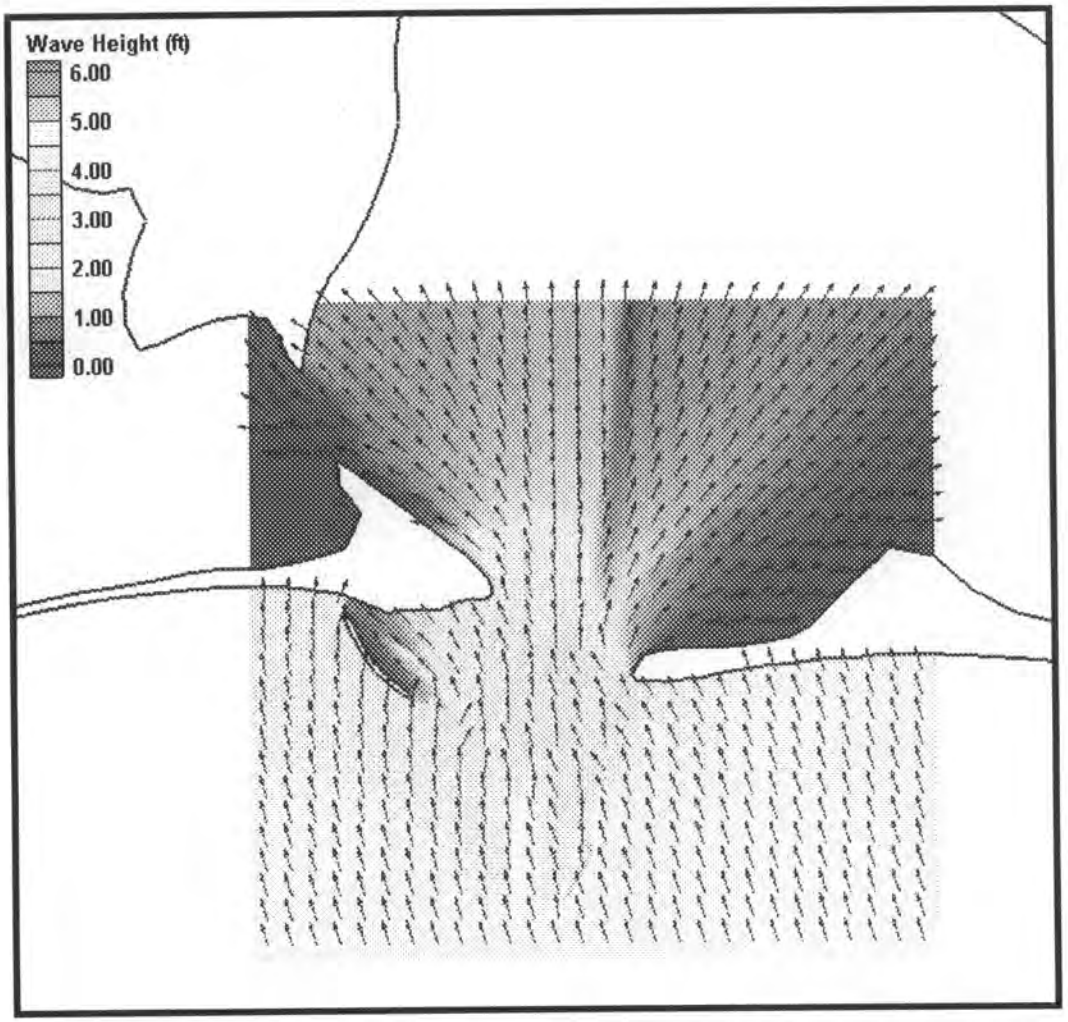

Figure H24. Fine grid (50m x 50m) wave results for Case 4, Mobile Pass. Wave heights are shown by color while wave direction is indicated by the arrow direction.

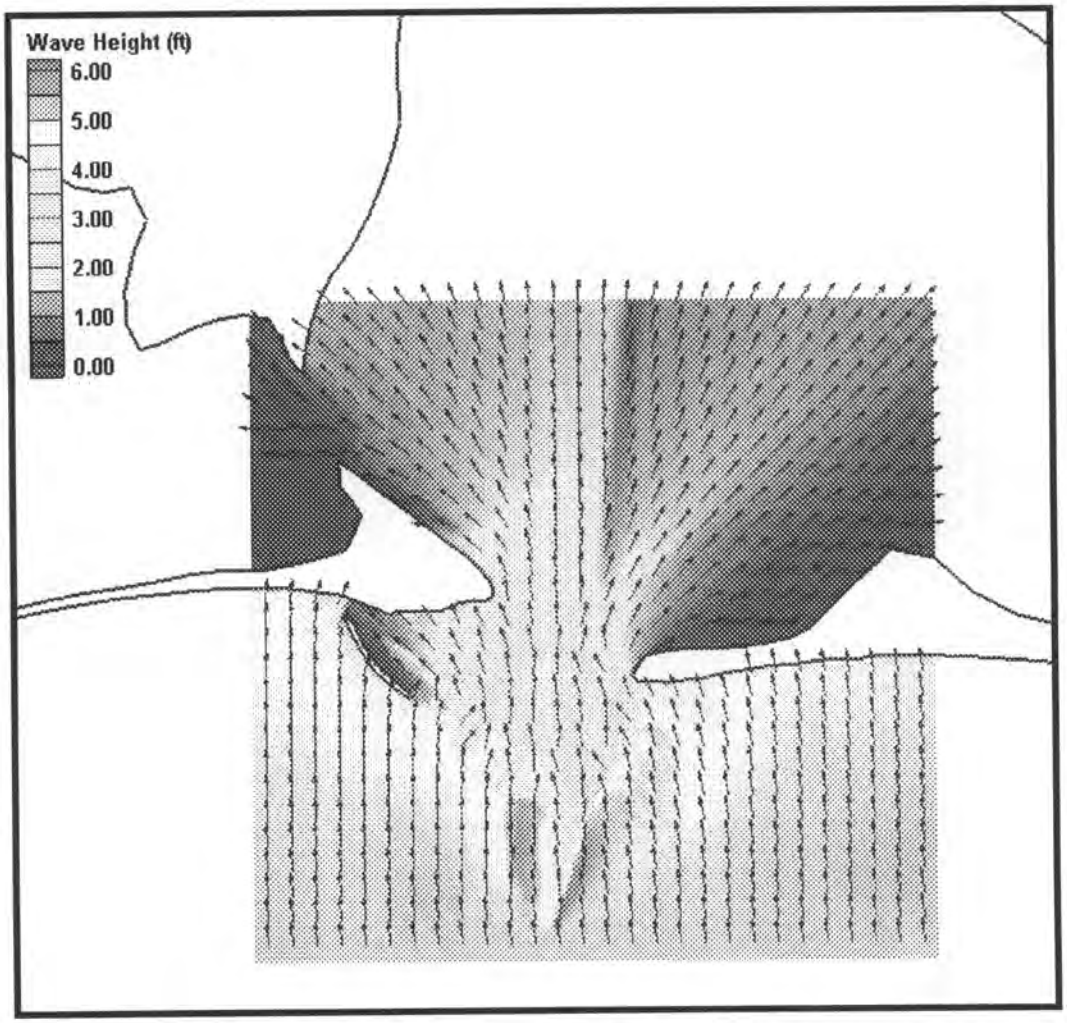

Figure H25. Fine grid (50m x 50m) wave results for Case 5, Mobile Pass. Wave heights are shown by color while wave direction is indicated by the arrow direction.

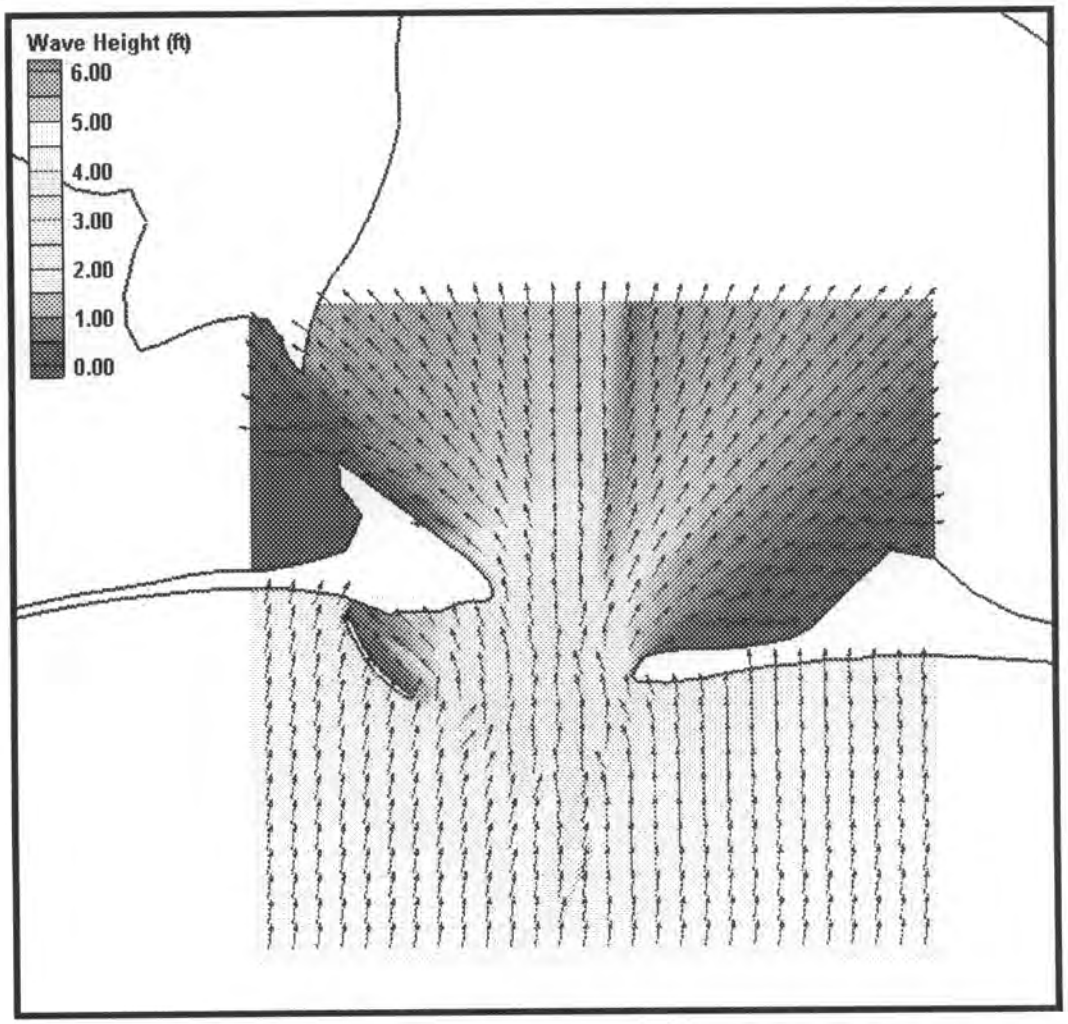

Figure H26. Fine grid (50m x 50m) wave results for Case 6, Mobile Pass. Wave heights are shown by color while wave direction is indicated by the arrow direction.

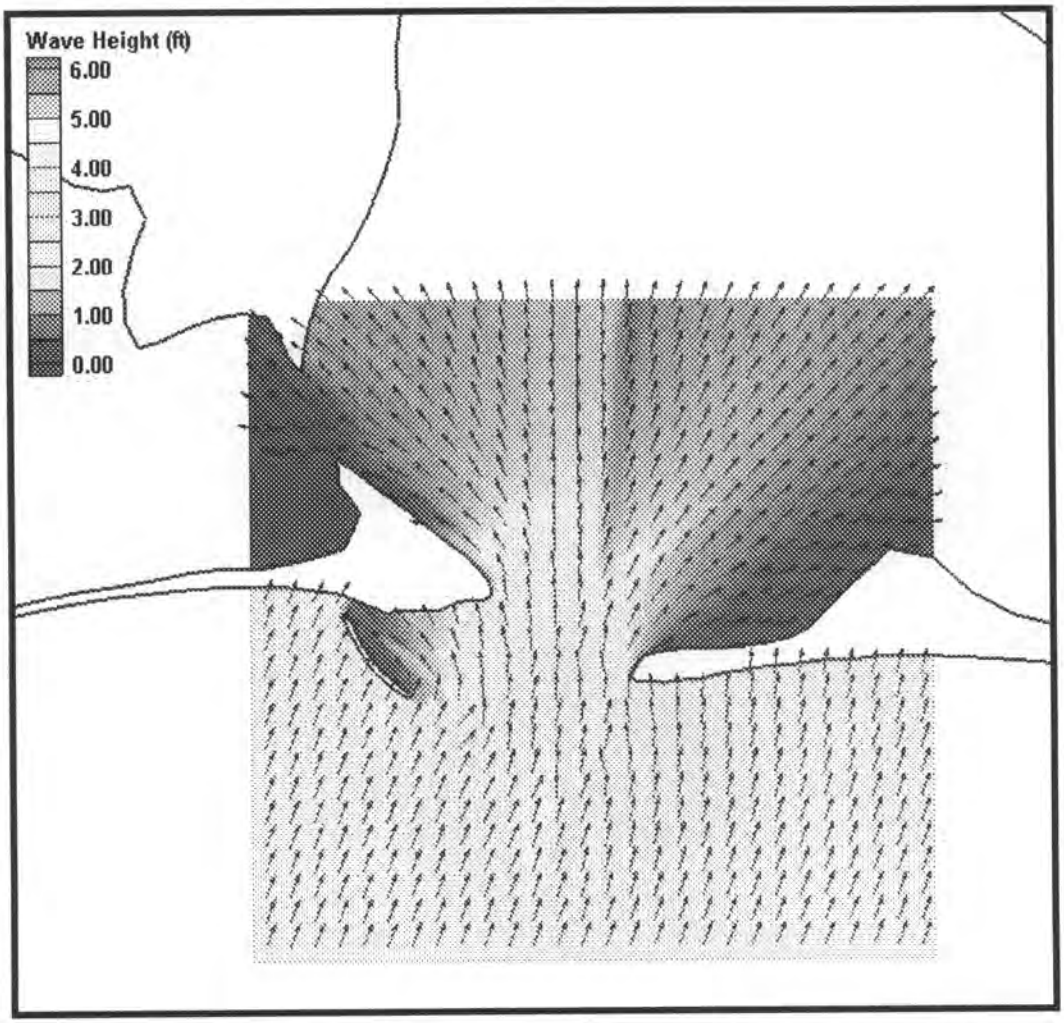

Figure H27. Fine grid (50m x 50m) wave results for Case 7, Mobile Pass. Wave heights are shown by color while wave direction is indicated by the arrow direction.

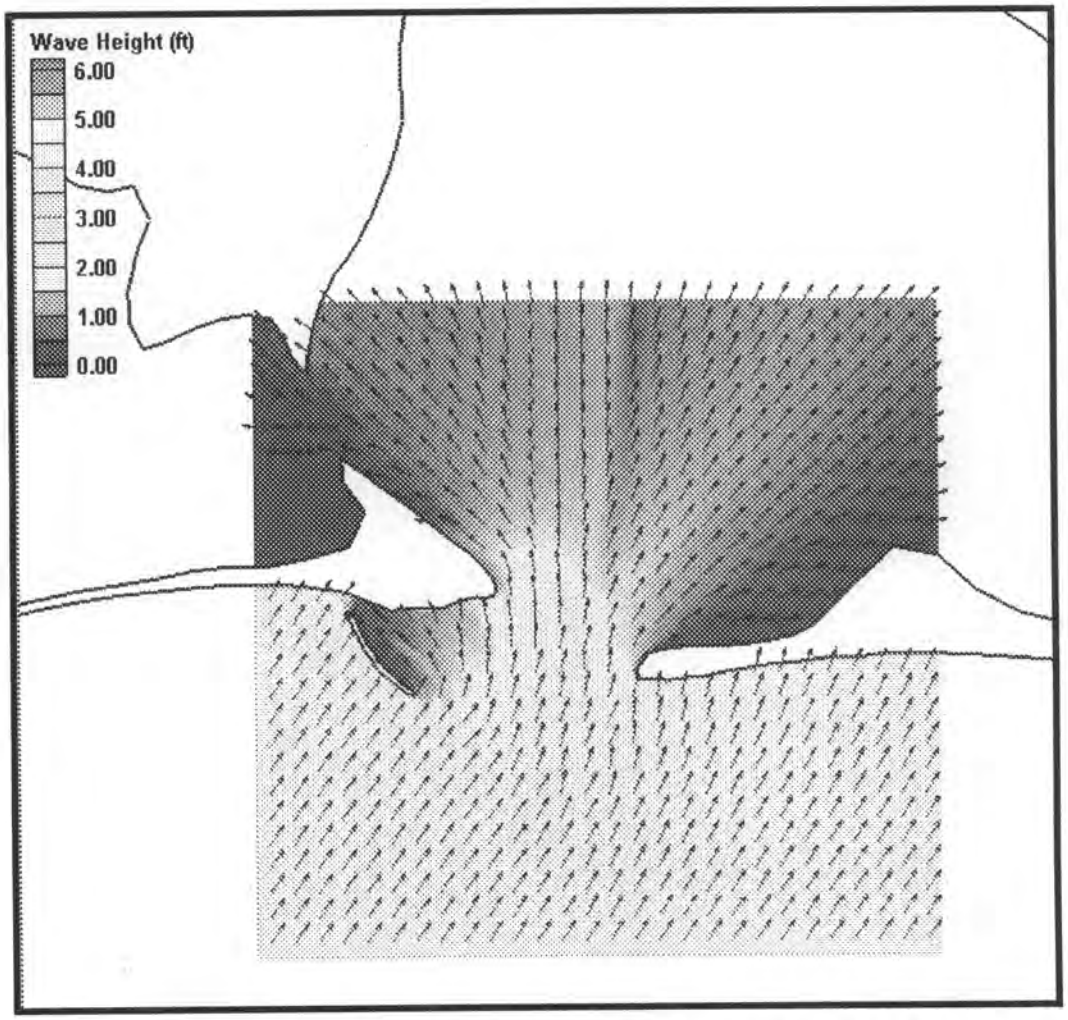

Figure H28. Fine grid (50m x 50m) wave results for Case 8, Mobile Pass. Wave heights are shown by color while wave direction is indicated by the arrow direction.

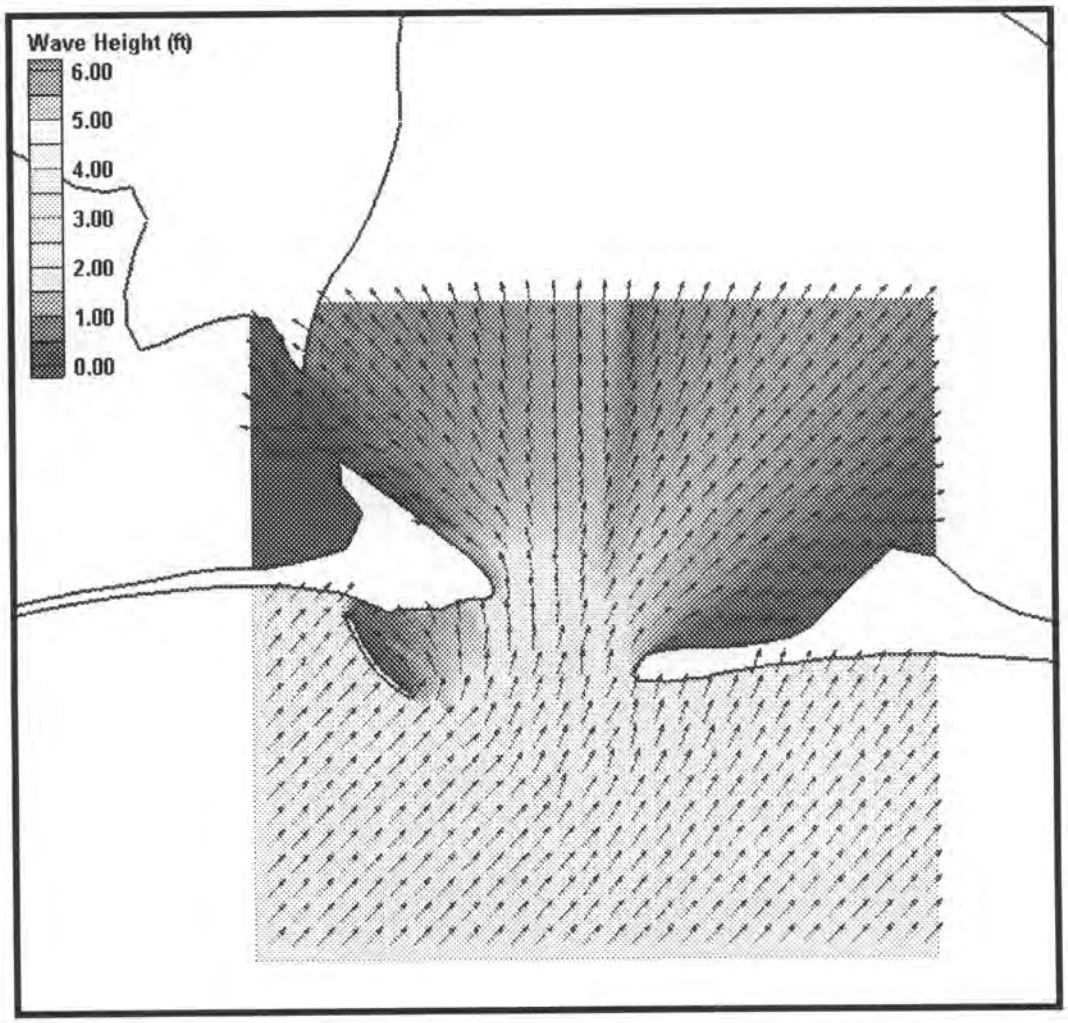

Figure H29. Fine grid (50m x 50m) wave results for Case 9, Mobile Pass. Wave heights are shown by color while wave direction is indicated by the arrow direction.

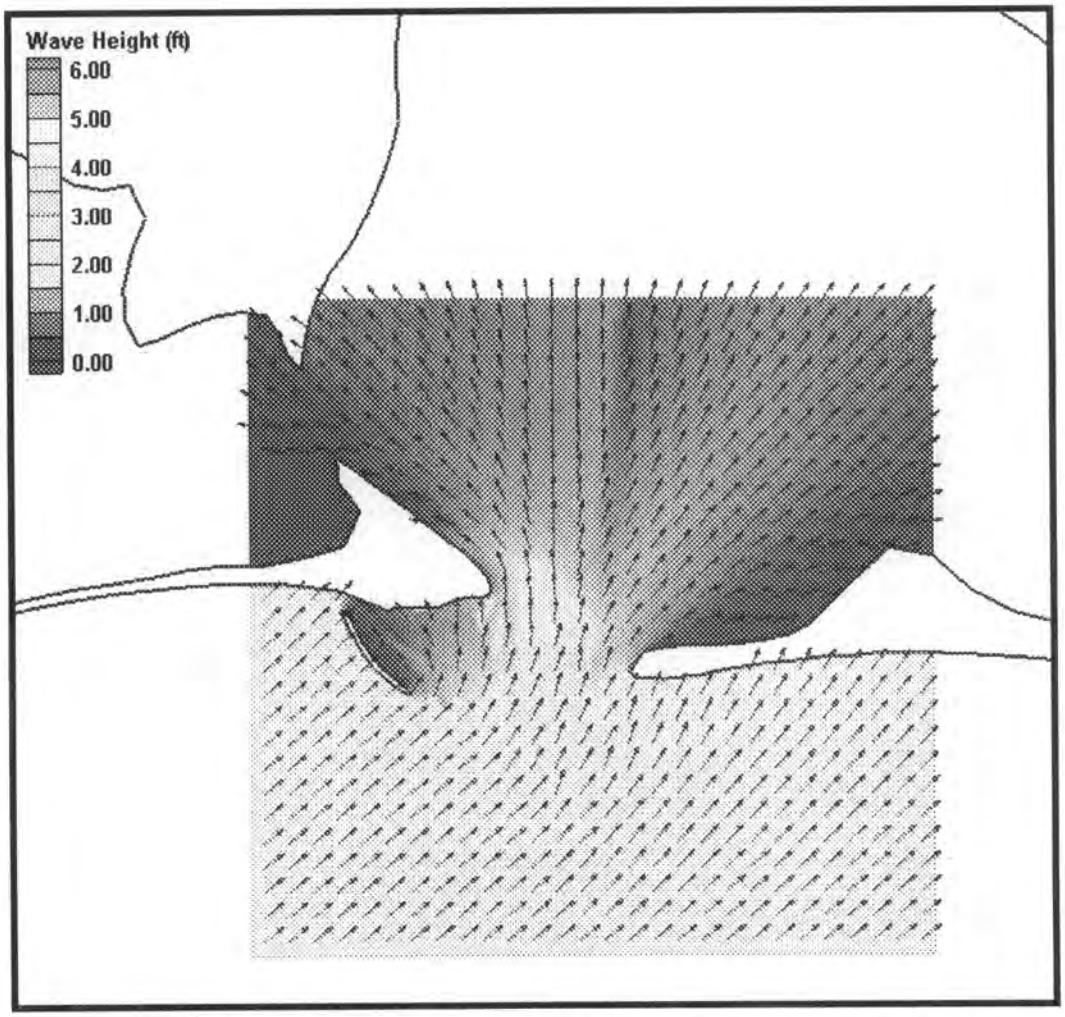

Figure H30. Fine grid (50m x 50m) wave results for Case 10, Mobile Pass. Wave heights are shown by color while wave direction is indicated by the arrow direction.

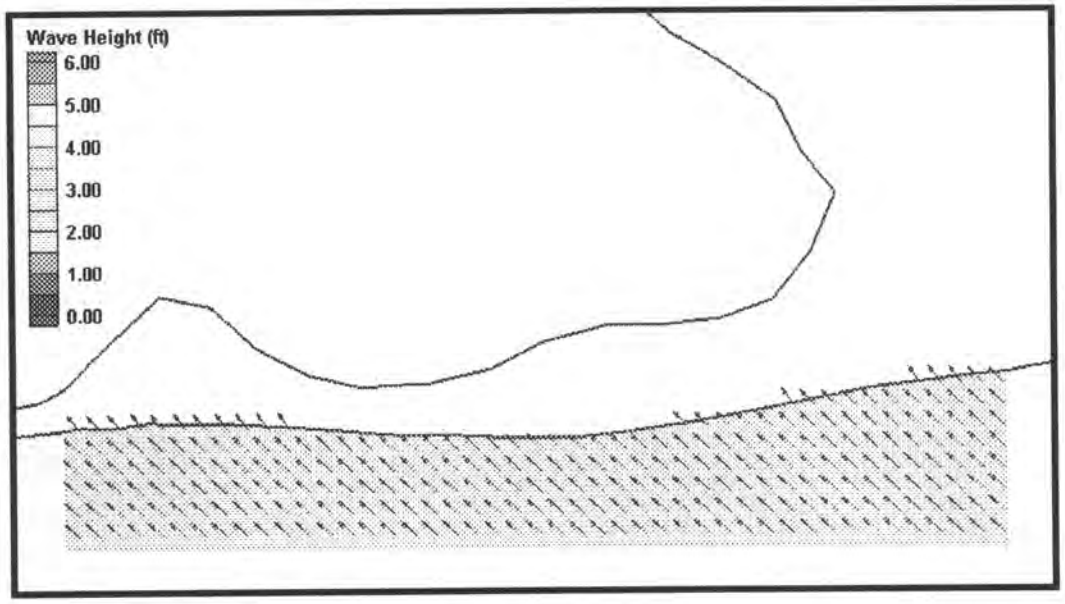

Figure H31. Fine grid (25m x 25m) wave results for Case 1, Morgan Peninsula. Wave heights are shown by color while wave direction is indicated by the arrow direction.

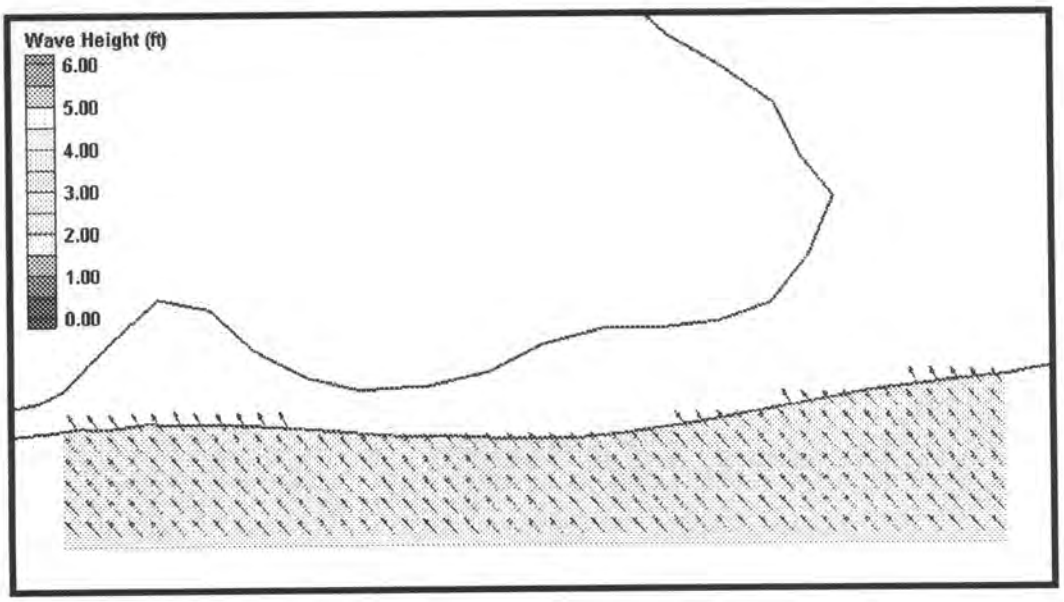

Figure H32. Fine grid (25m x 25m) wave results for Case 2, Morgan Peninsula. Wave heights are shown by color while wave direction is indicated by the arrow direction.

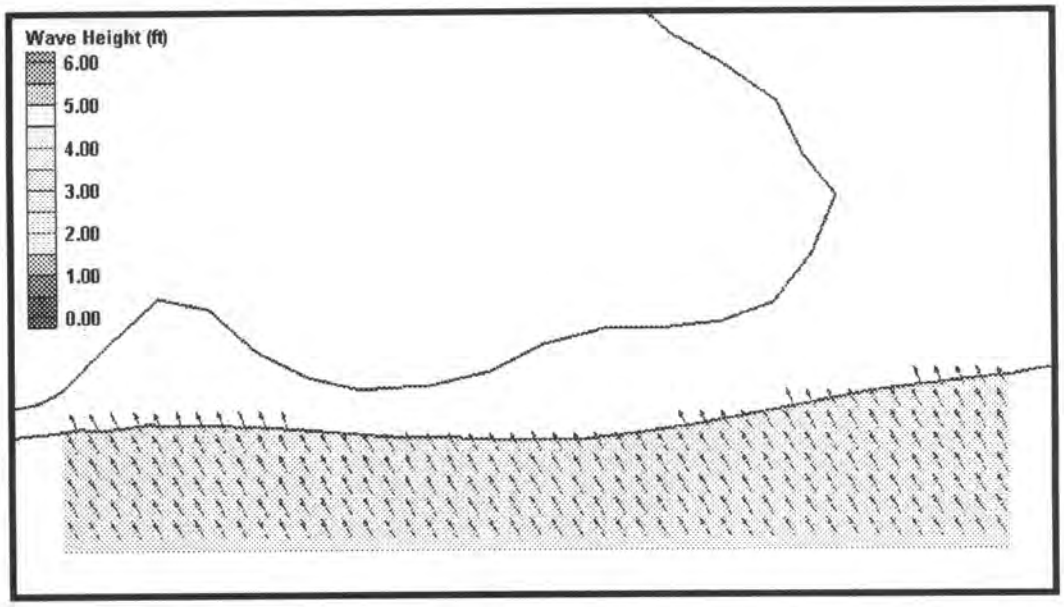

Figure H33. Fine grid (25m x 25m) wave results for Case 3, Morgan Peninsula. Wave heights are shown by color while wave direction is indicated by the arrow direction.

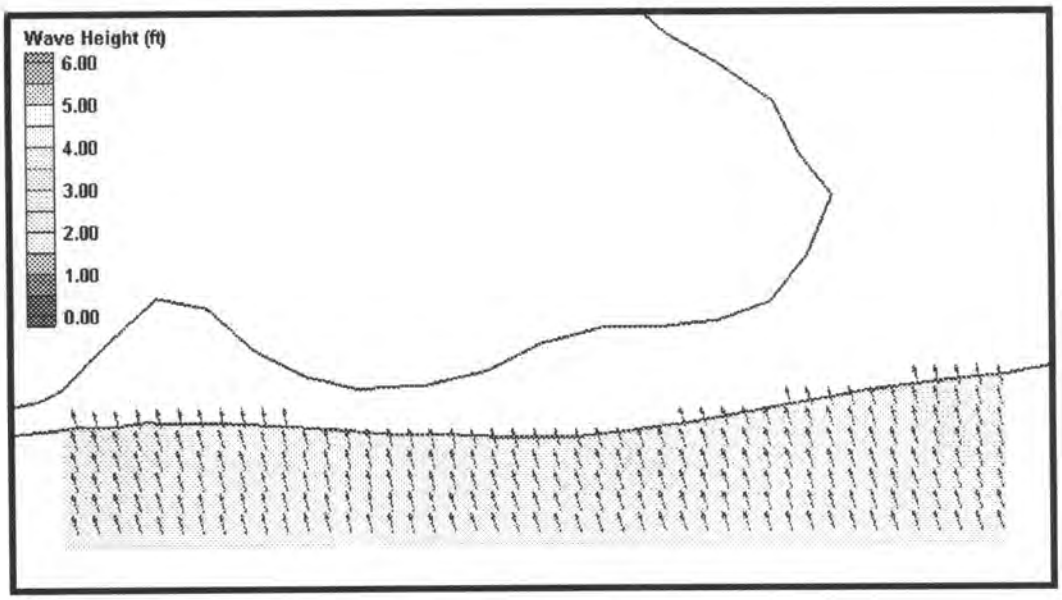

Figure H34. Fine grid (25m x 25m) wave results for Case 4, Morgan Peninsula. Wave heights are shown by color while wave direction is indicated by the arrow direction.

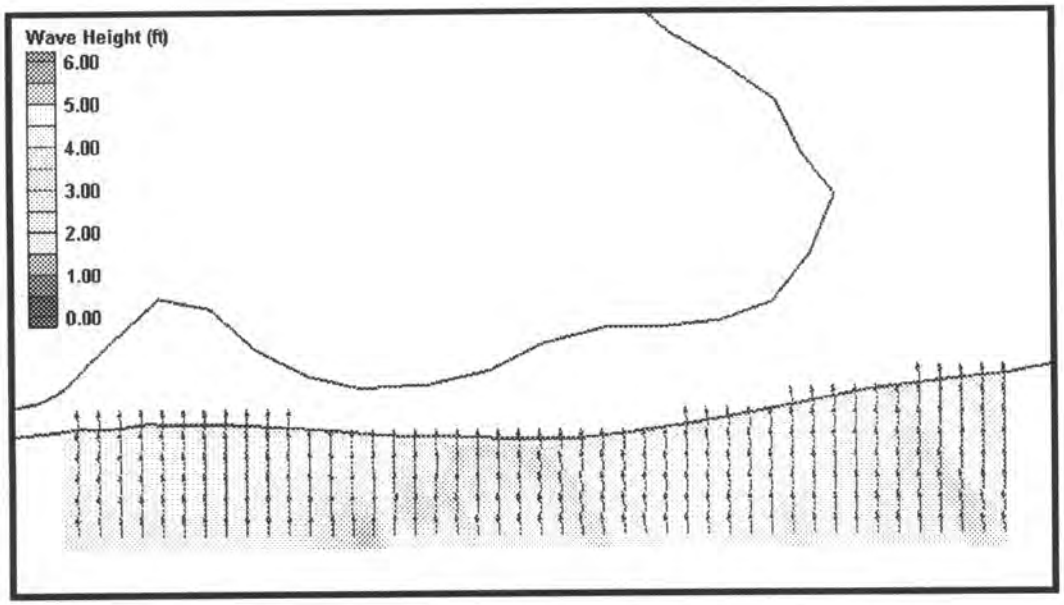

Figure H35. Fine grid (25m x 25m) wave results for Case 5, Morgan Peninsula. Wave heights are shown by color while wave direction is indicated by the arrow direction.

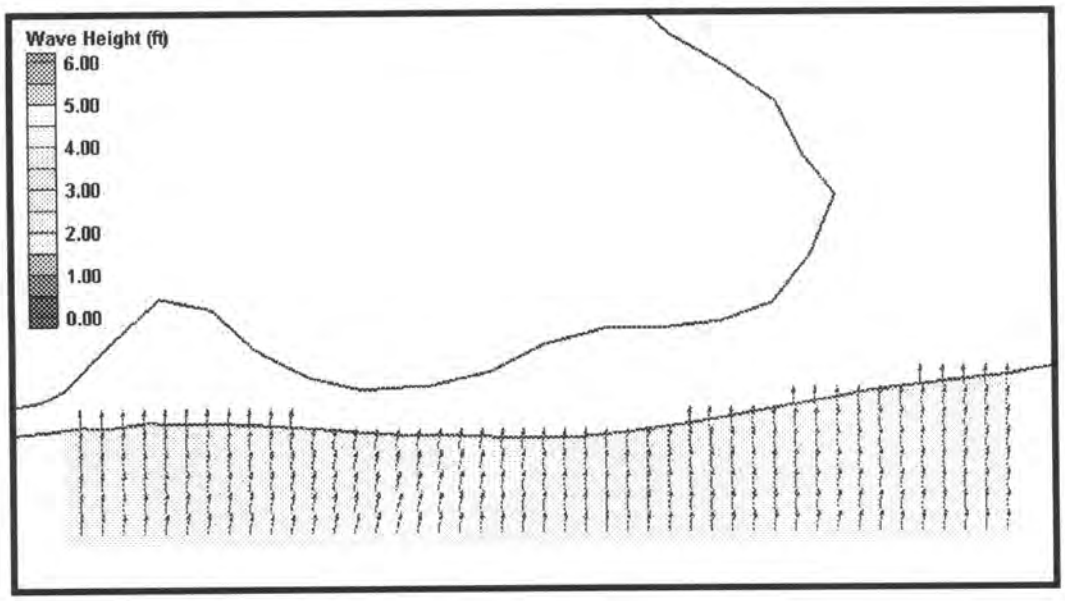

Figure H36. Fine grid (25m x 25m) wave results for Case 6, Morgan Peninsula. Wave heights are shown by color while wave direction is indicated by the arrow direction.

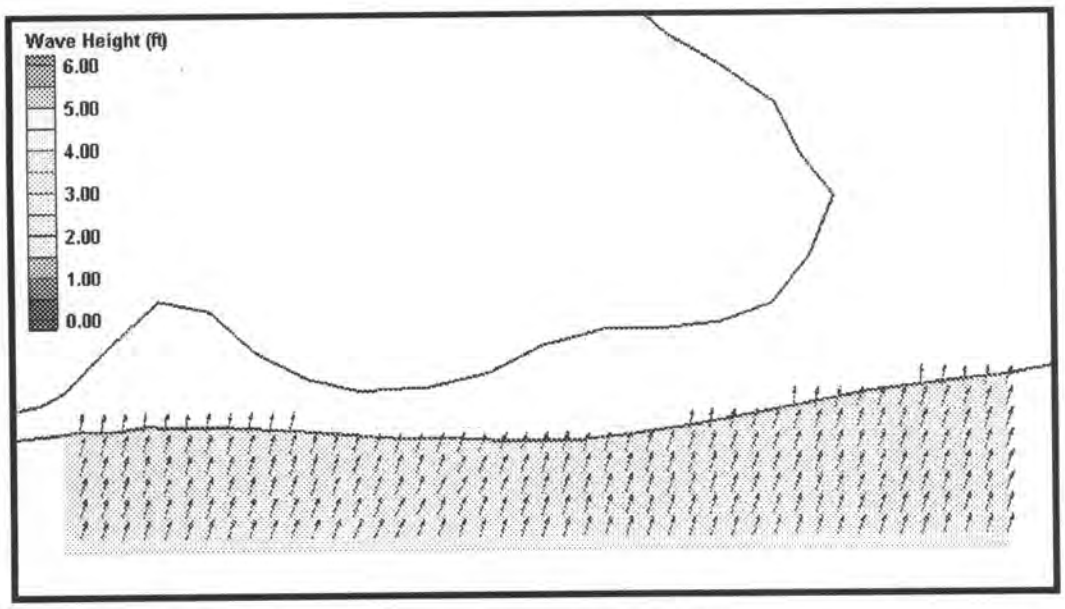

Figure H37. Fine grid (25m x 25m) wave results for Case 7, Morgan Peninsula. Wave heights are shown by color while wave direction is indicated by the arrow direction.

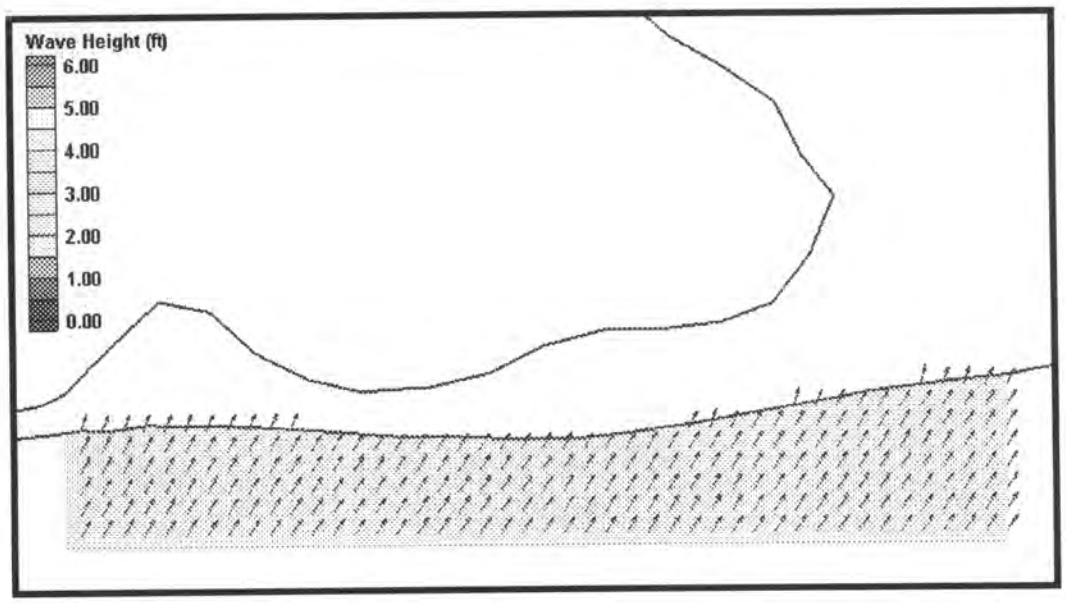

Figure H38. Fine grid (25m x 25m) wave results for Case 8, Morgan Peninsula. Wave heights are shown by color while wave direction is indicated by the arrow direction.

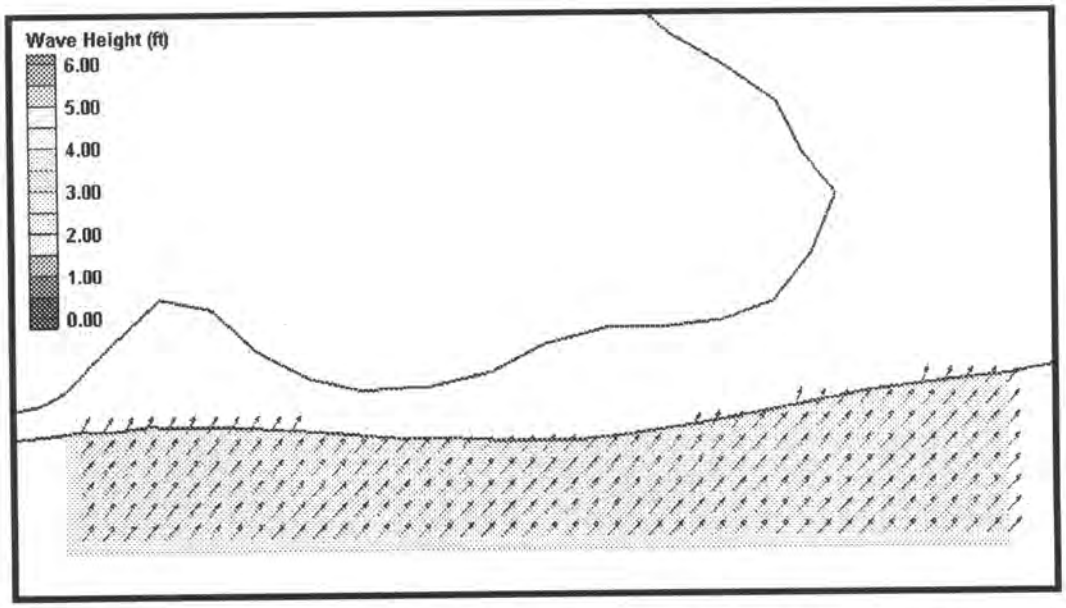

Figure H39. Fine grid (25m x 25m) wave results for Case 9, Morgan Peninsula. Wave heights are shown by color while wave direction is indicated by the arrow direction.

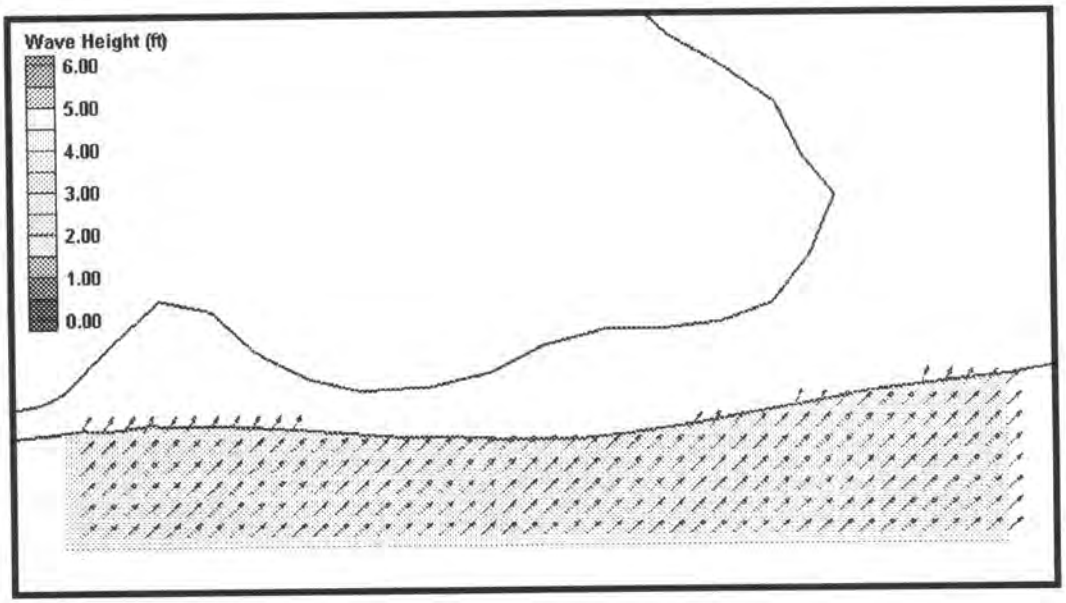

Figure H40. Fine grid (25m x 25m) wave results for Case 10, Morgan Peninsula. Wave heights are shown by color while wave direction is indicated by the arrow direction.